Phytochemical Analysis and Evaluation of Anticancer and Antimalarial Properties of Four Medicinal Plants

Fidelia Ijeoma Uche

Institute for Science and Technology in Medicine

Keele University

Thesis submitted to Keele University for the degree of

Doctor of Philosophy

March 2017

ABSTRACT

Cancer and malaria are among the most life-threatening diseases globally. Cancer is responsible for about 125,000 annual deaths globally. In 2015, the World Health Organization report estimated that 236000-635000 people died of malaria. These diseases are complicated by the development of resistance to available chemotherapeutic agents. Natural products have been recognized for their major applications in the identification of drug leads in drug discovery. *Viola philippica* Car, *Viola yedoensis* Makino (Violaceae), *Triclisia subcordata* Oliv (Menispermeaceae) and *Cyclicodiscus gabunensis* Harms (Fabaceae) are medicinal plants traditionally used for the treatment of various diseases including malaria or cancer in China and West Africa. However, the bioactive compounds are unknown. Therefore, this study evaluated the *in vitro* anticancer and antimalarial activities of the four medicinal plants and searched their bioactive compounds. The in vitro anti-ovarian cancer and antimalarial assays were demonstrated respectively using sulforhodamine B dye and Syber green 1 fluorescence assay methods. Bioassay-guided fractionation and purification were performed. Structural elucidation was performed by nuclear magnetic resonance spectroscopy and mass spectrometry analysis. Results revealed the anticancer and antimalarial activities of *T. subcordata*; *V. philippica,* and *V. yedoensis* to be bisbenzylisoquinoline alkaloids (cycleanine, isochondodendrine and 2′-norcocsuline) and/or cyclotides. The cycleanine analogues were synthesized and found to be more potent than cycleanine. Induction of apoptosis by these alkaloids has also been determined. This study could serve as basis for the support of use of these plants in cancer and/or malaria treatment. The BBIQ alkaloids and analogues could serve as lead compounds in drug discovery. Future *in vivo* studies need to be carried out on these alkaloids to get drug approval.

TABLE OF CONTENTS

LIST OF FIGURES

LIST OF TABLES

LIST OF ABBREVIATIONS

Apaf1	Apoptosis activating factor1
ATCC	American Type Culture Collection
Bak	BCL2 antagonist killer 1
Bax	BCL2 associated X protein
BBIQ	Bisbenzylisoquinoline
BCA	Bicinchoninic acid
Bcl-2	B-cell lymphoma protein 2
Bcl-XL	BCL2 related protein, long isoform
BSTFA	Bis(trimethylsilyl)trifluoroacetamide
Caspase	Cysteinyl aspartic acid-protease
CHCA	α-cyano-4-hydroxycinnamic acid
DMSO	Dimethlysulfoxide
DNA	Deoxyribonucleic acid
Endo-Glu-C	Endoproteinase Glu-C
ESI-MS	Electrospray ionization-mass spectrometry
Q-Tof	Quadruple Time of Flight
FADD	Protein associated with death domain
Fas	protein associated with tumour necrosis factor TNF1
FasL	Protein associated with Ligands
FBS	Fetal bovine serum
FITC	Fluorescein isothycanate
FOV	Field of view
GC-MS	Gas chromatography-Mass spectrometry

HOE	Human ovarian epithelial
HPLC	High performance liquid chromatography
IC_{50}	50% inhibition concentration
LC-MS	Liquid chromatography - mass spectrometry
MALDI	Matrix-assisted laser desorption/ionization
MDR	Multidrug resistance
MFI	Mean fluorescence intensity
NMR	Nuclear Magnetic resonance
PARP	Poly ADP (Adenosine-diphosphate)- ribose polymerase
PBS	Phosphate buffered saline
PE	Phosphatidylethanolamine
PSD	Post source decay
PVDF	Polyvinylidene fluoride
RNA	Ribonucleic acid
S.E.M.	Standard error of the mean
SDS	Sodium dodecyl sulphate
SPE	Solid phase extraction
SPPS	Solid phase peptide synthesis
SRB	Sulforhodamine B
TCA	Trichloroacetic acid
TCEP	Tris(2-carboxyethyl)phosphine
TFA	Trifluoroacetic acid
THPTA	Tris(3-hydroxypropyltriazolylmethyl)amine
TLC	Thin layer chromatography

TNF	Tumor necrosis factor
VP	*Viola philippica*
VY	*Viola yedoensis*

PUBLICATIONS

Journals

1. **Fidelia I. Uche**, Falko P. Drijfhout, James McCullagh, Alan Richardson and Wen-Wu Li. (2016) Cytotoxicity Effects and Apoptosis Induction by Bisbenzylisoquinoline Alkaloids from *Triclisia subcordata*. *Phytother. Res*. DOI: 10.1002/ptr.5660

2. Omar Aldulaimi, **Fidelia I. Uche,** Hamza Hameed, Haddijatou Mbye, Imran Ullah, Falko Drijfhout, Timothy D.W. Claridge, Paul Horrocks and Wen-Wu Li. (2017). A characterization of the antimalarial activity of the bark of *Cylicodiscus gabunensis* Harms, Journal of Ethnopharmacology. http://dx.doi.org/10.1016/j.jep.2017.01.014

Book Chapter

Wen-Wu Li, Okiemute Johnson-Ajinwa, **Fidelia Ijeoma Uche**. (2015) Potential of Phytochemicals and their Derivatives in the Treatment of Ovarian Cancer. Handbook on Ovarian Cancer: Risk Factors, Therapies and Prognosis. Nova Science. Publishers, Inc. 400 Oser Avenue, Suite 1600 Hauppauge, NY 11788 USA.

CONFERENCE ABSTRACTS

1 **Fidelia I. Uche**, Falko P. Drijfhout, James McCullagh, Alan Richardson and Wen-Wu Li. Cytotoxicity Effects and Apoptosis Induction by Cycleanine and Tetrandrine. 9th Joint Natural Product Conference, Copenhagen, Denmark, July 24- 27th 2016.

2 Omar Aldulaimi, **Fidelia I. Uche**, Imran Ullah, Hamza Hameed, Paul Horrocks, Wen-Wu Li. Investigation of the antimalarial compounds from *Cylicodiscus*

gabunensis Harms. 19th International Congress PHYTOPHARM 2015 Bonn, Germany, 21-24 July, 2015

3 **Fidelia I. Uche,** Alan Richardson, Falko Drijfhout, James Mccullagh, Trevor J. Greenhough, Sarah Hart , Elzbieta Piatkowska, Wen-Wu Li. Anti-ovarian cancer activities of Alkaloids from *Triclisia subcordata* and Cyclotides from *Viola yedoensis*. PharmSci 2014. Academy of pharmaceutical Sciences of Great Britain, University of Hertfordshire, Hartfield, United Kingdom; 09/2014 (Oral presentation).

4 **Fidelia I. Uche,** Wen-Wu Li, Alan Richardson, Trevor J. Greenhough (2014). Anticancer activities of cyclotides from *Viola yedoensis* Makino (Violaceae). Planta Medica: Annual meeting of American Society of Pharmacognosy and 14th Oxford international Conference on the Science of Botanicals, University of Mississippi Oxford, USA; 08/2014. PLANTA MEDICA, Volume: 80, Issue: 10, Pages: 818.

5 **Fidelia I. Uche,** Wen-Wu Li, Alan Richardson, Trevor J. Greenhough (2014). Anti-ovarian cancer activities of alkaloids from *Triclisia subcordata* Oliv. Planta Medica: Annual meeting of American Society of Pharmacognosy and 14th Oxford international Conference on the Science of Botanicals, University of Mississippi Oxford, USA; 08/2014. PLANTA MEDICA Volume: 80, Issue: 10, Pages: 813

ACKNOWLEDGEMENTS

I thank God for His divine grace and favor granted to me to accomplish this study. I thank Nigerian government for provision of scholarship for this study, through Education Trust Fund (ETF) and Niger Delta Development Commission (NDDC). I am grateful to Keele University for financial support.

My special thanks go to my lead supervisor, Dr. Wen-Wu Li for his dedicated and relentless efforts in directing and supervision of this study. I equally appreciate the contribution of Prof Trevor J. Greenhough as my second supervisor.

I am heavily indebted to my family, particularly my husband Uche C. Nwosu for his financial and moral support. I thank my children and siblings for moral support. I also appreciate all the moral support given to me by my sister in-laws, colleagues and friends like Dr. Homayemem Weli and Faiza Musa.

Finally, this study wouldn't have been easily successful without contributions of some collaborators in form of trainings and expert advice. Therefore, I appreciate the trainings given to me by the following collaborators: Dr. Alan Richardson and his group members such as Mohammed Abo Donia, Marwan Abdullah and Dr. Elizabeth Robinson for assistance in provision of cancer cell lines and training on cancer assays; Professor Paul Horrocks and his group for training me on in vitro malaria assays and his group members Dr. Imran Ullah and Haddijatou Mbye for assistance in malaria assays; Dr. Sarah Hart and Elzbieta Piatkowska for training on mass spectrometry proteomics; Dr. Falko P. Drijfhout training on LC-MS and use of preparative HPLC analysis, John Clew for training on use of NMR; Professors James McCullagh and Tim Claridge (Oxford University) for assistance in Mass

spectrometry and NMR spectroscopic analysis, respectively. Drs Sandhya Moise and Joshua C. Price for training me on flow cytometry and confocal microscopy, respectively.

CHAPTER ONE

INTRODUCTION

1.1 Natural Products

Natural products generally comprise products of life (Samuelson, 1999). In organic chemistry, natural products mainly denote organic compounds produced in living organisms by both primary and secondary metabolic pathways (Hanson, 2003). But in the areas of pharmacognosy and medicinal chemistry, natural products are limited to secondary metabolites from living organisms or natural sources (Bhat et al., 2005, Cragg et al., 2009, Williams & Lemke, 2002). The primary metabolites including the amino acids lipids, carbohydrates, and nucleic acids are the principal components or the molecular building blocks of life. The living organism cannot do without primary metabolites because they are produced for survival and the self-utilization by the organism. Primary metabolites exert innate influence on the organisms that produce them (Kossel, 1891, Kliebenstein, 2004, Karlovsky, 2008) The secondary metabolites are produced by organism for different reasons like symbiotic attraction or protection in a competitive predator environment (Kliebenstein, 2004, Karlovsky, 2008). Hence, they are species-limited in distribution. The secondary metabolites affect the biochemical signal and transduction pathways of the source organism (Demain & Fang, 2000, Cragg et al., 2009, Hanson, 2003) which could be attributed to their numerous pharmacological effects (Demain & Fang, 2000) Natural products could sometimes be used to denote pure compounds of plant origin (Heinrich et al., 2012). For this thesis, the discussion will focus mainly on natural products of plant origin.

Plants are the main source of chemical compounds with varied structural diversity known as phytochemicals (Crozier et al., 2008). A long history of the use of plants for food and medicines by human revealed an in-depth knowledge of medicinal properties and uses of many plants (Brouwer et al., 2005, Hesham et al., 2013). In many parts of the world, traditional medicines have found wide applications in treatment of various diseases including cancer and malaria (Adebayo & Krettli, 2011). Plants have been reported to exert wide influence and applications in the traditions and cultures of many developing countries (Delgado et al., 2011, Hesham et al., 2013). Per the World Health Organization reports (LeGrand & Wondergem, 1989, Cordell, 1995), about 80% of the global population use plants as primary source for health treatment. Besides, traditional medicines are still the only source of health treatment for about 60% of the worlds' population, especially in many rural areas of developing countries (Hesham et al., 2013).

Natural products of plants origin offer good sources for identification and discovery of drug leads or novel compounds in modern drug research (Cragg et al., 2009, Cragg et al., 1997). Reports showed that ethnobotany and ethnopharmacology exert significant contribution in drug discovery and development (Heinrich, 2000, Heinrich & Gibbons, 2001). It was reported that as at 1990, about 80% of drugs in use comprised of natural products or analogues derived or inspired by them (Li and Vederas 2009). It was also revealed that plant-derived drugs make up significant part of natural product-pharmaceuticals (Schmidt et al., 2007, Newman & Cragg, 2012). More than 100 natural product-based drugs were reported to be in clinical studies from 2001 to 2008 (Li & Vederas, 2009) .

1.2. Cancer and Anticancer Natural Products

1.2.1. Cancer

Cancer is a collective name that designates diseases of unregulated cell growth of abnormal cell. It may be transferred from one tissue to another through blood and lymph. Individual cancer is named after the affected or cancerous tissue. Cancer has been reported to be among the most lethal cause of deadly diseases of human and to be responsible for 25% death globally (Fouche et al., 2008, Jemal et al., 2009, Siegel et al., 2015). For example, ovarian cancer is an unregulated growth condition, arising from the cells in and around ovary and fallopian tube. Epithelia ovarian cancer ranks most common type and targets surface layer of ovary. Ovarian cancer is responsible for about 125,000 annual deaths with 204,000 incidences globally (Rauh-Hain et al., 2011). It is the most lethal of all the gynecological malignancies (Rauh-Hain et al., 2011). About 4,272 deaths were recorded from ovarian cancer in the UK in 2011 (Cancer research UK). Ovarian cancer is ranked the 5th cause of death among women in the UK (Rauh-Hain et al., 2011).

The increased challenges in failure of cancer treatment could be attributed to insufficient cancer measures such as chemotherapy, radiotherapy and surgical procedures (Fadeyi et al., 2013). Evidence has shown that plant products could offer a better option in the treatment and management of cancer because plants are inexhaustible reservoir of active agents for treatment of diseases (Cragg et al., 2009, Cragg et al., 1997, Fouche et al., 2008), as revealed by ancient traditional medicinal practices (Kim & Park, 2002, Lee, 2010, Mann, 2002). The major contributions of

ethnobotany and ethno-pharmacy in discovery and development of anti-cancer drugs has been revealed (Heinrich & Bremner, 2006).

1.2.2 Anticancer natural products

Plant-derived anticancer drugs include vinca alkaloids, vinblastine and vincristine isolated from the Madagascar *periwinkle* or *Catharanthus roseus* (L) (Guéritte & Fahy, 2005) and camptothecin derived from stem wood of the Chinese tree, *Camptotheca acuminate*. The analogues of camptothecin including topotecan and irinotecan are also anticancer drug approved by FDA (Li et al., 2015b) (Figure 1.1). Camptothecin and its analogues exert their mechanism of action by inhibition of DNA topoisomerase 1, with S-phase specific killing as their primary mechanism of killing (Liu et al., 2000). Another famous plant-derived drug is paclitaxel *('*Taxol') (Figure 1.2) isolated from the bark of the pacific yew tree, derived from *Taxus brevifolia* (Cragg et al., 1997). Paclitaxel binds to β-tubulin subunits of micro-tubules which disrupt the equilibrium between monomeric and polymeric tubulin, stabilizes the nucleation center (Rao et al., 1994, Schiff, 1997, Schiff et al., 1979).

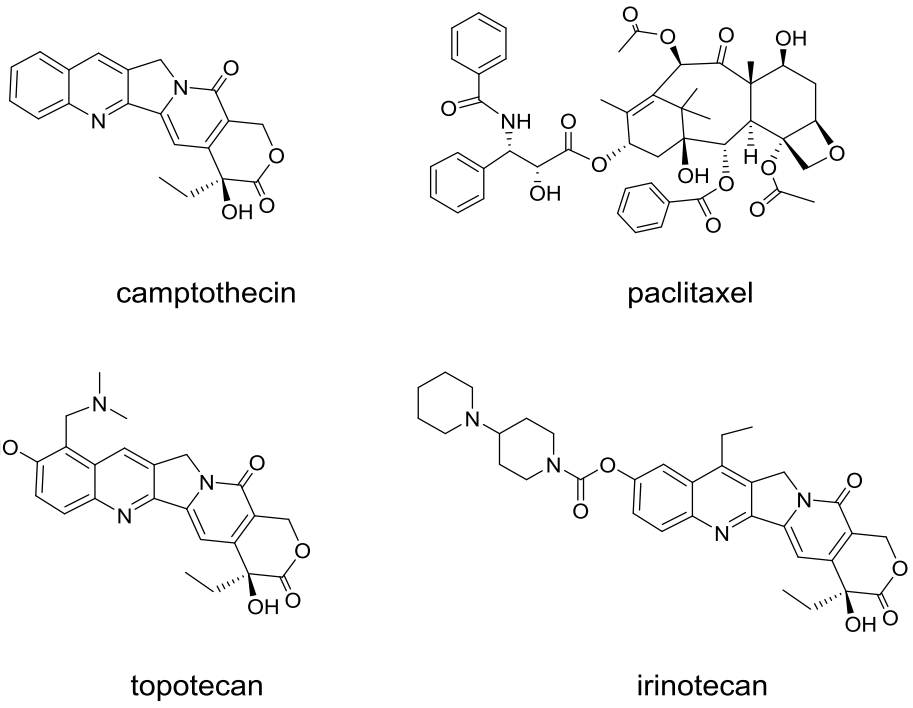

Figure 1.1 Structures of plant-derived natural products used for the treatment of cancer.

The most prevalent challenges in the treatment of cancer include resistance, toxicity, low specificity of the available cytotoxic agents and economic problems for developing countries (Hesham et al., 2013, de Mesquita et al., 2009). These problems, call for urgent need for research aimed at the investigation, identification and discovery of novel anticancer compounds. Bioassay-guided fractionation is an established reliable procedure used in identification of novel drugs of natural origin. It is most likely that many more efficient natural products for treatment of diseases, particularly cancer are yet to be discovered.

1.2.3 Apoptosis: programmed cell death

The drugs used in treatment of cancer can cause cell death. The type and magnitude of stimuli (drugs) could affect the nature of cell death elicited by the stimuli, which

could be due to necrosis or apoptosis. Drug – induced cell death in tumour is mostly carried out by apoptosis. It has been stated that at low doses, the cancer chemotherapeutic agents could cause apoptosis and at high dose they cause necrosis (Elmore, 2007)

Apoptosis is a programmed cell death involving coordinated destruction of cell, protein and DNA fragmentation. The cell to be eliminated stimulates enzymes that destroy the cells' nuclear DNA, or nuclear and cytoplasmic proteins. Apoptosis can also be caused by both physiological and other pathological factors (Elmore, 2007).

The morphological features of apoptosis include cell shrinkage, chromatin condensation, and cytoplasmic blebs formation, fragmentation of DNA or formation of apoptotic bodies and destruction of the apoptotic bodies by phagocytes or microphages and dendrites cells via phagocytosis. The unique feature of apoptosis is protein hydrolysis which is carried out by cysteine proteases members known as caspases. Apoptosis is controlled by two gene family namely: Bax, Bcl2 or $Bclx_L$ (anti-apoptotic) which obstruct the efflux of cytochrome *c* from mitochondria and block Apaf1.

The two major pathways involve in mechanism of apoptosis have been identified as intrinsic and extrinsic pathway or executioner pathways (Figure 1.2). During extrinsic pathway, DNA injury or stress stimuli activates the Fas (protein associated with tumour necrosis factor TNF1) and the cross-link ligands (FasL) which contain death domains receptors. The group of Fas associated death domain (FADD) receptors bind to procaspase 8 to activate cascade of caspases 8 which in turn activates caspases 3 to elicit execution pathways. This can lead to degradation or phagocytosis of the dead or injured protein by microphages or dendrite cells, or fragmentation of DNA completing

the apoptosis process. In the extrinsic pathway, DNA injury of stress stimuli triggers increased mitochondria permeability and efflux of cytochrome *c* causing apoptosis. The cytochrome c leaks out from mitochondria, and binds to the apoptosis activating factor 1 (Apaf1) which activates the cascades of caspase 9. This triggers activation of caspases 3 and 6 which also leads to the execution pathway causing apoptosis (Figure 1.2) (Robinson et al., 2013, Stephen, 2005).

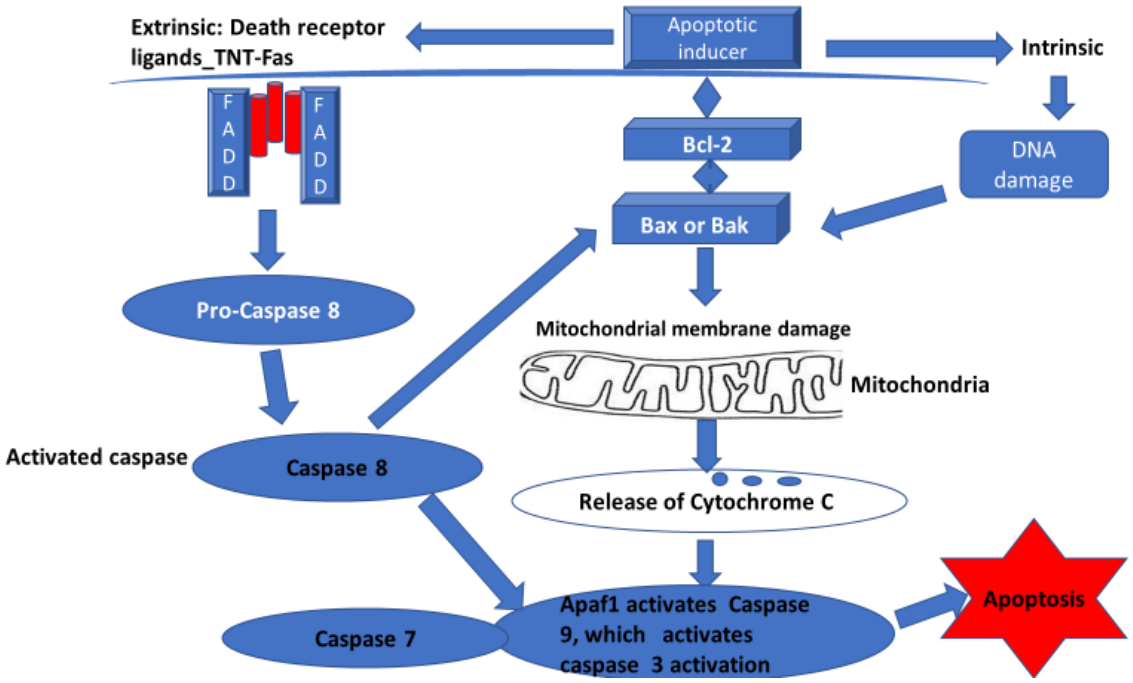

Figure 1.2 Schematic illustration of mechanism of apoptosis (Robinson et al., 2013, Stephen, 2005). The apoptosis mechanism comprises two major pathways namely: extrinsic and intrinsis pathways. The former is triggered by binding of death receptor ligands to group of FADD giving rise to activation of caspases 8, caspase 7 and caspase 3 which leads to apoptosis. Also, the intrinsic pathway involves the activation of Bax and Bak caused by DNA damage of stress . Activation of proapoptotic factor (Apaf1) induced by cytrochrome C leakage from mitochondrial membrane permeability leads to activation of caspase 9 which in turn activates caspase 3 causing apoptosis.

The detection of morphological change of cells, activity of caspases, DNA fragmentation, membrane alteration, and mitochondrial change have been developed to assay apoptosis and previously described in detail (Elmore, 2007).

1.3 Malaria and Antimalarial Natural Products

Malaria is caused by protozoan parasites from *Plasmodium* species and is among the most lethal infectious parasitic diseases globally. About three hundred million people are annually infected with malaria in developing countries such as Central and South America, Asia, and Sub-Saharan Africa (Greenwood & Mutabingwa, 2002, Snow et al., 2005). Besides, about 1.1-2.7 million people infected with malaria, especially children less than five years old die every year (Snow et al., 2005, Greenwood & Mutabingwa, 2002). Human malaria is transmitted by female *Anopheles* mosquitoes but caused by four *Plasmodium* species namely, *P. falciparum*, *P. vivax*, *P. ovale* and *P. malariae*. The most widespread and severe disease is caused by *P. falciparum*, which transiently infects the liver before invading red blood cells of the mammalian host (Figure 1.3).

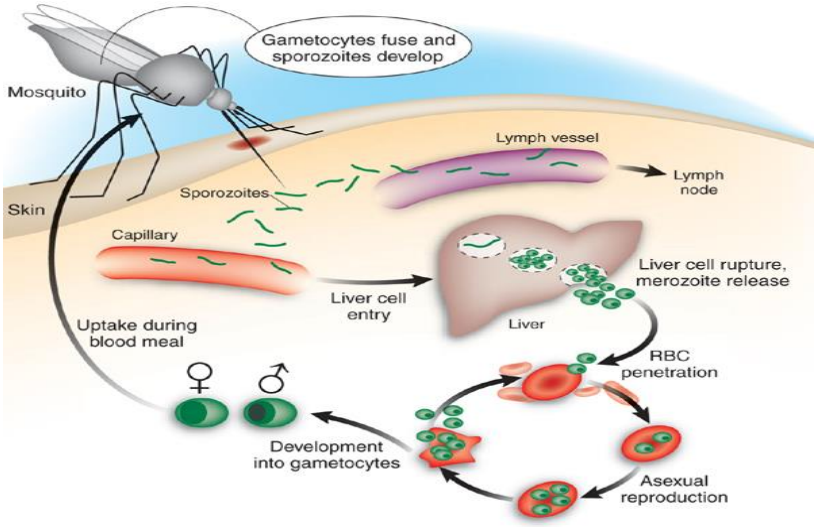

Figure 1.3 The life-cycle of malaria (Batista et al., 2009).

Clinical manifestations occur at the erythrocyte stage and can include fever, chills, and anemia, as well as delirium, metabolic acidosis, cerebral malaria and multi-organ system failure, which may be followed by coma and death (Batista et al., 2009).

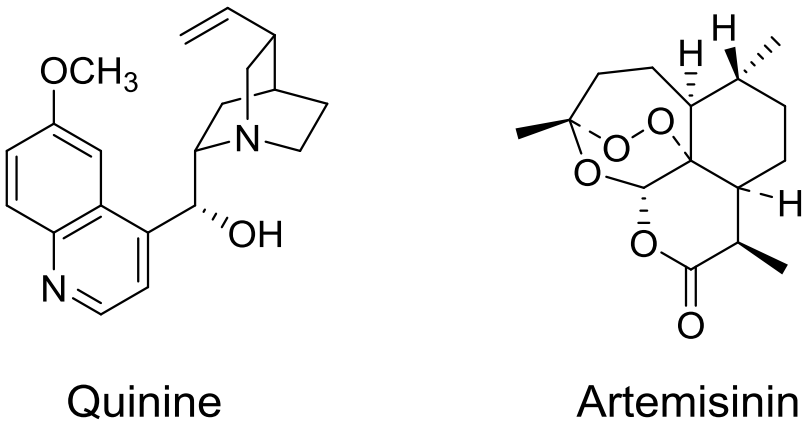

Figure 1.4 Structure of two potent antimalarial natural products.

Quinine (Figure 1.4) an aminoquinoline alkaloid isolated from the bark of *Cinchona* nitida(Rubiaceae) is one of the oldest and most important antimalarial drugs and is

still used today (Greenwood et al., 2005, White et al., 1983). Artemisinin (Figure 1.4) extracted from sweet wormwood (*Artemisia annua*) is the most potent antimalarial available (White, 2008, Klayman, 1985), rapidly killing all asexual stages of *Plasmodium falciparum*. Artemisinin is widely used to treat multidrug-resistant malaria (White, 2008). A Nobel Prize in Physiology and Medicine in 2015 was awarded for the discovery of artemisinin. A total of 266 antiplasmodial natural products belonging to the groups of alkaloids, terpenes, quassinoids, flavonoids, limonoids, chalcones, peptides, xanthones, quinones, sesquiterpenes, coumarins and miscellaneous compounds, as well as 37 promising semisynthetic antimalarial, have been reviewed and reported (Batista et al., 2009).

In the next two sections, two specific types of natural products from plants – cyclotides and bisbenzylisoquinoline (BBIQ) alkaloids will be reviewed regarding their structure, sources and biological activities including anticancer and/or antimalarial activities.

1.4 Plant Cyclotides

Cyclotides are highly stabilized cyclic peptides from plant family which are rich in disulfide bonds arranged in a knotted pattern that are connected to cysteine residues in a combinatorial cyclic backbone (Craik et al., 1999). The special structures of cyclic peptides bestow on them a remarkable stability and various biological activities. The cyclotides (28-37 aa) have been reported to be true gene products which differentiate them from a range of smaller cyclic peptides (5–12 aa) that are found in fungi and bacteria. The latter such as gramicidin and cyclosporine are typically synthesized by multi-enzyme complexes (Jennings et al., 2001). Therefore, cyclotides differ from other circular proteins in that they possess very distinct three-dimensional structures and, despite their small size, may be regarded as mini proteins (Jennings et al., 2001). This attribute arises mainly from the knotted network of disulfide bonds that stabilizes the structures.

1.4.1 Discovery of cyclotides

In the early 1970s, it was observed by a Norwegian Physician, Lorents Gran, on his Red Cross relief mission in Congo, Africa, that women from Lulua tribe of Congo were drinking the boiled water extract from the leaves of an African plant known as *Oldenlandia offinis* (Roam and Schult) DC (Rubiaceae) as tea to accelerate or speed up childbirth and to reduce time of labor (Gran, 1973, Gran et al., 2000). Some women applied it directly to the vagina during labor (Craik et al., 1999, Craik, 2009, Craik, 2010). He then came back to his laboratory in Norway, when he finished his Red Cross assignment, together with his colleagues and investigated the bioactive constituent of

the plant leaves that could be responsible for the oxytocic effect or the uteroactive function, inducing birth labour.

In women, oxytocin has been known for its wide application or function in induction of birth labour. It initiates the contraction of women womb or uterine muscle to stimulate or strengthen labour during child birth. Oxytocin also induces or improves the prostaglandins production thereby increasing contraction of uterine muscle and elicit or enhances delayed labour. Oxytocin could also cause production of breast milk with improved lactation for baby. Two different oxytocic bioactive constituents were isolated from the *O. affinis* extract, at the Department of Pharmacognosy, University of Oslo. These included serotonin and a polypeptide. As serotonin is easily degraded in the gastrointestinal tract, the oxytocic activity of the drug was reported to be due to the polypeptide (kalata B1), which was expressed at high levels in the plant (1-2 mg/g of dried crude powder of the plant) (Gran, 1973). After the analysis, Lorents Gran, partially characterized one of the major bioactive compounds-the polypeptide, which he discovered to be a peptide of 30-amino acids and named the bioactive compound ‘Kalata B1’ after the native or local name of that plant ‘Kalata Kalata’ (Gran, 1973). Conversely, it was about twenty-five years later that its full amino acid sequence and three-dimensional (3D) structure was revealed for the first time - this was later shown to be cyclic (Saether et al., 1995). It was amazing to note that the peptide did not have termini, it is head-to-tail cyclized and it had three disulfide bonds arranged in a knotted topology (Craik et al., 1999, Craik, 2001, Craik, 2009). It was reported that the N- and C-termini were blocked (Herrmann et al., 2008b) but it was not until 1995 that the macrocyclic nature of kalata B1 was revealed (Saether et al., 1995).

At that time three similar proteins had been reported from two additional Rubiaceae species: the circulins A and B from *Chassalia parvifolia* Schum (Gustafson et al., 2004, Gustafson et al., 2000), and cyclopsychotride A from *Psychotria longipes* Muell. Arg. (Witherup et al.,1994). In addition, a peptide, named Violapeptide-I, had been isolated and partially characterized from *Viola arvensis* Murr which belongs to the plant family of Violaceae (Schoepke et al., 1993). Many additional cyclotides have been discovered. These include the varv peptides A–H from *Viola arvensis* (Claeson et al., 1998; Goransson et al., 2004), several peptides from *Viola odorata*, *Viola hederaceae* and *Oldenlandia affinis* (Craik et al., 1999), several new circulins (Gustafson et al., 2000) and the cycloviolins (Hallock et al., 2000, Schoepke et al., 1993). It was reported that the number of cyclotides from Viola *odorata* L. was 30 (Ireland et al., 2006) but it has been suggested that the number of different cyclotides in one species may be over 100 and that the total number in the Violaceae alone might exceed 9000. It was suggested that if this is true, the cyclotides would be one of the largest protein families known (Simonsen et al., 2005).

1.4.2 Extraction, Purification and Isolation of Cyclotides

A range of approaches to isolate cyclotides from plant tissues has been established (Göransson et al., 2004, Craik et al., 1999, Claeson et al., 1998). During cyclotides extraction, three main features of cyclotides are usually considered for proper extraction purification and identification of cyclotides. These features of cyclotides applied in identification during extraction include the following after alcohol -based extraction: (1) identification of the late-eluting fractions on reversed-phase high performance liquid chromatography (RP-HPLC); (2) confirmation that their masses are consistent with typical cyclotides, i.e., 2700 - 3800 Da; and (3) observation of an

increase in mass of 18 Da on cleavage with endo-GluC (Gruber et al., 2008; Craik & Conibear, 2011, Craik et al., 2012, Tan & Zhou, 2006, Poth et al., 2011). The characteristic late elution on HPLC (Craik & Conibear, 2011) arises from the presence of a patch of hydrophobic residues on the surface of cyclotides (Rosengren et al., 2003).

A fractionation protocol for polypeptides isolation from plants biomass as developed by Claeson et al. is another good method adopted by many researchers (Claeson et al., 1998). The procedure enabled isolation of a highly-purified polypeptide fraction from plant biomass to be isolated and purified using HPLC (Tan & Zhou, 2006). The protocol is as follows: the dried ground plant materials are first defatted or pre-extracted with dichloromethane (CH_2Cl_2) to remove complex fat-soluble substances like chlorophyll, lipids and other low molecular–weight substances such as terpenoids, and phenylpropanoids. The polypeptides are not extracted by dichloromethane because of its insolubility in this solvent (Claeson et al., 1998). The polypeptide-rich crude extract (i.e. air-dried plant residues) is then re-extracted with a solvent such as 50% ethanol [EtOH-H_2O (1:1)]. It has been reported that many of the investigated polypeptides have good solubility in 50% alcohol than pure alcohol or water (Claeson et al., 1998). Besides, the use of aqueous alcohol in the extraction could confer protection against microbial invasion of the plant biomass and ethanol does not extract most polysaccharides or enzymes (Claeson et al., 1998). The acidified extract is filtered through polyamide gel to remove tannins before being partitioned between H_2O and *n*-BuOH and HPLC on a C18 (CH_3CN-H_2O) column for final purification (Claeson et al., 1998).

1.4.3 Method of detection of cyclotide

Chemical methods of detection test for cyclotides have been established (Tan & Zhou, 2006). A good specific method for detection of cyclotides has been reported to be 'TLC protosite' reaction with ninhydrin reagent. This is a sensitive chemical detection method for plant cyclic peptides. It can be effectively used to detect whether plant extracts contain cyclopeptides as well as a guide to isolation, separation and purification of cyclopeptides (Tan & Zhou, 2006). The details of this new method are as follows: the sample is dotted at one corner of each of two identical 25 mm x 50 mm silica gel plates (plates 1 and 2), and these plates are developed with $CHCl_3$-CH_3OH (8.5:1.5 or 9:1). After removal of the solvent, plate 2 is hung in a sealed glass vessel containing small bottle of 1 mL of concentrated HCl. The vessel is placed in in a drying incubator (110 °C) for 1-2 h to allow plate 2 to be hydrolyzed. After it is cooled for a few minutes, plate 2 is taken out, and the HCl is removed. Then plates 1 (nonhydrolyzed plate) and 2 (hydrolyzed plate) are sprayed with 0.2% ninhydrin- acetone reagent and colored after heating with a drier for several minutes. The above-mentioned process is repeated once more. If there are some purplish red spots in most cases and/or yellow spots in a few cases for plate 2, but there are no spots in the same locations on plate 1, this indicates that the detected samples contain cyclopeptides. This is because cyclopeptides got hydrolyzed by HCl to release amino group which reacted with ninhydrin to produce the purple colour product (Rheuman reaction). The plate that was not hydrolyzed by HCl did not release amino acid for ninhydrin reaction. Ninhydrin (triketohydrine) is oxidizing agent at slightly low PH which reacts with amino group to produce purple coloured Dikehydrine. Molecular mass of cyclotides should fall within 2700 - 3800 Da by mass spectrometry and on cleavage produces a difference of 18 Da (Tan & Zhou, 2006, Craik & Conibear, 2011).

1.4.4 Primary structures /Sequencing of cyclotides

Cyclic peptides exhibit sequencing problem because they neither contain an *N*- nor a *C*-terminus, thus blocking conventional sequencing approaches such as Edman degradation as well as more recent MS-based approaches (Craik & Conibear, 2011). Besides, cyclotides are highly resistant to enzymatic degradation in their natural oxidized state (Colgrave et al., 2005, Craik & Conibear, 2011, Colgrave, M.L., Craik, D.J., 2004). Therefore, the established method for preparing cyclotides for sequencing has been developed to reduce the disulfide bonds, alkylate the free thiols, and then cleave the cyclic peptide with selected enzymes to liberate termini for sequencing (Goransson & Craik, 2003, Göransson et al., 2009, Craik & Conibear, 2011). Endoproteinase Glu-C (endo-Glu-C) has been extensively used for this purpose and has the advantage that so far, all cyclotides, except for kalata B12, have a conserved Glu in loop 1 in addition to few other Glu residues in the sequence (Colgrave et al., 2004, Colgrave et al. 2005, Craik & Conibear, 2011). Thus, there is generally only one target site for endo-GluC. Trypsin has also been widely used in sequencing procedure, as has a combination of both enzymes (Chen et al., 2005). Edman sequencing has now been essentially replaced with MS-based approaches in which a series of fragment ions can be used to successfully trace the amino acid sequence (Craik & Conibear, 2011).

The identification of free cysteine residues and disulfide bond is important for clear observation of protein function and structure. The existences of Matrix-assisted laser desorption/ionization (MALDI) and electrospray ionization (ESI) has helped in very efficient detection and analysis of biomolecules (Ten-Yang et al., 2000; Aebersold &

Mann, 2003). Usually, when the concentration of protein for analysis is very small, the MS techniques are universal procedures to apply for knowledge of the free cysteine residues and disulfide linkages in the peptides. Chromatographic separation of the disulfide–linked peptides produced from chemical and enzymatic cleavage of protein is usually necessary for MS determination of the location of disulfide bonds (Cole et al., 1999, Yen et al., 2000). The purified disulfide-rich peptides are then ionized by MALDI or ESI-MS, and identified by means of mass mapping. To ascertain the location of the disulfide-linkage, the disulfide containing peptides could be further reduced and alkylated to measure the mass to charge ratio of each individual peptide contained in the disulfide bond. Otherwise disulfide—rich peptides could also be confirmed using tandem mass spectrometry (MS/MS) or post source decay (PSD) analysis without chemical modification (Cole et al., 1999).

Tandem MS sequencing after reduction and digestion of peptide fractions is an efficient method for the identification and elucidation of the primary structures of new and known cyclotides (Goransson & Craik, 2003). To characterize any given cyclotide and elucidate its structure effectively, the disulfide bonds of the cyclotides should be reduced and cleave to provide or expose the *C*-termini which usually contains Glu that would be cleaved and fragmented for proper MS/MS analysis. Therefore, the purified cyclotides compounds in the eluents, from reversed-phase preparative HPLC are chemically and enzymatically treated before proceeding to tandem mass spectrometry (MS-MS) for sequence analysis. They are first reduced to break the disulfide bonds using tris(2-carboxyethyl) phosphine (TCEP) and/or subsequently S-carbamidomethylated, and digested with trypsin or endoproteinase Glu-C: a procedure that increased the mass of each cyclotide, confirming the presence of six cysteine moieties. Either trypsin or endoproteinase Glu C or both

are used to prepare linear fragments of the modified proteins, yielding fragments cleaved at the C-terminus of cationic residues (Arg, or Lys) or anionic residue (Glu), respectively. The fragments are fully sequenced by MS-MS analyses. Another advantage of tandem MS sequencing is that it is possible to unambiguously define amino acid sequences for a mixture of cyclotides. However, it is also more common recently, to carry out the sequencing of natural peptides based on identification and utilization of their encoding nucleic acids, and this has been particularly successful for cyclotides (Craik & Conibear, 2011). A database that contains cyclotides sequences (www.cybase.org.au) has been developed to curate the sequences of cyclotides and other circular proteins, both at the amino acid and nucleic acid levels (Wang et al., 2008, Mulvenna, J.P., Wang, C., Craik, D.J, 2006, Craik & Conibear, 2011).

1.4.5 Three-dimensional structures (NMR and X-ray)

Nuclear magnetic resonance (NMR) spectroscopy and X-ray crystallography have immensely contributed to our in-depth knowledge of three-dimensional structure of proteins and the existence and structural necessity of disulfide bonds (Brunger, 1997). The elucidation of three-dimensional structures of cyclotides so far reported has been carried out almost exclusively by NMR (Craik & Daly, 2007, Craik & Conibear, 2011) with the exception of one cyclotide, varv F, which both NMR and X-ray structures were reported (Craik & Daly, 2007, Craik & Conibear, 2011). In all cases, the cystine knot forms the core of the molecule and is surrounded by a β-sheet structure comprising a well-defined β-hairpin and a less ordered third β-strand. The unique cyclic cystine knot structure of the prototypic cyclotide kalata B1 was first reported in 1995 using NMR (Saether et al., 1995).

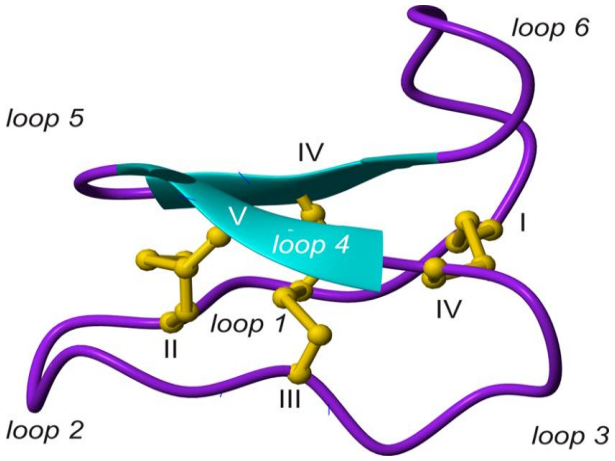

Figure 1.5 Ribbon structure of an exemplary cyclotide - Varv F (PDB code: 3E4H) (Burman et al., 2014).

1.4.6 Classification of Cyclotides

Cyclotides are grouped into two major subfamilies namely, the Mobius and Bracelet subfamilies based on topological differences, which are depending on the presence or absence of *cis*-Pro amide bond or motif (Figure 1.6) (Burman et al., 2014, Craik et al., 1999, Craik & Conibear, 2011). There is a recently discovered group known as circular trypsin inhibitors that comprise only two (MCoTI-I and MCoTI-II) from *Momordica cochinchinensis* of Curcubitaceae family (Burman et al., 2014). The bracelet subfamily group contains *trans*-amide bond but lack the *cis*-Pro bond. The Mobius subfamily contains a *cis*-Pro amide bond that creates a twist in the circular peptide backbone. In addition to the *cis*-Pro bond, Mobius and bracelet cyclotides differ in size, amino acid composition, and the nature of their inter-cysteine loops. A typical bracelet cyclotide contains one or two more residues than Mobius

counterparts. “Cyclization of any ribbon-like entity can be done in many ways but the two topologically simplest are by connection of the ends of the linear ribbon with no twist (i.e. bracelet-like), or with a single twist. The latter results in what is commonly known as a Mobius strip, which has the fascinating property of having just a single continuous side, compared to two sides of a bracelet” (Craik et al., 1999, Craik & Conibear, 2011).

There is no Pro amide bond at the corresponding position in circulin A, cycloviolacin O1 and other members of subfamily 1, and hence these can be regarded as bracelet-like molecules. It is therefore convenient to distinguish the two subfamilies of cyclotides as the bracelet cyclotides (subfamily 1) and the Mobius cyclotides (subfamily 2).

The major challenge or difficulty in extraction or study of cyclotides is head to tail cyclization of cyclotides. There is no free N- and C-terminal in cyclotides. Cyclotides are N-C cyclized. This offers great problem in study of cyclotides as series of steps or methods such as reduction, alkylation to free thiol group and enzymatic degradation to release cleave N and C- terminal bonds and fragment the long peptide residues need to be employed before sequence of cyclotides could yield good results. Also for chemical test for identification of cyclotides using ninhydrin test, acids hydrolysis needs to be applied to release free amid bond that could react to produce the colour reaction. Change. All these multiple processes are expensive and time-consuming procedures which render them very challenging in study of cyclotides.

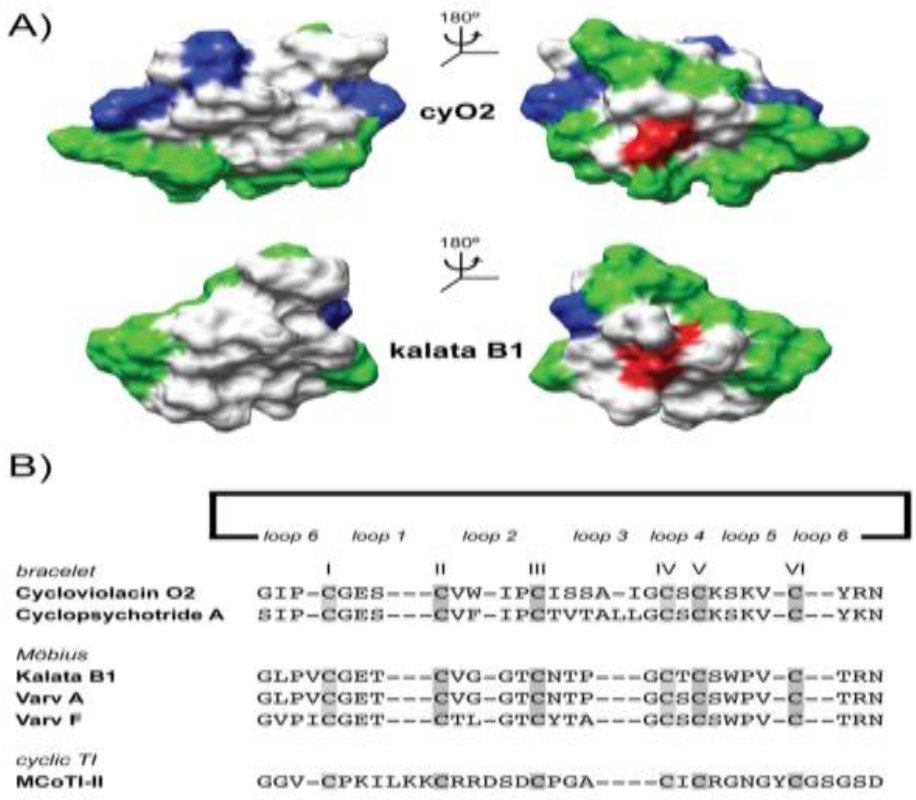

Figure 1.6 Surface and sequence representation of typical cyclotides (Burman et al., 2014). The backbone aligned models display the distribution of hydrophobic/hydrophilic regions on the protein surface and their amphipathic structure. Hydrophobic residues (Ala, Leu, Ile, Pro, Trp, Phe, Val) are in green, cationic (Arg, Lys) in blue, and anionic (Glu) in red. **A**) Cycloviolacin O2 and Kalata B1; **B**) Cycloviolacin O2 and cyclopsychotride (Bracelet); Kalata B1, Varv A, Varv F (Mobius); MCoT1-11 (Cyclic T) (Burman et al., 2014).

1.4.7 Production of cyclotides

Cyclotides can be extracted and purified in great quantity from plant materials as high as 1g/kg of plant tissue (Craik & Conibear, 2011), because the biosynthetic

procedure for cyclotides has been effectively and evolutionarily improved in nature (Reinwarth et al., 2012). This could be attributed to some important functions of cyclotides in plants. Such functions include protective functions (as plant defense), Cyclotides protect their plants from predators hence their uses as insecticides (insecticidal function) and anthelminthic. (Seather, 1995). Other biological function of cyclotides include antibacterial, cytotoxic and others stated in section 1.4.9

1.4.7.1 Chemical synthesis

Irrespective of the complex molecular scaffold of cyclotides, they are amazingly accessible by to solid phase peptide synthesis (SPPS). Chemical synthetic method for production of cyclotide can provide access to modified and “grafted” versions of cyclotides (Figure 1.7). Although naturally occurring cyclotides contain a wealth of sequence diversity, the capacity to chemically synthesize cyclotides provides opportunities to explore the structure–activity relationship of individual peptides by making mutants with specific sequence, and to develop cyclotides with new biological activities (Craik & Conibear, 2011). Chemical synthesis has been suggested to exhibit a clear benefit as against the recombinant route because it creates opportunity for an easy incorporation of synthetic element at any required position in the sequence (Reinwarth et al., 2012). Different procedures have been established over the previous years for the synthesis of cyclotides. The first step involved in cyclotide synthesis, is the assembly of the polypeptide chain. Chain assembly by SPPS, the routine method for peptide synthesis, involves coupling successive *N*-protected amino acids to a growing peptide chain which is attached, by the *C*-terminus, to a polymer resin (Craik & Conibear, 2011). The mixture of the reaction enables byproducts and excess reagents to be easily washed away, thereby greatly

simplifying purification and increasing yields. The process can also be automated, and this allows for rapid synthesis of peptides of up to approximately 50 residues in length (Craik & Conibear, 2011). It was stated that the most reasonable procedure applied in chemical synthesis of cycloids is a thioester-mediated approach or method in which linear cyclotide precursors are synthesized with a cysteine residue at the *N*-terminus and a thioester linker at the *C*-termini (Gunasekera et al., 2006).The complete synthesis of functional cyclotide involves sequential chain assembly, cyclisation and oxidation of the cysteine residues to form into their correct pairs of disulfide bonds i.e. oxidative folding (Cemazar et al., 2012, Craik & Conibear, 2011).

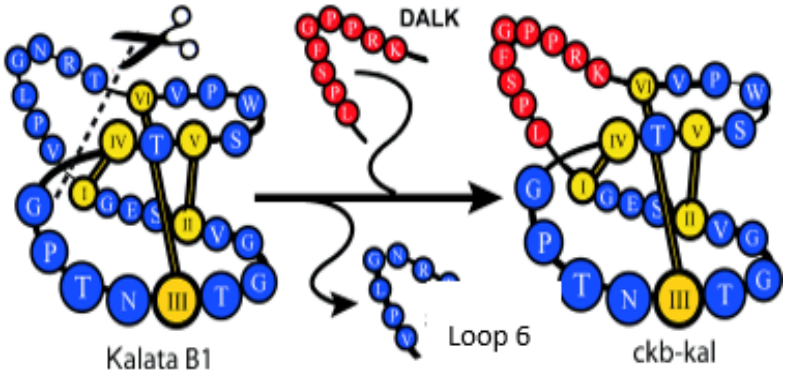

Figure 1.7 Application of cyclotide scaffold in peptide engineering (Wong et al., 2012).

The stability of scaffold of cyclotides makes them an ideal template for peptide engineering and drug design (Figure 1.7). By grafting natural peptide antagonists onto the cyclotide kalata B1, orally active peptides were engineered and potentially useful therapeutics for the treatment of inflammatory pain. In this case, the entire loop 6 of kalata B1 was replaced with the peptidic bradykinin B_1 receptor antagonist DALK (red in scheme) to obtain the cyclic bradykinin antagonist ckb-kal (Wong et al.,

2012). Generation of oxytocin-like peptide based on cyclotides with nanomolar affinity to G-protein-coupled receptor was also achieved (Koehbach et al., 2013) Reports showed that MCoTI-II is a significantly more potent matriptase inhibitor than SFTI-1. Deregulation of matriptase activity is implicated in several diseases including cancer. Therefore, inhibition of matriptase could have therapeutic potentials (Quimbar et al., 2013). The potential of bioengineered cyclic peptides for the treatment of multiple sclerosis (MS) was also demonstrated. This was achieved by grafting the active epitope (myelin oligodendrocyte glycoprotein) into the cyclotide scaffold to achieve improved stability and bioavailability of the epitope (Thell et al., 2016, Wang et al., 2013). Ji et al. reported the engineering of the cyclotide MCoTI-I to efficiently antagonize intracellular p53 degradation. The resulting cyclotide MCo-PMI could bind with low nanomolar affinity to both Hdm2 and HdmX, showed high stability in human serum, and was cytotoxic to wild-type p53 cancer cell lines by activating the p53 tumor suppressor pathway both *in vitro* and *in vivo* (Ji et al., 2013). Cyclotides are toxic against cancer and non-cancerous cells and their toxicity correlates with their ability to target and disrupt lipid bilayers that contain phosphatidylethanolamine phospholipids (Henriques et al., 2012, Troeira Henriques et al., 2014). It was suggested that cyclotides anticancer therapeutics activity could best be achieved by combination of their amenability to epitope engineering with their ability to bind cancer cell membranes (Henriques et al., 2012, Troeira Henriques et al., 2014).

1.4.7.2 Plant cell culture - based production of cyclotides

Plant cell culture is another way of production of cyclotide (Dörnenburg, 2008). Numerous problems connected with low production by cells slow growth, genetic instability of high–producing cell lines, poor control of cellular differentiation and inability to maintain photoautotrophic growth, have limited the expansion in the production of cyclotides using plant cell culture. Although considerable progress has been made to stimulate formation and accumulation of secondary metabolites using plant cell cultures during the past decades (Zhao, J & Verpoorte, R, 2007), few processes have proven to be economically viable. A strategy for enhancement of product yield has been reported (Dörnenburg, 2008, Dörnenburg, 2010).

1.4.7.3 Production by recombinant method

Bacteria possess the features for production of circular proteins and therefore can be used as expression systems. Bacteria do not produce cyclotide-like peptides in sufficient amount after transformation with the gene for their precursor proteins. So, they cannot be used for direct production of cyclotide (Dörnenburg, 2008, Katsara et al., 2006). Conversely an attempt to produce MCoTI-II inside living *E. coli* cells produced low expression (Dörnenburg, 2008, Katsara et al., 2006). The method reported by Avrutina et al to produce cyclotides has an advantage of the combination of economical and high efficient yield recombinant production of the linear peptide precursors that are already folded and oxidized, and chemical synthesis (Avrutina, 2008, Dörnenburg, 2008, Dörnenburg & Heike, 2010, Kimura et al., 2006).

1.4.8. Distribution of cyclotide in plants

About 280 different cyclotides have been isolated from more than 40 plant species since cyclotides were first discovered (Burman et al., 2014). Among the plant families found containing cyclotides include Violaceae, Rubiaceae, and Cucurbitaceae. Recently, cyclotides have also been found in Fabaceae, Solanaceae and linear cystine knot peptides from *Clitoria ternatea* of the pea (Fabaceae) (Nguyen et al., 2011, Poth et al., 2011c) and Petunia x hybrida (diamond pearly shades) a hybrid or species of the potato (Solanaceae) (Burman et al., 2014, Poth et al., 2011a, Poth et al., 2011b, Poth et al., 2013). Panitides L1-9 (linear peptides) were isolated from Poaceae (Nguyen et al., 2013). Violaceae seems to be the richest source of cyclotides with almost all the species investigated containing cyclotides unlike the Rubiaceae (Craik et al., 2012, Nguyen et al., 2012, Nguyen et al., 2013, Poth et al., 2011a, Pinto et al., 2012, He et al., 2011, Poth et al., 2012, Wang et al., 2008). It was reported that an estimate of the number of different cyclotides in the Violaceae could be about 5000-25,000, and proposed that cyclotides are ubiquitous among all Violaceae species (Burman et al., 2015). But this number was later proposed to be greater than 30000 with discovery of additional cyclotides *from Viola baoshanensis* (Zhang et al., 2015).The reason for the abundance of cyclotides in Violaceae is likely unknown. However, it could be probably because of adaptive measures of plants for protective and defensive mechanism naturally developed by violaceae to carry out their insecticidal and anthelminthic activities against insects, pests and nematodes which are likely more prevalent in geographical regions commonly found violaceae plants. Besides, violaceae are more common in temperate region than the tropical climate region. Therefore, it is likely that the enzyme (Butelase 1) which is responsible for backbone cyclization in the biosynthesis of cyclotides is favoured by temperate climate or cold region or might not withstand the relatively high climatic

temperature of the tropical region. Cyclotide-like genes and linear peptides have been found in Poaceae although there was no circular cyclotides identified in these plants (Burman et al., 2014, Nguyen et al., 2013).

1.4.9 Biological activities of cyclotides

The mechanism of action of cyclotides was reported to be the penetration of cell lipid bilayer membrane, preformation and destabilization through hydrophobic and phosphoethanolamin specific interaction (Wang et al., 2012).The presence of glutamic acid in loop 1 of the cyclotides improves stability and is essential for the membrane disrupting activity of cyclotides (Wang et al., 2012) .

Cyclotides exhibit a range of interesting bioactivities, including in vivo (rat model) uterotonic (Gran et al., 2000, Saether et al., 1995); and In vitro including anti-HIV (Gustafson et al., 2004), antimicrobial (Tam et al., 1999), cytotoxic (Hernandez et al., 2000, Lindholm et al., 2002, Svangard et al., 2004, Tang et al., 1999), hemolytic (Schoepke et al., 1993; Tang et al., 2010), neurotensin antagonistic (Witherup et al., 1994), insecticidal (Jennings et al., 2001), and trypsin inhibitory activities (Hernandez et al., 2000). Their natural function as plant defense agents was deduced from reports that cyclotides effectively inhibited the growth of two common cotton pests, *Helicoverpa punctigera* and *H. armigera*, when the larvae of these pests were fed with a cyclotide-containing diet (Jennings et al., 2005). Cycloviolacin VY1 from *Viola yedoensis* showed inhibition against influenza A H1N1 (Liu et al., 2014). Varv A, varv F, and cycloviolacin O2 showed potent activity in a panel of 10 different human tumor cell lines (Burman et al., 2014).

Anticancer activity of hedyotide B5 (HB5) to HB9 has been demonstrated (Ding et al., 2014). Cyclotides from *Citoria teratea* exerted anticancer and chemosensitizing activities in the lung cancer cell line A549 (Sen et al., 2013). Kalata B1, and kalata B2 caused antischistosome activity/anthelminthic effects against *Schistosoma japonicum* and *Schistosoma mansoni* (Malagón et al., 2013), Kalata (KB2) and Cycloviolacin O2 (CyO2) caused anti-staphylococcal activities (Fensterseifer et al., 2015). Cyclotides from *Hedyotis diffusa*, Diffusa cyclotide 1 to 3 (DC1-3) showed anticancer (activity in a cell growth assay or ability to cause cancer cell death) activities against prostate cancer cell lines. Cliotide (ctc13, ctc15, ctc17-ctc19, and ctc21-ctc53) exerted immunostimulating activity and antibacterial effect against Gram-negative bacteria (Nguyen et al., 2016). The vigno 5, a natural cyclic peptide from *Viola ignobilis*, induces apoptosis via the mitochondrial pathway in cervical cancer cells (Esmaeili et al., 2016).

A wide range of biological and pharmacological activities of cyclotides is listed in Table 1.1.

Table 1.1 In vitro biological activities of cyclotides.

Cyclotide	Plant source	Biological activity	Reference
MCoTI	*M. cochinchinensis*	Trypsin inhibitor	(Hallock et al., 2000)
MCoTII	*M. cochinchinensis*	Trypsin inhibitor	(Hallock et al., 2000)
Varv A	*V. tricolor, V. arvensis, and V. odorata*	Cytotoxic	Svangard et al. 2004; Lindodholm et al 2002.
Varv E	*V. tricolor*	Cytotoxic	Svangard et al. 2004; Lindodholm et al 2002
Varv B	*V. arvensis*	Cytotoxic	(Hernandez et al., 2000).
Varv C	*V. arvensis*	Cytotoxic	(Hernandez et al., 2000).
Varv D	*V. arvensis*	Cytotoxic	(Hernandez et al., 2000).
Varv E	*V. arvensis*	Cytotoxic	(Hernandez et al 2000)
Varv F	*V. arvensis*	Cytotoxic	(Hernandez et al., 2000, Lindodholm et al., 2002)
Varv G	*V. arvensis*	Cytotoxic	(Hernandez et al.,

			2000).
Varv H	*V. arvensis*	Cytotoxic	(Hernandez et al., 2000).
Cycloviolacin O2	*V. odorata*	Cytotoxic; Antibacterial against *Staphylococcal aureus*	(Svangard et al., 2004, Lindodholm et al., 2002, Fensterseifer et al., 2015, Pränting et al., 2010).
Vitri A	*V. tricolor*	Cytotoxic	(Goransson et al., 1999)
Kalata B2	*O. affinis* *H. punctigera* *H. armigera*	Insecticidal and antibacterial activity	(Jennings et al. 2005; Fensterseifer et al. 2015).
Kalata B1	*O. affinis*	Oxytocic activity	(Gran, 1973)
Cyclopay-chotride A	*P. longipes*	Antimicrobial activity	(Witherup et al., 1994)
Cycloviolacin O24	*Viola odorata*	Anti-HIV	(Ireland et al., 2008)
Cycloviolins A–D	*Leonia cymosa*	Anti-HIV	(Hallock et al., 2000)
Tricyclon A	*Viola tricolor*	Anti-HIV	(Mulvenna et al., 2005).

Circulins C	*C. parviflora*	Anti-HIV activity	(Shenkarev et al., 2006).
Circulins D	*C. parviflora*	Anti-HIV activity	(Shenkarev et al., 2006).
Circulins E	*C. parviflora*	Anti-HIV activity	(Shenkarev et al., 2006).
Circulins F	*C. parviflora*	Anti-HIV activity	(Shenkarev et al., 2006).
Palicourein	*P. condensata*	Anti-HIV activity	(Jennings et al, 2005)
Cycloviolin A-D	*L. cymosa*	Anti-HIV activity (2946.57)	(Jennings et al, 2001)
Cycloviolin A-D	*L. cymosa*	Anti-HIV activity (2910.33)	(Jennings et al. 2001)
Cycloviolin A-D	*L. cymosa*	Anti-HIV activity	(Jennings et al. 2001)
Palicourein	*P. condensata*	Anti-HIV activity	(Bokesch et al., 2001).
Cycloviolin A-D	*L. cymosa*	Anti-HIV activity	(Jennings et al. 2001)
Vhl-1	*V. hederaceae*	Anti-HIV activity	(Craik et al. 1999)
Cycloviolacin Y1	*V. yedoensis*	Anti-HIV activity	(Wang et al. 2008)
Cycloviolacin Y4	*V. yedoensis*	Anti-HIV activity	(Wang et al., 2008)

Cycloviolacin Y5	*V. yedoensis*	Anti-HIV activity	(Wang et al., 2008)
Cycloviolacin O3, O8, O14, O15, and O16	*V. odorata*	Anthelmintic activity	(Colgrave et al., 2008).
Cycloviolacin H4	*V. hederaceae*	Hemolytic activity	(Chen et al., 2005).
Cycloviolins A-D	*Leonia cymosa*	anti-HIV activity	(Hallock et al. 2000)
circulin A circulin B	*Chassalia parvifolia*	Antimicrobial and anti-HIV activities	(Tam et al., 1999)
Kalata B1	*O. offinis*	Uterotonic	(Gran, 1973)
cyclopsychotride A	*Psychotria longipes*	Neurotensin antagonist	(Witherup et al., 1994)
cycloviolacin VY1	*V. yedoensis (Violaceae)*	Anti-influenza A H1N1 virus	(Liu et al., 2014)
panitides L1-9,	*Panicum laxun* (Poaceae)	Cytotoxic against HeLa cells and antibacterial	(Nguyen et al., 2013)
hedyotide B5 - HB9	*Hedyotis biflora*	Cytotoxicity against pancreatic cancer cell lines.	(Ding et al., 2014).
kalata B1 / kalata B2	*O. offinis*	Antischistosome /anthelminthic activity	(Malagon et al., 2013)

cliotides	*Clitoria ternatea* (Fabaceae)	Gram-negative-specific antibacterial activity; anticancer and chemosensitizing activity against lung cancer cell line A549	(Nguyen et al., 2016; Sen et al., 2013)
Diffusa cyclotide 1 to 3 (DC1-3)	*Hedyotis diffusa*	Anti-prostate cancer activity	(Hu et al., 2015).
Cliotides: ctc13, ctc15, ctc17-ctc19, ctc21-ctc53	*Clitoria ternatae*	Antibacterial and immunostimulating activity.	(Nguyen et al., 2016)
vigno 5	*Viola ignobilis*	Anticancer cervical cancer activity	(Esmaeili et al., 2016)

The mechanism of action of cyclotides was reported to be the penetration of cell lipid bilayer membrane, preformation and destabilization through hydrophobic and phosphoethanolamin specific interaction (Wang et al., 2012). The presence of glutamic acid in loop 1 of the cyclotides improves stability and is essential for the membrane disrupting activity of cyclotides (Wang et al., 2012) .

The rapid kinetics and the broad spectrum of the toxic activities of cyclotides were likely due to their membrane disruption ability (Svanglard et al., 2007). Such activity was achieved by high affinity to the target membrane. This could be potentiated by the hydrophobic and electrostatic forces that drive adsorption of cyclotides toward the

lipid core and anionic surface of the target membranes (Burman et al., 2014). Reports showed that cyclotides were among the group of peptides with affinity for phosphatidylethanolamine (PE) membrane lipids, which was a characteristic feature among both subfamilies of cyclotides (Henriques et al., 2012).

1.4.10 Perspective and outlook

Foregoing data has demonstrated the potential for cyclotides to be used as anticancer therapeutics. The exceptional stability of cyclotides to heat, chemical and proteolytic degradation together with synthetic accessibility have bestowed them strong attraction for pharmaceutical, agrochemical industries as lead for drug discovery and as scaffolds in peptide–based drug design. For instance, linear peptides may have good potential features as drug lead but because they are prone to enzymatic and thermal cleavage and may have low bioavailability these could prevent their application as lead candidate in drug discovery and design by pharmaceutical industry. Cyclization of linear disulfide–rich peptides is a good strategy that has been adopted to enhance the stability of some potent but unstable peptides, to greatly improve their biopharmaceutical properties. The investigation of anti-ovarian cancer or other biological activities of cyclotides will be an interesting area to explore. Hence, there is increasing interest in exploring the plant kingdom to identify further cyclotides and more biological activities of this largest family of cyclized backbone of plant kingdom.

However, there have been some challenges in the study of cyclotides and the application of the cyclotides in preclinical or in vivo studies. Some of the challenges include the cyclic nature that hinders exposure of free N and C-terminus for easier sequence and characterization of cyclotides. Also, the low therapeutic index and

hemolytic features of some cyclotides could challenge more interest in further expansion and clinical application of cyclotides. Cyclotides tend to exert high toxicity or low therapeutic index hence not very much interest has been shown in clinical studies of cyclotides. All these could offer limitations to the exploration of research and interest in the cyclotides applications.

More so, in this study, there was limitation on the in vivo study of cyclotides in animal model due to financial challenges on high cost of animal studies, more facilities and limited time frame for PhD study.

1.5 Bisbenzylisoquinoline Alkaloids

Bisbenzylisoquinoline (BBIQ) alkaloids are among different large classes of alkaloids common in plant species. BBIQ alkaloids are prevalent in the families like Menispermeaceae, Annonaceae, Berberidaceae, Monimaiaceae and Ranunuclaceae (Angerhofer et al., 1999, Schiff, 1997, Schiff et al., 1979).

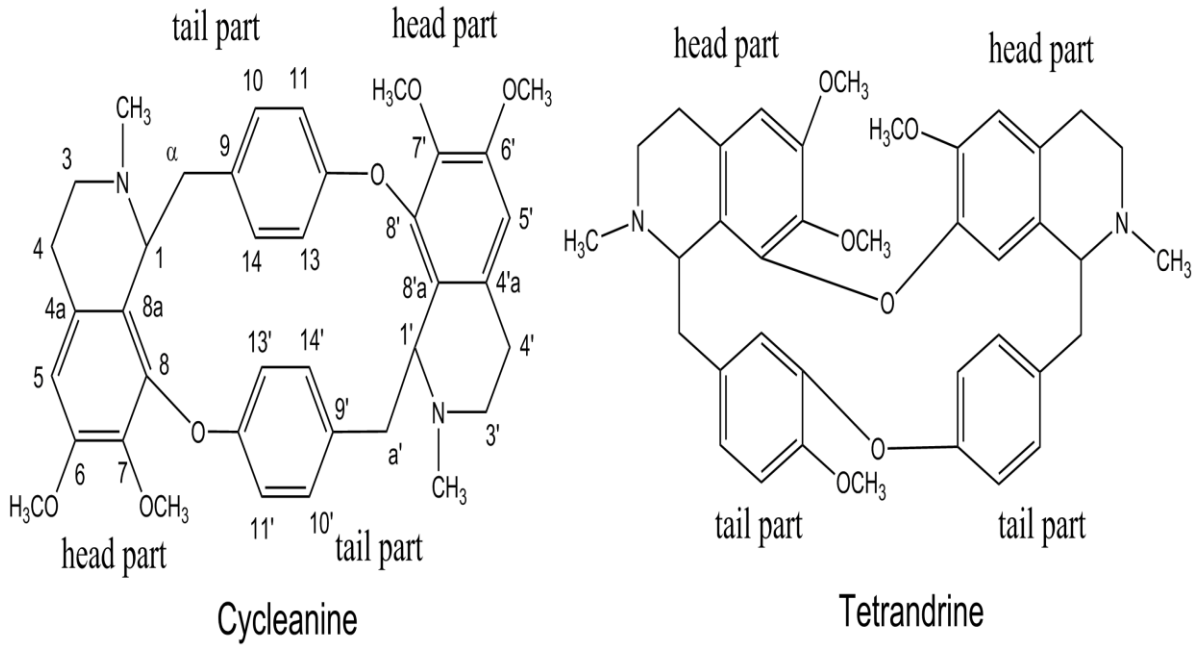

Figure 1.8 Chemical structures of cycleanine and tetrandrine: two typical examples of BBIQ alkaloids.

The BBIQ alkaloids are made up of two isoquinolines (‘head part’) linked to two benzyl moieties (‘tail part’) through two types of linkage such as head-to-tail (e.g. cycleanine) and head-to-head (e.g. tetrandrine). The majority of BBIQ alkaloids are produced by combination of two coclaurine units (biscoclaurines), a fewer number by combination of coclaurine and reticuline units (coclaurine-reticulines) and in some by

condensation of two moieties of reticuline (bisreticulines) (Angerhofer et al., 1999, Schiff, 1997, Schiff et al., 1979). The two moieties could often be largely joined by one or more diaryl ether bridge or occasionally by carbon bridges or methylene-oxy bridge (Angerhofer et al., 1999). The BBIQ alkaloids are therefore grouped based on the nature, the number and location where the bridge is attached.

Previous reviews on structure, spectra characteristics and botanical structures of BBIQ alkaloids have been reported (Guha et al., 1979, Schiff, 1997) . The differences in the chemical structures of BBIQ alkaloids are reported to be responsible for their varied pharmacological or biological activities (Angerhofer et al., 1999). Many of the plants that contain BBIQ alkaloids have been reported to exhibit history of medicinal applications traditionally, in treatment of various diseases such as malaria, cancer, amoebic dysentery, leishmaniasis, and bacterial infection (Likhitwitayawuid et al., 1993, Marshall et al., 1994, Angerhofer et al., 1999). The BBIQ alkaloids were reported to exhibit varied biological and pharmacological activities including cytotoxicity (Likhitwitayawuid et al., 1993), antimalarial (Angerhofer et al., 1999, Marshall et al., 1994, Ye & Van Dyke, 2016) anticancer activities (Sun & Wink, 2014, Wang et al., 2010), inhibition of histamine release (Nakamura et al., 1992), anti-leishmanial and anti-trypanosomal effects (Camacho et al., 2002).

Here, BBIQ alkaloids which have been reported to exert anticancer or antimalarial activities are listed or discussed. Lists of BBIQ alkaloids reported in the Web of Science from 1990 to 2016, to exert potent *in vitro* or *in vivo* anti-cancer or antimalarial activity (IC_{50} < 20 µM) are compiled (Table 1.4).

Tetrandrine and Fangchinoline

Previous reports have shown that Tetrandrine (**1**), fangchinoline (**5**) and tricordatine (**36**) (Table 1.4) were the only BBIQ reported in *Triclisia subcordata* to the best of our

knowledge (Tackie et al., 1974; Dwuma-Badu et al.,1975; Guha et al., 1979; Uche et al., 2016) . Tetrandrine (**1**) and fangchinoline were also isolated from the dried root of *Stephenia tetrandra* S Moore (Xu et al., 2011, Xiao et al., 2015, Wu et al., 2014, Schiff, 1997, Lin et al., 1993, Li et al., 2015) and other botanical sources (Table 1.4) (Schiff, 1997). Tetrandrine and fangchinoline exhibited in vitro pharmacological actions, including in vitro anti-cancer (Li et al., 2015, He et al., 2011b) and antimalarial activities (Marshall et al., 1994, Lin et al., 1993, Chea et al., 2010, Angerhofer et al., 1999, Ye & Van Dyke, 2016). They have been reported to cause in vitro inhibition of proliferation, and induced apoptosis of hepatoma, breast cancer and leukaemia cells (Sun & Wink, 2014, Chen et al., 2010, He et al., 2011b, Chen et al., 2009, Deng et al., 2015). Li et al showed that, in vitro antiproliferative effects of Fangchinoline on human prostate cancer cells could be due to its contributed by its suppression on of the proteasome β1 subunit (Li et al., 2015b).

Report from an in vitro study has shown that BBIQ alkaloids, such as tetrandrine could have clinical applications in China for treatment of diseases like lung cancer, leukaemia and amoebic dysentery (Mashall et al., 1994). Evidence showed that tetrandrine could suppress metastatic phenotype of prostatic cancer (Kou et al., 2016), induce apoptosis of colon cancer and inhibition of xenograft tumour growth by inhibition of Wnt-β-catenin signalling (He at al., 2011). Tetrandrine potentiated activity of the anti-cancer drugs like daunorubicin, vinblastine, doxorubicin in the P-glycoprotein (P-gp) expressing multi-drug resistance (MDR) cell line (Liu et al., 2013, Liu et al., 2000, Liu et al., 2015). Tetrandrine was reported to exert radio-sensitization effects, MDR reversal and anti-proliferation effects on the malignant brain tumour (gliomas) (Chen et al., 2010).

In one study, tetrandrine reduced the paclitaxel concentration required to achieve 50% inhibition of cell growth to HCT15 (P-gP-positive) cells about 3100-fold, while did not affect the accumulation and residual rate of rhodamine 123 in SK-OV-3 (P-gp-negative) cells (Yu-Jen, 2002, Li et al., 2015) . Therefore, tetrandrine was concluded to enhance the cytotoxicity of drugs via modulation of P-gP in the resistant cancer cells (Yu-Jen, 2002, Li et al., 2015). Tetrandrine could also increase growth suppression and apoptosis induced by cisplatin and cause redistribution of the cell cycle in ovarian cancer cells (Yu-Jen, 2002, Li et al., 2015). *In vivo* tetrandrine and cisplatin exhibited synergistic and growth inhibition effects, which supported the application of tetrandrine as an adjunct to cisplatin in the chemotherapy of ovarian cancer (Zhang et al., 2011). Tetrandrine in combination with doxorubicin showed a significant synergistic effect in multidrug resistant Caco-2 and CEM/ADR5000 cancer cells. It could also reverse the multidrug resistance by reducing the expression of P-glycoprotein (Sun & Wink, 2014, Liu et al., 2015) Tetrandrine has been demonstrated to exert potent antimalarial activities as well as synergism with chloroquine in both chloroquine sensitive and resistant strains of falciparum malaria (*Plasmodium falciparum*) with little toxicity (Ye & Van Dyke, 2016).

Ye and Van Dyke also demonstrated the in vitro antimalarial activities and the combination therapy of other BBIQ alkaloids like isotetrandrine (**2**), phaeanthine (**3**), pycynamine (**4**), fangchinoline (**5**), berbamine (**6**), obamegine (**7**), cycleanine (**8**), cepharanthine (**10**), methoxyadiantifolin (**11**), and thalicarpine (**12**) with respect to their IC_{50} and as ratio of chloroquine (CQ) sensitive to CQ resistant strain of *P. falciparum* respectively as shown (Table 1.4). The link between the ether bridges in the bisbenzylisoquinoline probably had essential contribution in the antimalarial function of BBIQ alkaloids (Ye and Van Dyke, 2015). Cepharanthine (**10**),

stephilababerine (**19**), Obaberine (**20**), daphnandrine (**21**), norobaberine (**22**), 2–norethalrugosine (**34**), and 2–norcepharanthine (**23**) all from tubers of *Stephania erecta* Craib (Menispermaceae) were reported to exert antimalarial and non-selective cytotoxicity (Likhitwitaywuid et al., 1993).

Reports have also shown the multidrug resistant (MDR) proteins in both cancer and malaria exhibit similar genetic sequence (Ye and Van Dyke, 2015). It was reported that decrease in the lipophilicity of BBIQ alkaloids could lead to decrease in cytotoxicity and anti-plasmodial activity due to alteration in cell membrane permeability (Angerhofer et al., 1997). The pharmacological activity of BBIQ alkaloids was demonstrated to be affected by their configurations and type of aromatic substituents present in the BBIQ alkaloids (Angerhofer et al., 1997). Since most of antimalarial and anticancer BBIQ alkaloids bind to MDR pump to elicit their effects, it is more likely that water soluble BBIQ alkaloids could exert more potent antimalarial and anticancer activities against MDR strains than the fat-soluble ones (Ye and Van Dyke, 2015). Penduline (**71**) was also shown to exert antiplasmodial effect (Valentin et al., 1997).

Angerhofer et al reported the antimalarial effects of 53 BBIQ on both chloroquine sensitive (D6) and resistant strains (W2) (Table 1.4 Compound **1** - **53**). This report revealed the IC_{50} of the 53 BBIQ to be in range of 29 – 1530 nM for the chloroquine sensitive D6 and 59 strains and greater than 16400 nM in the resistant W2 strain (Table 1. 4) (Angerhofer et al., 1999, Marshall et al., 1994, Likhitwitayawuid et al., 1993, Kaur et al., 2009, Saxena et al., 2003). The compounds with most antimalarial selectivity among the 53 BBIQ reported included cycleanine (**8**), tecmuconine (**14**), malekulatine (**15**), and repandine (**24**) (Angerhofer et al., 1999; Kaur et al., 2009). Mashall et al reported the antimalarial activities of 24 BBIQ on chloroquine resistant

strain of *P. falciparum* (Table 1.4; Compound (**55-69**)). Among the 24 BBIQ the range of IC_{50} of antimalarial agent was found to be 0.1 – 89 µM for thalisopidine (**58**) and cocsuline (**64**) (Table 1.4) (Mashall et al., 1994). Antimalarial activity of some other BBIQ alkaloids have also been reported, such as curine (**43**) (IC_{50} = 353 nM) and isochondodendrine (**63**) (IC_{50} = 892 nM) from the bark of *Isolona ghesquiereina* (Mambu et al., 2000, Kaur et al., 2009), Penduline (**71)** (2.8 µM) (Valentin et al., 1997), rodiasine (**72**) (1.1 µM) (Roumy et al., 2007, Kaur et al., 2009), norcepharanthine, cepharanoline and fangchinoline (0.2 - 0.3 µM) (Chea et al., 2010). Costaricine (**18**) was demonstrated to be the most bioactive antiplasmodial BBIQ alkaloids among the 16 isolated from *Nectandra sacicfolia* (H.B.K) Nees (Lauraceae) with IC_{50} of 50 ng/ml (the chloroquine-sensitive D6) and 294 ng/ml (the chloroquine-resistant W2) (Böhlke et al., 1996).Cepharanthine (**10**) was among the BBIQ alkaloids shown to be active against malarial parasites (Angerhofer et al., 1999).

Stebisimine (**73**), puetogaline B (**74**) ,1,2-dehydrotelobine (**75**), and 2′-norcocsuline (**40**), and isolated from *Anisocycla grandidieri* Baill. (Menispermaceae) were reported to exert antiproliferative activity against cancer cell lines including ovarian, breast and hepatocellular carcinoma (Liu et al., 2013). Marshall et al demonstrated the antiplasmodial activity and cytotoxicity of 16 BBIQ (Table 1.4; **5-7**, **55**, **56**, **60-69**). Berbamine (**6**), obamegine and thalisopidine (**59**) showed very potent antiplasmodial activity relative to other BBIQ alkaloids, with IC_{50} less than 1 µM. Berbamine (**6**) also exerted the highest cytotoxicity. Cyleapeltine (**15**), homoaromaline (**27**), limacine (**28**), and tharugosine (**29**) all from *Cyclea barbata* (Wall) (Menispermaceae) were reported to exhibit cytotoxicity and antimalarial activities (Lin et al., 1993).

Table 1.2 List of antimalarial BBIQ alkaloids with IC_{50} on *P falciparum* CQ-sensitive and resistant strains.

Antimalarial BBIQ, Compound number and / botanical source(s) (family)	Chemical Structures	IC_{50} (µM)		References
		D6	W2	
Tetrandrine (1) *Stephania tetrandra* S. Moore; *Cocculus pendulus; Cyclea barbata; Cyclea burmanni; Pachygone dasycarpa,* (Menispermaceae)	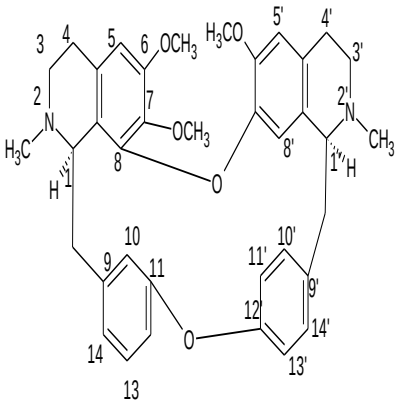 Tetrandrine S, S Isotetrandrine R, S Phaeanthine R, R	0.2-2.9	0.2-1.2	Ye and VanDyke, 2015, Angerhofer et al., 1999; Lin et al. 1993.
Isotetrandrine (2) *Stephania erecta*. Cocculus pendulus, *Stephania cepharantha* (Menispermaceae) *Berberis heteropoda. B. koreana, B. nummularia B. valdiviana* (Berberidaceae)		0.3 - 4.8	0.1 - 1.4	Ye and VanDyke, 2015, Angerhofer et al. 1999, Marshal et al.1994, Schiff, 1997.
Phaeanthine (3) *Phaenthus Ebractedatis* Cyclea burmann, *Phaeanthus crassipetalus* (Menispermaceae).		0.3 - 6.0	0.5-5.0	Ye and Van Dyke, 2015; Angerhofer et al., 1999 Marshal et al., 1994.
Pycnamine (4) *Pycnarrhena manillensis* Vidal		0.8 - 3.8	0.8 - 4.2	Ye and Van Dyke, 2015; Marshal et al.1994
Fangchinoline (5) *Stephania rotunda* Lour., *S. tetrandra* Radix *Pachgona dasycarpa*, *Strychnopsis thourasil* (Menispermacaea).		-	0.3 - 2.2	Ye and Van Dyke, 2015, Desgrouas et al. 2014, Chea et al., 2010, Angerhofer et

	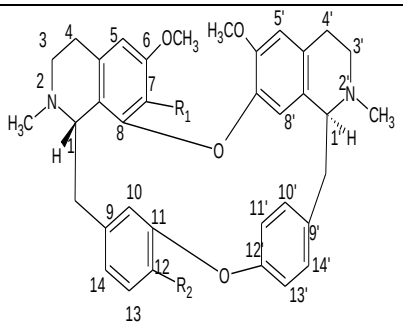			al., 1999, Marshal et al. 1994, Schiff. 1997
Berbamine (6) *Berberis aggregata (Berberidaceae), Cyclea barbata, Stephena cepharantha* (Menispermaceae)	 R1 R2 Pycnamine R, R OCH_3 OH Fangchinoline S, S OH OCH_3 Berbamine R, S OCH_3 OH	0.1-4.6	0.3-1.9	Ye and Van Dyke, 2015; Angerhofer et al., 1999; Marshal et al. 1994, Schiff 1997.
Obamegine (7) *Stephania cepharantha Hayata* (Menispermacaea).	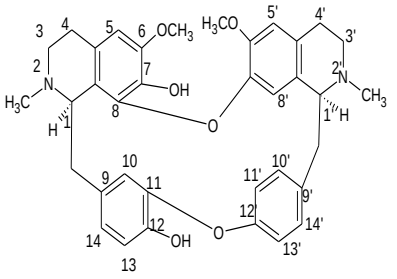 Obamegine R, S	0.4 - 6.6	0.5-4.8	Ye and Dyke, 2015, Angerhofer et al. 1999, Marshal et al. 1994, Schiff, 1997.
Cycleanine (8) *Stephania cepharantha* Hayata (Menispermaceae)	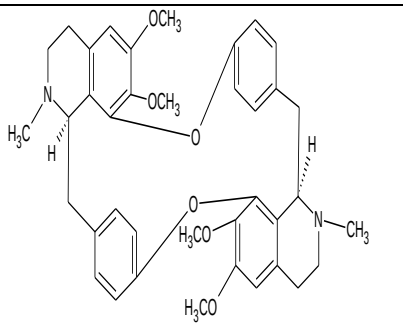 Cycleanine R, R	7.0	9.7	Ye and Van Dyke, 2015, Angerhofer et al., 1999.

Hernandezine (9) *Cocculus pendulus* (Menispermaceae) Thalictrum flavun L (Ranunculaceae)	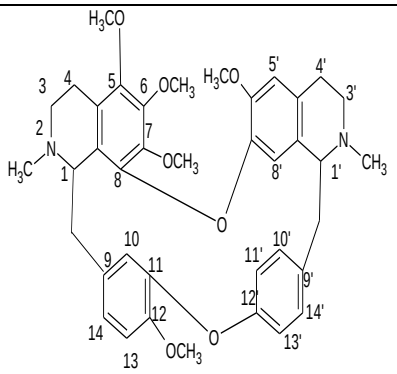 Hernandezine S, S	3.7	1.3	Ye and Van Dyke, 2015, Schiff, 1997.
Cepharanthine (10) *Stephania cepharantha Hayata* *Stephania erecta* Criab (Menispermaceae)	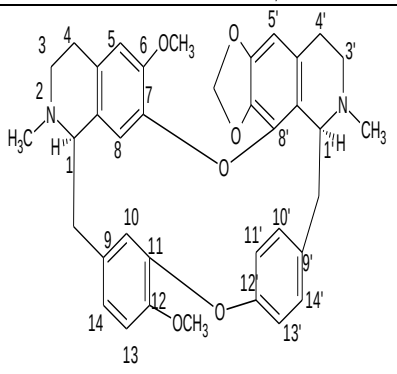 Cepharanthine R, S	0.2 - 17	1.2-13 0.5 – 1.3	Ye and Van Dyke 2015; Angerhofer et al. 1999, Likhitwitayawuid et al.,1993; Saxena et al., 2003
Methyoxyadiantifoline (**11)**	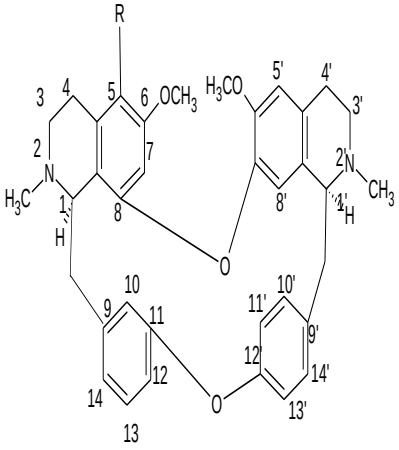 Methoxyadianthifoline S, S R = OCH_3 Thalicarpine S, S R = H	32	42	Ye and Van Dyke, 2015
Thalicarpine (12) *Thalictrum dasycarpum* Fish & Lall (Rannuclaceae)		10	9.4	Ye and Van Dyke, 2015

Antimalarial BBIQ alkaloids	**Chemical structure**	**IC_{50} (µM)**		**References**
		D6	**W2**	
Neothalibrine **(13)** Thalictrum revolutum DC.	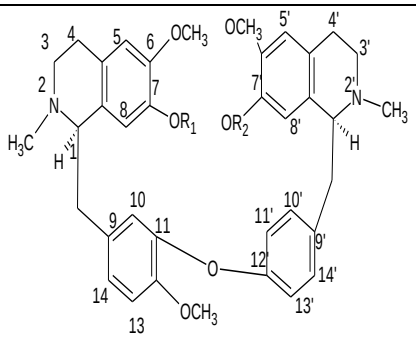 R1 R 2 Neothalibrine S, S H CH_3 Temuconine R, S CH_3 H	0.047	0.215	Angerhofer et al.,1999
Temuconine **(14)** *Aristolochia elegans* (Aristolochiaceae)		0.213	0.227	Angerhofer et al.,1999
Malekulatine **(15**) *Hernandia Sonora L* (Hernandiaceae)	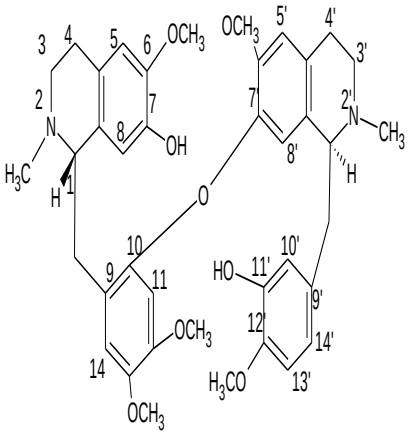 Malekulatine R, S	0.061	0.164	Angerhofer et al., 1999 Schiff ,1997
Cycleapeltine (**16**) Cyclea barbata (Wall) Miers (Menispermaceae)	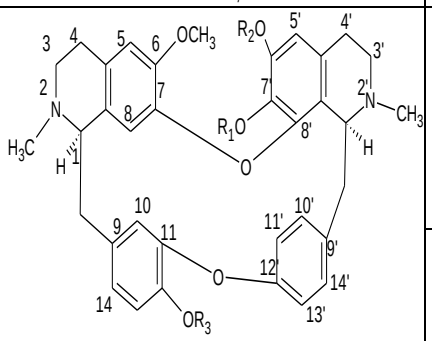 R1 R 2 R 3 Cycleapeltine S, S H CH_3 CH_3 limacusine R , R H CH_3 CH_3	0.048	0.067	Angerhofer et al.,1999
Limacusine **(17)** *Anisocycla jollyana* (Menispermaceae)		0.064	0.192	Angerhofer et al., 1999

Costaricine **(18)** *Nectandra sacicfolia* (H.B.K) Nees (Lauraceae)	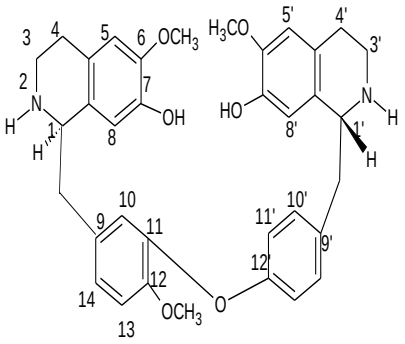 Costaricine	0.050	0.294	Bohlke et al., 1996
Stephibaberine (**19**) *Stephania erecta* (Menispermaceae).	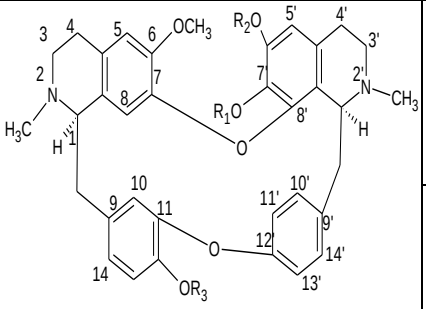	0.214	0.510	Angerhofer et al.,1999 Likhitwitaywuid et al., 1993
Obaberine **(20)** *Berberis heterobotrys* (Berberidaceae) *Stephenia erecta Craib* (Menispermaceae)		0.371	0.341	Angerhofer et al.,1999 Schiff, 1997
Daphnandrine **(21)** *Stephania erecta Craib*. (menispermaceae)	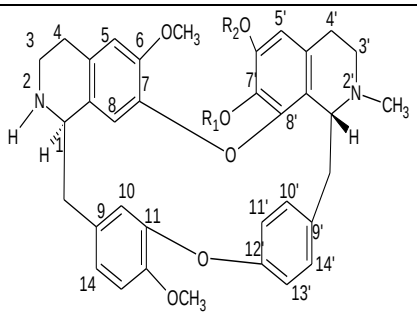	0.106	0.375	Angerhofer et al.,1999 Schiff, 1997
2-norobaberine **(22)** *Stephania erecta Craib*. (menispermaceae)		0.075	0.154	Angerhofer et al.1999; Schiff, 1997
2-norcepharanthine **(23)** *Stephania totunda* Lour. (Menispermacaea*)*		0.079	0.219 0.300	Angerhofer et al.,1999; Chea et al., 2010; (Desgrouas et al., 2014).
Repandine **(24)**				Angerhofer et

Cyclea barbata (Menispermacaea)	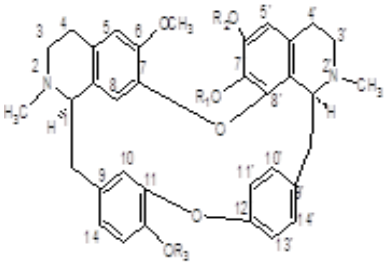	0.042	0.067	al.1999; Schiff ,1997
Candicusine **(25**) *Curarea candicans* Barneby & Kurkoff (Menispermaceae)	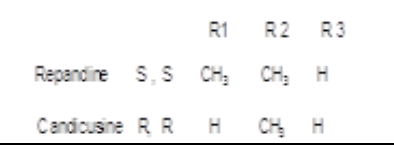 R1 R2 R3 Repandine S , S CH_3 CH_3 H Candicusine R, R H CH_3 H	0.029	0.105	Angerhofer et al.,1999
Aromoline **(26)** *Berberis heteropoda* (berberidacaea) *Stepehania cepharantha* Hayata (Menispermaceae)	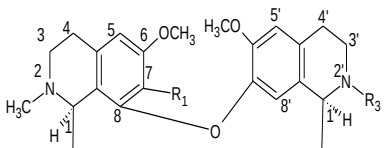	0.446	1.4	Angerhofer et al.,1999; Marshall et al. 1994 Schiff 1997
Homoaromaline **(27**) *Cyclea barbata* (Wall) Miers *Anisocycla jollyana(Pierre)* Diels (Menispermaceae)	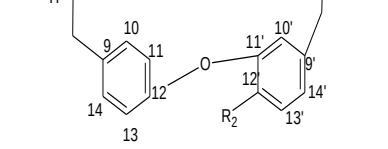 R_1 R_2 R_3 Aromaline R, S OH OH CH_3 Homoaromaline R, S OH OCH 3 CH_3	0.173 0.232	0.474 ; 0.451	Angerhofer et al.1999; Marshall et al. 1994; Lin et al., 1993; Schiff, 1997
Limacine **(28)** *Spirospermum penduliforum* Thou *Phaeanthus crassipetalus Becc (Menispermaceae)*	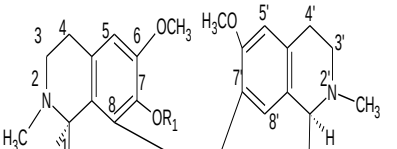	8653	263164	Angerhofer et al.,1999; Lin et al.., 1993
Thalrugosine **(29)** *Cyclea barbata, Stephenia erecta* (Menispermaceae)	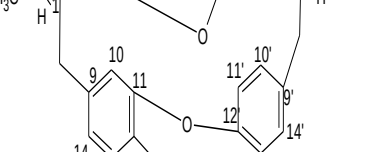 R1 R 2 Limacine R, R H CH 3 Thalrugosine R, S H CH 3	0.199; 0.065	0.374 ; 0.078	Angerhofer et al.,1999; Lin et al.., 1993
Atherospermoline **(30)** *Pachygone dasycarpa*	Artherospermoline S, S H H	0.232	0.623	Angerhofer et al.1999

N-methyl-7-O-desmethylpeinamine (**31**) *Pachygone dasycarpa*	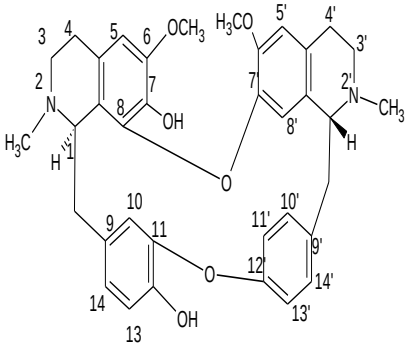 N-methyl -7- O-desmethylpeinamine S, R	0.134	0.609	Angerhofer et al.1999
2-Norberbamine **(32)** *Pycnarrhena ozantha* Diels (Menispermaceae)	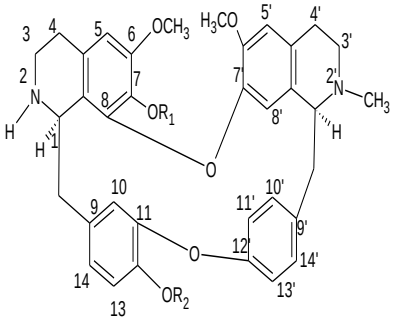 R1 R 2 2 - norberbamine S,S CH_3 H 2 - northalrugosine S, S H CH_3	0.047	0.193	Angerhofer et al.1999
2-norisotetrandrine **(33)**		0.106	0.728	Angerhofer et al.1999
2-northalrugosine **(34)** *Pycnarrhena ozantha Diels* (Menispermaceae)		0.115	0.21	Angerhofer et al.,1999
Tricordatine **(36)** *Pachygone dasycarpa* (Menispermaceae)	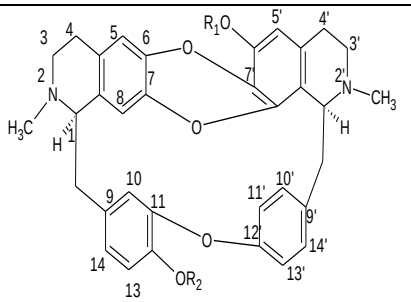 R1 R 2 Tricordatine S, R H H 12 -O - methyltricordatine S, R H CH_3 N - methyltelobine S, R CH_3 CH_3	0.09	0.259	Angerhofer et al.1999, Schiff, 1997
12-O-methyltricordatine **(37)** *Pachygone dasycarpa*		0.03	0.112	Angerhofer et al.1999
N-methyltelobine **(38)**		0.169	0.451	Angerhofer et al.1999

Cepharanoline (**39**) *Stephania rotunda Lour*. (Menispermacaea)	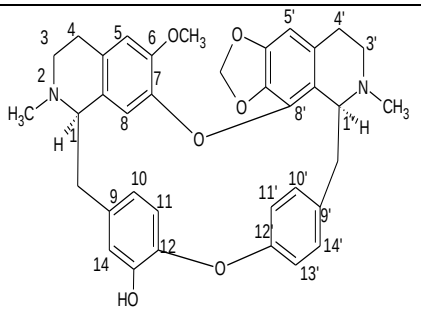 Cepharanoline	0.2	-	Chea et al., 2010; Desgrouas et al. 2014
2′-Norcocsuline (**40**) *Pachygone dasycarpa* (Menispermaceae)	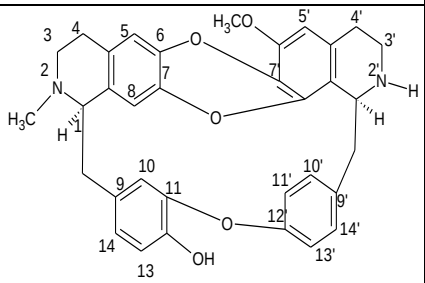 2' - norcocsuline	0.48	0.281	Angerhofer et al.,1999
1,2-dehydrotelobine (**41**) *Anisocycla Jillana* (Pierre) Diels (Menispermaceae)	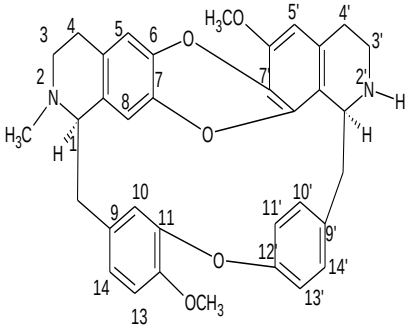 1, 2 - dehydrotelobine	0.554	0.464	Angerhofer et al.1999; Schiff, 1997

Antimalarial BBIQ alkaloids	Chemical structure	IC_{50} (µM)		References
		D6	W2	
Thalmirabine (**42**) *Thalictrum foetidum Thalictum minus* (Ranunculaceae)	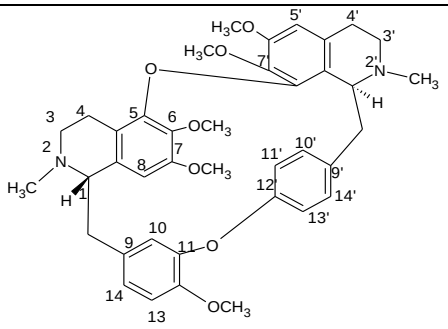 Thalmirabine	0.224	0.110	Angerhofer et al.,1999
(-)-curine (**43**) *Cissampelos muccronata, Cyclea barbata, Stephania epigeae* (Menispermacaea)	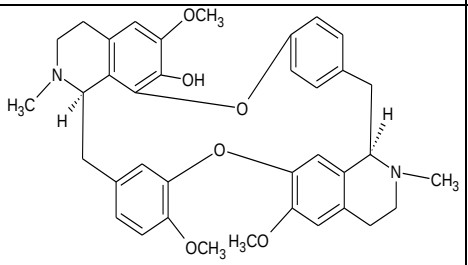 Curine	0.128	0.387; 0.353	Angerhofer et al.,1999; Mambu et al., 2000, Kaur et al., 2009 Schiff, 1997
(+)-2′-norcuricycline **(44)**	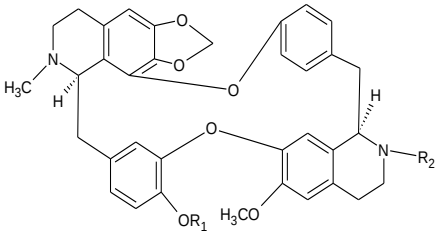 R1 R 2 2'- norcuricycline R, S CH_3 H 2' - norisocuricycline R , R CH_3 H Curicycleatjenine S, R CH_3 $COCH_3$ Isocuricycleatjine R. R H $COCH_3$ Isocuricycleatjenine R, R CH_3 $COCH_3$	0.53	0.676	Angerhofer et al.,1999
2′-norisocuricycline **(45)**		1.27	0.662	Angerhofer et al.,1999
curicycleatjenine **(46)** *Cyclea* atjehensis Forman (Menispermaceae)		2.32	1.20	Angerhofer et al., 1999
Isocuricycleatjine **(47)** *Cyclea atjehensis* Forman (Menispermaceae)		6.89	4.03	Angerhofer et al., 1999
Isocuricycleatjenine **(48**) *Cyclea atjehensis* Forman (Menispermaceae)		0.6	1.05	Angerhofer et al.,1999

Isocuricycleatjehimine **(49)** *Cyclea atjehensis* Forman (Menispermaceae)	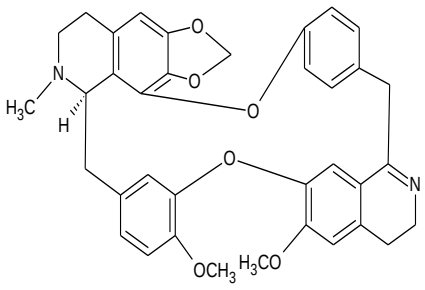 Isocuricycleatjehimine	4.98	2.10	Angerhofer et al.,1999
Cycleatjehenine **(50)** *Cyclea atjehensis* Forman (Menispermaceae)	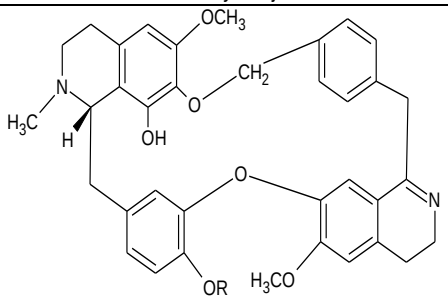 Cycleatjehinine R = CH_3 Cycleatjehine R = H	0.115	0.066	Angerhofer et al.,1999
Cycleatjehine **(51)** *Cyclea atjehensis* Forman (Menispermaceae)		0.11	0.059	Angerhofer et al.,1999
3′,4′-dihydrocycleatjehenine **(52)** *Cyclea atjehensis* Forman (Menispermaceae)	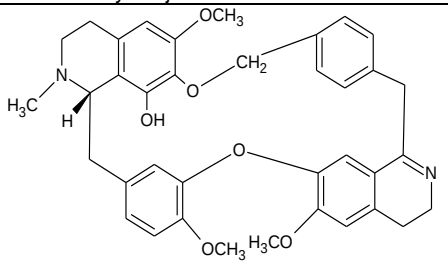 3', 4'-dihydrocycleatjehenine	0.346	0.169	Angerhofer et al.,1999
2′-noratjecycline **(53)** *Cyclea atjehensis* Forman (Menispermaceae)	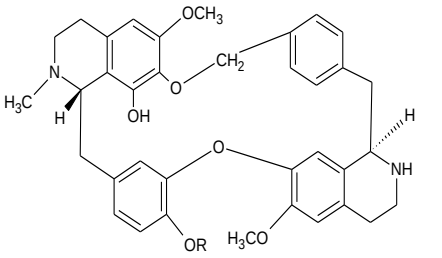 2' - noratjecycline R = H N - acetyl¨2'-noratjeecycline R = $COCH_3$	0.348	0.199	Angerhofer et al.,1999
N-acetyl-2′-noratjecycline **(54)** *Cyclea atjehensis* Forman (Menispermaceae)		1.03	0.605	Angerhofer et al.,1999
Funiferine **(55)** *Guatteria boliviana* (Annonaceae)		-	0.6	Marshall et al., 1994

Tiliageine **(56)** *Guatteria boliviana* (Annonaceae)	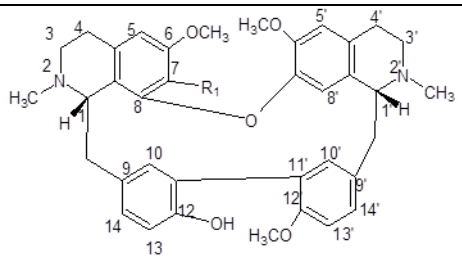 Funiferine S, R R1 = OCH_3 Tiliageine S, R R1 = OH	-	6.3	Marshall et al., 1994
Daphnoline **(57)** *Pachygone dasycarpa* (Menispermaceae)	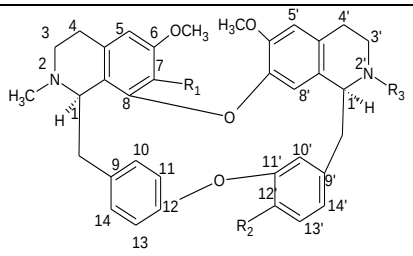	-	1.0	Marshall et al., 1994
Oxyacanthine HCl **(58)** Berberi spp *Berberis amurensis* (Berberidaceae)	R_1 R_2 R_3 Daphnoline R, S OH OH H Oxyacanithine R, S OCH_3 OH CH_3	-	1.1	Marshall et al., 1994, Angerhofer et al.1999; Lin et al., 1993; Schiff, 1997
Thalisopidine **(59)** *Triclisia patens* (Menispermaceae)	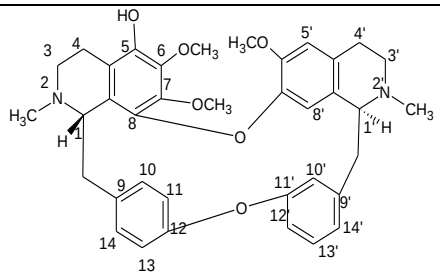 Thalisopidine S, S	-	0.1	Marshall et al., 1994, Marshall et al., 1994, Camacho et al., 2002
Tetrandrine methiodide **(60)**	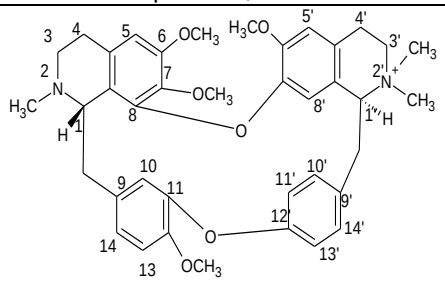 Tetrandrine methiodide S, S	-	>0.065	Marshall et al. 1994.

Dinklacorine **(61)** Tiliacora dinklagei Engl (Menispermaceae)	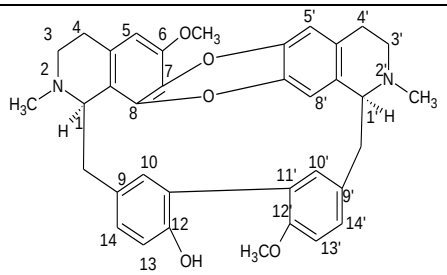 Dinklacorine R, S	-	3.9	Marshall et al., 1994
Trigilletimine **(63)** *Triclisia gilletii* (De Wild.) Staner and T. patens Oilv., (Menispermaceae)	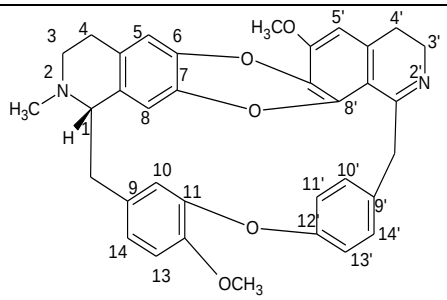 Trigilletimine	-	42	Marshall et al., 1994
Cocsoline **(64)** *Cocculus pendulus* (Menispermaceae)	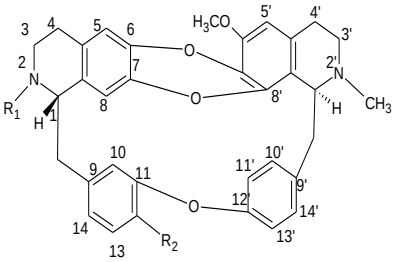 R 1 R 2 Cocsoline S, S H CH Cocsuline S, S CH_3 OH Isotrilobine S, S CH_3 OCH_3	-	1.2	Marshall et al., 1994
Cocsuline **(65)** *Cocculus pendulus* (Menispermaceae)		-	0.5	Angerhofer et al., 1999
Isotrilobine **(66)** Anisocycla jollyana (Menispermaceae)		-	2.1	Marshall et al., 1994
Cocsuline methiodide **(67)**		-	>18	Marshall et al., 1994
Gilletine **(68)** *Stephania cepharantha* Hayata (Menispermacaea) .	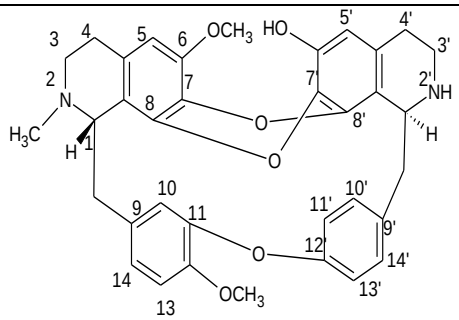 Gilletine S, R	-	1.8	Marshall et al., 1994

Insularine **(69)** *Cissampelos insularis* Makino, *C. ochiaiana* Yamamoto (Menispermaceae)	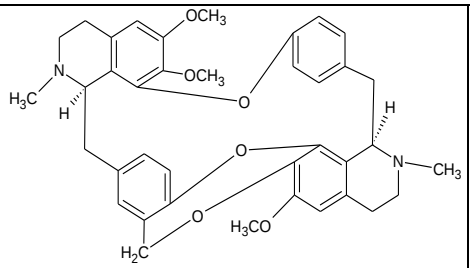 Insularine R, R	-	2.1	Marshall et al., 1994
Cepharanoline (**70**) *Stephania rotunda Lour*. (Menispermacaea*)*	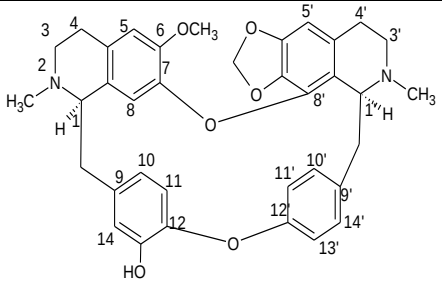 Cepharanoline	-	0.2	Chea et al. 2010; Desgrouas et al., 2014
Penduline **(71)** *Isopyrum thalictroides* (Ranunculaceae)	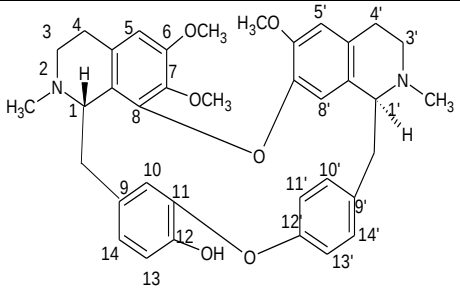 Penduline	-	2.8	Valentin et al., 1997
Rodiasine (**72**) *Pseuoxandra cuspidata* (Annonaceae).	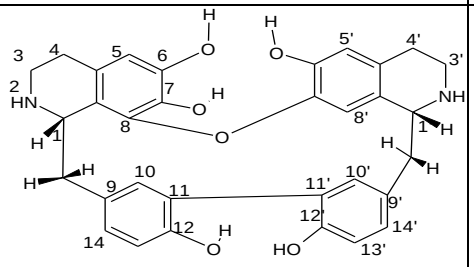 Rodiasine S, R	-	1.140	Roumy et al., 2006; Kaur et al., 2009

D6 and W2 represent CQ-sensitive and resistant strains of *P. falciparum*, respectively.

Table 1.3 List of anticancer BBIQ alkaloids.

Anticancer BBIQ alkaloids/botanical source	**chemical structure**	**Cell lines**	**IC_{50} (μM)**	**Reference**
Tetrandrine (1) Stephania tetrandra	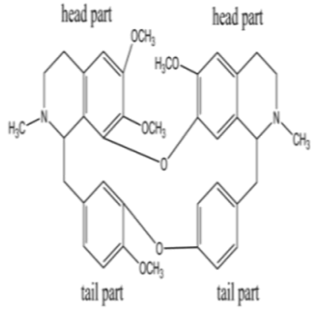 Tetrandrine	HelaG2 Hepatocellular carcinoma cells Huh7, U251, HCT116 and A549 cells	9.0	Likhitwitaywuid et al., 1993 (Likhitwitaywuid et al., 1993a, Mei et al., 2015)
Cycleanine (8) *Triclisia subcordata*	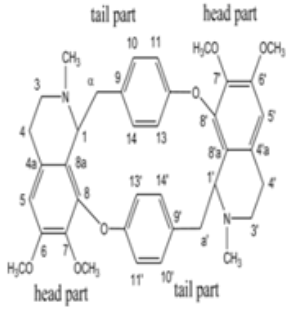 Cycleanine	Ovcar-8	7.4	Uche et al., 2016
Stebisimine (73) *Anisocycla grandidieri* Baill (Menispermaceae)	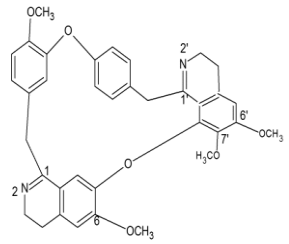 Stebisimine	A2780 H460 MCF-7 UACC-257	>10	Liu et al., 2013

Puetogaline B (74) *Anisocycla grandidieri* Baill (Menispermaceae)	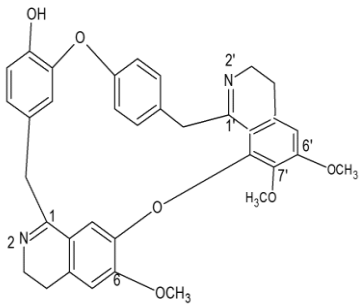 Puetogaline B	A2780 H460 MCF-7 UACC-257	>10	Liu et al., 2013
1,2-dehydrotelobine **(75)** *Anisocycla grandidieri* Baill (Menispermaceae)	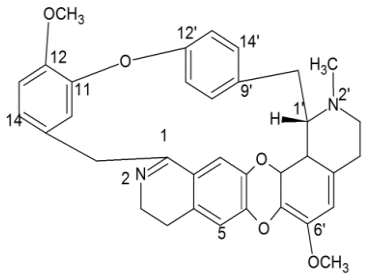 1, 2 - Dehydrotelobine	A2780 H460 MCF-7 UACC-257	1.1 – 6.3	Liu et al., 2013
2'-norcocsuline (40) *Anisocycla grandidieri* Baill (Menispermaceae)	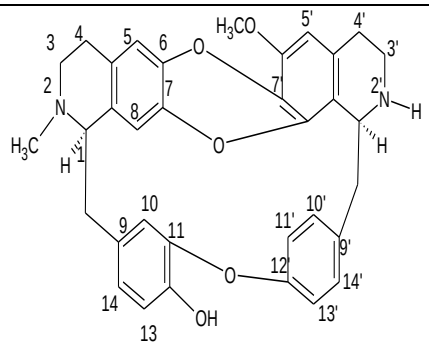 2' - norcocsuline	A2780 H460 MCF-7 UACC-257	2.2 – 4.2	Liu et al., 2013
Isoliensinine (77) *Nelumbo nucifera* Gaertn. (Nymphaeaceae)	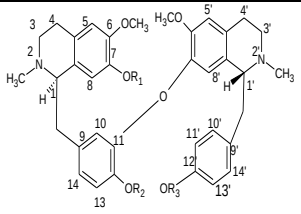	breast cancer cells MDA-MB-231cells	18.3	Zhang et al., 2015 Paudel and Panth, 2015
liensinine (78) *Nelumbo nucifera Gaertn.* (*Nymphaeaceae*	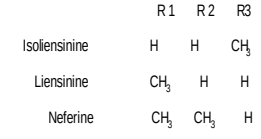 R1 R2 R3 Isoliensinine H H CH_3 Liensinine CH_3 H H Neferine CH_3 CH_3 H	breast cancer cells MDA-MB-	>18	Zhang et al., 2015 Paudel and

)		231		Panth, 2015
Neferine (79) *Nelumbo* nucifera Gaertn. (Nymphaeaceae)		breast cancer cells MDA-MB-231cells lung cancer cells Hepatocellular carcinoma HCC Hep3B cells	>18	Zhang et al., 2015, Yoon et al., 2013, Paudel & Panth, 2015, Poornima et al., 2014
Fangchinoline (5)		Prostate PC-3 cells and LnCap cells	-	Li et al., 2015
Cepharanthine (10) *Stephania epigeae* (Menispermaceae)	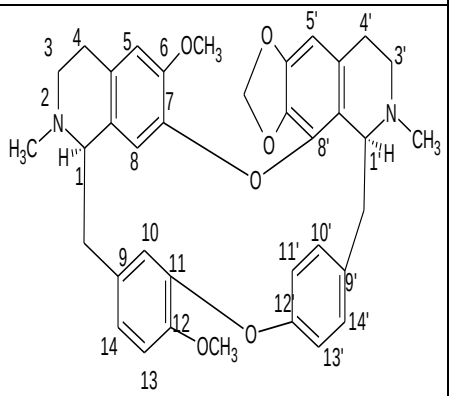 Cepharanthine R, S	cancer cell lines A-549, HL-60, MCF-7, SMMC-7721, and SW480	-	Lv et al., 2013

Liu et al demonstrated the anticancer activities of four BBIQ alkaloids (Table 1.4) alkaloids isolated from *Anisocycla grandidieri* Baill (Menispermaceae) on ovarian cancer cell line (A2780), lung cancer cell line (H460), breast cancer (MCF-7), and UACC-257 melanoma (Liu et al., 2013). The BBIQ showed anticancer activities with IC_{50} ranging from 1.1 to 20 µM. 2′-Norcocsuline exhibited most growth inhibition activity.

Murebwayire et al reported that phaentharine (**3**) isolated from *Triclisia sacleuxii* (Pierre) Diels showed cytotoxicity and antiplasmodial activity (Murebwayire et al., 2008). The configuration at chiral center and substitution on the aromatic rings of BBIQ affect the cytotoxicity and antiplasmodial actions of BBIQ (Angerhofer et al., 1999). Cepharanthine (**10**) was reported to exhibit potent anticancer activity on six human cancer cell lines (Lv et al., 2013). Fangchinoline **(5)** caused cytotoxicity in prostate breast cancer (Li et al., 2015, Deng et al., 2015). Isoliensinine (**77**), liensinine (**78**) and Neferine (**79**) all from *Nelumbo nucifera* Gaertn (Nymphaeaceae) (Mukerhjee et al., 2006) showed cytotoxicity effect on human breast cancer cell lines with isoliensinine (**77**) exerting highest anticancer activity (Zhang et al., 2015). Neferine (**79**) was also demonstrated to exhibit anticancer activity against lung cancer cells and hepatocellular carcinoma HCC Hep3B cells (Poornima et al., 2014, Yoon et al., 2013).

1.6. Selected plants used in this research Study

1.6.1. *Viola philippica Car*

Viola philippica Car (family Violaceae) is a perennial shrub that bears an ornamental flower (Figure 1.9). It is geographically distributed in China, Japan and North Korea. *Viola philippica* is used in Chinese traditional medicines for the treatment of cancer (Deng et al., 2013, He et al., 2011a), pains, inflammatory conditions, detoxification, and heat-cleansing (He et al., 2011a, Deng et al., 2013). The young leaves are used as edible vegetable (Peng, 2003). Previous studies have shown that *Viola philippica* contains flavone, actinomycetes (Deng et al., 2013) and cyclotides like Viphi A, ViphiB, Mram 8, Viphi D–G, Viba 17, Viba 15, Varv A, Kalata B1 and Cycloviolacin O2 (He et al., 2011a).

Figure 1.9 Photograph of *Viola philippica* Car.

1.6.2 Viola yedoensis Makino

Viola yedoensis Makino Violaceae is a perennial shrub that produces violet flowers (Figure 1.10). Its' geographical distributions include China, Japan, and Korea. (Wang et al., 2007). The dried whole plant of *Viola yedoensis* ("Zi Hua Di Ding") is an important constituent of the Chinese traditional medicines for the treatment of infectious diseases, detoxificant, anti-inflammatory and analgesic. The tender leaves are used as vegetable. (Wang et al., 2007)

Figure 1.10 Photograph of *Viola yedoensis* Makino.

In Chinese traditional medicine, the decoction of *Viola yedoensis* is taken as a tea and used to resolve toxic heat, swelling, carbuncles, sores, boils, treat snake bites, bronchitis, hepatitis, acute nephritis, appendicitis, and enteritis (Wang et al., 2007).

Some bioactive constituents have been isolated from *V. yedoensis* and identified (Wang et al., 2007) Cyclotides from *Viola yedoensis* have been reported to inhibit the growth of human immunodeficiency virus (HIV) (Wang et al., 2007) and certain

bacteria. Some of already identified cyclotides from *V. yedoensis* include kalata B1, varv A, varv E, cycloviolacins Y1, Y2, Y3, Y4, and Y5 (Wang et al., 2007)

1.6.3 *Triclisia subcordata* Oliv

Triclisia subcordata Oliv (Family Menispermaceae) is called Izuzu and Alugboran in Ibo and Yoruba (in Nigeria) languages, respectively. It is a slender woody twiner of low land rain-forest, with broad- vein and reticulate leaves (Figure 1.11), small flowers in short pedunculated clusters and pubescent fruits. Traditionally, the root of *T. subcordata* is used in south eastern part of Nigeria for the treatment of cancer, malaria, snake bite, edema, anemia, gout, debility, malnutrition, dropsy, bacterial infection, infertility (Abo et al., 2011), anti-inflammatory and as a pain killer (oral interview and reports from traditional medicine practitioners in Nigeria). Previous studies have been done on pharmacological activities of *T. subcordata* such as antibacterial (Abo et al., 2011), antiulcer and antihistamine activities (Asuzu & Anaga, 1996). But there is gap in the anticancer and antimalarial *in vitro* activities of *T. subcordata.* It is therefore, a novel study to evaluate the *in vitro* these activities of *T. subcordata* and to elucidate the structure of the bioactive principle(s) of *T. subcordata. A* previous study has identified and reported a few alkaloids from *T. subcordata*. Phytochemical studies in the 1970s revealed the presence of only three BBIQ alkaloids such as tricordatine (Tackie et al., 1973; Guha et al., 1979), fangchinoline (Tackie et al., 1974), and tetrandrine (Dwuma-Badu et al.,1975; Guha et al., 1979) from T. subcordata. It is possible that *T. subcordata* may likely contain more alkaloids. Plants from Menispermaceae family have been revealed to be rich in alkaloids. BBIQ alkaloid is among the commonest alkaloids present in

Menispermaceae family. This study therefore, also targets to identify and semi-synthesize novel bioactive anticancer and antimalarial alkaloids.

It is in the light of this, that this study seeks to contribute in the closure of this gap created. It probably could help to establish for the first time, a scientific data on the anticancer and more information on antimalarial activities of *T. subcordata*.

Figure 1.11 Photograph of *Triclisia subcordata***.**

1.6.4 Cylicodiscus gabunensis Harms

Cylicodiscus gabunensis Harms is a member of the plant family of Mimosaceae. It is a large tree of about 180-200ft (Okokon et al., 2006) in height which is prevalent in tropical rain forest of west and central Africa (Tene et al., 2011) The stem bark is traditionally used in Nigeria and Cameroon for the treatment of cancer, malaria, fever, headache, filariases, rheumatism and gastrointestinal problems (Okokon et al., 2006, Tene et al., 2011). Some studies have reported on the antibacterial, antidiarrheal, *in vivo* antimalarial activities, and bioactive constituents like triterpenoid saponins, a diterpene derivative called cyclodione and coumestan glycosides of *C. gabunensis* (Tchivounda et al., 1991, Kouitcheu et al., 2006, Okokon et al., 2006, Tane et al., 1995, Nchancho et al., 2009, Tene et al., 2011). Therefore, the rationale for the use of this plant as traditional remedy has created the need to demonstrate scientifically that the molecules in this plant may possess therapeutic effect against cancer and malaria.

Figure 1.12 Photograph of *Cylicodiscus gabunensis* (Ayarkwa & Owusu, 2008).

1.7 Aims and Objective of this study

1.7.1 The aims of this research are to:

- ❖ investigate the anticancer or antimalarial activities of *Viola philippica, V. yedoensis, Triclisia subcordata, and Cylicodiscus gabunensis;*
- ❖ evaluate and characterize the anticancer-cyclotides of *Viola philippica* and *yedoensis*
- ❖ Evaluate the anticancer and antimalarial activities and elucidate the structures of alkaloids from *Triclisia subcordata.*
- ❖ Carry out semi-synthesis or modification of bioactive alkaloids of *T. subcordata* (cycleanine) and determine the anticancer and antimalarial effects of the semi-synthesized products.
- ❖ Determine the molecular mechanism of cell death caused by the identified alkaloids on ovarian cancer cell lines.
- ❖ monitor cell distribution and uptake of cycleanine and semi-synthesized cycleanine by cells
- ❖ To evaluate the anticancer and antimalarial effects of extract of *C. gabunensis*

1.7.2 Objectives of this study include:

- To carry out the extractions of *V. philippica and yedoensis, T. subcordata, and C. gabunensis.*
- To screen *V. philippica, V. yedoensis, T. subcordata,* and *C. gabunensis* extracts and fractions for *in vitro* anticancer activities.
- To carry out *in vitro* antimalarial activities of *T. subcordata, and C. gabunensis* fractions and extracts.

- To isolate, purify and identify purified cyclotides *from V. philippica and yedoensis.*
- To carry out electrospray mass spectrometry, MALDI-TOF mass spectrometry analysis, to determine the masses and characterize the cyclotides of *V. philippica and yedoensis.*
- To characterize bioactive cyclotides responsible for the anticancer activities of *V. philippica and yedoensis.*
- To carry out bio-assay guided assay on the crude extracts, fractions and total alkaloids of *T. subcordata.*
- To isolate and purify the bioactive alkaloids of *T. subcordata* by chromatography techniques such as silica gel column, thin layer chromatography (TLC), and both analytical and semi-preparative HPLC.
- To carry out liquid chromatography-mass spectrometry (LC-MS) and nuclear magnetic resonance (NMR) spectroscopy analysis, to determine the structures of anticancer and antimalarial bioactive alkaloids of *T. subcordata.*
- To carry out caspase 3/7 activity assay on the identified alkaloids and cyclotides to determine the level of caspase activation.
- To do western blot or immunoblotting assay to check for the cleavage of poly ADP ribose (PARP cleavage) on cancer cell lines.
- To quantitatively and qualitatively evaluate the DNA fragmentation caused by apoptosis of some of the identified alkaloids on ovarian cancer cell line by use of flow cytometry.
- To evaluate the cell fluorescence activity/cell distribution of the semi-synthesized cycleanine by use of fluorescence microscopy and azide-containing dye (via click chemistry).

Hypothesis

The overarching research question that prompted this study has been the traditional uses of *Viola philippica, V. yedoensis*, *Triclisia subcordata*, and *Cylicodiscus gabunensis* in treatment of cancer and malaria. This issue has generated hypotheses in this study which states that:

Viola philippica, V. yedoensis, Triclisia subcordata, and Cylicodiscus gabunensis exert cytotoxicity on ovarian cancer cells and antimalarial activity on plasmodium falciparum. The molecular mechanism of cell death induced by bioactive compounds from *Triclisia subcordata* is probably by apoptosis.

Therefore, to test the above hypotheses in this study, four different ovarian cancer cells were employed in this research to demonstrate the cytotoxicity of the identified bioactive novel or test compounds (natural products) on both sensitive and chemo resistant strains of ovarian cancer cells and on plasmodium falciparium strain for antimalarial activity.

Therefore, the rationale for this study is the use of these plants as traditional remedies has created the need to identify the molecules in them that may possess therapeutic activity.

Also, the choice of combination of plant families used in this study was based on diverse interest of financial sponsor, student and supervisor since there was no relationship among the plant families used in this research. As a pharmacognosist, I developed interest on the identification of novel bioactive compounds responsible for the cytotoxicity and antimalarial activity of *Triclisia subcordata* after an oral interview with traditional medicine practitioner in Nigeria who claimed that *Triclisia subcordata* is ‘a very powerful remedy ‘in Nigeria for traditional treatment of malaria and cancer.

Already I had pre-existing research proposal on evaluation of stem bark of *Cylicodiscus gabunensis* for its malaria and cancer treatment because throughout my childhood, *Cylicodiscus gabunensis* was used by my parents as traditional remedy in treating us malaria. So, having recognized these two plants as strong traditional remedy for both cancer and malaria, a research proposal was made and gained funding from Nigerian government (NDDC and ETF) to sponsor this research. The aim was to determine the bioactive components of these plants and to ascertain authenticity of the claims by the traditional medicine practitioners.

However, my supervisor (Dr Wen-Wu Li) had different research interest focused on *Viola yedeonsis* and *Viola philippica* which he revealed to me after presenting my sponsor's approved research proposal. Literature also revealed that *Viola yedeonsis and Viola philippica* have application in Chinese traditional medicine, in combination therapy for treatment of cancer. This prompted the combination of the four plants selected in this study. This was to marry the interest of financial sponsor, supervisor and student.

CHAPTER TWO

MATERIALS AND METHODS

2.1 Viola philippica Cav. and Viola yedoensis Makino

2.1.1 Plant materials and reagents

The aerial parts of *Viola philippica* Cav. were collected from Yongchuan, Chongqing, China in April 2012. The plant was identified by Prof. Qian Wang, Chengdu Institute of Biology, Chinese Academy of Sciences, and a voucher specimen was deposited in the herbarium of Chengdu Institute of Biology, Chinese Academy of Sciences. The aerial parts of *Viola yedoensis* Makino (Synonym for *V. philippica* var. philippica) produced in Jiangsu Province, China were purchased from herbal medicine shop, Chongqing, China. A voucher specimen (No. ISTM004) was deposited in the Institute for Science and Technology, Keele University.

All the chemicals used were of analytical grade. Methanol, ethyl acetate, dichloromethane, chloroform, acetonitrile and trifluoroacetic acid (TFA) were products of Sigma-Aldrich. Trypsin-ultra, mass spectrometry grade (Bio Labs), endo-proteinase GluC (Bio Labs), formic acid, zip tip (Millipore), ammonium bicarbonate (NH_4HCO_3), Tris (2-caboxyethyyl) phosphine hydrochloride (TCEP) (Thermo Scientific, UK).

2.1.2 Extraction and purification of cyclotides from *V. philippica* and *V. yedoensis*

The extraction of *V. philippica and V. yedoensis* crude powder was done by previously established method with little modification (Claeson et al., 1998, Göransson et al., 2004). Briefly, *V. philippica and V. yedoensis* crude powder (800g)

was pre-extracted with 3.5 L of dichloromethane (CH_2Cl_2, or DCM) and filtered after 24 h. This was repeated thrice within 96h. After evaporation of DCM, the DCM extract of *V. philippica* (VP-DCM) and *V. yedoensis* (VY-DCM) were obtained and kept aside. The plant residues were dried and macerated with 3.5 L methanol/water ($MeOH/H_2O$, 3:2) daily for 96 h (Figure 2.1). The pre-extraction with dichloromethane was important to remove the chlorophyll, fats, and low molecular weight compounds that could interfere with the isolation of our targeted metabolites – cyclotides (Claeson et al., 1998). The $MeOH/H_2O$ crude extract was concentrated, using a rotary evaporator, water bath (Grant JB series, temperature at 40-50^oC) and vacuum pump (V-700 by Buchi). The yields of methanol/water extract for *V. philippica* (VP-MW) *and V. yedoensis* (VY-MW) were 14.6% (116.9g) and 13.9% (111.8g), respectively. These crude extracts were subjected to liquid-liquid partition using n-butanol and H_2O. A crude $MeOH/H_2O$ extract was dissolved with equal volumes of 100ml/100ml butanol/H_2O and poured into a separating conical flask. Then 250 ml of butanol and 250 ml of distilled water were poured into the separating column/flask containing the dissolved extract, properly shaken and allowed to settle for 10 - 20 minutes. The lower aqueous phase was collected and this was repeated thrice (Figure 2.1). Their *butanol* fractions denoted as VP-MW-BU and VY-MW-BU, and **a**queous fractions denoted as VP-MW-A and VY-MW-A, were separately mixed together and dried with rotary evaporator and lyophillizer, respectively. Ninhydrin reagent test for cyclotides was used with thin layer chromatography (TLC) to detect the presence of cyclotides in these fractions, per already known procedure with little modification (Tan & Zhou, 2006). The Isolation of cyclotides from *V. philippica* and *V. yedoensis* was done with gel column chromatography of column of 3 x 42 cm length loaded with silica gel of 70 – 230 mesh (Sigma-Aldrich) by washing with a mixture of

$CHCl_3$ and MeOH with increasing the percentage of MeOH until 100% at the rate of 70 drops/minute. The mixture of cyclotides was further purified using semi-preparative HPLC. The reversed-phase HPLC was adopted for purification because cyclotides have been reported to appear as late eluting peaks in HPLC (Claeson et al., 1998, Goransson et al., 2004, Tan & Zhou, 2006b). Semi-preparative HPLC was carried out using Agilent 1220 LC, USA. The mobile phase was a mixture of 0.1 % TFA (A) and 80% acetonitrile containing 0.1 % TFA (B). The composition of the mobile phase was rising from 10 % to 70 % B over a period of 25 min and kept at 100 % B for 6 min or 11 min on a semi-preparative HPLC column (Phenomenex, UK; Jupiter C18 reverse phase, 300 A, 5 µm particle size, 9.4 × 250 mm) at a flow rate of 4 ml/min. Eluted fractions at different retention times were collected and freeze-dried on a lyophilizer to give purified cylcotides. Thus, two main fractions from *V. philippica* eluted at 18 mins and 19 mins were collected and lyophilized to give VP18 (5mg) and VP19 (4mg). Similarly, two major fractions of *V. yedoensis* eluted at 18 and 19 mins were obtained and denoted as VY18 (6mg) and VY19 (5mg), respectively. For analysis of the purity of the isolated cyclotides, a gradient from 20 % B to 80 % B over a period of 25 min and 100% B for 6 min was applied on an analytical HPLC column (Phenomenex, UK; Jupiter C18 reverse phase, 300 A, 5 µm particle size, 4.6 × 250 mm) at a flow rate of 1 ml/min.

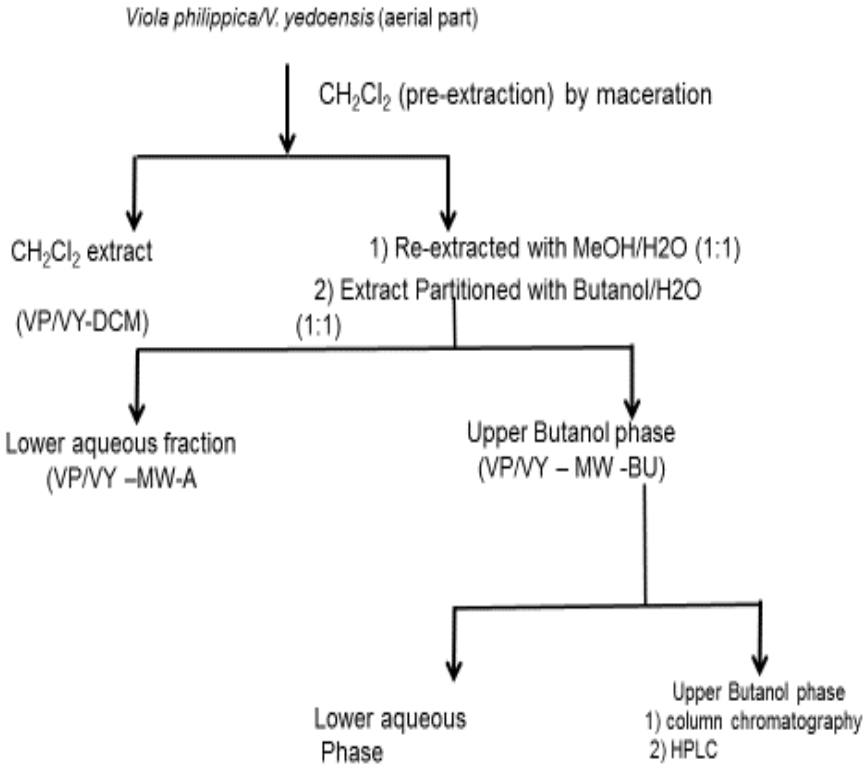

Figure 2.1 Flowchart of the extraction and enrichment of cyclotides from plants.

2.1.3 Mass spectrometric analysis of cyclotides from *V. philippica* and *V. yedoensis*

2.1.3.1 Methods for cyclotides reduction, and enzyme digestion

Reduction of cyclotides *by TCEP*

To ca. 6 nmol of cyclotide (~20 µg) in 20 µL of 0.1 M NH_4HCO_3 (pH 8.0) was added 1 µL of 0.1 M tris(2-carboxyethyl) phosphine hydrochloride (TCEP) in 0.1 M NH_4HCO_3 (pH 8.0), and the solution was incubated at 65 °C for 10 min (Wang et al., 2008).

Trypsin digestion ONLY

To the 10 µL reduced peptide (10 µg), 0.5 µL of trypsin (0.5 µg/µL) was added, to give a final peptide-to-enzyme ratio of 40:1. The trypsin incubation could proceed for

1 h at 37 °C. The digestions were quenched by the addition of an equal volume 10 µL of 0.5% HCO_2H and desalted using Zip tips (Millipore), which involved four washing steps [step 1: washing with100% acetonitrile; step 2: washing with 0.5 % HCO_2H; step 3: absorb digestion peptide samples; step 4: elution in 10 µL of 80% CH_3CN (0.5% HCO_2H)]. Samples were stored at 4 °C prior to analysis.

A combination of trypsin and endoGlu-C digestion

To the 10 µL reduced peptide (10 µg), 0.5 µL of trypsin (0.5 µg/µL) was added. The trypsin incubation could proceed for 1 h at 37 °C, then 0.5 µL of endoGlu-C (0.5 µg/µL) was added and a further 3 h incubation at 37 °C. The digestions were quenched by the addition of an equal volume of 0.5% HCO_2H and desalted using Zip tips (Millipore), which involved four washing steps as described above. Samples were stored at 4 °C prior to analysis.

Chymotrypsin digestion ONLY

To the 10 µL reduced peptide (10 µg), 0.5 µL of chymotrypsin (0.5 µg/µL) was added, to give a final peptide-to-enzyme ratio of 40:1. The chymotrypsin incubation could proceed for 3 h at 37 °C. The digestions were quenched by the addition of an equal volume 10 µL of 0.5% HCO_2H and desalted using Zip tips (Millipore), which involved four washing steps as described above. Samples were stored at 4 °C prior to analysis.

2.1.3.2 MALDI 4800 MS and MS/MS

Digested peptides were mixed in a 1:1 ratio (v/v) with α-cyano-4-hydroxycinnamic acid (CHCA, 10 $mgml^{-1}$ in 0.1% TFA, 80% acetonitrile) on a stainless steel MALDI target plate, and analysed by a MALDI time-of-flight (TOF/TOF) instrument (MALDI 4800, AB Sciex, Warrington, Cheshire).

2.1.3.3 Liquid chromatography electrospray ionisation/ Mass spectrometry (LC ESI/MS)

Cyclotides, digested and reduced peptide samples were injected onto a Dionex - Ultimate 3000 HPLC system (Thermo Scientific) using a 100% buffer A (5% acetonitrile (MeCN), 0.1% formic acid) in a 20 µl loop. Samples were then separated using a silica C18 column (Acclaim PepMap 100 C18, Thermo Scientific) following a gradient of 0 to 100% buffer B (95% MeCN, 0.1% formic acid) in 60 min. Spectra were accumulated using API 3200 triple quadrupled mass spectrometer (AB Sciex) using a Nano spray ion source. Spectra were acquired in Q1 mode in 400-1600 amu mass range.

Q-TOF waters micro mass, Q-Tof premier mass spectrometer was also employed in LC-MS, and MS/MS of digested peptides or cyclotides. Mass spectra were acquired and analysed to determine the peptide sequence based on both b-series of ions for the *N*-terminal fragments and y-series of ion for *C*-terminal fragments from MS/MS data.

2.2 *Triclisia subcordata* Oliv

2.2.1 General experimental Procedures

^{1}H NMR, ^{13}C NMR, DEPT, and 2D-NMR (COSY, HMQC and HMBC) spectra were obtained on a Bruker 400 or 500 MHz instruments. Chemical shifts were reported in δ (ppm) using the solvents ($CDCl_3$ or CD_3OD) standard and coupling constants (J) were measured in Hertz. Silica gel (Sigma-Aldrich) was used as an adsorbent for flash column chromatography. Dragendorff's reagents were purchased from Sigma-Aldrich.

2.2.2 Plant Material

The plant materials from *Triclisia subcordata* were collected in batches (1 and 2) in April 2012 and 2014 from Imo state, Nigeria, respectively, and identified by a taxonomist, H.D Onyeachusim. The voucher specimens (number: UUH1817) was deposited at University of Uyo, Akwa Ibom state, Nigeria. The root bark of the plant was cut into pieces, air-dried and pulverized.

2.2.3 Extraction and fractionation of *T. subcordata*.

First Batch: The powdered root bark of *Triclisia subcordata* (250 g) was extracted with 1L of 50 % ethanol by a Soxhlet apparatus. The extract was concentrated to dryness using rotary evaporator. The total extract (TSS) was subjected to further solvent partition per a previously established procedure (Kikueta et al. 2013) to yield the chloroform fraction containing enriched alkaloid (TSS1), the aqueous extract (TSS2), and the aqueous methanol fraction (TSS3) (Figures 2.2).

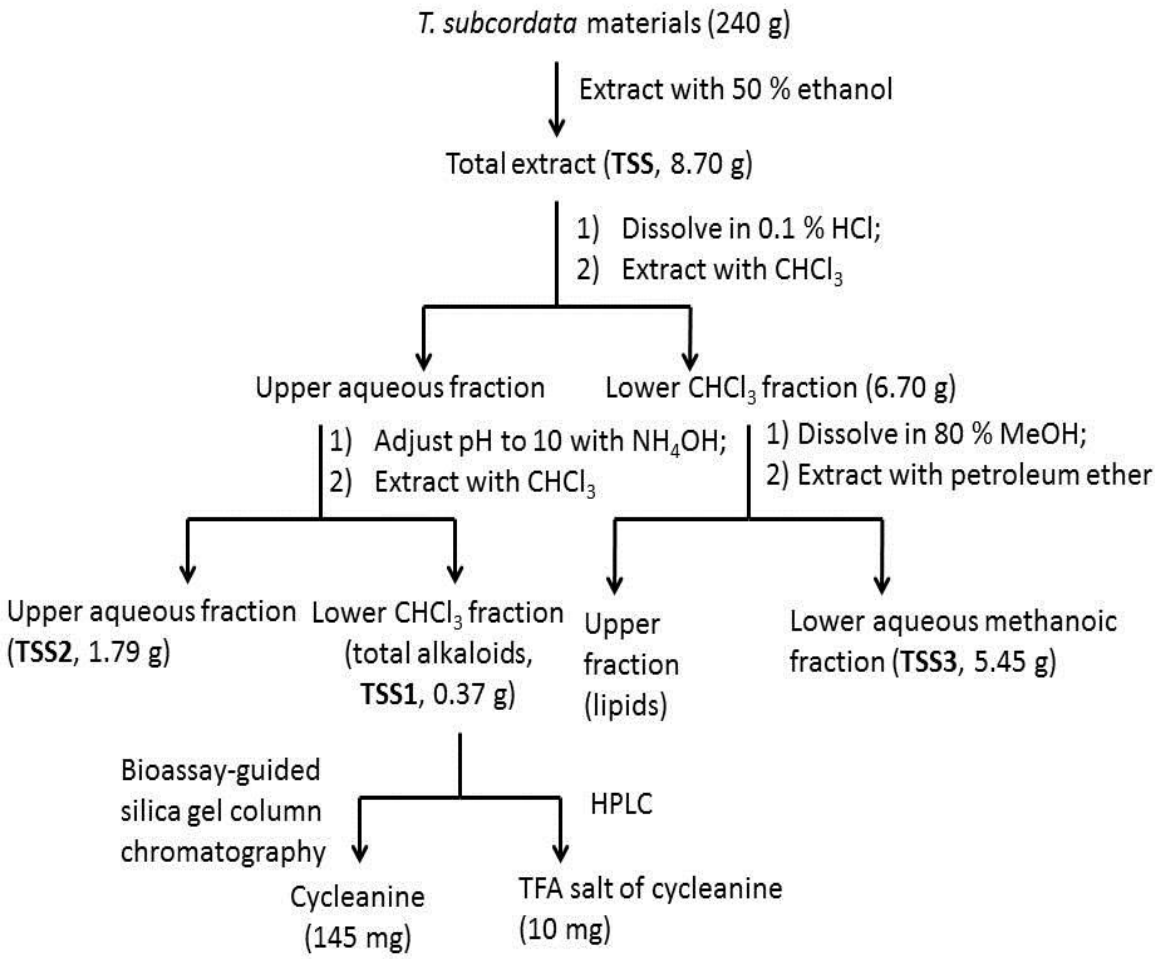

Figure 2.2 Scheme of extraction by Soxhlet apparatus, fractionation, purification and isolation of anti-cancer alkaloids from *T. subcordata* (Batch 1)

After first batch extraction and preliminary assay of fractions and compounds got, it was discovered that the method needed little modification and optimization to make it simpler steps for economic reasons. Also, to rule out the possibility of some alkaloids being destroyed by heat from Soxhlet apparatus. New method was therefore employed in second batch extraction to take care of the possible problems eminent in the first extraction. The second method was also specific method for alkaloid extraction since it became obvious from our first batch extraction and preliminary

assay that the targeted bioactive compound of *T. subcordata* were likely to be mainly alkaloids. These were subsequently targeted during second batch extraction. It is also a well-known fact that some alkaloids could be degraded by heat. So, high temperature was not employed in the second batch extraction. It was by simple maceration at room temperature to ensure that our targeted bioactive components were not degraded products.

Second batch: The 1.8kg powdered root of *T. subcordata* was extracted by maceration using 8 L of 5% acetic acid for 48h three times. The extract was combined and dried with a rotary evaporator. The crude extract was subjected to alkaloid extraction by alkalinisation with ammonium hydroxide (NH_4OH) (pH 9-10) and subsequent partition with chloroform to get 22.6 g total alkaloid (Figure 2.3).

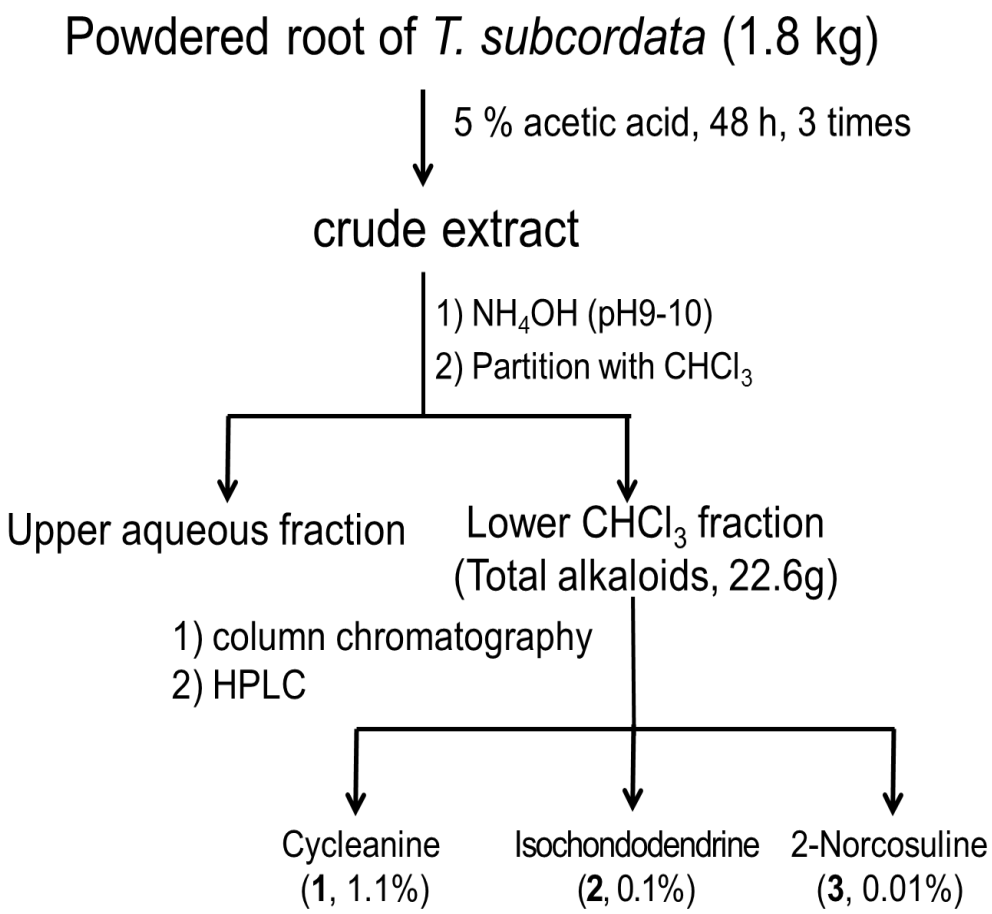

Figure 2.3 Scheme of extraction by maceration, fractionation, isolation and purification of anti-cancer alkaloids from *T. subcordata* root.

2.2.4 Phytochemical screening

Preliminary phytochemical tests were carried out on plant extracts to screen them for preliminary bioactive constituents using a characteristic colour reaction changes to detect the presence of phyto-constituents according to previously established procedures (Harborne, 1998, Trease & Evans, 1998, Uche & Ezugwu, 2009, Ijeoma et al., 2011, Edeoga et al., 2005, Sofowora, 1982) (Table 2).

Table 2.1 Preliminary Phytochemical screening of crude extract of *Triclisia subcordata*

root.

Test	observation	inference
Test for Alkaloids A 2.0 g extract + 5 mL 1% HCl + warmed, and filtered. Then 1 mL filtrate + 2mL Dragendorff's reagent.	Formation of Orange, precipitate observed.	Alkaloids present +++
A 1mL filtrate + 1 mL Mayer's reagent	Formation of milk /white precipitate observed	Alkaloids present +++
A 1mL filtrate + 1mL Hager reagent (picric acid)	Formation of yellow precipitate observed	Alkaloids present +++
Test for Saponins **A 0.5**g extract + shaken with water in a test tube	Formation of Frothing which persisted on warming. This was confirmed by Hemolysis test.	Evidence for presence of Saponins ++
Test for Tannins A 1.0g of extract + 5ml distilled water+ filter, 2mL filtrate + Ferric chloride test	Blue black precipitate observed	Evidence for the presence of tannin +++
Detection of diterpene **Copper acetate Test:** A 1.0g extracts were	Formation of emerald green color.	indicates the presence of

dissolved in water and treated with 3 drops of copper acetate solution.		diterpenes. ++
Liebermann-Burchard test: A 2.0g extracts were treated with chloroform and filtered. The filtrates were treated with few drops of acetic anhydride, boiled and cooled. Conc. Sulphuric acid was added.	Formation of brown ring at the junction	indicates the presence of phytosterols. ++
Salkowiski's test: A 2.0g extracts were treated with chloroform and filtered. The filtrates were treated with few drops of Conc. Sulphuric acid, shaken and allowed to stand.	Appearance of golden yellow color	indicates the presence of triterpenes ++
<u>Test for Flavonoids</u> **Alkaline Reagent Test:** A 1.0g extracts were treated with three drops of sodium hydroxide solution.	Formation of intense yellow color, which becomes colorless on addition of dilute acid,	indicates the presence of flavonoids ++
Lead acetate test: A 1.0g extracts were treated with three drops of lead acetate solution.	Formation of yellow color precipitate	indicates the presence of flavonoids. ++
Shinoda reduction test	Orange coloration observed	++

Cardiac glycosides A 2.0g extracts were treated with sodium nitropruside in pyridine and sodium hydroxide.	No pink to blood red colour formed.	indicate the absence of cardiac glycosides. -
Modified Borntrager's Test: A 3 .0g extracts were treated with Ferric Chloride solution and immersed in boiling water for about 5 minutes. The mixture was cooled and extracted with equal volumes of benzene. The benzene layer was separated and treated with ammonia solution.	No coloration formed in the ammonia layer, indicates the absence of anthranol glycosides.	No anthranol glycoside observed
Carbohydrates: **Molisch's Test:** A 2-mL filtrate from the extract was treated with 2 drops of alcoholic α-naphthol solution in a test tube + 2 drops of H_2S04	formation of the violet ring at the junction	indicates the presence of Carbohydrates ++

+ represent trace; ++ moderately present: +++ much present, --absence

2.2.5 Liquid chromatography-mass spectrometry (LC-MS)

1µL of alkaloid sample in methanol (0.1 mg/ml) was injected onto a Waters BEH C18 (2.1x100 mm 1.7 µm particle size) reversed phase column via a Thermo Scientific Ultimate U3000 ultra-performance liquid chromatography (UPLC) system. Alkaloids were separated using a linear gradient method utilising mobile phase A (Milli-Q water with 0.1% formic acid) and mobile phase B (acetonitrile with 0.1% formic acid). The

gradient consisted: 0 min (95% A), 1 min (95% A), 7 min (100% B), 7.01 min (95% A) and 10 min (95% A). The flow rate was maintained at 0.4 ml/min throughout.

The outlet from the chromatography system was directly coupled to a HESI II electrospray ion source on a Thermo Scientific Q-Exactive Orbitrap mass spectrometer system which was used to generate ions from the LC eluent and create a mass chromatogram and spectra. The MS method utilised a full-MS mode experiment in positive ion mode, 140,000 resolution, an AGC target of 3e6, max ion injection time of 200 ms and a scan range of 300-2500.

2.2.6. Isolation of alkaloids of *T. subcordata*.

2.2.6.1 Isolation of cycleanine from batch 1 plant.

The TSS1 (273 mg), which showed most cytotoxic activity, was subjected to silica gel chromatography eluting with $CHCl_3$ with increasing amount of MeOH to give 40 fractions. The eluted fractions were tested, identified and combined as guided by Dragendorff's reagent test, thin layer chromatography and UV detector at 254 nm and 365 nm. Dragendorff's and Mayer's reagents were used as the preliminary test for alkaloids using chemical colour reaction tests of alkaloids (Sofowora, 1998, Trease and Evans, 1998). The combined fractions were concentrated in vacuum with a rotary evaporator. Cycleanine (145 mg) was recrystallized from 1-4th fraction (TSS1.1). Fractions 5-8 were combined as TSS1.2 (27.8 mg) and further purified by using HPLC on an Agilent 1220 LC system (USA). UV detector was set at 254 nm wavelength. The mobile phase was a mixture of 0.1 % TFA (A) and 80% acetonitrile containing 0.1 % TFA (B). The composition of the mobile phase was rising from 10 % to 70% B over a period of 25 min and kept at 100 % B for 6 min on a semi-preparative HPLC column (Phenomenex, UK; Jupiter C18 reverse phase, 300 Å, 5

μm particle size, 9.4 × 250 mm) at a flow rate of 4 ml/min. Eluted fractions at different retention times were collected and freeze-dried in a lyophilizer. For analysis of the purity of the isolated alkaloids, a gradient from 10 % B to 70% B over a period of 25 min and 100% B for 6 min was applied on an analytical HPLC column (Phenomenex, UK; Jupiter C18 reverse phase, 300 A, 5 μm particle size, 4.6 × 250 mm) at a flow rate of 1 ml/min.

Cycleanine (**1**), white powder. ^{1}H and ^{13}C NMR ($CDCl_3$) (Tables 4.3 and 4. 4). LC-ESI-MS, *m/z*: 623.3118 $[M + H]^{+}$; 312.1610 $[M + 2H]^{2+}$.

TFA salt of cycleanine (**1a**), white powder. ^{1}H and ^{13}C NMR ($CDCl_3$) (Tables 4.3 and 4.4). LC-ESI-MS, *m/z*: 623.3074 $[M + H]^{+}$; 312.1579 $[M + 2H]^{2+}$.

2.2.6.2 Isolation of BBIQ alkaloids (from Batch 2)

The total alkaloid (22.6 g) was purified using combined methods of column chromatography described above, recrystallization and HPLC procedure to yield three pure alkaloids including cycleanine (**1**, 83.7%), isochondodendrine (**2**, 7.5%) and 2′-norcocsuline (**3**, 1%). Cycleanine was obtained by crystallization, isochondodendrine was isolated from silica gel column chromatography and 2′-norcocsuline was isolated by HPLC.

Isochondodendrine (**2**), white powder, ^{1}H and ^{13}C NMR ($CDCl_3$) (Table 4.3 and 4.4). Positive HR-ESI-MS, *m/z*: 595.2807 (Calcd. mass for $C_{36}H_{39}N_2O_6$, $[M + H]^{+}$, 595.2808).

TFA salt of 2′-Norcocsuline (**3**), ^{1}H and ^{13}C NMR ($CDCl_3$) see Table 4.5 and 4.6. Positive HR-ESI-MS, *m/z*: 549.2384 (Calcd. mass for $C_{34}H_{33}N_2O_5$, $[M + H]^{+}$, 549.2389).

Conversion of 2'-norcocsuline (**3**) TFA salt to its free base, 2'-norcocsuline was carried out by first alkalinisation and subsequent extraction with $CHCl_3$ to give its free base form. ^{1}H and ^{13}C NMR ($CDCl_3$) of **3** are also listed in Table 4.5 and 4.6.

2.2.7 Semi-synthesis of (aminoalkyl)cycleanine analogues

2.2.7.1 Synthesis of 5-[(dimethylamino)methyl] cycleanine (**4**)

Cycleanine (**1**, 1.0 g, 1.6 mmol) isolated from this plant was combined with 10 ml concentrated HCl and paraformaldehyde (0.1 g, 3.4 mmol) and the reaction mixture was stirred on ice for 3h. The reaction mixture was concentrated to dryness. After evaporation of HCl under vacuum, the mixture product was dissolved in 30 mL acetonitrile, treated with 1.6mL of 2 M dimethylamine in THF and NaOH pellet (128 mg), and stirred at room temperature for 3h. After filtration, a yellow powder was obtained. The product was further purified by silica gel column chromatography (5 - 50 % $CHCl_3$/MeOH). The fractions containing the product were combined and evaporated to produce a yellow powder (20 mg, yield 7.8%, purity > 98%). ^{1}H and ^{13}C NMR (CD_3OD) for **4** (Table 5.1 and 5.2). Positive HR-ESI-MS, *m/z*: 680.3692 (Calcd. mass for $C_{41}H_{50}N_3O_6$, $[M + H]^+$, 680.3700).

2.2.7.2 Synthesis of 5-[(propargylamino)methyl] cycleanine (**5**)

Cycleanine (1g, 1.6mmol) was combined with 10 ml concentrated HCl and paraformaldehyde (0.1 g, 3.4 mmol) and the mixture was stirred on ice for 3 h. The reaction mixture was concentrated to dryness and the residue was dissolved in 30 mL acetonitrile, treated with 200µL propargylamine and NaOH pellet (128 mg), and stirred at room temperature for 3h. After filtration, a yellow powder (1.29 g) was obtained and further purified by silica gel column chromatography as described above for compound **5**. ^{1}H and ^{13}C NMR (CD_3OD) for **5** (Table 5.1 and 5.2). Positive HR-ESI-MS, *m/z*: 690.3507 (Calcd mass for $C_{42}H_{48}N_3O_6$, $[M + H]^+$, 690.3538).

2.3 *Cylicodiscus gabunensis*

2.3.1 Plant materials

The stem bark of *Cylicodiscus gabunensis* Harms (Mimosaceae) was collected from Orlu L.G.A., Imo state Nigeria in September 2011. The plant materials were identified and authenticated by H.D Onyeachusim, a taxonomist. A voucher specimen (UPH1028) was deposited in the Herbarium of Botany department, University of Port Harcourt, Nigeria.

2.3.2 Extraction of *Cylicodiscus gabunensis*

Cylicodiscus gabunensis stem bark was cut into pieces, air dried and reduced to powder. The crude powder (200g) was pre-extracted with 1L hexane by maceration. The extract was dried and extracted thrice with 1L of 70% ethanol using cold maceration. The combined extracts were dried using rotary evaporator to get the ethanol extract (CGE, 24g).

2.3.3. Fractionation of the ethanol extract of *C. gabunensis* (CGE)

CGE (24 g) was dissolved in water and partitioned with ethyl acetate and n-butanol sequentially to give the ethyl acetate fraction (CGEEA, 1.8g), butanol fraction (CGEBU, 16.6g) and aqueous fraction (CGEAQ, 3.2g). These fractions were screened for both anticancer and antimalarial activities.

2.4 Anticancer activity of plant extracts and pure compounds

2.4.1 In vitro cytotoxicity

2.4.1.1 Cell lines

The human ovarian cancer cell lines (Ovcar-8, Ovcar-4, A2780 and Igrov-1) and normal human ovarian epithelial (HOE) cells were used in this study. Ovarian cancer cell lines were products of American tissue culture collection (ATCC). The Ovcar-8

cell line originated from ovarian carcinoma that was resistant to carboplatin (Robinson et al., 2013). The Igrov-1 cell line originated from an ovarian carcinoma that was sensitive to chemotherapy treatment (Robinson et al., 2013). The Ovcar-4 cell line was produced from the cisplatin resistant ovarian cancer patient (Robinson et al., 2013). A2780 was obtained from a human ovarian carcinoma before exposure to drug treatment (Robinson et al. 2013). Human Ovarian Epithelial (HOE) cells were bought from Applied Biological Materials (ABM) Inc. HOE originated from normal ovarian epithelium and immortalized using SV40 large T antigen (Robinson et al. 2013).

2.4.1.2 Cell culture.

HOE, Ovcar-8, Ovcar-4, A2780 and Igrov-1 cells were grown in Roswell Park Memorial institute (RPMI 1640, Lonza) medium was employed in culturing of human ovarian cancer cell lines (. The medium was supplemented with 10% fatal bovine serum (FBS, Lonza), penicillin-streptomycin (50 µg/ml: Lonza) and glutamine (2 mM: Lonza). These were incubated and maintained in a standard humidified incubator (Pamassonic incubator: MCO-18AC: S/N 13020089) conditions of 37 $^{\circ}$C, 5% carbon dioxide (CO_2).

All cells were routinely sub-cultured when they were more than 80% confluent (as determined using an Olympus CKX41 light microscope). To detach adherent cells from the culture flask for routine passage or experimentation, cells were washed with 1 mL phosphate buffered saline (PBS; Lonza) and subsequently exposed to 1 mL 0.01% trypsin (Lonza) in PBS. The cells were shaken and incubated at 37°C to facilitate detachment. After complete detachment of cells, 1.1 mL of RPMI 1640 enriched medium was used to neutralize the trypsin. This was transferred into a sterile 15 mL polypropylene tube (Sarstedt) and centrifuged at 150 g for 3 minutes at

room temperature using a Thermo Scientific (Heraeus Megafuge 8) centrifuge. The cell pellets were re-suspended in fresh medium after aspiration of the culture. The cells were maintained in T75 sterile tissue culture flasks (Sarstedt). For assay, a minimum number of cells (100 cells) was counted with Neubauer hemocytometer. The required number of cells were seeded into an appropriate tissue culture plates (96-well or 6-well plates Sarstedt) as described below.

2.4.1.3 Cell growth assay with sulforhodamine B (SRB) assay

Plant extracts or pure compounds were solubilized in dimethyl sulfoxide (0.2% DMSO; but the maximum concentration of DMSO is usually 0.5%) (or PBS for carboplatin) to obtain the following stock concentrations: 100mg/ml of total plant extracts or fractions; 20 mM of cyclotides and BBIQ alkaloids (cycleanine, isochondodendrine, 2′-norcocsuline, tetrandrine, and semisynthetic cycleanine derivatives), 13.5 mM carboplatin (Sigma-Aldrich), and 10 mM paclitaxel (Sigma-Aldrich). Sulforhodamine B (SRB) and trichloroacetic acid (TCA) were bought from Sigma-Aldrich, UK, and acetic acid from Fisher scientific, UK.

The SRB assay (Vichai & Kirtikara, 2006) was used to evaluate the effects of the plant extracts and pure compounds on the growth of ovarian cancer cell lines (A2780, Ovcar-8, Ovcar-4, Igrov-1) and on normal human ovarian epithelia (HOE) cells. To demonstrate the level of sensitive of our test compounds to pre-and post-chemotherapy exposed ovarian cancer cell lines, the four-different ovarian cancer cells were selected in this study. The reason is, for good identification of new or bioactive compounds in ovarian cancer research, it is considered ideal to demonstrate the activity of such compounds in chemo-resistant as well as sensitive strains of ovarian cancer, probably due to common low prognosis of cancer patients.

Cancer cells have been known to be prone to development of resistant to chemotherapy because of post exposure or treatment with a cancer chemotherapy. Therefore, the four cell lines used in this study include:

A2780 cell line was produced from a human ovarian carcinoma prior to chemotherapy treatment. A2780 used was to investigate test compound sensitivity on cancer cells that have no history of chemotherapy treatment and thus could be sensitive to cancer drug treatment.

Ovcar-4 cell line was got from the ascites of cisplatin - resistant ovarian cancer patient. This was to ascertain the sensitivity of our test compounds to ovarian cancer cells that had developed resistant to cisplatin which is already known cancer chemotherapeutic agent.

Ovcar-8 cell line originated from carboplatin -resistant ovarian carcinoma. This was chosen to evaluate the sensitivity the compounds to ovarian cancer cells that had developed resistant to carboplatin, a well-known cancer chemotherapeutic agent commonly used either as single or in combination therapy for treatment of different cancer

Igrov-1 cell line was derived from a post- chemotherapy sensitive ovarian carcinoma. The reason for the choice of Igrov-1 was to determine the sensitivity of our test compounds on ovarian cancer cells that have been previously exposed to chemotherapeutic agents. HOE was employed to determine the therapeutic index or selectivity of the test compounds. 2000 cells (A2780, Ovcar-8), and 5000 (Ovcar-4, Igrov-1, or HOE) cells were seeded in 80 µl of growth medium in each well of a 96-well plate. After 24 hours 20 µl of plant extracts or pure compounds dissolved in the medium (final DMSO concentration 0.2%). After 72 hours, the medium was decanted

and the cells were fixed with 10% TCA on ice for 30 min before drying. The cells were stained with 0.4% SRB in 1% acetic acid for 30 min, washed with 1% acetic acid and dried. Then, 200 µL of Tris-base (10 mM) were added to the dried plates and shaken for 5 min to solubilise the SRB dye. The absorbance at 540 nm or 570nm was measured using a spectroscopic plate reader (Multi-mode microplate reader BioTEK Synergy 2, USA). DMSO or medium was used as negative control while paclitaxel or carboplatin or both were used as positive drug controls. The data was analysed by non-linear regression using the Graph Pad PRISM 6.0 software to fit a 4-parameter sigmoidal dose-response curve.

2.4.1.4 Trypan blue Cell Viability counting

The viability of cancer cells was measured using trypan blue exclusion method (Invitrogen) before seeding cells and after drug treatment of the cells. The cells (A2780, Ovcar-8, Ovcar-4, or Igrov-1) (200, 000 cells/well) were seeded into 6 good plates, and medium (control), carboplatin, plant extracts, fractions, isolated compounds-cycleanine, isochondodendrine, 2′-norcocsuline or tetrandrine (20 µM) including semisynthetic cycleanine derivatives were administered to the cells after 24hr incubation. Then cell viability was determined using Neubauer haemocytometer and trypan blue exclusion after 48h treatment. Briefly, 20 µL cells culture were collected after trypsinization and mixed with and equal volume of 0.4% trypan blue thoroughly. Then 20 µL of the suspension mixture was analysed with a Countess™ Automated Cell Counter (Life Technologies, USA) to determine cell viability.

2.4.2 Apoptosis detection by Caspase – Glo 3/7 activity assay

The effect of BBIQ alkaloids, cycleanine, isochondodendrine, 2′-norcocsuline, tetrandrine and cycleanine derivatives, 5-[(dimethylamino)methyl]cycleanine and 5-

[(propargylamino)methyl]cycleanine on the caspase-3/7 activities was carried out using assay kits caspase-Glo 3/7 (Promega Corp., Madison, WI, USA) on a 96-well microplate as described previously with little modification (Robinson et al., 2013) (Robinson et al. 2013). Briefly, A2780 and Ovcar-8 (2000 cells/well), and Igrov-1 and Ovcar-4 (5000 cells/well) cells were incubated in 80 µL growth medium in a 96-well plate for 24 hours. Cells were then supplemented with growth medium (control), carboplatin, cycleanine or isochondodendrine, 2′-norcocsuline, tetrandrine or cycleanine derivatives, 5-[(dimethylamino)methyl] cycleanine (**4**) or 5-[(propargylamino)methyl] cycleanine (**5**) (final concentration 20 µM) for 48 hours. Before adding caspase agents, the morphological changes were observed and the images were captured under an inverted light microscope. Then, 100 µL of the culture was treated with 25 µL caspase-Glo 3/7 reagent and incubated at room temperature on a Rocker (Gyro shaker) for 30 minutes, protected from light. The luminescence reading was measured at 570 nm by Multi-Mode Microplate Reader BioTEK Synergy 2 (USA).

2.4.3 Western blot assay for PARP cleavage

To evaluate apoptosis, 200,000 Ovcar-8 cells/ml were seeded in a 6-well plate, n = 5 (usually cell density of 10^5 - 10^6 range could give sufficient protein for analysis per manufacturer's specifications). These were separately treated with cycleanine, isochondodendrine, 2′-norcocsuline, tetrandrine, cycleanine derivatives, 5-[(dimethylamino)methyl] cycleanine or 5- [(propargylamino)methyl] cycleanine, carboplatin (20 µM) or medium for 48 h. Cells were collected by trypsinization, lysed, protein concentration determined by the bicinchoninic acid (BCA) assay. Equal amounts of proteins (10µg) from total cellular extracts were resolved on 4-20% Tris-Glycine polyacrylamide gradient gel (Nusep) with hepes running buffer (100 mM

hepes, 100 mM Tris and 1% sodium dodecyl sulphate). After electrophoresis, the proteins on the gel were transferred to polyvinylidene fluoride (PVDF) membrane. The membrane was then incubated with Tris Buffered Saline with Tween (TBST) buffer (50 mM Tris hydrochloride (Tris HCl, pH 7.4, 150 mM NaCl, 0.1% Tween 20) containing 5% skimmed milk powder for 1.0 hour with gentle rocking on a Stuart Scientific Platform Shaker STR6 at room temperature. The membrane was then probed with poly (ADP) ribose polymerase (PARP) from rabbit (Cell Signalling Technology Inc., USA) (1:1000) for 16 hours at 4°C overnight and washed. Then probed with antibodies against poly (ADP) ribose polymerase (anti-rabbit). Then incubated with glyceraldehde-3-phosphate dehydrogenase (GAPDH) from mouse (Millipore, USA) (1:5000) for 1 hour at room temperature. Then treated with anti-mouse after incubation. Proteins were visualised using UptiLight HRP chemiluminescent substrate (Uptima) on a FluorChem M Imager.

2.4.4 Apoptosis analysis by flow cytometry

0.5 ml of Ovcar-8 cells (300,000 cells/ml) were seeded in 12 well plates for 24h, and exposed to medium as control, carboplatin, cycleanine, isochondodendrine, 2-norcocsuline, tetrandrine or cycleanine derivatives -5-[(dimethylamino)methyl]cycleanine or 5-[(propargylamino)methyl]cycleanine (20 µM). After incubation for 48 h, the cells were washed with PBS, trypinsized and stained with fluorescein isothycanate (FITC)-conjugated annexin V using Annexin V-FITC kit (Miltenyi Biotec, Germany) and propidium iodide (PI) following the manufacturer's protocol. Apoptotic and live cells were measured using a Beckman Coulter Cytomics 500 flow cytometer with CXP software (High Wycombe UK). Flow cytometry data was analyzed using Flowing Software (Perttu Terho, Turku Centre for Biotechnology, University of Turku, Finland). The percentage of early and

later apoptotic, and live cells in three independent experiments were statistically analyzed using Graph Pad Prism 6 software.

2.4.5 Cell cycle analysis by flow cytometry

Ovcar-8 1 × 10^6 cells/well were seeded in a 6-well plate. The different cell density was considered here because during our pilot study, where different preliminary experiments were performed using flow cytometer, it became necessary to optimize each assay to get perfect results for specific procedure, provided the cell density falls within the manufactures' range or specifications. The 6- well seeded cells were treated with cycleanine, tetrandrine, isochondodendrine, 2′-norcocsuline, or cycleanine derivatives, 5-[(dimethylamino)methyl] cycleanine or 5-[(propargylamino)methyl] cycleanine carboplatin (20μM), and medium (control) for 48 hr. The adherent cells were trypinized and washed with PBS. The cells were then fixed with 70% ethanol in cold PBS, and incubated at 4^{o}C for 24 hr. The fixed cells were centrifuged at 200 g for 10 mins and the cell pellets were washed twice with PBS. Cells were suspended in PBS containing PI (50 μg/mL), Triton X-100 (0.1%, v/v), and DNase-free RNase (1 μg/mL). (Robinson et al. 2013). DNA contents were determined by flow cytometry using a Beckman Coulter Cytomics 500 flow cytometer with CXP software (High Wycombe UK). Flow cytometry data was analysed using Flowing Software (Perttu Terho, scattering (FSC) (Turku Centre for Biotechnology, University of Turku, Finland). The flow cytometer, FC 500 was used (Beckman Coulter (UK) LTD Cytomics FC500, High Wycombe UK).

2.4.6 Imaging alkaloids uptake inside cells using click chemistry and confocal fluorescence microscopy

The imaging of alkaloids uptake was done using click chemistry and confocal fluorescence microscopy per previous with little modification (Luo et al., 2013). Briefly, human Ovcar-8 cell line was maintained in a culture medium consisting of RPMI supplemented with 10% FBS and 50µg/mL penicillin-streptomycine and 2mM glutamine (Lonza). The cells (5 $x10^4$ cells/mL) were seeded in 96 good plates and incubated at 5% CO_2 and 37^oC overnight. The cells were respectively treated with Alexa 488 azid alone with cell (control), 20 µM cycleanine, or 20 µM 5-[(propargylamino)methyl] cycleanine (**5**) for 5h. Cells were fixed with 3.7% formaldehyde at 4 $^{\circ}C$ for 30 min and washed 3 times with excess PBS. The fixed cells were incubated with the click chemistry reaction buffer (0.1 M Tris buffer, pH 8.5, with 0.05 % Triton, 20 µM of Alexa 488 azide; 50 µM of $CuSO_4$, 25 µM of Tris(3-hydroxypropyltriazolylmethyl) amine (THPTA), 2.5 mM ascorbic acid) for in situ specifically labelling of 5 with an azide-containing fluorophore in the dark at room temperature for 30 mins. After the labelling reaction, the reaction buffer was removed and the cells were washed two times with PBS. Florescence signal was measured by use of confocal microscope (Olympus U-TBI 90 Olympus 1 X 83 confocal microscope 3G14189, Japan). Excitation and emission filters for imaging the intracellular uptake of monoalkynyl cycleanine (**5**) were taken at 470/15nm and 515 – 550 nm respectively (Luo et al., 2013). The mean fluorescence intensity (MFI) of individual cells within selected field of view (FOV) of the fluorescence microscopy data was calculated by using ImageJ (Public domain, NIH) software (Luo et al., 2013). The MFI of individual cells was corrected by subtracting the background fluorescence signal.

The average MFI was calculated by averaging the MFI from selected FOVs (with approximately 30−40 cells in total).

2.5 Antimalarial activity of plant extracts and pure compounds

2.5.1 Materials

The following materials or instruments were used: Lumina flow hood-ICN flow. BS5726 class11 MSC Gelaik BSB. Incubator/Oven- NUAIRE^{TM} DH Auto flow incubator, Model No NU.5500E series 11 (CO_2 air – jacketed incubator). Centrifuge-U-320R, BOECO Germany, light microscope (Olympus CX21), Water bath, Luminator-Glo-Max Multimode Reader Luminator: Glomax Multi Detection system (Promega UK), Tissue culture plates: White 96 multi-good plates - Flat bottom suspension cells plates made by Sarstedt. Syber green 1 MSF lysis buffer (100 µl of 20mM Tris (PH 7.5), 5 nM EDTA, 0.008% (w/v) saponin and 0.08% (V/V) Triton X-100 containing syber green 1(1 x final concentration from 5000x stock Invitrogen). Most of the materials /chemicals used were products of Sigma Aldrich.

2.5.2 *In vitro* antimalarial assay

The previously established standard procedure for in-vitro antimalarial screening or assay using MSF containing Syber green 1 fluorescence assay techniques was employed with little modification, as described by (Hasenkamp et al., 2013, Smilkstein et al., 2004, Wong et al., 2011). Briefly, *Plasmodium falciparum* Dd2 strain was employed for these assays. Transgenic Dd2 chloroquine resistant P. falciparum was cultured in standard continuous culture conditions (RPMI 1640), supplemented with 37.5mMHEPES, 10mM D glucose, 2mM L-glutamine, 100µM Hypoxanthine-(growth biomarker), 8%v/v human serum at 2% haematocrit in atmosphere of 1%, O_2, 3% CO_2 and 96% N_2 ;5nM WR99210 and 2.5ug/mL blastidin. (Hasenkamp et al.,

2013, Smilkstein et al., 2004, Wong et al., 2011). Parasitaemia level and stage were determined by light microscopy by use of Giemsa staining of thin blood smears. Synchronization of culture was done by sequential sorbitol treatment. The 100uL of Dd2 culture mixed with different drug concentrations in 96 well plate and incubated for 48h. Then 100uL of the drug treated culture was mixed with Malaria fluorescence syber green 1 (MFS) with lysing buffer ((100 µl of 20mM Tris (PH 7.5), 5 nM EDTA, 0.008% (w/v) saponin and 0.08% (V/V) Triton X-100). This was thoroughly mixed and incubated in dark for 1h at room temperature. A two-fold serial dilution was employed for a 48hour assay of a trophozoite synchronised culture. Then fluorescence emission at 490 measured at excitation 510-570 using Glomax multi-detector laminator reader. Each biological replicate recorded, comprises three technical replicates on the same 96-well plate. Following capture of the fluorescent signal, the parasitaemia was calculated as follows: $100 \times [\mu_{(S)} - \mu_{(-)}/\mu_{(+)} - \mu_{(-)}]$, where $\mu_{(S)}$, $\mu_{(+)}$ and $\mu_{(-)}$ represent the means of the fluorescent signals for the sample in question and 100% and 0% controls, respectively. Then % growth (parasitaemia) was plotted against $\log_{10}$-transformed drug concentration and to get $IC_{50,}$ which was determined using a nonlinear regression (sigmoidal dose–response/variable slope equation) in Graph Pad Prism v5.0 (Graph Pad Software, Inc., San Diego, CA). Chloroquine was used as reference control. The antiplasmodial activity is expressed as the 50% inhibitory concentrations (IC_{50}).

2.6 Statistical analysis

Pharmacological data was analysed by non-linear regression using the GraphPad Prism software (GraphPad Software Inc.) to fit a four-parameter sigmoidal dose-response curve (Hill-equation). The concentration that caused 50% cell growth inhibition (IC_{50}) and Hill coefficient were determined. This was repeated at least thrice

and the results (IC_{50}) were expressed as mean ± SEM (standard error of mean) of at least three or more observations. Analysis of variance (ANOVA) or Student t-test was further used to compare the mean of the control with test drugs using statistical software of the GraphPad prism. n = 5 independent observations and $P < 0.05$ as shown in individual pages.

CHAPTER THREE

ANTICANCER EFFECTS OF *VIOLA PHILIPPICA* CAV AND *VIOLA YEDOENSIS* MAKINO

3.1 Isolation, identification and structures of cyclotides from *V. philippica* and *V. yedoensis*

The combined acid hydrolysis and ninhydrin test indicated that butanol fractions of *Viola philippica* and *Viola yedoensis* (VP-MW-BU and VY-MW-BU) contained rich cyclotides. In order to identify the sequence and structures of the cyclotides, the butanol fractions were separately passed through silica gel column chromatography with $CHCl_3$:MeOH solvent system with increasing percentage of MeOH for isolation of cyclotides-rich fractions according to pre-established procedure (Claeson et al., 1998, Göransson et al., 2004, Tan & Zhou, 2006, Wang et al., 2007, He et al., 2011a). Then different fractions of the cyclotides- enriched fractions of *V. philippica* and *V. yedoensis* respectively (Table 1 and 2) were further tested for the presence of cyclotides using Ninhydrin test per previously established procedure for cyclotides colour reactions tests (Tan & Zhou, 2006) (Table 1 and 2). Different fractions of the Viola exhibited varied degree of colouration with ninhydrin tests. These were further confirmed by MALDI-MS. The most highly cyclotides - rich fractions VPF7- VPF9 (**Table 3.1**) of *V. philippica* and VYF7- VY9 for *V. yedoensis* (**Table 3.2**) were further purified with reversed-phase HPLC and detected by UV light spectroscopy (215 nm) (Figure 3.1 and 3.2).

Table 3.1 Silica gel column chromatography fractions from butanol fraction of *Viola philippica* (VP-MW-BU) and their ninhydrin test results. Fractions VPF7 –VPF9 were purified by HPLC to obtain cyclotides VP18 (5 mg) and VP19 (4 mg) (Figure 3.1).

Code used for fractions (F1-F 9)	Description of solvent system used for elution of each fraction	Weight (mg)	Test for cyclotides
VPF1	$CHCl_3$:MeOH (4:1)	102	+
VPF2	$CHCl_3$:MeOH (3:1)	390	++
VPF3	$CHCl_3$:MeOH (2:1)	300	++
VPF4	$CHCl_3$:MeOH (1:1)	341	++
VPF5	$CHCl_3$:MeOH (1:2)	219	++
VPF6	$CHCl_3$:MeOH (1:3)	83	++
VPF7	$CHCl_3$:MeOH (1:4)	61	+++
VPF8	MeOH (100%)	137	+++
VPF9	MeOH: H_2O (3:1)	71	+++

Table 3.2 Silica gel column chromatography fractions from butanol fraction of *Viola yedoensis* (VY-MW-BU) and ninhydrin tests. Fractions F7 – F9 was purified by HPLC to get two major cyclotides fractions eluted at 18 and 19 min. These were lyophilized to give VY18 (5 mg) and VY19 (6 mg).

Code used Fractions (F1 – F9)	Description of Solvent system used for elution of each fraction.	Weight	Test for cyclotide observation
VYF1	$CHCl_3$: MeOH (4:1)	2.8g	+
VYF2	$CHCl_3$: MeOH (3:1)	2.3g	+
VYF3	$CHCl_3$: MeOH (2:1)	430mg	++
VYF4	$CHCl_3$: MeOH (1:1)	2.1g	++
VYF5	$CHCl_3$: MeOH (1:2)	728mg	++
VYF6	$CHCl_3$: MeOH (1:3)	250mg	++
VYF7	$CHCl_3$: MeOH (1:4)	117mg	++++
VYF8	MeOH	200mg	++++
VYF9	MeOH: H_2O (3:1)	680mg	++++

The cyclotides eluted from the RP-HPLC chromatogram peaks VP18 and VP19 from *V. philippica* (Figure 3.1), and VY18 and VY19 from *V. yedoensis* (Figure 3.2).

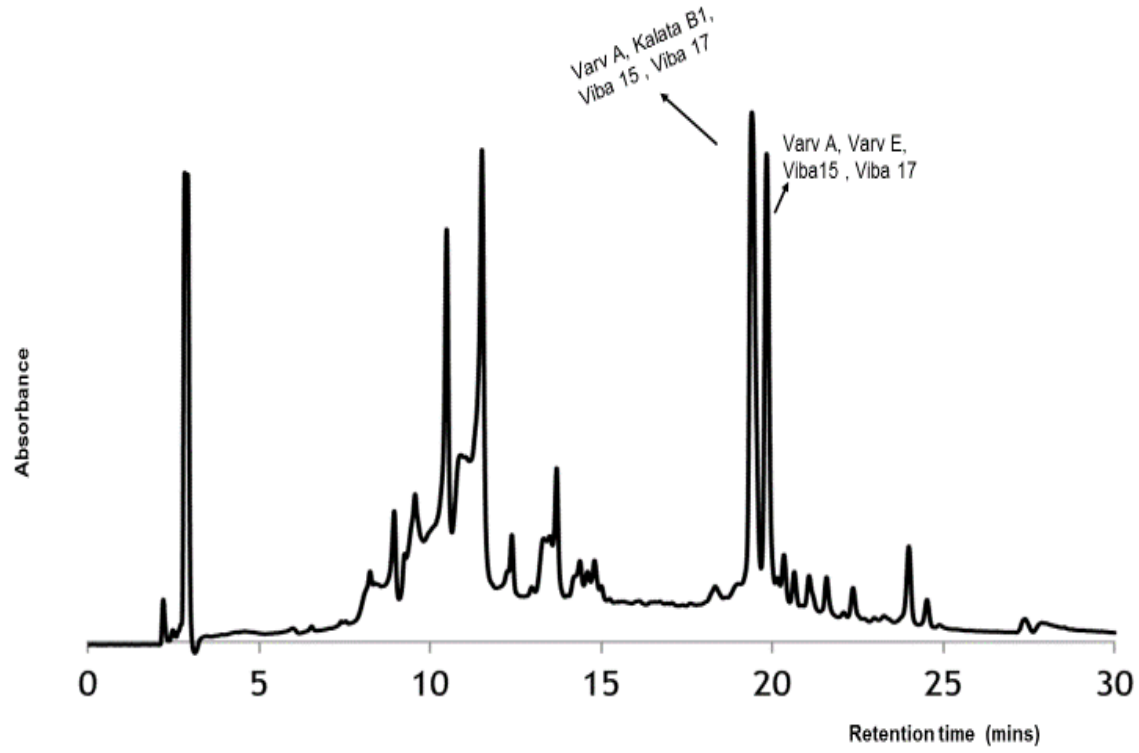

Figure 3.1 Semi-preparative HPLC chromatogram of the butanol fraction of *Viola philippica (*VP-MW-BU). VP18 (Varv A, Kalata b1, Viba 15, Viba 17 and VP19 (Varv A, Varv E, Viba 15, Viba 17; Solvent: Acetonitrile 80%: 0.1% trifloroacetic acid; UV-detector 215nm.

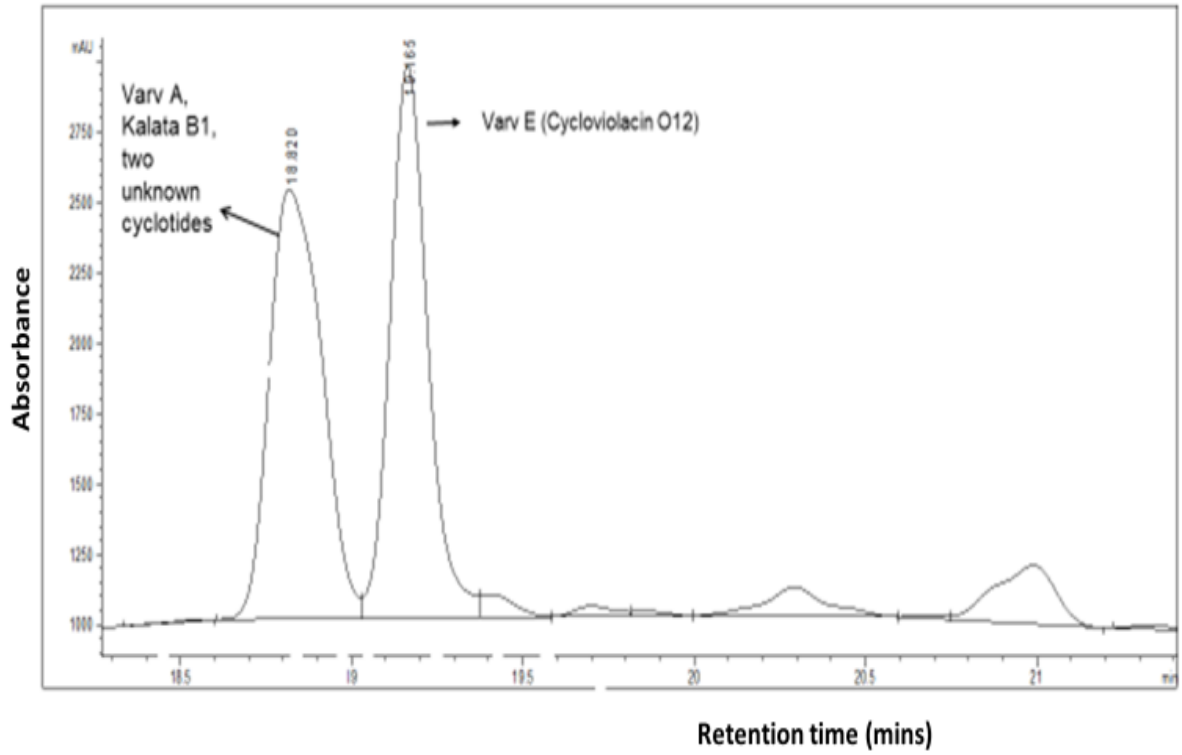

Figure 3.2 Semi-preparative HPLC chromatogram of cyclotides from *Viola yedoensis* (VY). VY18 (Varv A, Kalata b1, and two unknown peptides) and VY19 (Varv E = cycloviolacin O12). The average molecular masses of the two unknown cyclotides which were determined by liquid column chromatography -mass spectrometer (LC-MS) electron-spray ionization (Waters Micromass Q- TOF premium mass spectrometer) were found to be 2907.960 and 2894.006 Da. Solvent gradient at initial time: (A: 5% Acetonitrile: 0.1% Formic acid) and final time (B: 95% Acetonitrile: 0.1% formic acid) increased from low organic to high organic. Ion source is electron spray ionization (ESI-nano spray); Fragmented mode is CID, CAD, IRMPD (y and b-ions); MS scan mode is Quadrupole; MS-MS mode is Time of Flight (TOF).

The molecular masses of the cyclotides, VP18, VP19, VY18 and VY19 were evaluated using HPLC directly coupled (online) to mass spectrometer (LC-MS) by electronspray ionization potential (Figure 3.3) and by tandem mass spectrometer(MS/MS) using Quadrupole- Time of flight (Q-TOF) mass spectrometer. There was an observed increase in molecular mass of cyclotides by 6Da after reduction by TCEP (Figures 3.4 and 3.5) which could signify the presence of three disulphide bonds in cyclotides. This is consistent with previous studies (He et al 2011). The MS/MS sequencing of TCEP-reduced and enzymes (trypsin/Endo-Glu-C/chymotrypsin) digested cyclotides resulted to identification of primary structures of alignments of the sequences of the cyclotides from *V. philippica* (VP) and *V. yedoensis* (VY) (Figures 3.6 and 3.7). The primary structures (sequence) of the cyclotides were identified by comparison of alignments of the sequences of the cyclotides obtained with the literature search from CyBase (database of known cyclotides) (He et al., 2011). For instance, VP18 were identified to contain Varv A (Figure 3.6), Kalata b1, Viba 15, Viba 17 (42:26:21:11). VP19 contained cyclotides Varv A, Varv E, Viba 15, and Viba 17 (44:11:17:28) (Figure 3.7). VY18 contained Varv A, Kalata b1, and two unknown peptides co-eluted in this peak and VY19 was Varv E (Cycloviolacin O12). The monoisotopic molecular masses of the two unknown cyclotides co-eluted in VY18 are 2907.960 and 2894.006 (Figure 3.3 and 3.4). The data obtained were in consistent with previous works (Wang et al. 2008; He et al. 2011a).

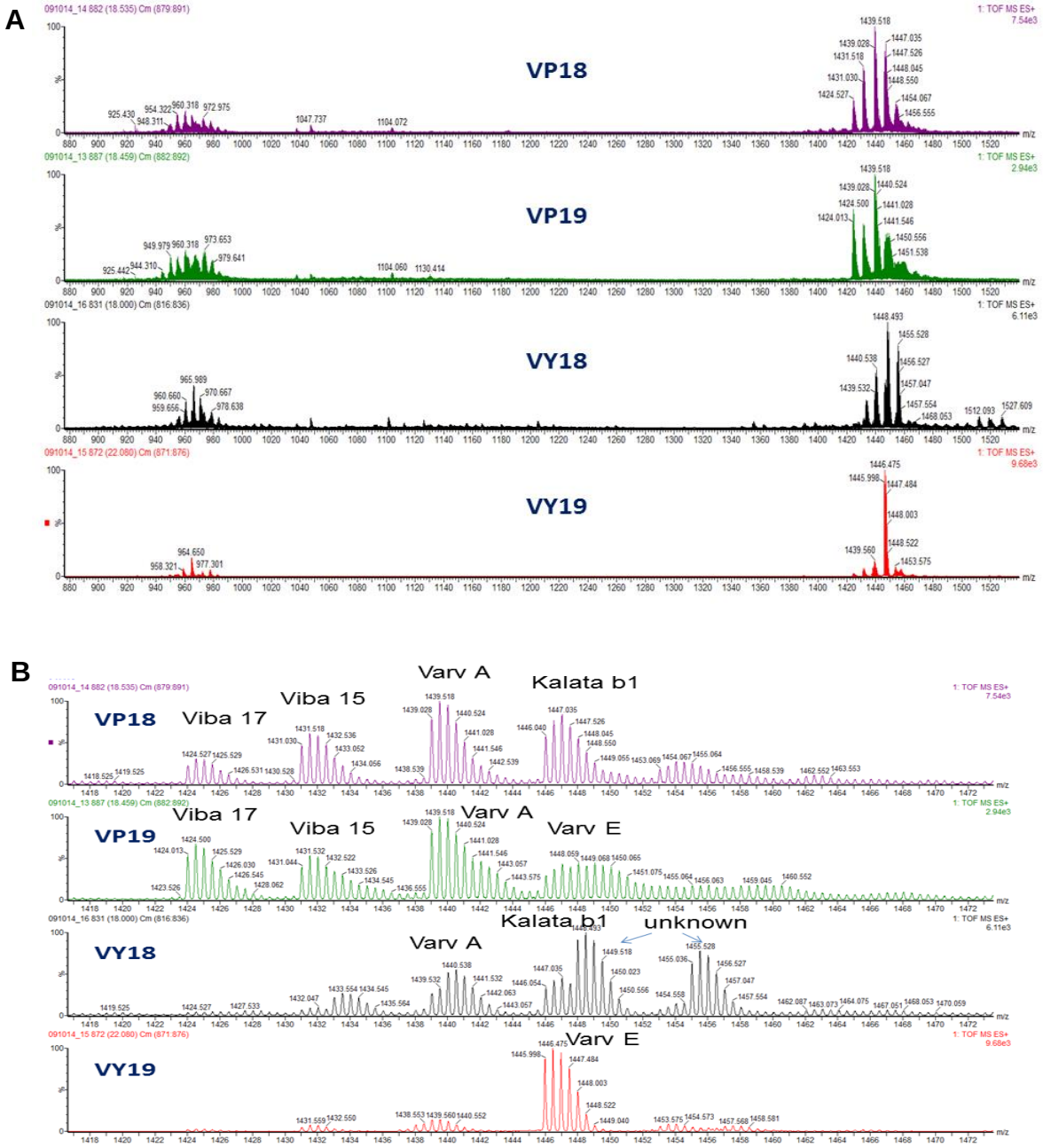

Figure 3.3 LC-MS analysis of cyclotides of *Viola philippica* 10µL (VP18 and VP19) and *Viola yedoensis* 10µL (VY18 and VY19) after reduction and enzyme digest were injected into HPLC -MS (ESI) The bottom graph is an expansion of top graph. Solvent gradient at Initial time: (A: 5% Acetonitrile: 0.1% Formic acid) ending time (B: 95% Acetonitrile: 0.1% formic acid) increased from low organic to high organic.

After first semi - HPLC purification, 200µL of the major chromatogram peaks - 20µg (VP18, VP19, VY18 or VY19) were separately subjected to reduction and alkylation

of cysteine with 1µL of 0.1M buffered TCEP to identify the presence of three disulfide residues which suggested the presence of cyclotides. These peaks were subsequently subjected to enzymatic cleavage using Endo- GluC that targets C-terminal bond cleavage and further digested using trypsin which cleaves at carboxyl - terminal of arginine and lysine residues to create a sequence specific peptides with basic carboxyl terminal (Steen and Mann, 2004). Also in ESI the tryptic peptides are double charged and y-ions are common. The final products, 10 µL each peptide was further injected to HPLC which was directly coupled online to mass spectrometer (LC-MS)- The Waters Q-TOF premium Mass spectrometer. The peptides were separated and analyzed (Figure 3.3) by mass to charge ratio through electron spray ionization potential mechanism (Steen and Mann, 2004). The signal intensity or mass spectrum is directly proportional to analyte concentration (Steen and Mann, 2004). Here the peptides were eluted per their hydrophobicity using gradient solvent elution with increasing organic solvent (0.1% Formic acid: 95% Acetonitrile). The most hydrophobic would be late -eluted and the most hydrophilic would be first eluted (Steen and Mann, 2004). The peptides produced at this stage are known as tryptic peptides (which are usually doubly charged in electron-sprayed ionization) or precursor peptides (Figures 3.3 -3.5) with quadrupole mode. These ions were further fragmented by MS-MS using Tandem - mass spectrometer (MS/MS) by time of flight (TOF) mass spectrometer scan mode to obtain the final Tandem-MS spectrum of the peptides sequence which produced y-ions or b-ions (Steen and Mann, 2004). Usually y-ions are common in tryptic peptides. The sequence specific ions were further analyzed by Peptide-search, to identify the peptide sequence using mascort generic file search engine and Denovosequence auto software. The results of the sequence alignment obtained were compared to or matched with existing peptide database –

search in CyBase library of cyclotides sequence to identify the actual sequence (Figures 3.6 - 3.7).

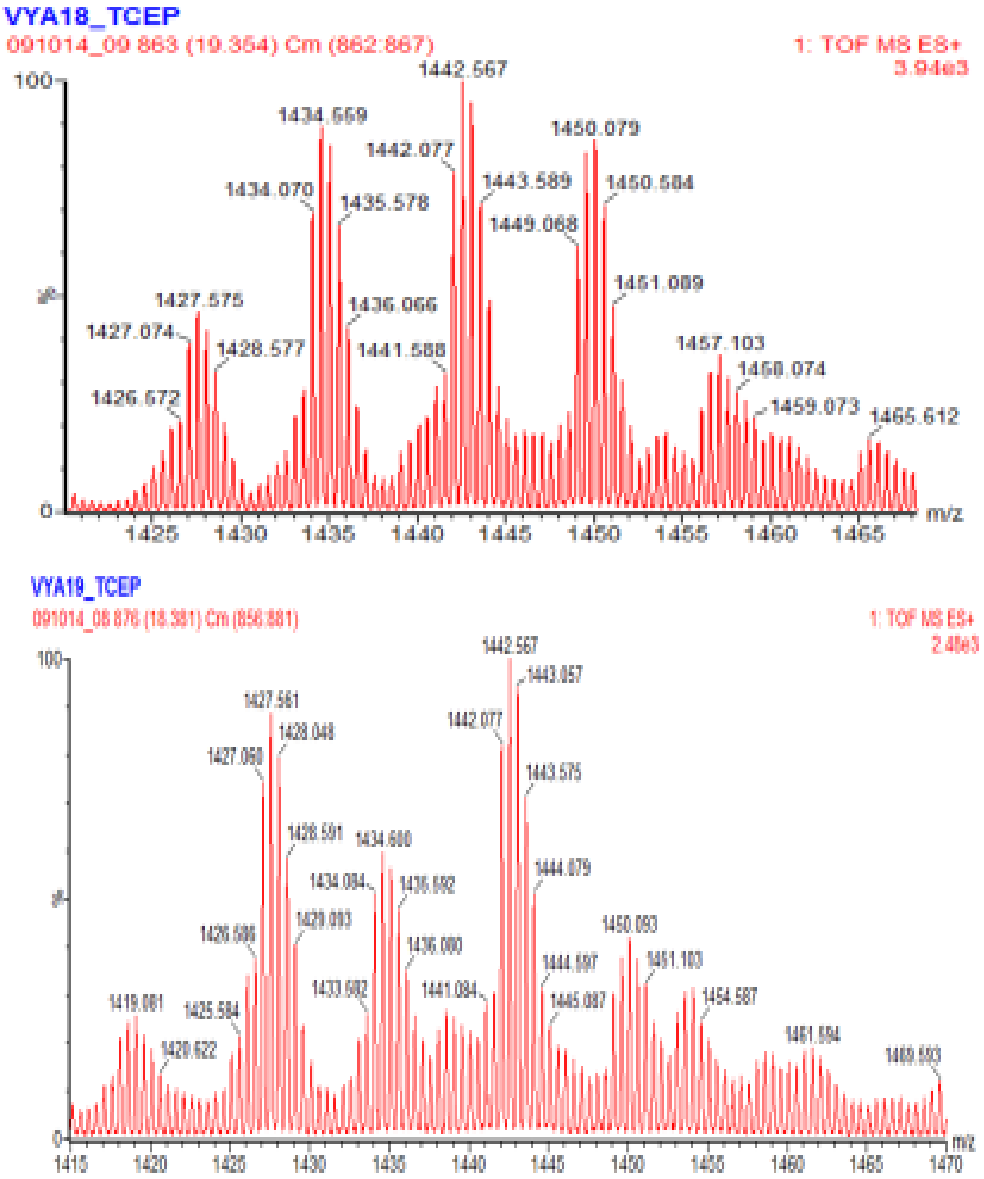

Figure 3.4 ESI-MS of *Viola philippica* cyclotides - VP18 (top) and VP19 (bottom) after TCEP reduction. Ion source is electronspray ionization (ESI-nano spray).

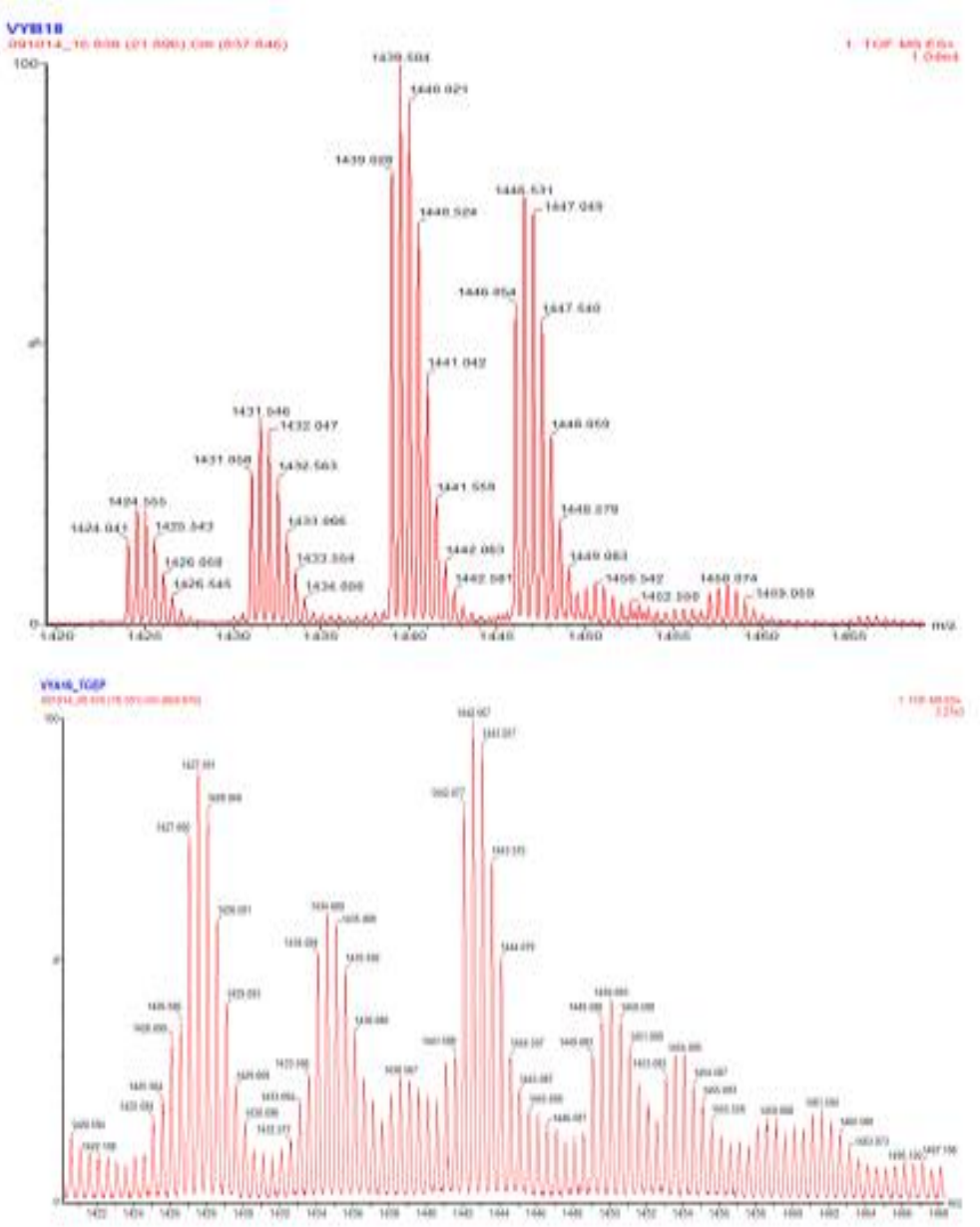

Figure 3.5 ESI-MS of cyclotides VY18 (top) and VY19 (bottom) from *Viola yedoensis* after TCEP reduction. Ion source is electronspray ionization (ESI-nano spray).

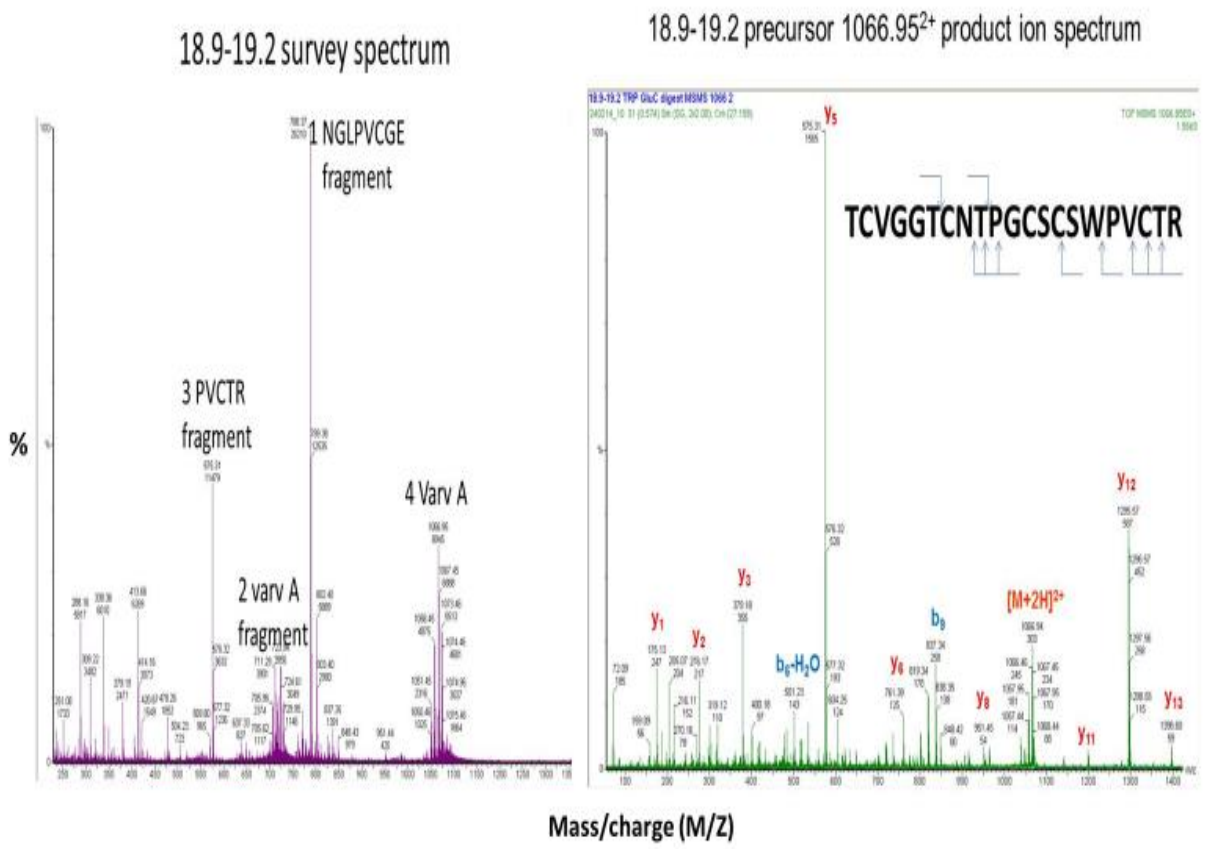

Figure 3.6 Mass Spectrum of Varv A cyclotide in VP18 after TCEP reduction, enzymatic digestion (left) and MS/MS spectrum of a fragment peptide-4 (right). Ion source is electronspray ionization (ESI-nano spray); Fragmented mode is CID, CAD, IRMPD (y and b-ions); MS scan mode is Quadrupole; MS-MS mode is Time of Flight. This shows the bioactive cyclotide to be Varv A (GLPVCGETCVGGTCNTPGCSCSWPVCTRN).

The isolated column chromatography fraction of Viola yedeonsis extract were purified by HPLC to identify major peaks and separate the pure compounds. The major peaks were subjected to reduction and alkylation of cysteine to identify the presences of

three disulfide residues which suggest the presence of cyclotides. These peaks were separately subjected to enzymatic cleavage using Endo- GluC that targets C-terminal bond cleavage and further digested using trypsin. The final products were further subjected to separation by HPLC with direct online couple to mass spectrometer (LC-MS) which separated and analyzed the peptides by mass to charge ratio through electronspray ionization potential mechanism (Steen and Mann, 2004). The signal intensity or mass spectrum is directly proportional to analyte concentration (Steen and Mann, 2004). Here the peptides were eluted per their hydrophobicity using gradient solvent elution with increasing organic solvent (0.1% Formic acid: 90% Acetonitrile). The most hydrophobic would be late -eluted and the most hydrophilic would be first eluted (Steen and Mann, 2004). The electron-sprayed ionized, purified and separated peptide ions were which was scanned by quadrupole mode were further fragmented using tandem Mass Spectrometer (MS-MS) by time of flight (TOF) scan mode .Then the cyclotides sequence were determined or identified using Mascort generic file search engine and Denovosequence computer auto software peptide-search applications to analyze the peptide ions for sequence (Steen and Mann, 2004).The results of sequence alignment obtained were compared or matched with already known sequence in the peptide sequence database - searching of library of cyclotides sequence (CyBase) (Figure 3.6 - 3.87).

cyclotides	loop4 I loop1 II loop2 III loop3 IV V loop5 VI loop 6	Theoretic mass (monoisotopic)	Expt. mass
Varv A	CGETCVGGTCNTPGCSCSWPVCTRNGLPV	2876.17	2876.06
Kalata b1	CGETCVGGTCNTPGCTCSWPVCTRNGLPV	2890.14	2890.11
Viba 15	CGETCVGGTCNTPGCACSWPVCTRNGLPV	2860.18	2860.12
Viba 17	CGETCVGGTCNTPGCGCSWPVCTRNGLPV	2846.02	2846.08
Varv E = Cylcoviolacin O12	CGETCVGGTCNTPGCSCSWPVCTRNGLPI	2890.14	2890.00

Figure 3.7 Alignment of the sequences of the cyclotides isolated and identified from *V. philippica* (VP) and *V. yedoensis* (VY). The cysteine residues numbered as I-VI are highlighted in red colour and the backbone loops are numbered as loop1-6.

3.2 Anticancer activities of the crude extracts and cyclotides of *V. philippica* and *V. yedoensis*

The anti-cancer activities of extracts and cyclotides of *V. philippica* and *V. yedoensis* on different ovarian cancer cell lines (Igrov-1; A2780 and Ovcar-8) were done using cell growth assay. The results showed that the butanol fraction and the cyclotides of *V. philippica* (VP18 and VP19) and *V. yedoensis* (VY18 and VY19) exhibited significant growth inhibition activities on different ovarian cancer (Igrov-1, A2780 and Ovcar-8) cell lines (Tables 3.3 and 3.4; Figures 3.8 – 3.11). The cyclotide, Varv E

appeared to be mostly potent against the three ovarian cell lines tested (Table 3.4 and Figure 3.8). All the cyclotides identified possess glutamic acid residues in loop 1 (Figure 3.7). This is consistent with previous reports which revealed that glutamic acid residues in loop 1 and hydrophobicity of cyclotides are essential for cytotoxicity of cyclotides (He et al. 2011a; Hermann et al. 2006; Tang et al. 2010).

Table 3.3 Cytotoxicity IC_{50} of fractions and cyclotides from V. philippica (VP). Data represented as mean ± SEM of the IC_{50}, n = 5 independent experiments.

Sample code	cyclotides	50% concentration inhibition (IC_{50}) on cell lines		
		Igrov-1	A2780	Ovcar-8
VP-MW-BU	n-Butanol fraction	6.9±0.1 µg/mL	6.5± 0.4 µg/mL	14.7±1.0 µg/mL
VP18	Varv A, Kalata b1, Viba 15, Viba 17 (42:26:21:11)	8.6±0.5 µM	4.1±0.3 µM	9.9±0.6 µM
VP19	Varv A, Varv E, Viba 15, Viba 17 (44:11:17:28)	10.8±1.8 µM	6.9±0.6 µM	11.1±0.8 µM

Table 3.4 Cytotoxicity of fractions and cyclotides from V. yedoensis (VY). Data represented as Mean ± SEM of the IC_{50}, n = 5 independent experiments.

Sample Code	**cyclotide**	**50% concentration (IC_{50}) on cell lines**		**inhibition**
		Igrov-1	A2780	Ovcar-8
VY-MW-BU	n-Butanol fraction	6.7±0.1 µg/mL	6.4±0.4 µg/mL	14.5±1.0 µg/mL
VY18	Varv A, Kalata b1, and two unknown peptides	11.5±0.4 µM	9.5±0.3 µM	11.2±0.3 µM
VY19	Varv E=Cycloviolacin O12	5.5±0.3 µM	5.7±0.2 µM	6.5±0.4 µM

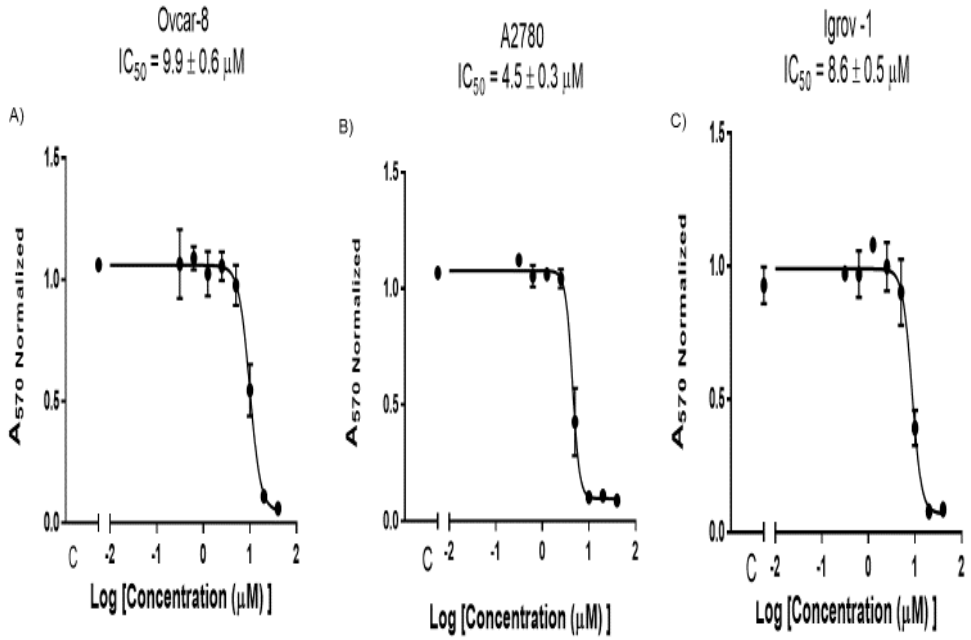

Figure 3.8 Concentration-response curves of VP18 [Varv A, Kalata b1, Viba 15, Viba 17 of *Viola philippica* against Ovcar-8 (A), A2780 (B), Igrov-1 (C) ovarian cancer cell lines with normalized (to control) absorbance at 570nm. At concentrations or dose range tested (0.16 – 40µM), VP18 showed cytotoxicity of the ovarian cancer cell at doses of 5, 10, 20 and 40µM.There was no observed cytotoxicity effects observed below 5µM of VP18. A_{570} on y-axis, represents normalized absorbance at 570nm (optical density). Graph determined by four parameters fitting sigmoid curve (graph pad prism). Data represented as mean ± SEM of IC_{50}. C represents IC_{50} of control (no drug, only medium). n = 5 independent experiments.

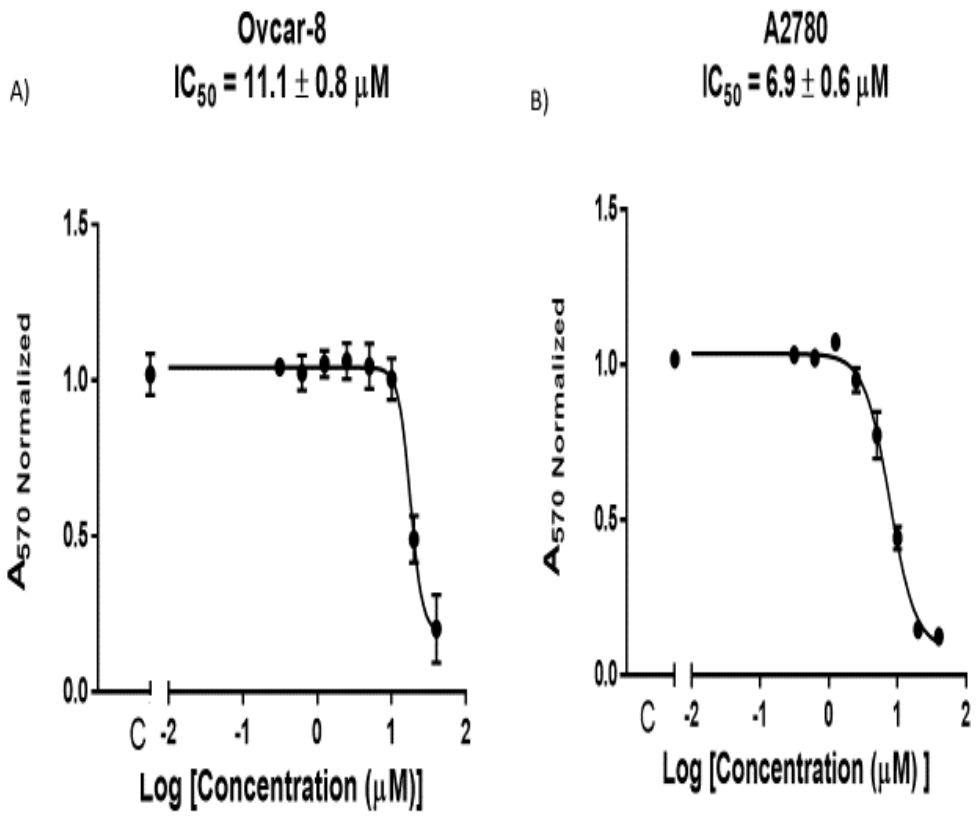

Figure 3.9 Concentration-response curves of VP19 [Varv A, Varv E, Viba 15, Viba 17 of *Viola philippica* on Ovcar-8 (A) and A2780 (B) ovarian cancer cell lines with normalized (to control) absorbance at 570nm. At concentrations or dose range tested (0.16 – 40μM), VP19 showed cytotoxicity of the ovarian cancer cell at doses of 5, 10, 20 and 40μM.There was no observed cytotoxicity effects observed below 5μM of VP19.A_{570} on y-axis represents absorbance at 570nm (optical density) normalized. Graph determined by four parameters fitting sigmoid curve (graph pad prism). Data represented as mean ± SEM of IC_{50}. C represents IC_{50} of control (no drug). n = 5 independent experiments

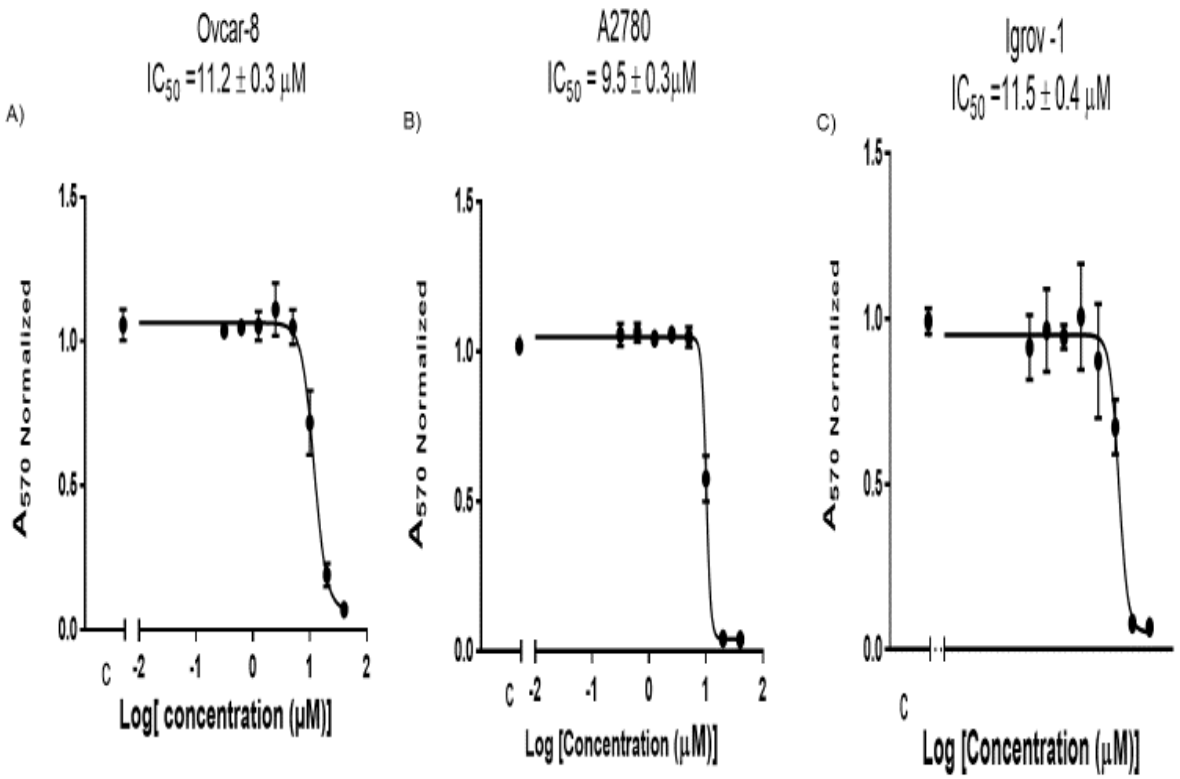

Figure 3.10 Concentration-response curves of VY18 [Varv A, Kalata b1, and two unknown peptides] of Viola yedoensis on Ovcar-8 (A), A2780 (B), Igrov-1 (C) cancer cell lines with normalized (to control) absorbance at 570nm. At concentrations or dose range tested (0.16 – 40µM), VY18 showed cytotoxicity of the ovarian cancer cell at doses of 5, 10, 20 and 40µM.There was no observed cytotoxicity effects observed below 5µM of VY18. A_{570} represents absorbance at 570nm. (optical density). Graph determined by four parameters fitting sigmoid curve (graph pad prism). Data represented as mean ± SEM of IC_{50}. C represents IC_{50} of control (no drug). n = 5 independent experiments.

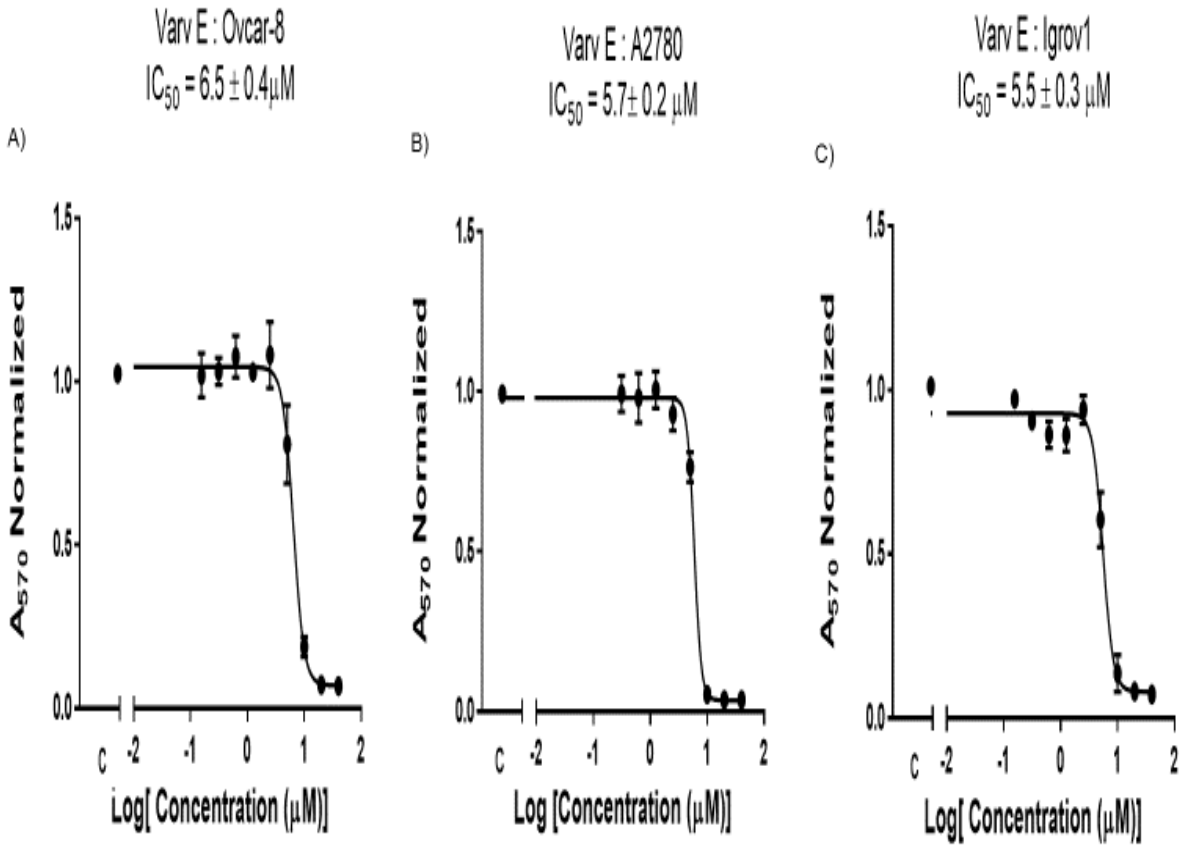

Figure 3.11 Concentration-response curves of VY19 (Varv E = Cycloviolacin O12) of *Viola yedoensis* on Ovcar-8 (A), A2780 (B), Igrov-1 (C) cancer cell lines with normalized (to control) absorbance at 570nm. At concentrations or dose range tested (0.16 – 40μM), VY19 showed cytotoxicity of the ovarian cancer cell at doses of 5, 10, 20 and 40μM.There was no observed cytotoxicity effects observed below 5μM of VP19. A_{570} represents absorbance at 570nm (optical density) normalized. Graph determined by four parameters fitting sigmoid curve (graph pad prism) Data represented as mean ± SEM of IC_{50}. C represents IC_{50} of control (no drug). n = 5 independent experiments.

3.3 Anti-malarial activities of the fractions of *V. philippica*

The preliminary *in vitro* anti-malarial activities of *V. philippica* extracts and fractions were assayed on chloroquine- resistant malaria strain *of Plasmodium* falciparum. Results showed that different extracts and fractions of *Viola philippica,* at concentrations of 5µg/mL, 50µg/mL and 500µg/mL caused decrease in percentage growth (parasitamia) of the malaria parasites (Figure 3.12). The butanol fraction (VP-MW-BU), aqueous extract (VP-MW-A1), aqueous fraction seaparated from butanol/water factionation (VP-MW-A2), dichloromethane crude extract (VP-DCM), the methanol crude extract (VP-MW) inhibited growth of malaria parasites (Figure 3.12).

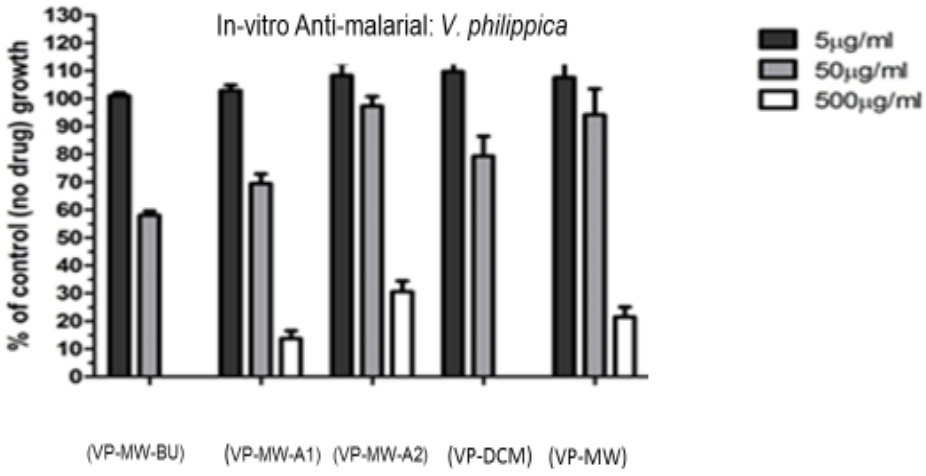

Figure 3.12 *In-vitro* preliminary antimalarial assay of different doses (5, 50 and 500 µg/mL) of extract and fractions of *Viola philippica.* VP-MW-BU represents butanol fraction; VP-MW-A1, water extract; VP-MW-A2, aqueous lower fraction; VP-DCM, dichloromethane extract, and VP-MW, crude MeOH extract.

From the results of *V. philippica* (Figure 3.12), at 50µg/mL the butanol fraction (VP-MW-BU) showed highest percentage growth inhibition about 55% while aqueous fraction (VP-MW-A2) exhibited the least percentage parasite growth inhibition (Figure 3.12).

The butanol fraction (VY-MW-BU) of *Viola philippica* was subjected to silca gel column chromatography ($CHCl_3$:MeOH) as previously described (Tab 3.1). The different column fractions at concentrations (0.5, 5 and 50µg/mL) showed different percentage growth inhibition (Fig 3.13). The significant percentage growth inhibition was observed at concentration of 50µg/mL in all the fractions (Fig 3.13). Fraction VPF6 exhibited most significant percentage growth inhibition with 10% growth of malaria parasite at 50µg/mL. VPF5 showed about 15% parasite growth at 50µg/mL, VPF3 20% and VPF1 30% (Fig 3.13). The rest of the fractions (VPF2, VPF4, VPF7 and VPF8) exerted 50% and above parasite growth at 50µg/mL (Figure 3.13). This suggested that *V.philipicca* exhibited moderate *in vitro* anti-malarial activity. No further identification was carried out at this stage.

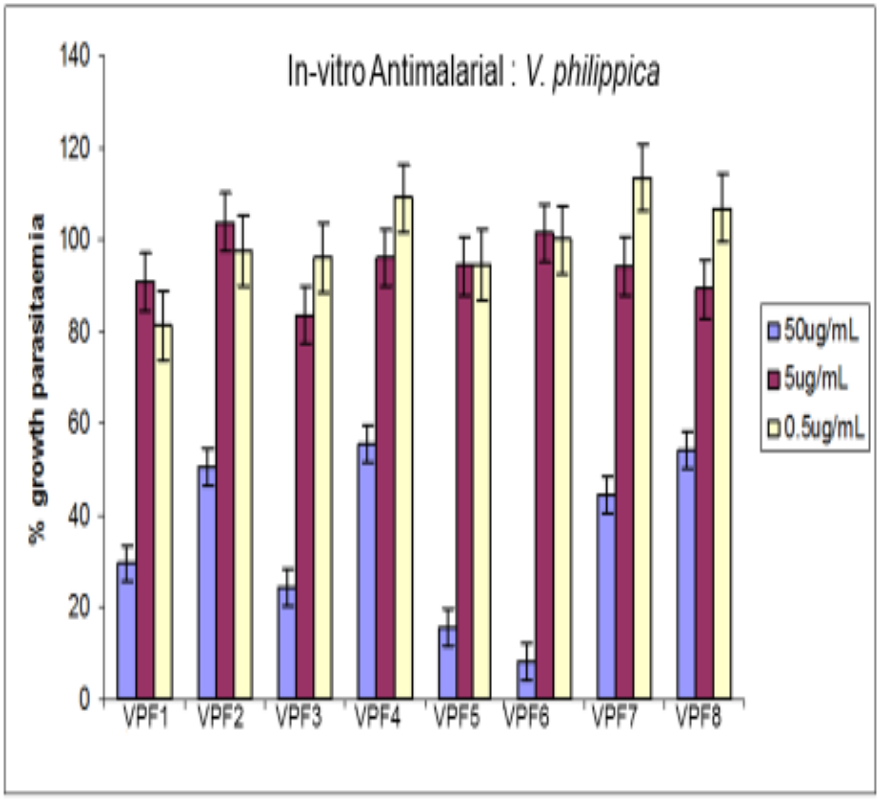

Figure 3.13 Antimalarial activities of silica gel column chromatography fractions of butanol extract of *Viola philippica*. VPF1 represents first silica gel column chromatography (chloroform: MeOH) fraction (Table 3.1) of butanol fraction of *V. philippica* (VY-MW-BU).

3.4 Discussion

In this study, we have isolated, purified, characterized, identified and elucidated primary structures of cyclotides from *V. philippica* [(VP18: Varv A, Kalata B1, Viba 15, and Viba 17) and (VP19: Varv A, Varv E, Viba 15, and Viba 17)] and *V. yedoensis*

[(VY18: Varv A, Kalata B1, and two unknown peptides) and (VY19: Varv E)]. All the identified cyclotides are known. The two unknown cyclotides with molecular masses of 2907.960 and 2894.006 Da, found co-eluted in VY18 are still undergoing further analysis for their proper identification and structure elucidation.

We have also carried out scientific investigation and could establish scientific data on the *in vitro* anti-ovarian cancer activities of the cyclotides of *V. philippica* and *V. yedoensis.* Although the cytotoxicity of cyclotides had previously been reported (Herrmann et al., 2008, Wang et al., 2007, Tang et al., 2010, Svangård et al., 2004, Lindholm et al., 2002, He et al., 2011a) this is a novel report of the anti-ovarian cancer activities of Varv E and anti-cancer activities of *V. yedoensis.* Varv E could serve as a starting material in drug discovery in search of anti-ovarian cancer drug with more potent or improved anti-ovarian cancer activity. However structural elucidation of the unknown peptides from *V. yedoensis* is on-going. We have equally done some preliminary in-vitro antimalarial screening of extracts or fractions from *V. philippica*. This report therefore, is a novel report of antimalarial effects of *V. philippica.* However, further study needs to be done to determine the IC_{50} of *V. philippica* on malaria parasite.

CHAPTER FOUR

ISOLATION, IDENTIFICATION AND ANTI-CANCER ACTIVITY OF ALKALOIDS FROM TRICLISIA SUBCORDATA

4.1 Results of phytochemical screening tests of extract of *T. subcordata* root

The preliminary phytochemical screening of ethanol extract of *Triclisia subcordata* root was carried out to identify possible metabolites of crude extracts of *Triclisia subcordata* root. The preliminary screening tests revealed the presence of alkaloids, saponins, tannins, steroids (phytosterols), flavonoids, and terpenes (Table 4.1 and 4.2).

Table 4.1 Preliminary phytochemical screening results of ethanol extracts *Triclisia subcordata* root.

Phytoconstituents	Inference
Alkaloids	+++
Saponins	++
Tannins	+++
Flavonoids	++
Free Anthraquinone	-
Combined anthraquinones	-
Terpenes/sterols	++
Carbohydrates	+
Cardiac glycosides	-

+ Slightly present; ++ moderately present; +++ much present; - absent.

The extraction and fractionation of *T. subcordata* (Figure 2.2 and 2.3) yielded the total crude extract (TSS), the total alkaloid (TSS1), the aqueous fraction (TSS2) and the aqueous methanol fraction (TSS3). Both TSS1 and TSS3 showed positive Dragendorff's tests, which indicated the presence of alkaloids in these fractions. The TSS1 was further fractionated by silica gel column chromatograph using $CHCl_3$: MeOH gradient elution to get different fractions F1 - F47 (Table 4.2).

Table 4.2 Isolated alkaloids and fractions from total alkaloids (TSS1) of *T. subcordata* by silica gel column chromatography.

Codes for fractions from TSS1	Dragendorff's test	weights	TLC and Dragendorff's tests observation.
F1-4	--	106mg	No colouration.
F5	+++	727mg	Single spot (cycleanine)
F6	+++	5. 82g	Single spot (cycleanine)
F7	+++	1.40g	Single spot
F8	+++	1.28g	Single spot
F9	+++	1.76g	Double spots
F10-11	+++	3.17g	Double spots
F12	+++	140mg	Single spot
F13-17	+++	300mg	Double spots
F18-19	+++	350mg	Double spots
F20	+++	125mg	Double spot
F21-22	+++	150mg	Double spot
F23- 25	+++	409 mg	Double spot Recrystallization: MeOH
F26 -27	++	118mg	Multiple spots
F28-30	++	300mg	Multiple spots
F31-32	++	40mg	Double spots
F33-35	+++	120.9mg	Double spots
F36-38	++	106mg	Double pots
F39	++	30.3mg	Double spots
F44-47	++	36mg	Single spot

+ represents alkaloids present trace; ++ moderately present: +++ much present; -- absent

Different fractions eluted from $CHCl_3$: MeOH (99:1) to $CHCl_3$: MeOH (1: 99) as gradient elution gave non- alkaloids fraction (F1-4) that showed negative test results

with Dragendorff's test (Table 4.2); pure alkaloid fractions as F5-6 (identified as cycleanine); and other alkaloid fractions such as F7-47 with respective weights (Table 4.2). TLC under UV-lamp 360/540nm and using iodine tests and Dragendorff's tests also showed different degree of spots and intensity of orange coloration with these compounds, confirming the presence of alkaloids in these fractions (Table 4. 2).

4.2 Isolation and structure elucidation of alkaloids from *T. subcordata*

4.2.1 Structure elucidation of anticancer alkaloids from *T. subcordata*

Bioassay-guided fractionation of TSS1 resulted in isolation of three pure alkaloids using silica gel chromatography and/or HPLC (Figure 2.2, 2.3). The analytical HPLC and LC-MS were carried out to confirm the purity of the isolated componds in Figure 4.1. These were identified on the basis of spectroscopic data including LC-MS, ^{1}H NMR, and ^{13}C NMR (Figure 4.2-4.4 and Tables 4.3-4.6) as the BBIQ alkaloids cycleanine (**1**), isochondodendrine (**2**) and 2′-norcocsuline (**3**) in comparison with their spectroscopic data in the literature (Kanyinda et al., 1997, Liu et al., 2013). The quantitative analysis of analytical HPLC of total alkaloids (TSS1) revealed the percentage of pure BBIQ in *T. subcordata* as cycleanine 83.7%; isochondodendrine 7.5% and 2′-norcocsuline 1% (Figure 4.1A).

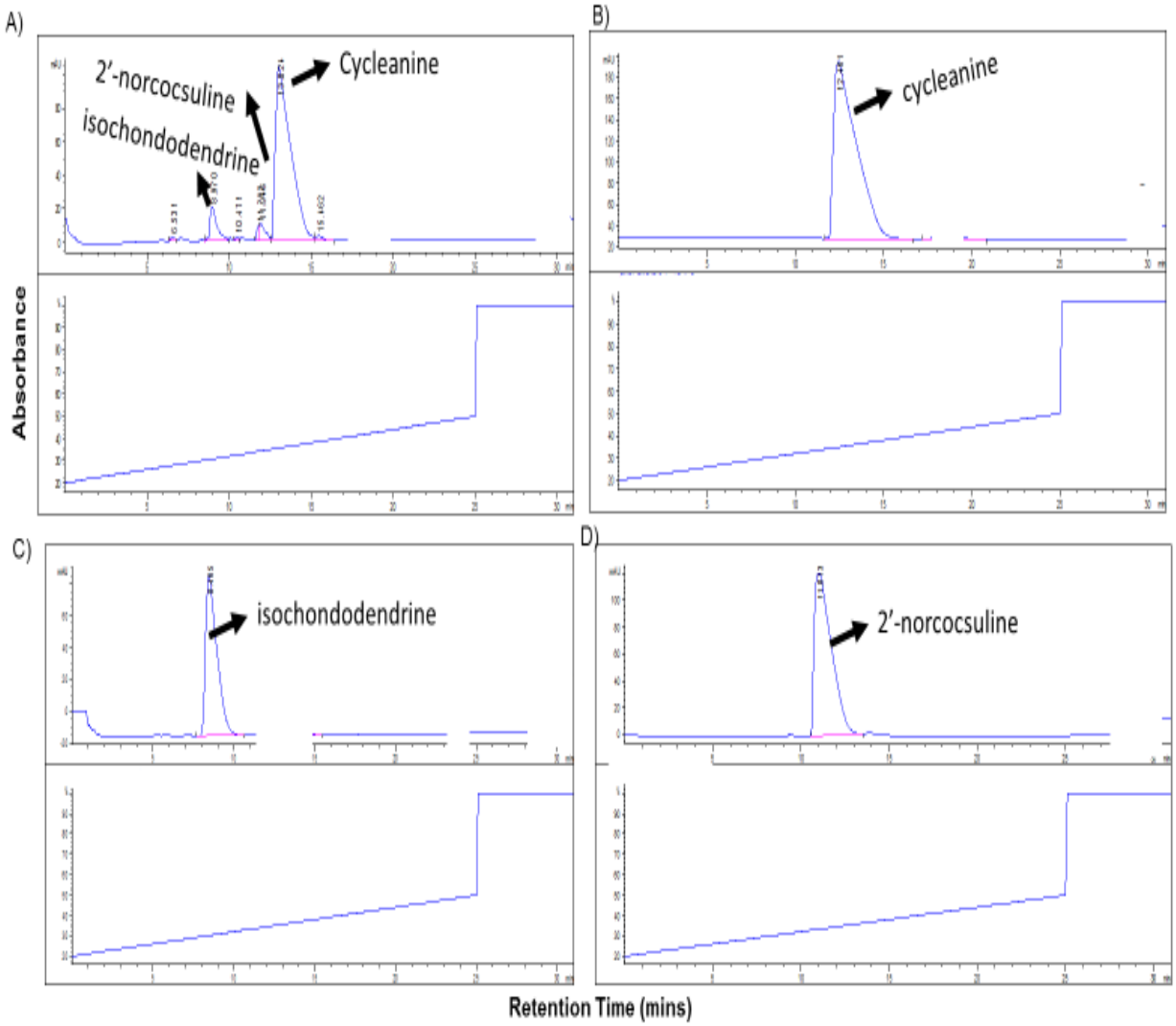

Figure 4.1 Chromatograms of analytical HPLC of total alkaloids (A), purified cycleanine (B), isochondodendrine (C) and 2′-norcocsuline (D). The peaks were correlated to the original peaks in the total alkaloid TSS1 (A) chromatogram from where they were purified.

Cycleanine was also isolated as a TFA salt form when using HPLC where the solvent system contained 0.1 % TFA. ^{1}H NMR and ^{13}C NMR of the TFA salt of cycleanine showed slight difference from those of cycleanine (Table 4.3 and 4.4). The structures of the three BBIQ alkaloids from *T. subcordata* were shown in Figure 4.2. Also, the

TFA salt of 2′-norcocsuline exhibited slight difference in ^{1}H NMR and ^{13}C NMR from 2′-norcocsuline, but when the pure alkaloid (base) from the TFA salt was re-extracted by the normal procedure for alkaloid extraction (previously described in Chapter 2) the observed ^{1}H NMR and ^{13}C NMR of 2′-norcocsuline became similar and comparable to the literature data for 2′-norcocsuline (Tables 4.5 and 4.6).

Cycleanine (Figure 4.2) has been isolated from many other plants species of the Menispermaceae family (Schiff, 1997). Cycleanine was shown to increase the intracellular doxorubicin accumulation in the resistant MCF -7 /Adr cell lines (Tian and Pan, 1997). Here cycleanine is being isolated and characterized from Triclisia subcordata as part of novel contribution to knowledge.

Tetrandrine, (Figure 4.2) an isomer of cycleanine is also a common BBIQ reported in different plants including *Triclisia subcordata* (Dwum-Badu et al 1995).Tetrandrine has been shown to exert various biological activities including anticancer, (Chen, 2002), antiallergic, anti-inflammatory, anti-malarial, and cardiovascular effects (Schiff, 1997).Tetrandrine inhibited the growth of various types of cancer cell line (Chen, 2009; He etal 2011; Xu et al 2011) and could reverse multi-drug resistance by inhibiting P-glyco protein activity (Sun and Wink, 2014).

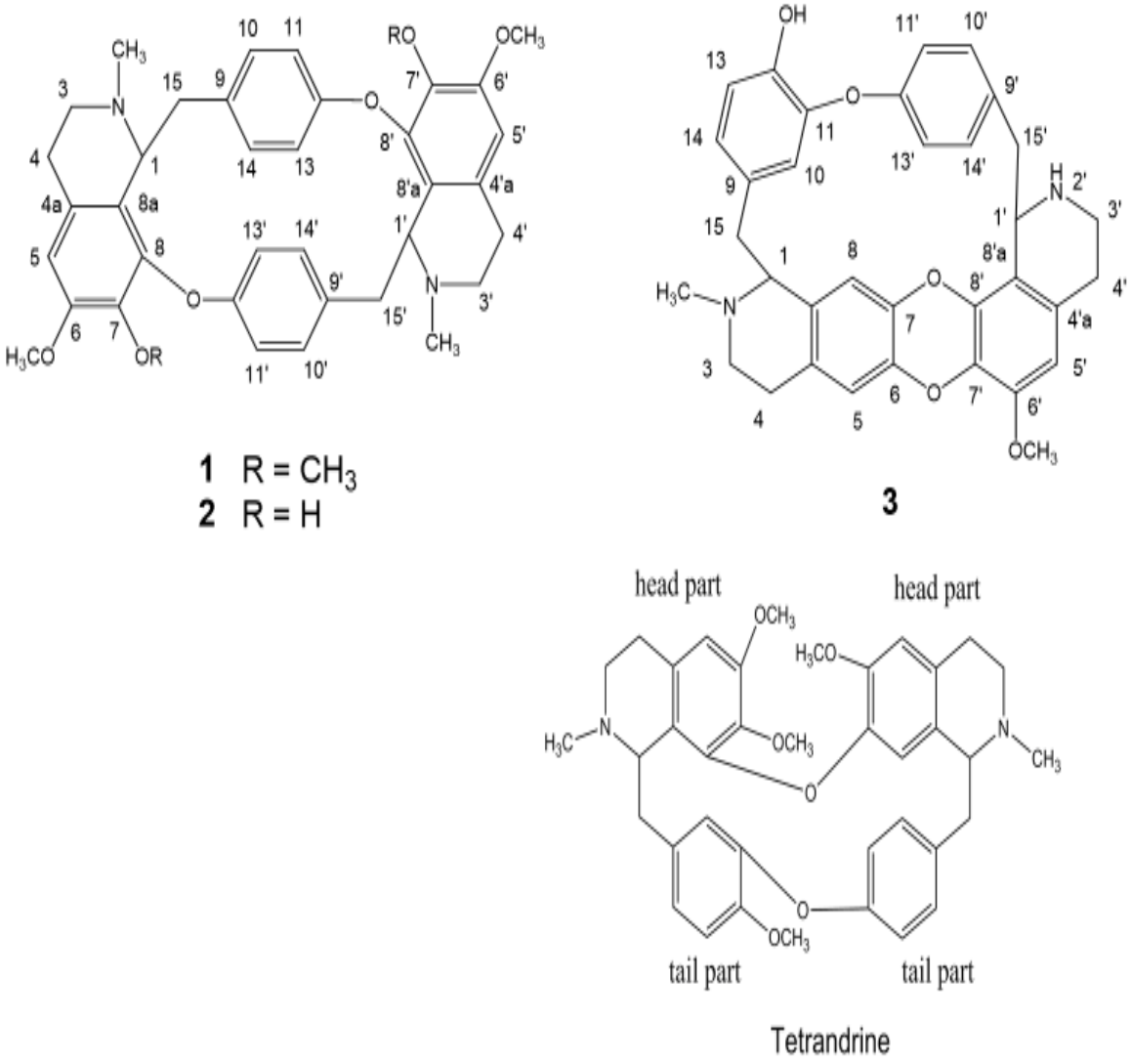

Figure 4.2 Structure of three BBIQ alkaloids, cycleanine (**1**), isochondodendrine (**2**) and 2′-norcocsuline (**3**) from *T. subcordata.* Tetrandrine is an isomer of cycleanine previously reported in *T. subcordata.* Structures reported per analysis of results from spectroscopic data from ^{1}H NMR (400 MHz, $CDCl_3$) (Table 4.3) and ^{13}C NMR (100 MHz, $CDCl_3$) (Table 4.4)

Table 4.3 ^{1}H NMR (400 MHz) chemical shift data (δ, ppm) for cycleanine (**1**), the TFA salt of cycleanine ($CDCl_3$), isochondodendrine ($CDCl_3$ + CD_3OD (1:1) (Figure 4.3) (**2**) (*J* values, in Hz, in parentheses).

Position	Compound (δ_H)		
	Cycleanine (**1**)	TFA salt of cycleanine	Isochondodendrine (**2**)
H-1	4.29, d (10.39)	4.97 br d (6.48)	4.28, d (10.72)
H-1′	4.29, d (10.39)	4.97 br d (6.48)	4.28, d (10.72)
H-3	α, 3.28 m; β, 2.92 m	α, 4.00 m; β, 3.24 m	α, 3.28 m; β, 2.92 m
H-3′	α, 3.28 m; β, 2.92 m	α, 4.00 m; β, 3.24 m	α, 2.92 m; β, 2.92 m
H-4	α, 3.05 m; β, 2.92 m	α, 3.46 m; β, 3.24 m	α, 3.15 m; β, 2.90 m
H-4′	α, 3.05 m; β, 2.92 m	α, 3.46 m; β, 3.24 m	α, 2.92 m; β, 2.92 m
H-5	6.57 s	6.66 s	6.57 s
H-5′	6.57 s	6.66 s	6.57 s
H-10	7.05 dd (8.44; 2.08)	7.27 (overlapped, brs)	7.00 (brd)
H-10′	7.05 dd (8.44; 2.08)	7.27 (overlapped, brs)	7.00 (brd)
H-11	6.66 dd (8.44; 2.81)	6.66 (overlapped, brs)	6.49 dd (8.29; 2.64)
H-11′	6.66 dd (8.44; 2.81)	6.66 (overlapped, brs)	6.49 dd (8.29; 2.64)
H-13	5.82 dd (8.31; 2.81)	5.79 br d (6.85)	5.74 dd (8.29; 2.64)
H-13′	5.82 dd (8.31; 2.81)	5.79 br d (6.85)	5.74 dd (8.29; 2.64)
H-14	6.28 dd (8.44; 2.20)	6.28 br d (7.70)	6.19 dd (8.29; 1.51)
H-14′	6.28 dd (8.44; 2.20)	6.28 br d (7.70)	6.19 dd (8.29; 1.51)
H-α	α, 2.52 m; β, 3.28 m	α, 2.77 m; β, 3.66 m	α, 2.50 m; β, 3.29 m
H-α′	α, 2.52 m; β, 3.28 m	α, 2.77 m; β, 3.66 m	α, 2.50 m; β, 3.27 m
6-OMe	3.81 s	3.87 s	3.75 s
6′-OMe	3.81 s	3.87 s	3.75 s
7-OMe	3.40 s	3.42 s	
7′-OMe	3.40 s	3.42 s	
N-Me	2.53 s	2.80 s	2.41s
N′-Me	2.53 s	2.80 s	2.41s
CF_3COOH		12.26 s	

Table 4.4 ^{13}C NMR (100 MHz) chemical shift data (δ, ppm) for cycleanine (**1**), the TFA salt of cycleanine ($CDCl_3$), isochondodendrine ($CDCl_3$ + CD_3OD (1:1) (Figure 4.4) (**2**).

Carbon	Compound (δ_C)		
	Cycleanine (**1**)	TFA salt of cycleanine	Isochondodendrine (**2**)
1 (1′)	60.09	60.81	59.65
3 (3′)	44.63	43.89	44.15
4 (4′)	24.67	21.64	23.20
4a (4a′)	130.31	129.35	129.27
5 (5′)	109.22	108.87	108.21
6 (6′)	152.01	153.95	148.04
7 (7′)	139.02	140.20	136.18
8 (8′)	143.77	144.79	138.29
8a (8a′)	125.11	125.49	123.60
9 (9′)	129.53	128.48	128.58
10 (10′)	128.73	127.20	128.11
11 (11′)	117.47	118.49	117.53
12 (12′)	154.15	154.13	154.25
13 (13′)	114.05	114.11	113.99
14 (14′)	128.25	125.49	128.11
α (α′)	37.96	40.71	37.90
6-OMe (6′-OMe)	56.07	56.16	55.43
7-OMe (7′-OMe)	59.63	60.38	
N-Me (N′-Me)	42.34	41.42	41.06
CF_3COOH		116.18	

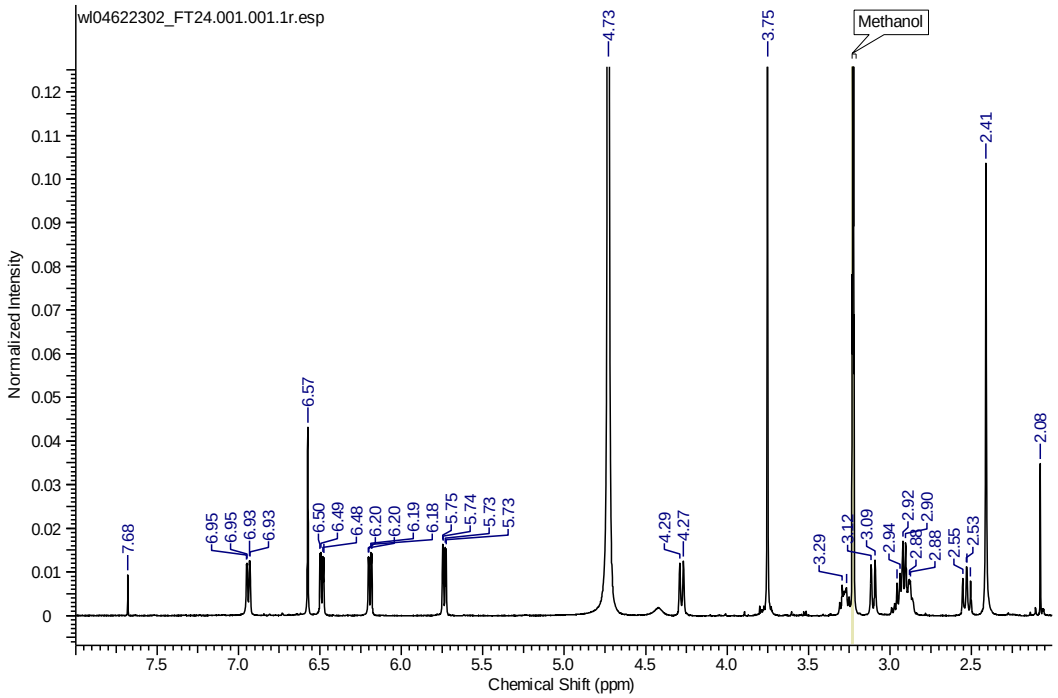

Figure 4.3 ^{1}H NMR of isochondodendrine ($CDCl_3$ + CD_3OD (1:1)).

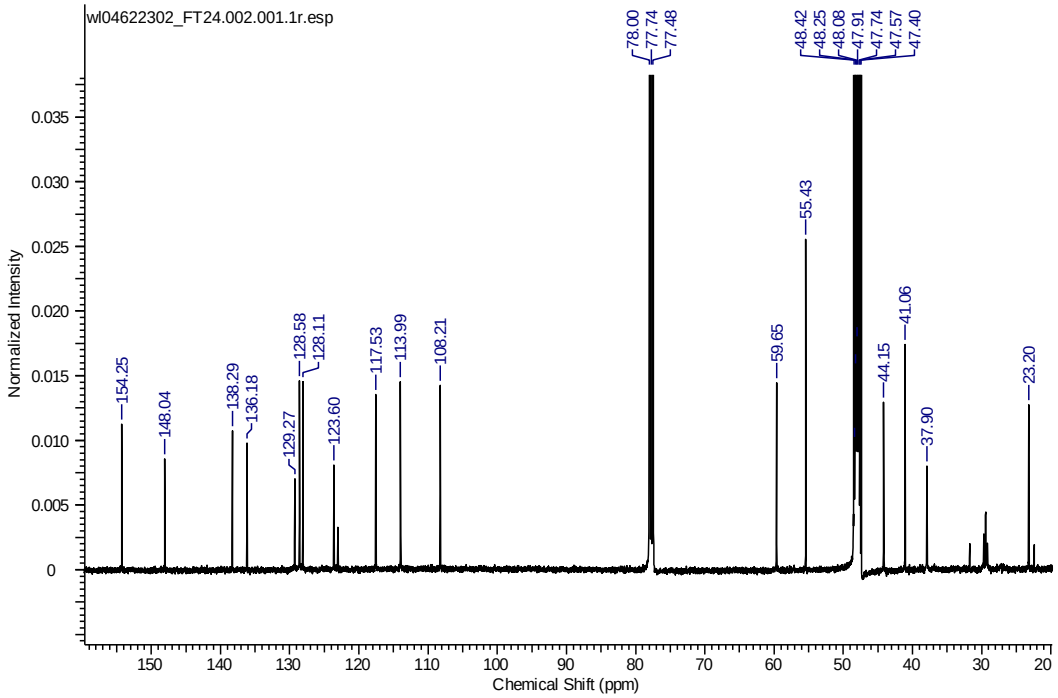

Figure 4.4 ^{13}C NMR of isochondodendrine [$CDCl_3$ + CD_3OD (1:1)]

Table 4.5 ^{1}H NMR chemical shift data (δ, ppm) for 2′-norcocsuline (**3**) and (+)-2′-norcocsuline-TFA salt (500 MHz, MeOD + $CDCl_3$).

proton	2'-norcocsuline-TFA salt	2'-norcocsuline (3)	2'-norcocsuline (3) (Liu et al. 2013)	proton	2'-norcocsuline-TFA salt	2'-norcocsuline (3)	2'-norcocsuline (3) (Liu etal. 2013)
H-1	4.32	3.34 m	3.32 m	H-1′	4.78	4.36 brs	4.35 brs
H-3	3.15, 3.07	2.65 m	2.67 m;	H-3′	3.05, 3.23	2.86 m; 3.33 m	2.86 m; 3.17 m
H-4	3.12, 2.95	2.65 m	2.67 m;	H-4′	2.95,3.12		
H-5	6.62s	6.63 s	6.62 s	H-5′	6.69 s	6.33 s	6.31 s
H-8	6.51s	6.17 s	6.15 s	H-8'	-		
H-15	3.67, 3.56	2.72 m; 2.98 dd	2.67 m; 2.95 dd (14.2, 2.0)	H-15′	3.32, 3.12	3.15 m; 3.27 dd	2.62 m; 3.32 dd (15.0, 2.3)
H-10	6.88 d	6.53 (d, 1.9)	6.52 brs	H-10′	7.12	7.20 dd (7.9, 2.1)	7.19 brd
H-11	-			H-11′	6.91	6.97 (dd, 8.2, 2.5)	7.00 (dd, 8.2, 2.4)
H-13	6.84d	6.93 d (8.2)	6.91 d (8.1)	H-13′	7.23	7.22 (dd, 8.2, 2.4) 7.17	7.21 brd
H-14	6.90 dd	6.85 dd (8.0; 1.6)	6.82 dd (8.1; 1.6)	H-14′	7.59 brd	7.68 (dd, 8.4, 1.3)	7.66 brd
N-Me	2.53 (brs)	2.46 s	2.44 s	6′-OMe	3.86 s	3.88 s	3.86 s

Table 4.6 ^{13}C NMR (125 MHz, CD_3OD (48.0 ppm as reference) + $CDCl_3$) chemical shift data (δ, ppm) for 2′-norcocsuline (**3**) and the 2′-norcosculine-TFA salt.

Carbon	2′-norcocsuline-TFA salt	2′-norcocsuline (3)	2′-norcocsuline (Liu et al. 2013)	Carbon	(+)-2′-norcocsuline-TFA salt	2′-norcocsuline (3)	2′-norcocsuline (Liu et al. 2013)
1	62.8	67.4	67.5	1′	51.8	54.0	54.2
3	47.5	49.3	49.6	3′	40.0	44.6	44.9
4	23.6	27.7	27.7	4′	23.1	27.7	28.3
4a	131.2	-	134.8	4a′	129.7	-	129.8
5	118.4	115.4	115.5	5′	107.9	106.3	106.7
6	138.5	-	139.5	6′	146.2	-	146.1
7	139.8	-	139.7	7′	130.6	-	135.7
8	114.4	113.8	114.1	8′	138.5	-	140.6
8a		-	133.8	8a′	121.5	-	122.0
15	36.1	40.7	41.3	15′	40.2	38.4	38.7
9	126.5	-	129.6	9′	139.9	-	138.9
10	116.1	116.2	116.6	10′	130.8	-	131.3
11	146.2	-	143.7	11′	123.0	121.2	121.3
12	148.3	-	148.1	12′	161.7	-	153.9
13	115.9	115.3	115.8	13′	122.4	122.4	122.5
14	116.8	122.4	122.2	14′	130.0	128.2	128.2
***N*-Me**	35.4	42.4	43.0	6′-OMe	55.7	56.1	56.3

-, peaks are not observed due to dilute sample in ^{13}C NMR recording.

4.3 Anticancer activities of fractions and alkaloids from *T. subcordata*

4.3.1 Cell growth assays of fractions of *T. subcordata*

All the extracts and fractions except aqueous fraction (TSS2) showed different levels of growth inhibition of ovarian cancer cells (Table 4.7 and Fig. 4.5). The most potent activity was exhibited by the alkaloid-enriched fraction (TSS1). The TSS1 also showed some selectivity for the cancer cells because the growth of normal human ovarian epithelia cells HOE was inhibited with almost 10-fold lower potency (Table 4.7).

Table 4.7 The IC_{50} and SI values of the total extracts and fractions of *T. subcordata* on Ovcar-8, A2780, and normal human ovarian epithelia (HOE) cells (the data are expressed as mean ± SEM (n=3). Selective index (SI) is defined as the ratio of IC_{50} in OSE cells to that in the cancer cells. ND represents not determined.

Sample and SI	IC_{50} (μg/ml)		
	Ovcar-8	A2780	HOE
TSS	4.2 ± 1.1	2.6 ± 1.2	ND
TSS1	2.4 ± 0.5	2.1 ± 0.9	20 ± 1.3
SI for TSS1	8.2	9.5	-
TSS2	53 ± 3.0	39 ± 2.4	ND
TSS3	6.0 ± 2.1	3.5 ± 1.1	8.2 ± 1.1
SI for SS3	1.4	2.4	-

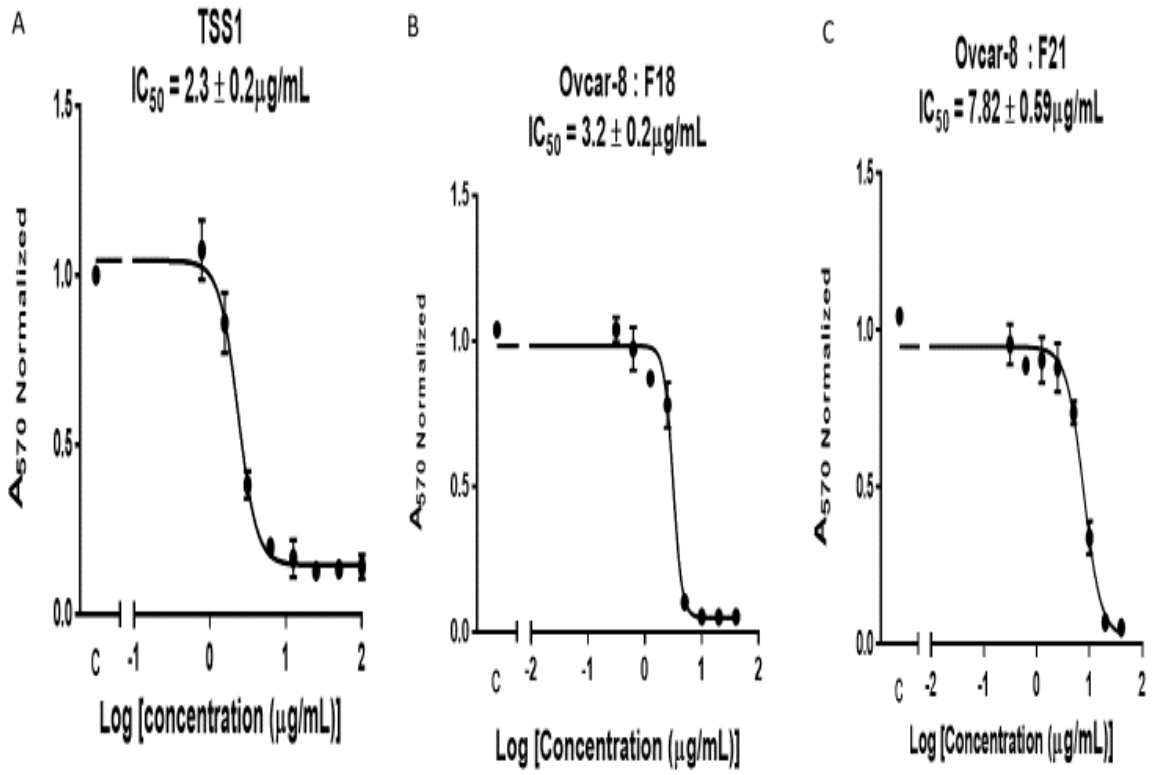

Figure 4.5 Anticancer activities of the total alkaloid extract and other bioactive fractions from *T. subcordata* in Ovcar-8 cells. (A) Total alkaloid extract; (B) F18; (C) F21 on ovarian cancer cell lines. The Ovcar-8 ovarian cancer cell lines treated with different concentrations of fractions (0.16 – 40 µM) and total alkaloid extract A (0.16 – 40 µg/mL) over 72h showed significant IC_{50}. Data determined by four parameters fitting sigmoid curve represented as mean ± SEM, n = 5. A_{570} in y-axis represents normalized (to control) absorbance at 570nm (optical density). C represents IC_{50} of

control (no drug, only medium). The IC_{50} of total alkaloids was shown to be 2.3 ± 0.2 µg/ml, R^2= 0.9835.

4.3.2 Cell growth assays of BBIQ alkaloids of *T. subcordata*

The IC_{50} of the BBIQ alkaloids of *T. subcordata* (cycleanine, isochondodendrine, 2'-norcocsuline and tetrandrine) were determined on different ovarian cancer cell lines and normal HOE cells, to evaluate their potency on these cell lines. These BBIQ alkaloids exhibited different IC_{50} values ranging from 0.8 ± 0.1 to 17.4 ± 0.3 µM (Table 4.8). Tetrandrine was previously reported in *T. subcordata* while cycleanine, isochondodendrine and 2′-norcocsuline are new report in *T. subcordata* in this study.

Also, this is the first-time report of cytotoxic effects of cycleanine and isochondodendrine on ovarian cancer, to the best of our knowledge. Carboplatin and paclitaxel were used as positive controls (Table 4.8). The selective index (SI), an indicator of safety of these drugs on normal HOE cells is also shown (Table 4.8). The SI of cycleanine ranged between 3 and 5 consistent with the preliminary evidence for moderate selectivity of TSS1 for cancer cells.

Table 4.8 The IC_{50} and SI values of the BBIQ alkaloids of *T. subcordata* on Ovcar-8, A2780, Igrov-1 and Ovcar-4 cells (the data are expressed as mean ± SEM (n=3).

Sample name	Cell lines/IC_{50} ± SEM (μM)				
	Ovcar-8	A2780	Igrov-1	Ovcar-4	HOE
Carboplatin	12 ± 0.9	16 ± 1.0	8 ± 0.7	16 ± 1.1	-
Cycleanine	7.9 ± 0.6	5.6±0.5	7.2 ± 0.4	14 ± 1.0	35 ± 0.1
SI	3.4	4.6	4.8	2.6	
Isochondodendrine	3.5 ± 0.1	8.0±0.6	9.0 ± 0.5	17 ± 0.3	10.5 ± 1.2
SI	3	2.5	> 1	<1	-
2′-norcocsuline	1.9 ± 0.2	2.9±0.1	0.8 ± 0.1	6.2 ± 0.5	8.0 ± 0.2
SI	1.5	> 1	3.5	> 1	-
Tetrandrine	12 ± 1.4	7.7 ± 0.2	6.9 ± 0.6	9.3±0.4	
Paclitaxel	5.8 nM	4.6 nM	ND	8.7 nM	-

Carboplatin and paclitaxel served as positive control. ND represents not determined.

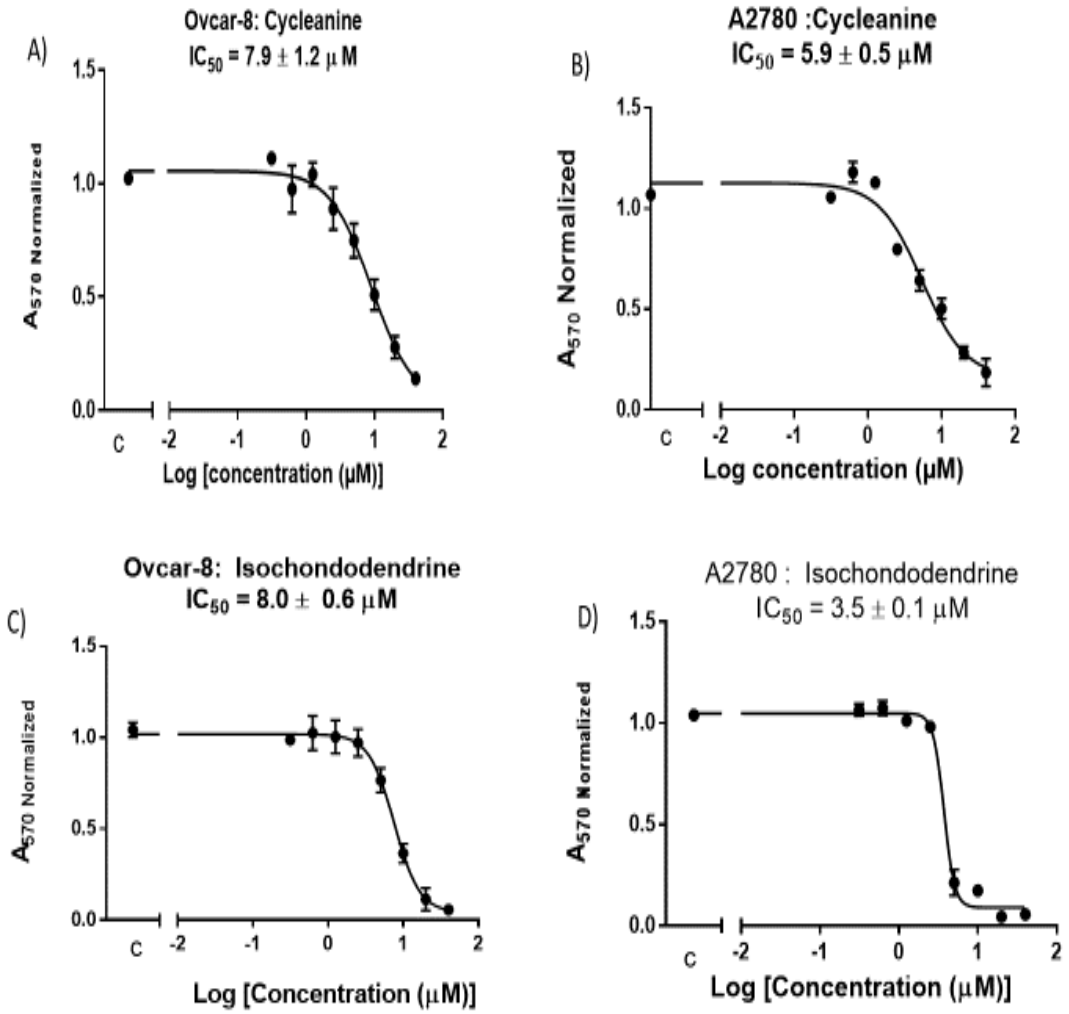

Figure 4.6 Anticancer activities of cycleanine and isochondodendrine on ovarian cancer cell lines. Concentration-response curves of cycleanine on Ovcar-8 (A) and A2780 (B), isochondodendrine on Ovcar-8 (C) and A2780 (D), respectively. Cycleanine and isochondodendrine at dose range of 0.16 – 40 µM over 72h showed cytotoxicity on ovarian cancer cells. The dose range that showed most activities includes 2.2- 40 µM. Data determined by four parameters fitting sigmoid curve represented as mean ± SEM, n=5. A_{570} in y-axis represents normalized (to control) absorbance at 570nm (optical density). C represents IC_{50} of control (no drug, only medium).

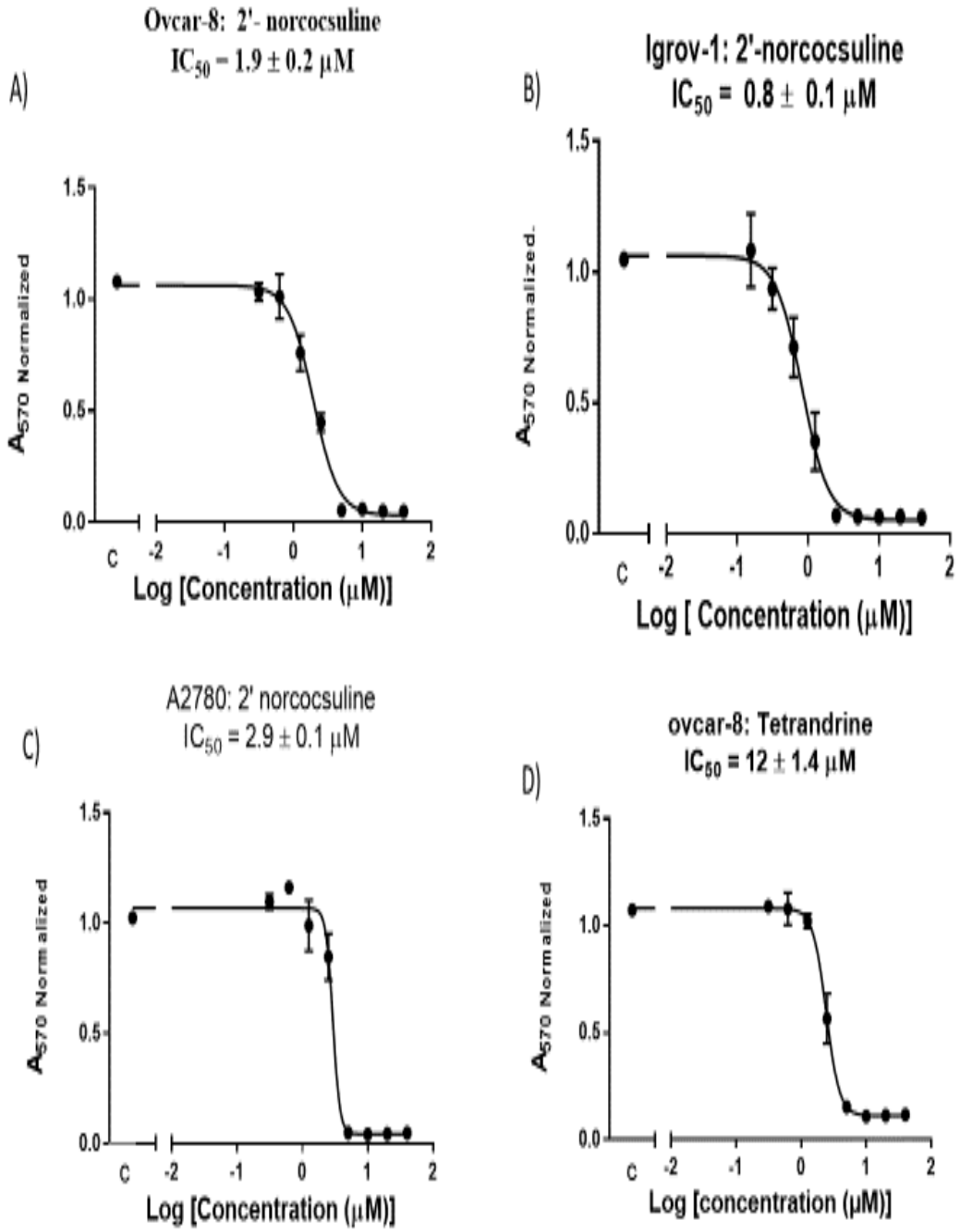

Figure 4.7 Cytotoxicity of 2′-norcosculine and tetrandrine from *T. subcordata.* The concentration versus response curves of 2′-norcosculine (A-C) on Ovcar-8, Igrov-1, A2780 and tetrandrine on Ovcar-8 (D) cancer cell lines. A_{570} represents normalized (to control) absorbance at 570nm. (optical density). 2′-norcosculine and tetrandrine at dose range of 0.16 – 40 µM over 72h, showed cytotoxicity on ovarian cancer cells. The dose range that showed most activities includes 2.2- 40 µM. Results determined

by four parameters fitting sigmoid curve. Data represented as mean ± SEM, n = 5. C represents IC_{50} of control (no drug, solvent).

4.3.3 Cytotoxicity

The trypan blue exclusion method was employed to distinguish cytotoxic and cytostatic effects. The viability of A2780, Ovcar-8, Igrov-1 and Ovcar-4 cells was reduced substantially by cycleanine, isochondodendrine, 2′-norcocsuline and tetrandrine, as well as by the positive control carboplatin, when the four cancer cell lines were exposed to the BBIQ alkaloids for 48 h (Figure 4.8).

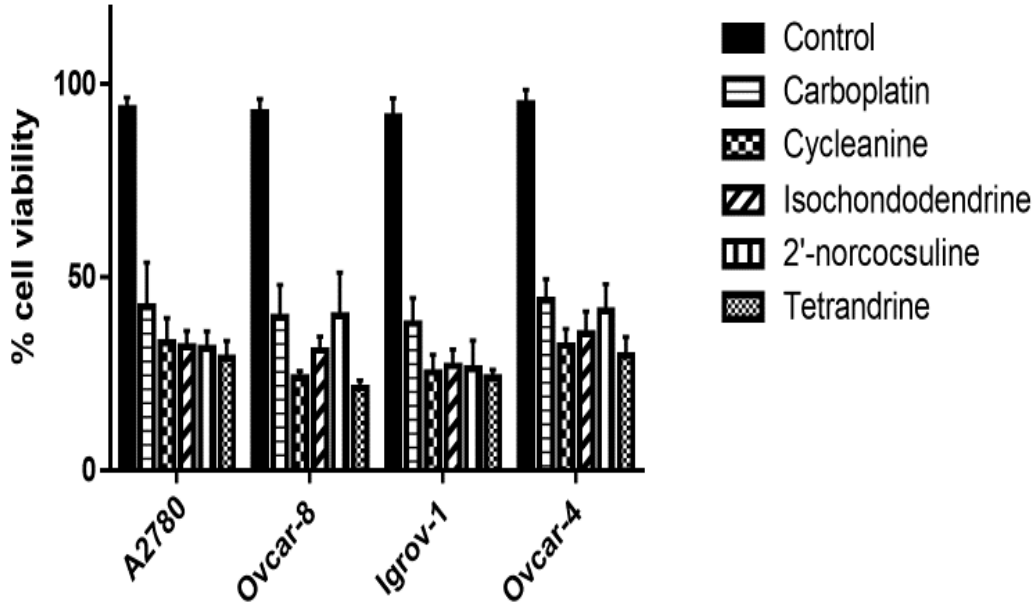

Figure 4.8 Trypan blue exclusion test of cell viability of ovarian cancer cell lines exposed to carboplatin, cycleanine, isochondodendrine, 2′-norcocsuline and tetrandrine. The percentage of viable cells of A2780, Ovcar-8, Igrov-1 and Ovcar-4

cell lines, 48h post-treatment with 20µM carboplatin (positive control), cycleanine, isochondodendrine, 2′-norcocucsuline and tetrandrine was determined by countess automated cell counter using trypan blue exclusion counting method. Negative control group was treated with solvent (medium, no drug). The data were recorded as mean ± SEM, n = 5. The cell viability of each cell line was significantly decreased (increased dead cells) in the treatment group, compared to control (non-treatment group). Two-way ANOVA analysis was used, P= 0.0005; post hoc multiple comparison t- test P<0.05 using Graph Pad prism software.

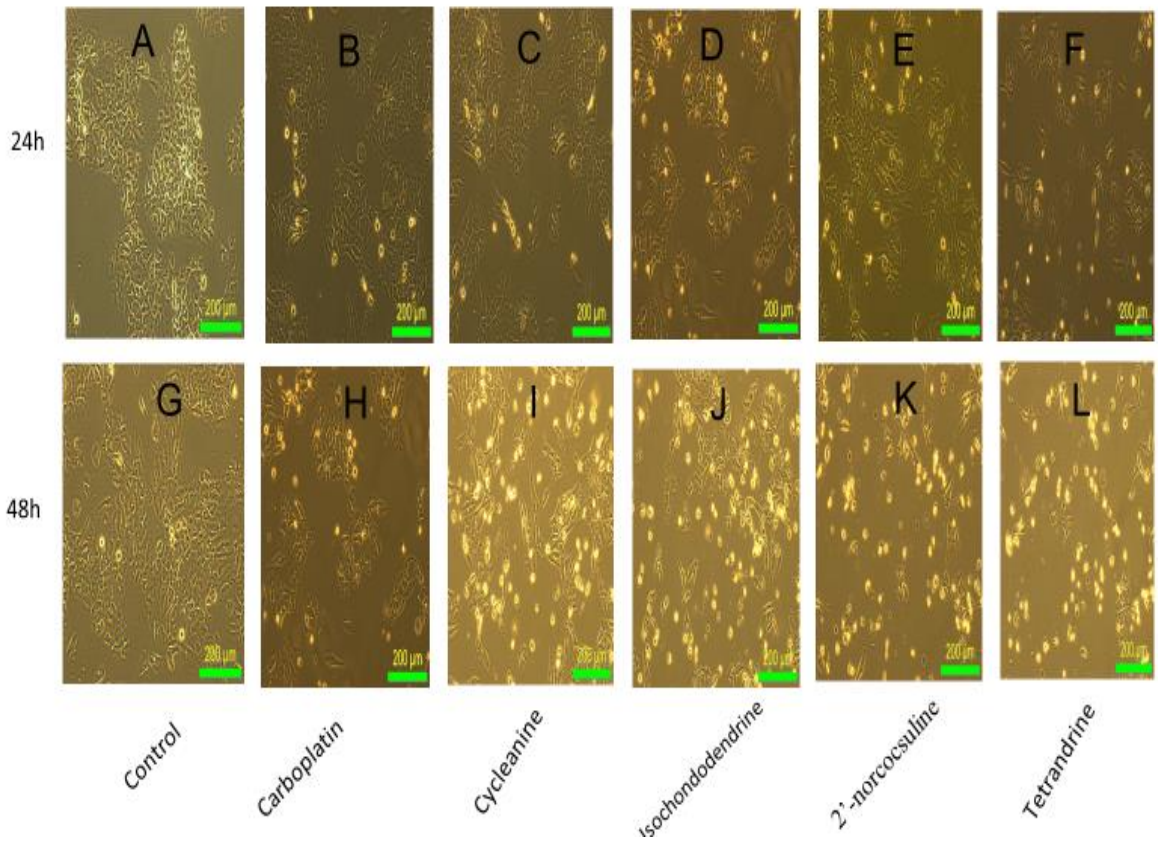

Figure 4.9 Morphological effects of BBIQ alkaloids on Ovcar-8 cells. Time-dependent effects of control (A and G), carboplatin (B and H), cycleanine (C and I); isochondodendrine (D and J); 2′-norcocsuline (E and K) and tetrandrine (F and L) on the morphology of Ovcar-8 cells. There were morphological alterations of Ovcar-8

cells observed, after treated with carboplatin, cycleanine, isochondodendrine, 2′-norcocsuline and tetrandrine (20 µM). These effects were reproducible in all experiments. (A and G) without drug. These were representative of five independent experiment.

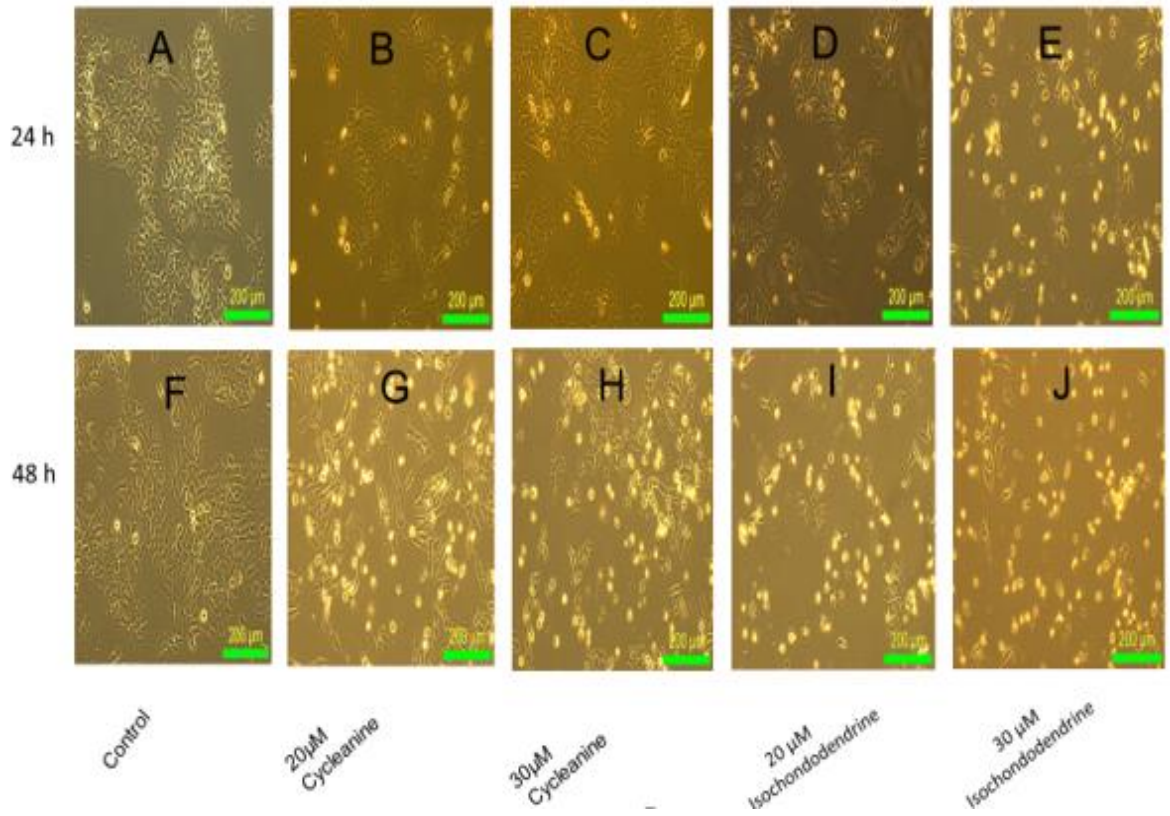

Figure 4.10 Concentration and time-dependent effects of BBIQ on the morphology of Ovcar-8 cells. Cycleanine (B, C, G and H); isochondodendrine (D, E, I and J); and control without drug treatment (A and F). Ovcar-8 cells exposed to different concentrations of Cycleanine and isochondodendrine (20 and 30 µM) for 24 and 48h respectively exhibited dose dependent effects on the morphology of the Ovcar-8 as

observed under phase contrast light microscope. These effects were reproducible in all experiments. These are representative of five independent observations.

4.3.4 Apoptosis

To evaluate whether the decrease in viabilities caused by cycleanine, isochondodendrine, 2′-norcocsuline and tetrandrine were due to apoptosis, the activation of caspase 3/7 activities by these compounds were evaluated. Increased level of caspase activities in Ovcar-8, A2780 and Igrov-1 cells were observed (Figure 4.11). Cycleanine, isochondodendrine, 2′-norcocsuline and tetrandrine increased caspase activity comparably to control, while tetrandrine and 2′-norcocsuline augmented caspase activity noticeably more, up to 8-fold (Figure 4.12). Morphological alterations of Ovcar-8 cells treated with carboplatin, cycleanine, isochondodendrine, 2-norcocsuline and tetrandrine were also consistent with apoptosis including membrane blebbing, rounding up and cell detachment (Figure 4.9 - 4.10).

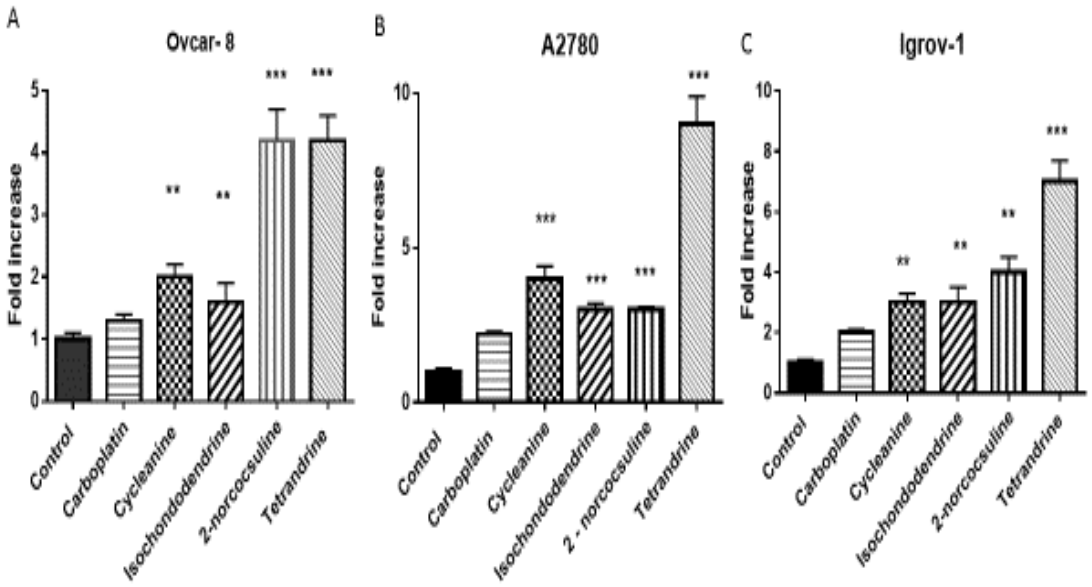

Figure 4.11 Caspase/apoptotic activities of BBIQ alkaloids from *T. subcordata* on three cancer cell lines. Enzymatic activities of caspase 3/7 after 48 h treatment of Ovcar-8 (A), A2780 (B) and Igrov-1 (C) cells with control (medium), carboplatin (positive control), cycleanine, isochondodendrine, 2′-norcocsuline and tetrandrine (20 μM). The caspase activity is expressed as fold increase relative to control cells (mean ± SEM; n = 6). The caspase activity was significantly increased following carboplatin, cycleanine and tetrandrine exposure compared to cells treated with medium (control) where indicated (one-way ANOVA for group analysis, $P<0.0001$) Post hoc paired t-test ($P<0.05$, t-test) Culture medium served as negative control, carboplatin positive control.

To confirm the cells under-went apoptosis, PARP cleavage, a marker of apoptosis, was assessed by immunoblotting. Exposure of Ovcar-8 cells to cycleanine, isochondodendrine, 2′-norcocsuline, tetrandrine, or carboplatin resulted in significant PARP cleavage (Figure 4.13).

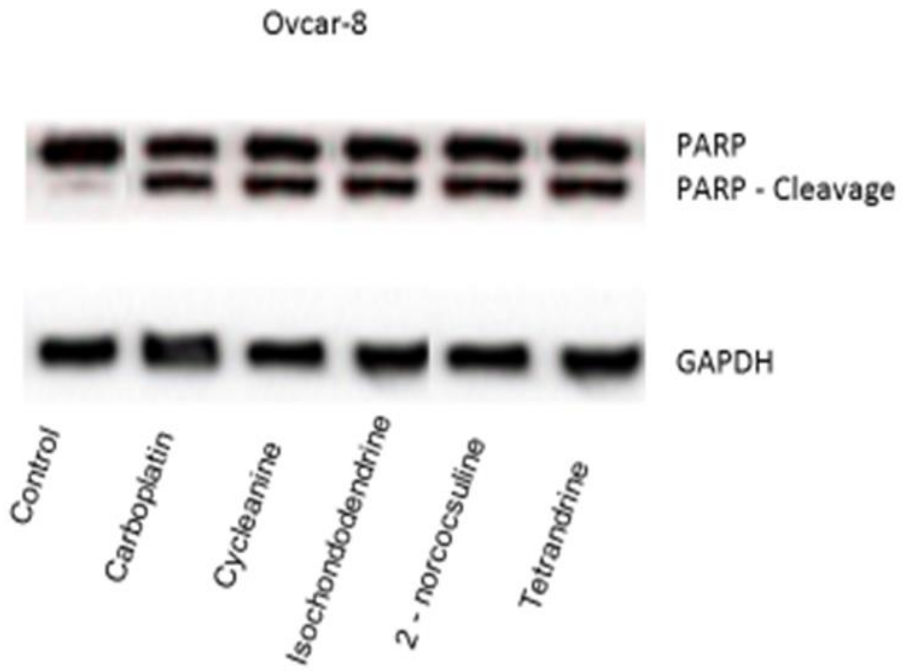

Figure 4.12 Western blot (PARP-cleavage) for cycleanine, isochondodendrine, 2′-norcocsuline and tetrandrine from *T. subcordata* on Ovcar-8 cancer cell line. Western blotting analysis of the PARP-1 cleavage marker in Ovcar-8 cells after treatment with carboplatin, cycleanine, isochondodendrine, 2′-norcocsuline and tetrandrine. GAPDH was used as a loading control. A representative of three different observations is presented. The results showed that the treatment of carboplatin, cycleanine, isochondodendrine, 2′-norcocsuline and tetrandrine led to significant cleavage in PARP compared to control cells, respectively. There was no significant PARP-cleavage observed in negative control.

To further quantify the percentage of apoptotic cells after treatment of these alkaloids, the cells were stained by Annexin V and PI and analysed by flow cytometry (Figure 4.13). Carboplatin, cycleanine isochondodendrine, 2′-norcocsuline and tetrandrine treatment after 48 h caused significant increase of the population of both early and late apoptotic cells compared to the control cells (Figure 4.13), quantified in 4.13 G Ovcar-8 was selected to be used alone in western blot, Annexin V or cell cycle experiment among other four cells being used, for basic economic reasons. Also, particularly because ovar-8 is known to be most resistant or least sensitive among all the ovarian cells being used in this study. The assumption is that if ovcar-8 could respond positively, then it is likely that other ovarian cells being used in this study (which are more sensitive than ovcar-8) probably would give positive response too. Due to limited resources, which was considered a challenge in this research all other ovarian cells could not be used in western blot, cell cycle and Annexin V.

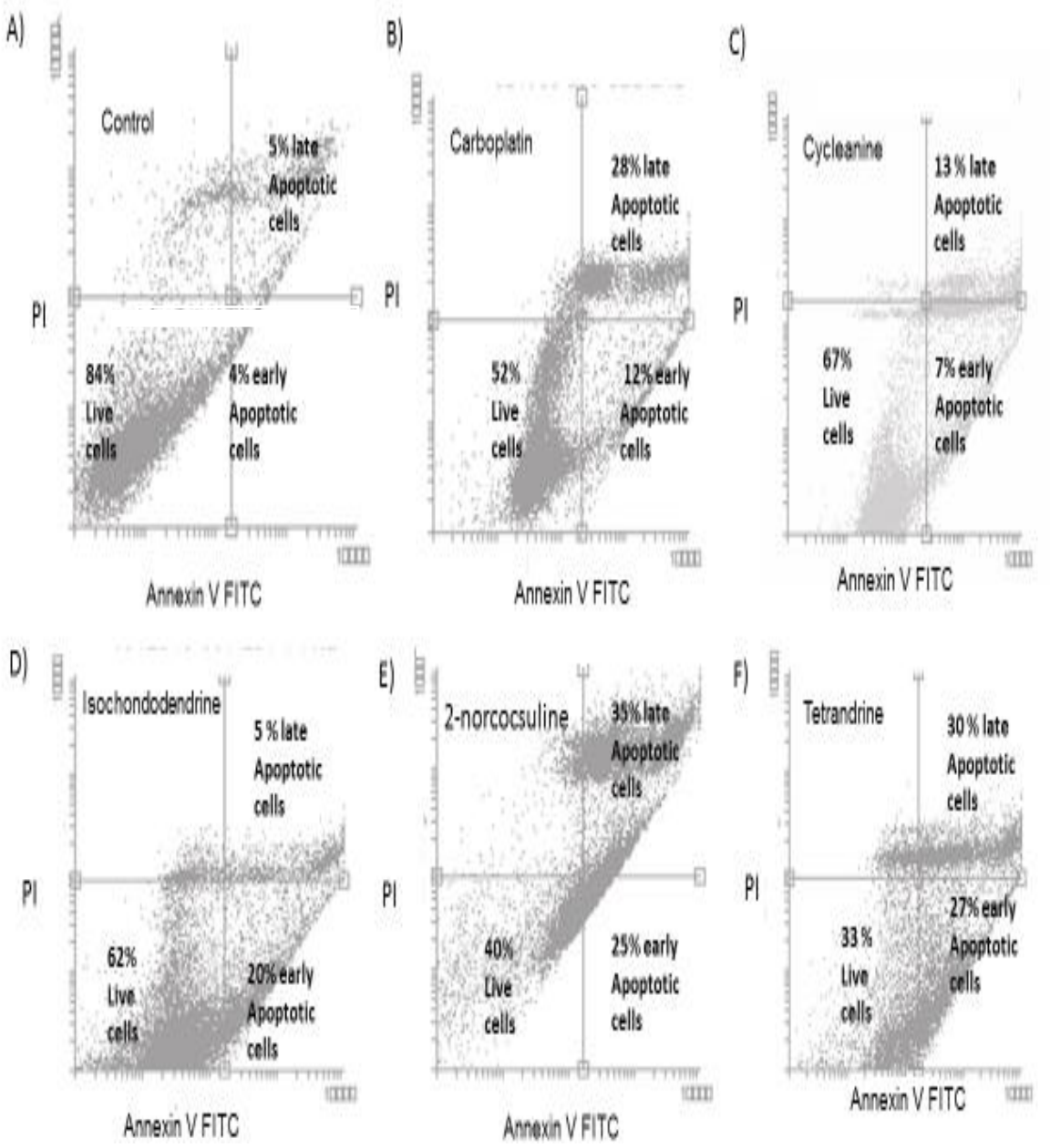
A)
Control
5% late Apoptotic cells
PI
84% Live cells
4% early Apoptotic cells
Annexin V FITC
B)
Carboplatin
28% late Apoptotic cells
PI
52% Live cells
12% early Apoptotic cells
Annexin V FITC
C)
Cycleanine
13 % late Apoptotic cells
PI
67% Live cells
7% early Apoptotic cells
Annexin V FITC
D)
Isochondodendrine
5 % late Apoptotic cells
PI
62% Live cells
20% early Apoptotic cells
Annexin V FITC
E)
2-norcocsuline
35% late Apoptotic cells
PI
40% Live cells
25% early Apoptotic cells
Annexin V FITC
F)
Tetrandrine
30 % late Apoptotic cells
PI
33 % Live cells
27% early Apoptotic cells
Annexin V FITC

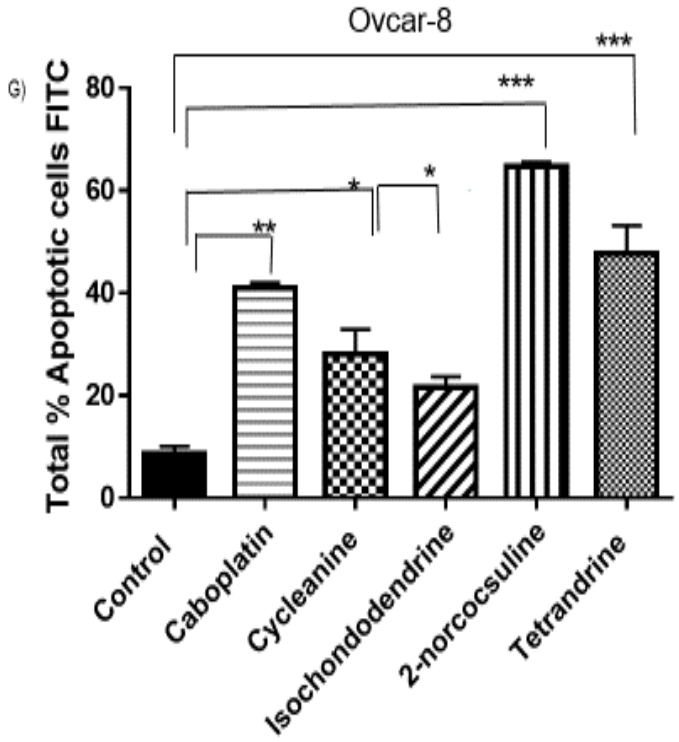

Figure 4.13 Flow cytometry analysis of apoptotic effects of carboplatin, cycleanine, isochondodendrine, 2′-norcocsuline and tetrandrine on Ovcar-8 cells. The scattering dot plots indicating the percentage of live, early and late apoptotic cells under treatment of medium (control) (A), carboplatin (B), cycleanine (C), isochondodendrine (D), 2′-norcocsuline (E), and tetrandrine (F) (20 μM) for 48 hours by using Annexin V & PI assay. The percentages of the total apoptotic cells caused by carboplatin, cycleanine, isochondodendrine, 2′-norcocsuline and tetrandrine were significant compared to control (G) (one-way ANOVA for group analysis, $P<0.0001$; post hoc paired *t*-test relative to control was done (*P <0.05; ** P <0.001 *** P <0.0001 t-test).

4.3.5 Cell cycle analysis

The effects of cycleanine, isochondodendrine, 2′- norcocsuline and tetrandrine on cell cycle distribution of Ovcar-8 cells are shown in Figure 4.15. The percentage of Ovcar-8 cells in subG$_1$ increased after exposure to carboplatin, cycleanine, isochondodendrine and tetrandrine for 48h compared to negative control, consistent with apoptosis (Figure 4.14).

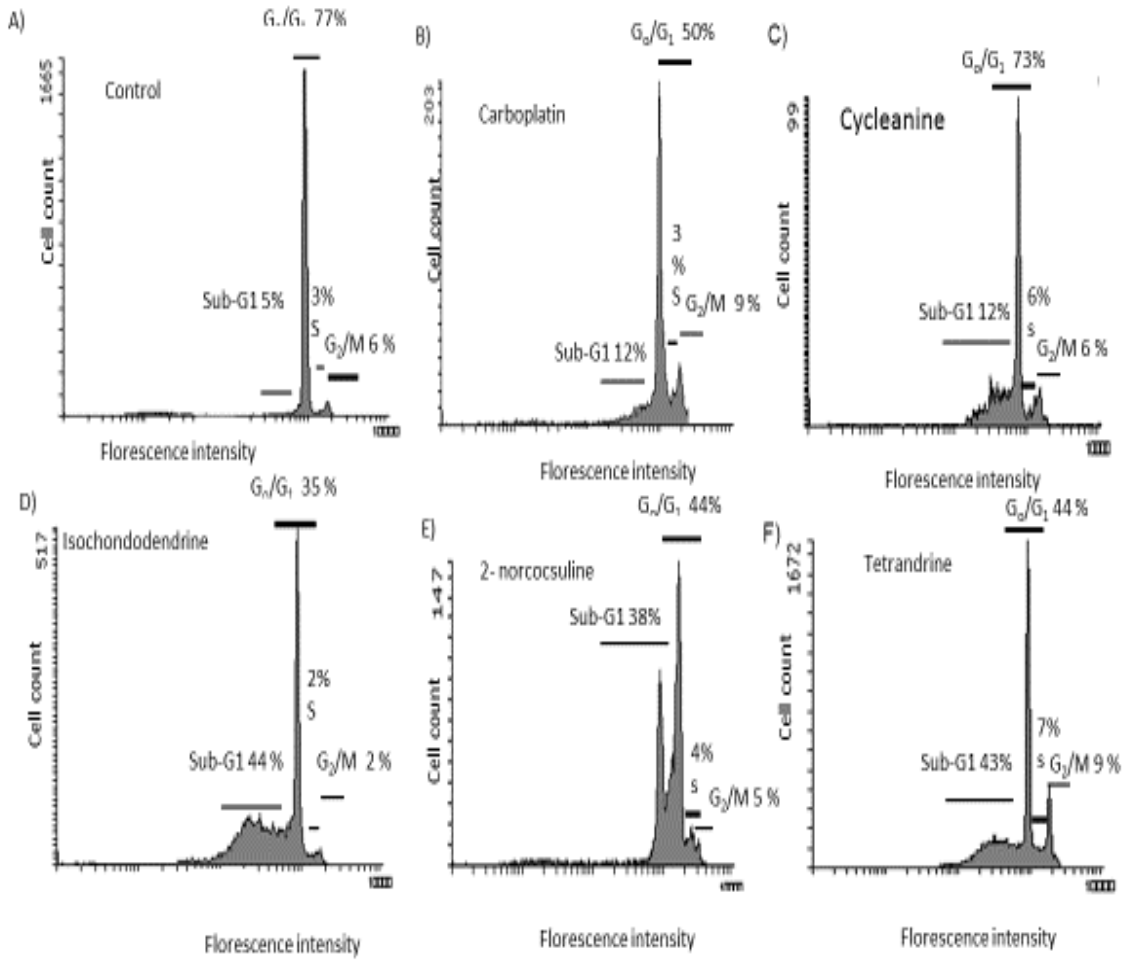

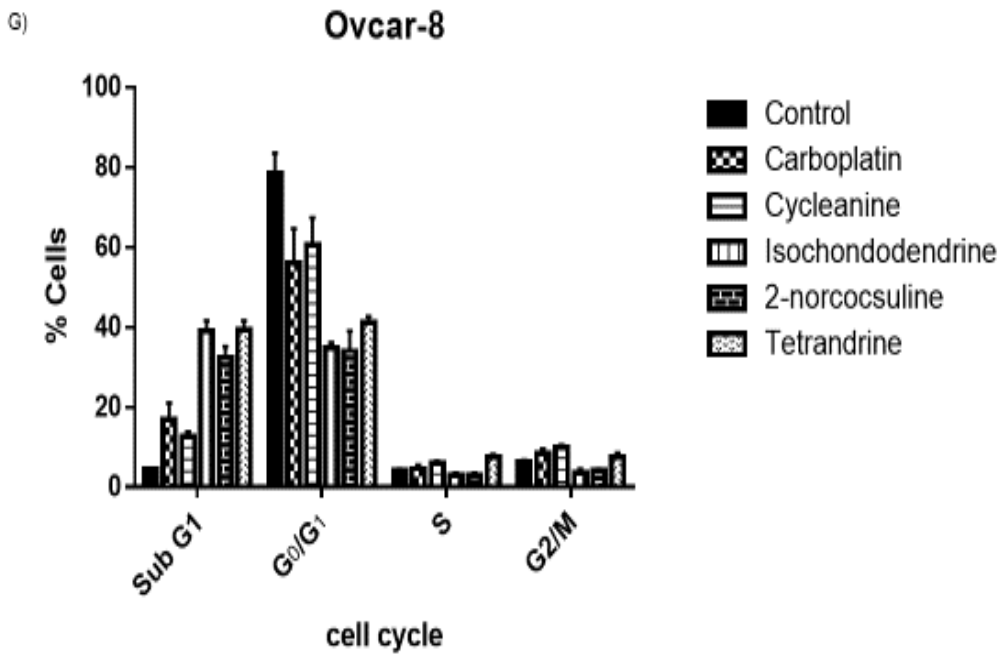

Figure 4.14 Effects of BBIQ alkaloids on cell cycle of Ovarc-8 by flow cytometry. The effects of medium (control) (A), carboplatin (B); cycleanine (C); isochondodendrine (D), 2′-norcocsuline (E); and tetrandrine (20 μM) (F) on the Ovcar-8 cell cycle by use of flow cytometry analysis. The percentage of in subG_1 phase (apoptotic cells) of the Ovcar-8 cell cycle was significantly increased compared to cells exposed to solvent-control. While G_0/G_1 phase (live cells) decreased significantly compared to control $P<0.0001$, two-way ANOVA. This figure was a representation of n=3 observations.

4.4 Discussion

Cycleanine, isochondodendrine, 2′-norcocsuline and tetrandrine have been isolated from other plant species of the Menispermaceae family (Angerhofer et al., 1999, Mambu et al., 2000, Schiff, 1997, Liu et al., 2013). Cycleanine was shown to increase

the intracellular doxorubicin accumulation in the resistant MCF-7/Adr cell lines (Tian & Pan, 1997). Tetrandrine is also a common BBIQ alkaloid found in different plants as well as in *T. subcordata* (Dwuma-Badu et al., 1975). It showed various biological activities including anticancer, anti-allergic, anti-inflammatory, anti-malarial, and cardiovascular effects (Yu-Jen, 2002, Schiff, 1997). Tetrandrine inhibited the growth of various types of cancer cells (Yu-Jen, 2002, Xu et al., 2011, Xiao et al., 2015, Wu et al., 2014, He et al., 2011b) and could reverse multidrug resistance by inhibiting P-glycoprotein activity (Sun & Wink, 2014).

Here, cycleanine, isochondodendrine and 2′-norcocsuline have been isolated and characterized from *T. subcordata*, as part of novel contribution to knowledge. The analytical data (ESI-MS and NMR) were consistent with literature data for cycleanine, isochondodendrine (Kanyinda et al., 1997) and 2′-norcocsuline (Liu et al., 2013). The change of ^{1}H NMR signals of cycleanine by TFA was observed and such features were often found for the other alkaloids (Verpoorte, 1986). Furthermore, we showed that both a head-to-tail BBIQ cycleanine (including TFA salt of cycleanine) and a head-to-head BBIQ tetrandrine which is an isomer of cycleanine and was previously isolated from *T. subcordata* (Figure 4.5) showed potent anti-ovarian cancer activities. While such a structural difference in BBIQ alkaloids was key to the inhibition of histamine release as only the head-to-tail BBIQ such as tetrandrine showed the inhibition (Nakamura et al., 1992).

The induction of apoptosis by tetrandrine was observed previously in human lung carcinoma (Lee et al., 2002), bladder cancer (Li et al., 2011), colorectal cancer (He et al., 2011b), gallbladder carcinoma and prostate cancer cells (Liu et al., 2015). The combination of tetrandrine and cisplatin caused enhanced cytotoxicity through apoptosis as well as redistribution of the cell cycle in ovarian cancer cells in vitro and

vivo (Zhang et al., 2011). To confirm that these four BBIQ alkaloids (cycleanine, isochondodendrine, 2′-norcocusuline and tetrandrine) could induce apoptosis in ovarian cancer cell lines, two markers of apoptosis including caspases 3/7 and cleavage of PARP to its 89 kDa fragment were measured. Cycleanine, isochondodendrine, 2′-norcocusuline and tetrandrine significantly increased caspase 3/7 activity in all cell lines tested, indicating the induction of apoptotic cell death (Figure 4.12). The apoptotic activity was further confirmed by the detection of the PARP-1 fragment in cycleanine, isochondodendrine, 2′-norcocusuline and tetrandrine-treated Ovcar-8 cells using immunoblotting assay (Figure 4.13). The percentage of the apoptotic cells caused by 2′-norcocsuline and tetrandrine are greater than those by isochondodendrine, cycleanine and carboplatin (Figure 4.12 and 4.13). Tetrandrine increased population of both apoptotic sub-G_1 and G_1 phase in the lung cancer cells (Lee et al., 2002). The increase of cell fraction of sub-G_1 caused by the BBIQ alkaloids was also observed in ovarian cancer cell in this study indicating the induction of apoptosis because such sub-G_1 peak is often regarded as a characteristic indicator of apoptosis (Kajstura et al., 2007). Interestingly, cycleanine, and isochondodendrine were shown in this study to cause apoptosis in ovarian cancer cells similar as tetrandrine but with less potency (Figure 4.12 - 4.16). Also in this study, 2’-norcocsuline was proved to cause apoptosis comparable to tetrandrine. All these were significant compared to control.

In this study, also, the extracts and BBIQ alkaloids of *T. subcordata* were demonstrated to contain alkaloids (Figure 4.1) and exert significant *in vitro* anti-ovarian cancer activities (Figure 4.8), which provided a scientific basis for future potential use of this plant for the treatment of ovarian cancer. Importantly, cycleanine showed a modest selectivity towards ovarian cancer cells over normal cells via

apoptosis, which may be used as a hit to modify its structure by semi-synthesis to improve its anti-cancer activity (Uche et al., 2016). To be approved as anticancer drugs, in vivo activities of these alkaloids and analogues must be evaluated. This work is ongoing in our laboratory and will be reported in the future. This study therefore could serve as novel scientific documentation of cycleanine, isochondodendrine and 2′-norcocsuline as bioactive constituents of *T. subcordata.* It could also provide scientific proof of *in vitro* anti-ovarian cancer activities and apoptosis induction of ovarian cancer cells by cycleanine, isochondodendrine and 2′-norcocsuline.

CHAPTER FIVE

SEMI-SYNTHESIS OF ANALOGUES OF CYCLEANINE AND THEIR ANTI-CANCER ACTIVITIES

5.1 Semi-synthesis of analogues of cycleanine

The search for more potent anti-cancer bisbenzylisoquinoline (BBIQ) alkaloids with high selective index - SI (minimum toxicity) motivated our further study aimed at modification or semi-synthesis of analogues of cycleanine which was previously isolated from *T. subcordata* in this study. Cycleanine (**1**) was preferred as a hit drug among the three BBIQ isolated from *T. subcordata* because even though it was less potent than isochondodendrine (**2**) or 2′-norcocsuline (**3**), it showed the modest selectivity relative to others (SI > 3) in normal human ovarian epithelial cells (Uche et al., 2016).

Besides, cycleanine was the most abundant in *T. subcordata* (about 98% yield of the total alkaloids); hence sufficient quantity was produced for semi-synthesis process. Though, 2'-norcocsuline showed high potency against ovarian cancer (IC_{50} 0.8 – 3µM), its SI was smaller than that of cycleanine and its percentage yield in *T. subcordata* total alkaloid was too small to guarantee sufficient quantity for semi-synthesis.

In this study, therefore, semi-synthesis of cycleanine analogues was carried out to produce chloromethylcycleanine which can subsequently react with dimethylamine,

and propargylamine to produce 5-[(dimethylamino)methyl]cycleanine (**4**), and 5-[(propargylamino)methyl]cycleanine respectively (**5**) (Figure 5.1).

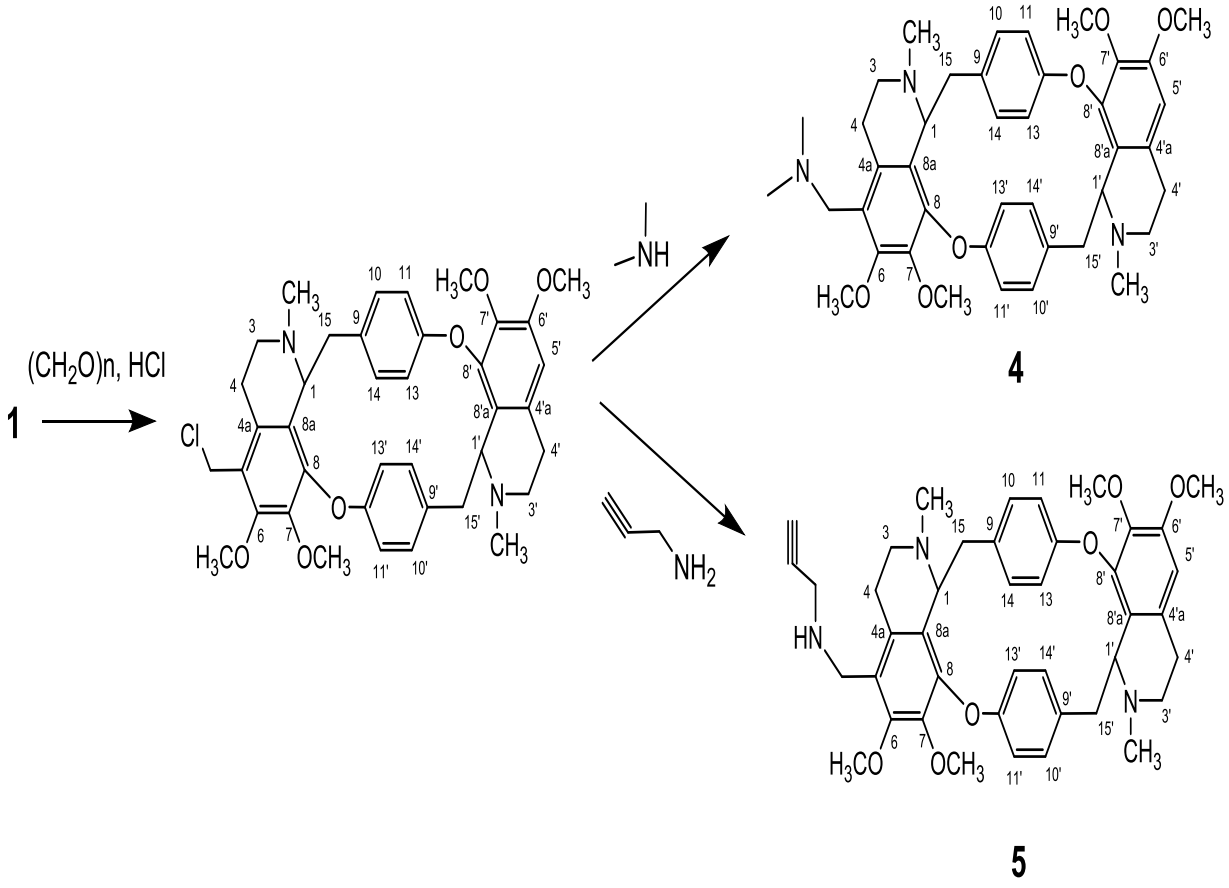

Figure 5.1 Scheme for the semi-synthesis of (aminoalkyl)cycleanine analogues. Structural elucidation based on results analysis of spectroscopic data from ^{1}H NMR (500 MHz, $CDCl_3$) (Table 5.1) and ^{13}C NMR (100 MHz, $CDCl_3$) (Table 5.2).

To determine the purity and molecular mass of the cycleanine analogues, the LC-MS analysis of the semi-synthesized products were analyzed. The results revealed the two products as pure (purity > 98%) and supported the structure of 5-[(dimethylamino)methyl]cycleanine (**4**) and 5-[(propargylamino)methyl]cycleanine (**5**) (Figure 5.2 and 5.3).

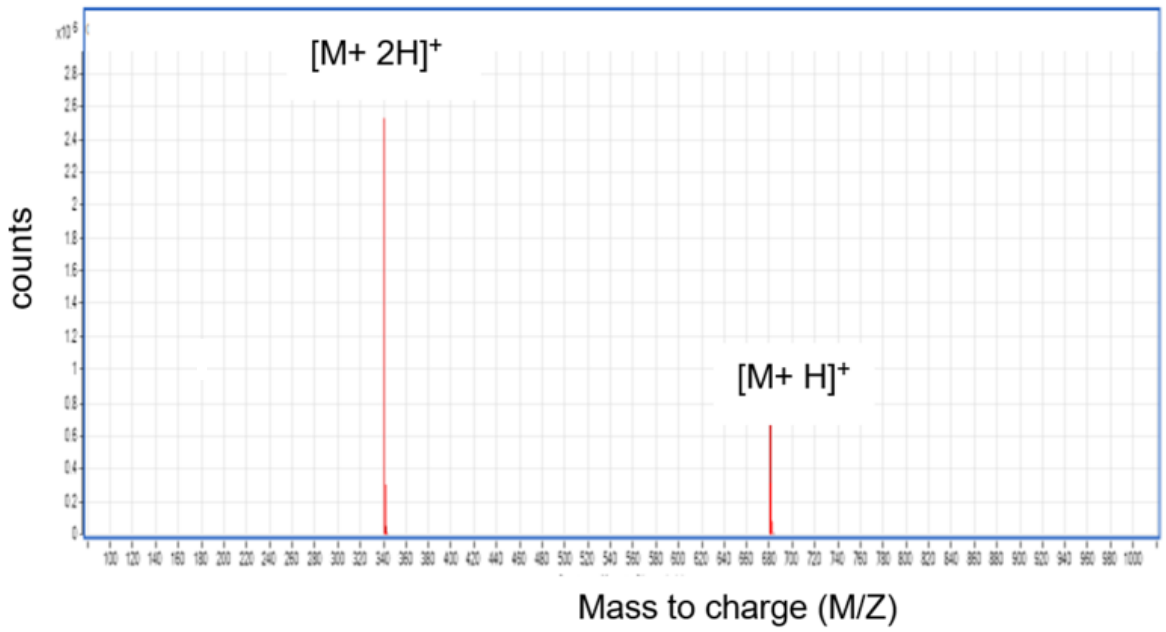

Figure 5.2 The LC-MS spectrum of 5-[(dimethylamino)methyl] cycleanine (**4**).

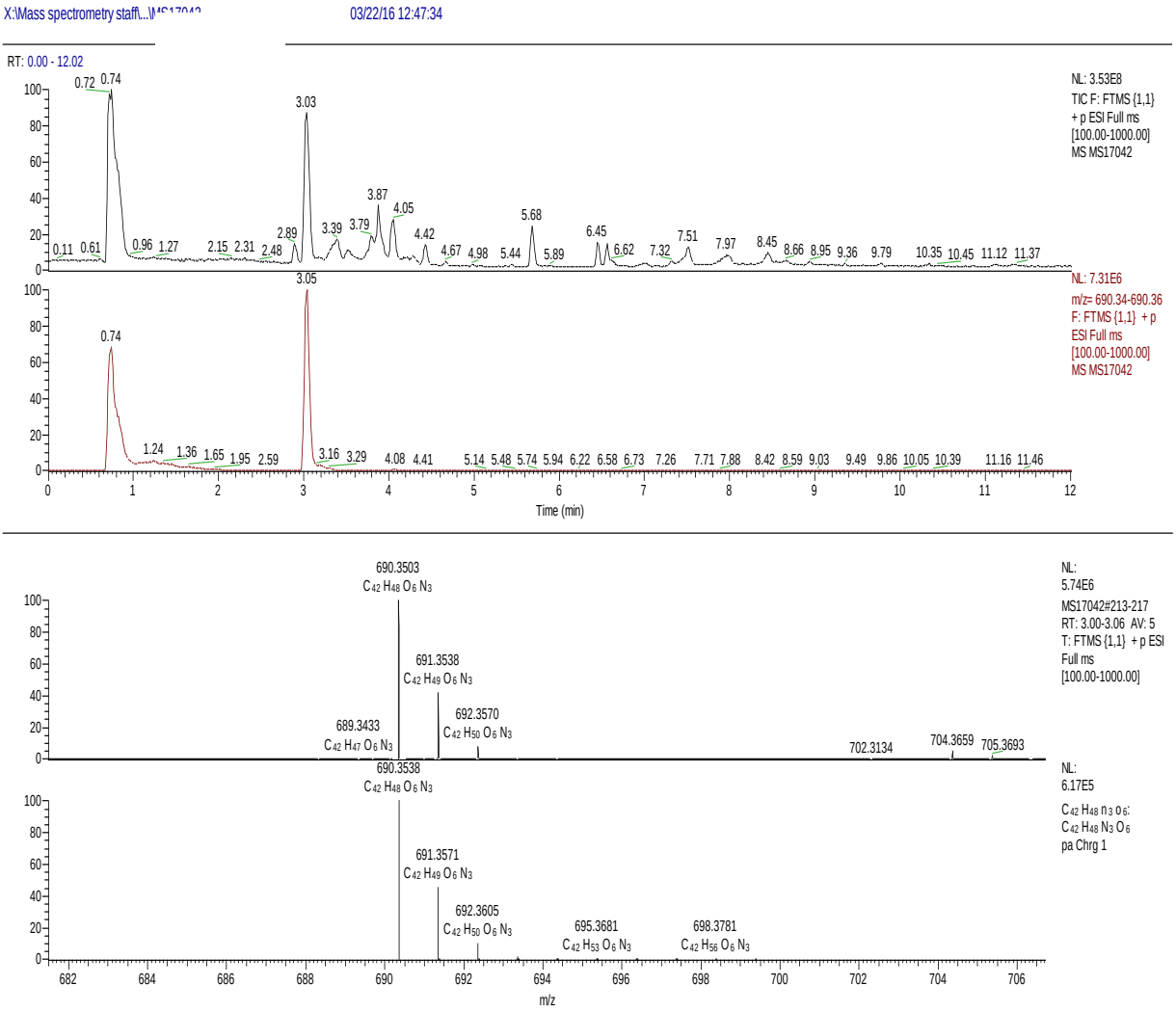

Figure 5.3 The LC-MS spectrum of 5-[(propargylamino)methyl] cycleanine (**5**).

Further NMR analysis confirmed these structures. The new compounds were identified based on the analysis of spectroscopic data of ^{1}H NMR (500 MHz, CD_3OD) and ^{13}C NMR (125 MHz, CD_3OD), HMBC, HMQC (Tables 5.1 and 5.2: Figures 5.1) respectively. The symmetry of cycleanine was lost after the chemical modification, and the peak for H-5 or 5' in ^{1}H NMR of cycleanine was shifted and corresponded to only one proton in compound **4** (Figure 5.5) or **5** which indicated the substitution of amino group at H-5 of cycleanine.

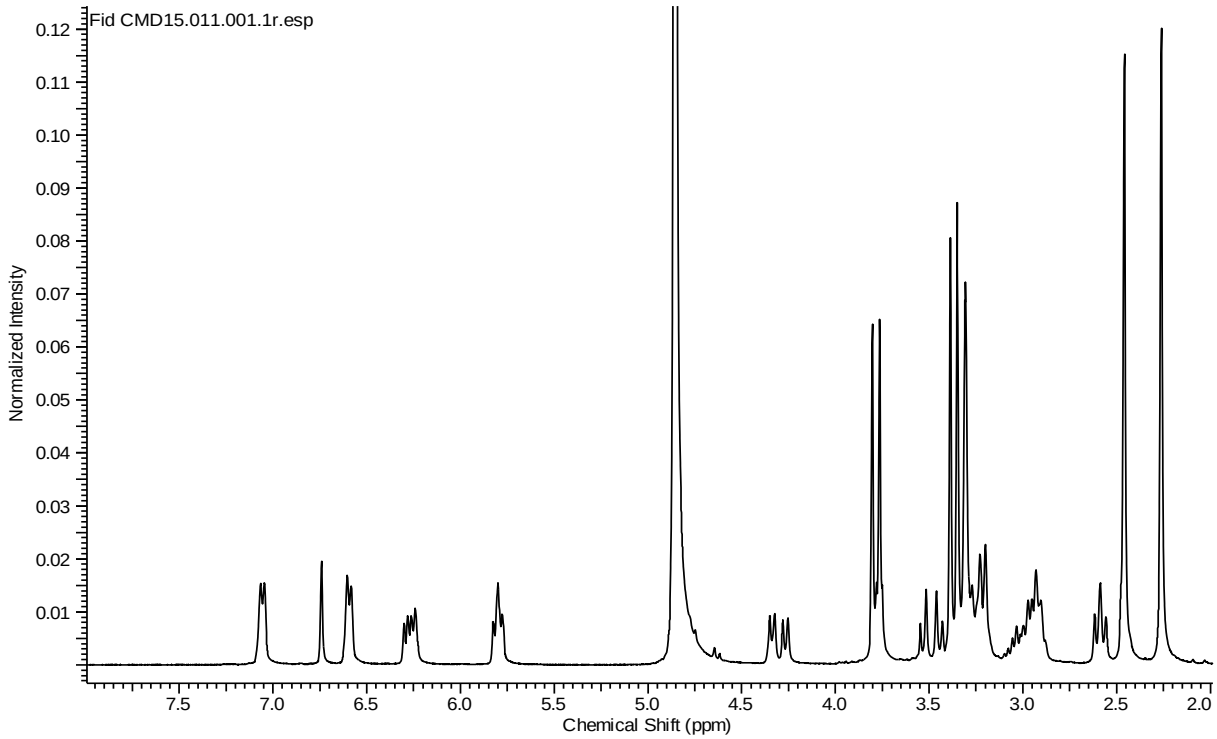

Figure 5.4 ^{1}H NMR spectrum of **4** (500 MHz, CD_3OD).

Table 5.1 ^{1}H NMR (500 MHz, $CDCl_3$) chemical shift data (δ, ppm) for two synthetic cycleanine analogues (**4** and **5**) (*J* values, in Hz, in parentheses).

proton	4	5	proton	4	5
H-1	4.27 d (10.4)	4.70 d (10.6)	H-1′	4.34 d (10.4)	4.70 d (10.6)
H-3	3.29 m; 2.92 m	3.65 m; 3. 28 m	H-3′	3.32 m; 2.94 m	3.65 m; 3. 28 m
H-4	2.96 m; 3.24 m	3.19 m; 3.30 m	H-4′	3.05 m; 3.00 m	3.23 m; 3.23 m
H-5	-	-	H-5′	6.74 s	6.85 s
H-10	7.04	7.18 brd	H-10′	7.07	7.20 brd
H-11	6.58	6.66 dd (8.4, 2.7)	H-11′	6.60	6.65 dd (8.4, 2.7)
H-13	5.86	5.86 dd (8.7, 2.7)	H-13′	5.81	5.81 dd (8.7, 2.7)
H-14	6.25	6.32 dd (8.2, 1.7)	H-14′	6.29	6.31 dd (8.2, 1.4)
H-15	2.57 m; 3.21 m	2.70 m; 3.37 m	H-15′	2.60 m; 3.25 m	2.70 m; 3.37 m
6-OMe	3.78 s	3.88, s	6′-OMe	3.82 s)	3.84 s
7-OMe	3.37, s	3.41 s	7′-OMe	3.40, s	3.38 s
N-Me	2.48	2.75 s	N′-Me	2.48 s	2.72 s
CH_2	3.54 d, 12.2; 3.47 d, 12.2	3.44 m			
N-$(CH_3)_2$	2.28 s				
NH-CH_2-CCH		3.47 m; 3.38 m			

Table 5.2 ^{13}C NMR (100 MHz, $CDCl_3$) chemical shift data (δ, ppm) for synthetic cycleanine analogues (**4** and **5**).

Carbon	**4**	**5**	**Carbon**	**4**	**5**
1	59.2	60.0	1′	59.2	59.5
3	44.1	43.9	3′	43.9	43.7
4	23.8	22.0	4′	20.9	19.6
4a	130.4	128.8	4a′	130.4	128.7
5	124.5	123.6	5′	109.2	109.2
6	152.3	153.5	6′	151.7	152.5
7	142.6	143.2	7′	138.8	139.4
8	143.5	144.0	8′	143.2	143.8
8a	127.4	127.9	8a′	126.3	128.4
9	129.8	128.6	9′	130.3	128.7
10	128.1	128.1	10′	128.0	127.9
11	117.4	117.7	11′	117.3	117.6
12	154.3	154.4	12′	154.1	154.1
13	114.0	114.1	13′	113.9	114.0
14	128.5	128.1	14′	128.4	128.1
15	37.3	37.8	15′	37.3	37.5
6-OMe	59.7	60.0	6′-OMe	54.9	54.7
7-OMe	58.8	58.7	7′-OMe	58.4	58.7
N-Me	40.9	39.8	N′-Me	40.9	39.8
CH_2	53.0	57.0			
$-N(CH_3)_2$	44.5				
- $NHCH_2CCH$		43.5; 72.9; 79.2			

5.2 Anticancer activities of semi-synthetic analogues of cycleanine on cancer cell lines

To assay the cytotoxicity or anti-proliferative activities of 5-[(dimethylamino)methyl] cycleanine **(4)** and 5-[(propargylamino)methyl]cycleanine (**5**), the IC_{50} of the new compounds were evaluated on different ovarian cancer cell lines (Igrov-1, A2780 and Ovcar-8) after treatment for 72h. The results revealed the IC_{50} of **4** and **5** as ranging from 3.6 ± 0.5 µM to 5.2 ± 0.6 µM and from 5.6 ± 0.2 to 6.3 ± 0.6 µM respectively on the three ovarian cancer cell lines (Table 5.3; Figures 5.4 and 5.5). The results (Table 5.3) suggest that **4** and **5** probably, exert about 2-3 times improved potency against ovarian cancer cells than the cycleanine with IC_{50} ranging from 7 to 14 µM (Table 4.8).

Table 5.3 The IC_{50} of 5-[(dimethylamino)methyl] cycleanine (**4**) and 5-[(propargylamino) methyl]cycleanine (**5**) in ovarian cancer cells.

compound	**Ovarian cancer Cell lines**		
	Igrov-1	A2780	Ovcar-8
4	4.4 ± 0.1 µM	3.6 ± 0.5µM	5.2 ± 0.6 µM
SI (4)	> 2	3	> 2
5	6.1 ± 0.5 µM	6.3 ± 0.6 µM	5.6 ± 0.2 µM
SI (5)	> 5	>5	6
Carboplatin	8 ± 0.7 µM	16 ± 1.0 µM	12 ± 0.9 µM

Data represented as mean ± SEM (n= 5). The results were significant $P<0.05$ (one-way ANOVA). HOE (**4**) IC_{50} = 10 ± 0.2 µM; (**5**) 32 ± 1.6 µM. SI means selective index.

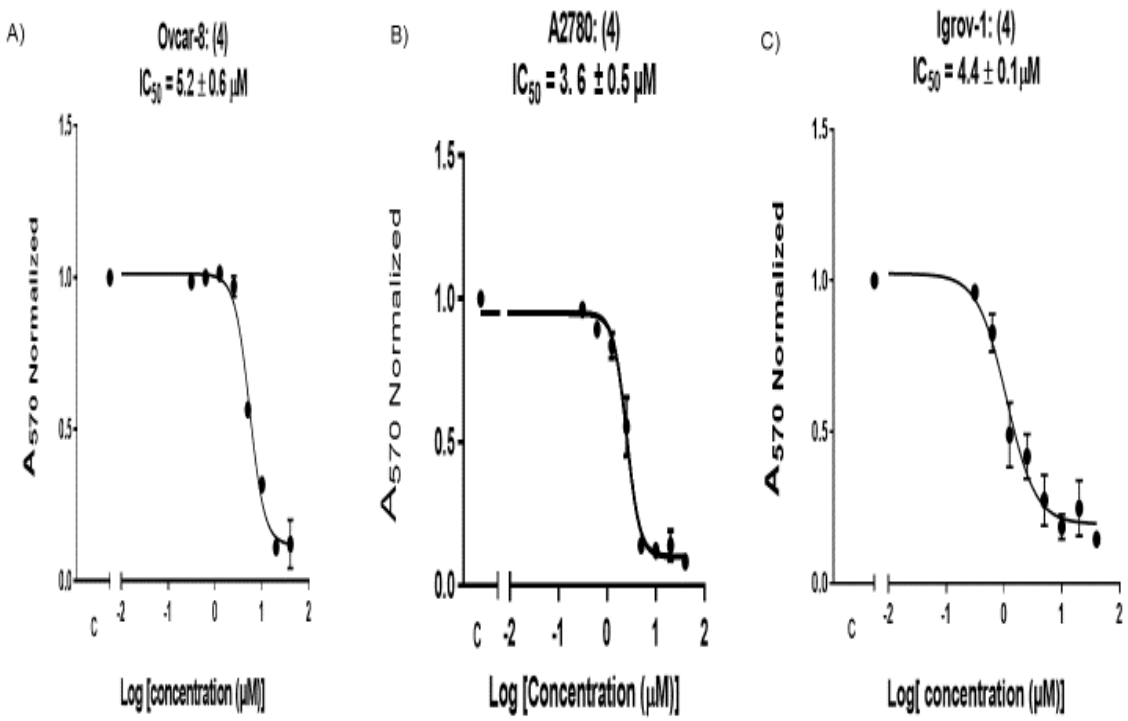

Figure 5.5 Concentration-response curves of **4** in ovarian cancer cell lines with absorbance at 570nm normalized to control. The Ovcar-8 (A), A2780 (B) and Igrov-1 (C) ovarian cancer cell lines treated with different concentrations of **4** (0.16 – 40 µM) (Table 5.3, Figure 5.5-5.6) over 72h. Graph determined by four parameters fitting sigmoid curve (GraphPad prism demo 6.1). Data represented as mean ± SEM n= 5. *C* represents IC_{50} of control.

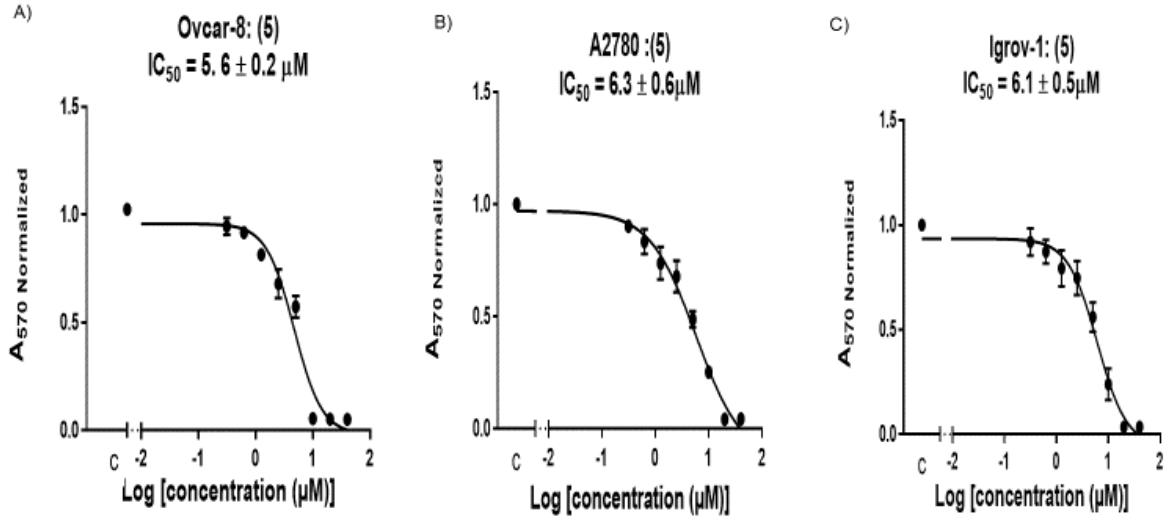

Figure 5.6 Concentration-response curves of (**5**) in ovarian cancer cell lines with absorbance at 570nm normalized to control. The Ovcar-8 (A), A2780 (B), and Igrov-1 (C). Ovarian cancer cell lines treated with different concentrations of **5** (0.16 – 40 µM) over 72h.The dose range that showed cytotoxic activities include 2.2- 40 µM. The graph determined by four parameters fitting sigmoid curve (Graph Pad prism). Data represented as mean ± SEM, n = 5 independent experiments. A_{570} in y-axis represents normalized absorbance at 570nm (optical density). C represents control (DMSO). Results were significant at $P<0.05$ (one way ANOVA)

However, having demonstrated the in vitro cytotoxity of cycleanine analogues together with the selective index future work needs to be done to determine the in vivo or preclinical assay of these compounds.

To have better understanding of the morphological effects of 5-[(dimethylamino) methyl] cycleanine (**4**) and 5-[(propargylamino)methyl] cycleanine (**5**) on ovarian

cancer cell lines, different concentrations of **4** and 5 (5 - 20 µM) were exposed to Ovcar-8 cells over 24 and 48 hours.

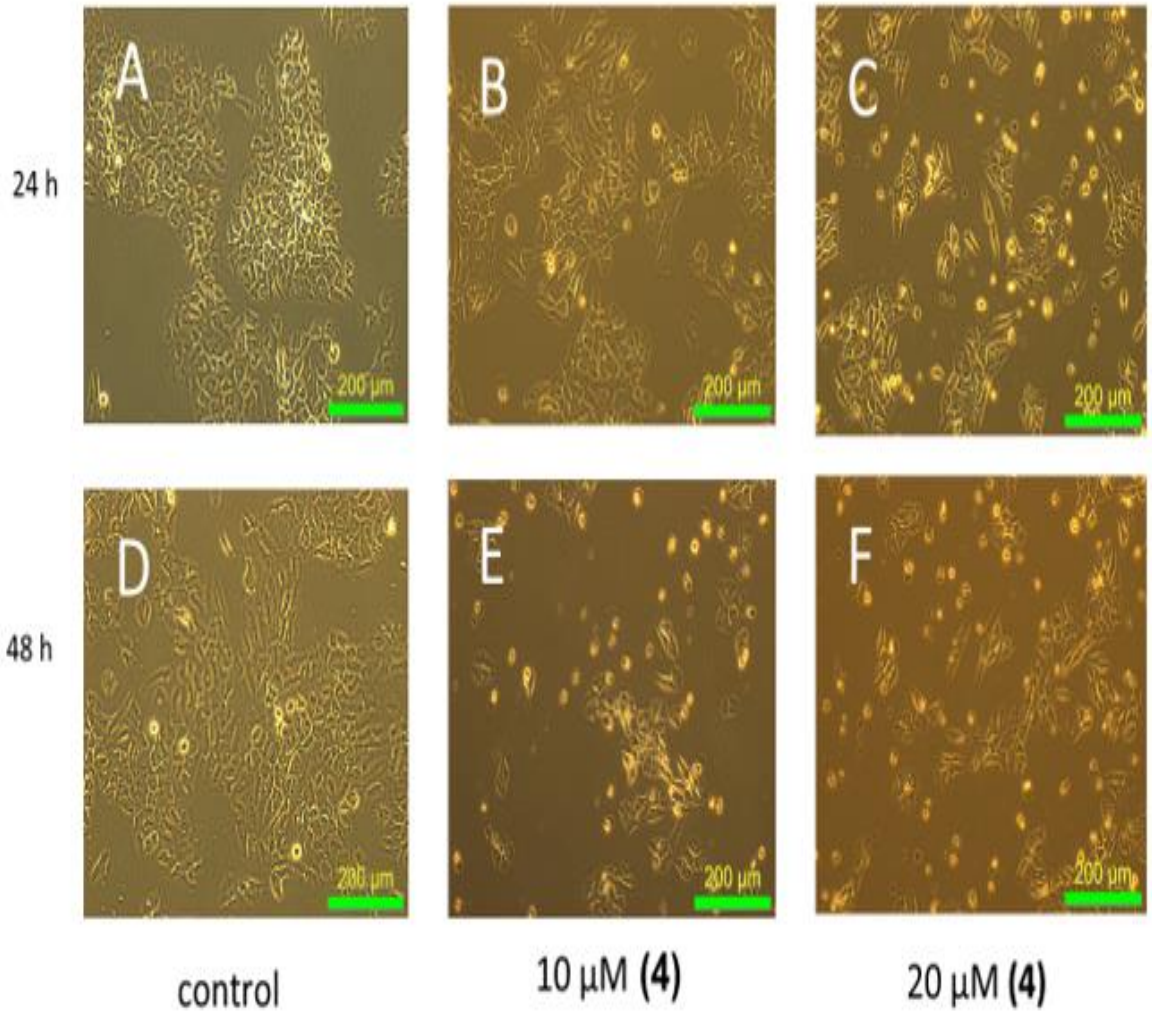

Figure 5.7 Effects of 5-[(dimethylamino) methyl] cycleanine (**4)** on the morphology of Ovcar-8 cancer cells. A and D are control (no drug) for 24 and 48h respectively. B and E are 10 µM of **4** - treated cells after 24 and 48hrs respectively. C and F are 20 µM of **4** - treated ovcar-8 cells after 24 and 48 h respectively. At 10- 20 µM, over 24 and 48h, compound **4** induced two-time point – (B and E) and two concentrations (C and F) –induced t changes on the morphology of Ovcar-8 as seen under phase

contrast light microscope. These changes were reproducible in 5 independent experiments. There was observed morphological alterations on ovcar-8 cells post-treatment with two timepoint and two concentration of 5-[(dimethylamino) methyl] cycleanine (figure 5.7). These changes were reproducible in 5 independent experiments.

The effects of 5-[(propargylamino)methyl] cycleanine (**5**) on morphology of Ovcar-8 cancer cells were also found to be time- and concentration-dependent (Figure 5.8).

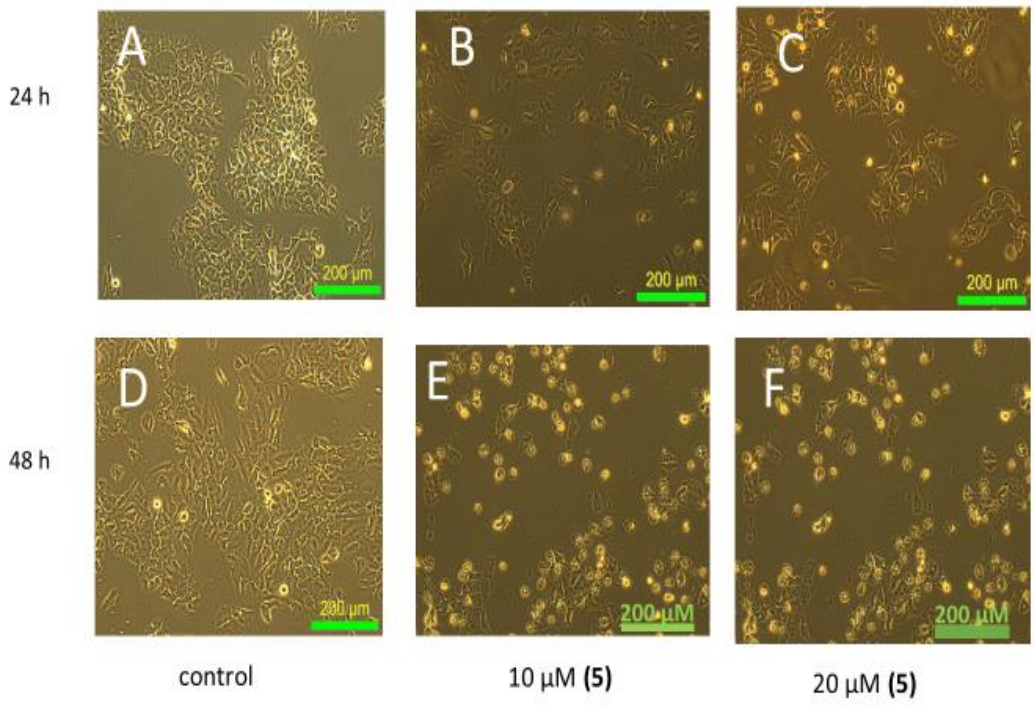

Figure 5.8 Effects of 5-[(propargylamino)methyl] cycleanine **(5)** on morphology of Ovcar-8 cancer cells. Ovcar-8 showed morphological changes when treated with two concentration of **5** (10 and 20 µM) over two time points of 24h (B and E) and 48h (D

and F). A and D are controls for 24 and 48h, respectively; B and E were morphological changes observed when ovcar-8 was treated with 10 µM of **5** over after 24 and 48h respectively, as seen under phase contrast light microscope.; C and F were observed at 20 µM of **5**-treated ovcar-8 cells after 24 and 48 h, respectively. There was observed morphological alterations on ovcar-8 cells post-treatment with two time point and two concentration for **5** (figure 5,8). These changes were reproducible in 5 independent experiments.

5.3 Caspase or apoptotic activities of cycleanine derivatives on cancer cell lines

The results of anticancer activities of 5-[(dimethylamino)methyl] cycleanine (**4**) and 5-[(propargylamino)methyl] cycleanine (**5**) prompted a detail study of the mechanism of cell death induced by these drugs on ovarian cancer cell lines. This study therefore further investigated the apoptosis induction of **4** and **5** in cancer cells by evaluation of caspase 3/7 activation (Figure 5.9), cleavage of PARP (Figure 5.10) and cell cycle assays (Figure 5.11 – 13). The aim was to determine the apoptotic effects of the new analogues in ovarian cancer cells.

Results showed that 5-[(dimethylamino)] cycleanine and 5-[(propargylamino) methyl]cycleanine (20µM) after exposure to Ovcar-8, A2780 and Igrov-1 for 24h, caused activation of caspase Glo 3/7 activities which was manifested as elevation of caspase levels on the three ovarian (Ovcar-8: (A), A2780: (B) and Igrov-1: (C) cell lines (Figure 5.9). The increase in caspase activity was represented as fold increase

relative to the control (Figure 5.9 A, B, C). Medium without treatment served as (negative) control while carboplatin was used as positive control (Figure 5.9).

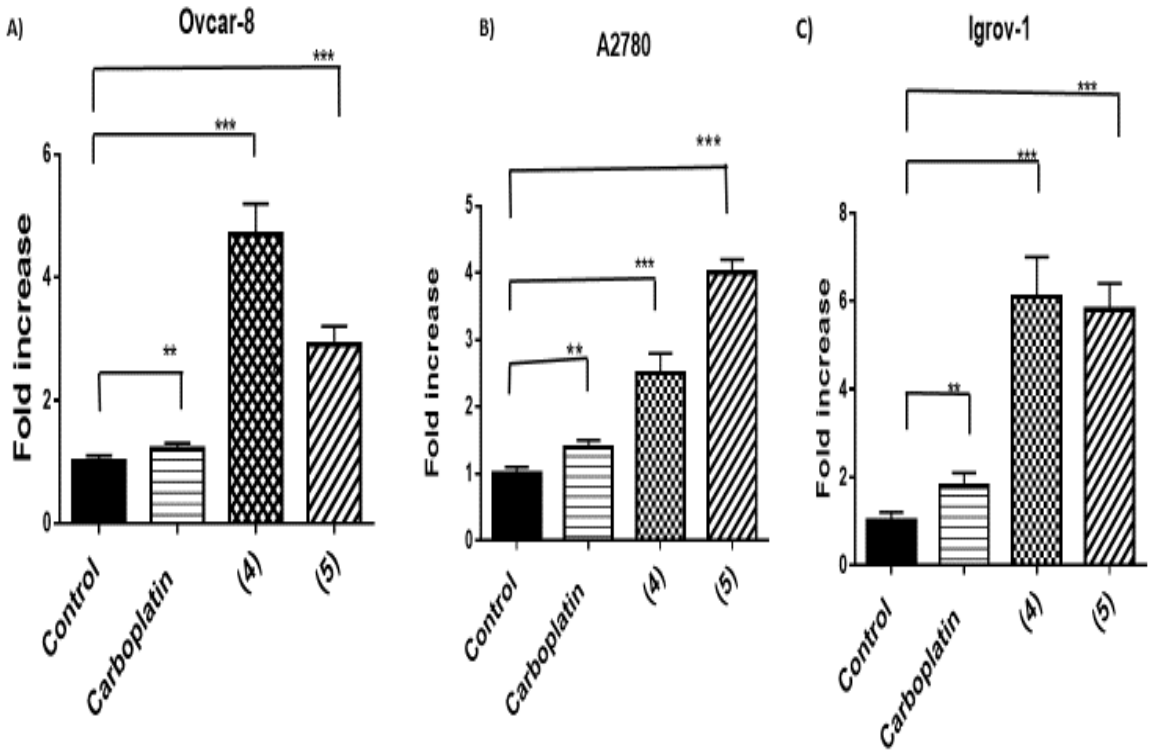

Figure 5.9 The apoptotic effects (caspase 3/7 activities) of **4** and **5** on three ovarian cancer cell lines. Data represented as mean ± SEM, n = 6 observations, negative control was the solvent without drug, carboplatin used as positive control; **4** and **5** (20 μM) test compounds. **4** and **5** are 5-[(dimethylamino)] cycleanine and 5-[(propargylamino) methyl] cycleanine respectively. Results were significant compared to control *** P<0.0001(one-way ANOVA) post hoc analysis multiple t- test compared with control P<0.001 (t-test).

5.4 Western blot (PARP cleavage) analysis for cycleanine analogues

The Western or immunoblotting was carried out as further confirmation of apoptosis induction on cancer cells of 5-[(dimethylamino)methyl]cycleanine (**4**) and 5-[(propargylamino)methyl]cycleanine (**5**). The results showed that the Ovcar-8 cancer cell line by treatment of **4** and **5** caused a significant cleavage in PARP in a similar way as cycleanine compared to control cells (Figure 5.10). There was no significant PARP-cleavage observed in negative control.

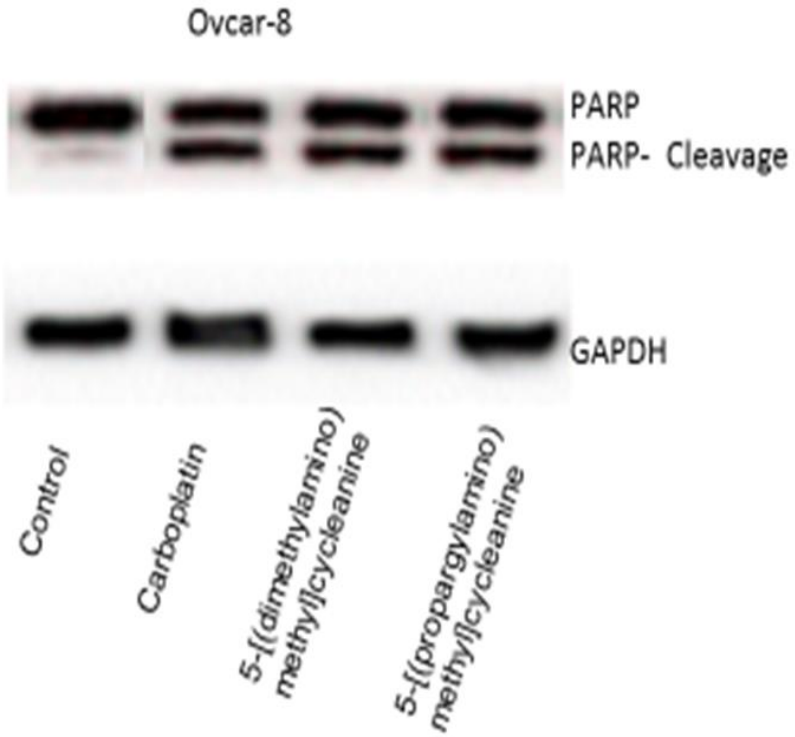

Figure 5.10 Western blotting analysis of the PARP-1 cleavage (marker) in Ovcar-8 cells after treatment with carboplatin, **4** and **5**. GAPDH was used as a loading control. A representative of three independent experiments is shown.

5.5 Evaluation of apoptotic effects of 4 and 5 on Ovcar-8 cells using flow cytometry

For quantification of the percentage of apoptotic cells post - treatment with **4** and **5**, Ovcar-8 cells were treated and stained with Annexin V and propidium iodide (PI) and analysed by flow cytometry (Figure 5.11). Treatment of Ovcar-8 with carboplatin, **4** and **5** over 48h caused significant increase in the population of both early and late apoptotic cells compared to the control (no drug) cells (Figure 5.11).

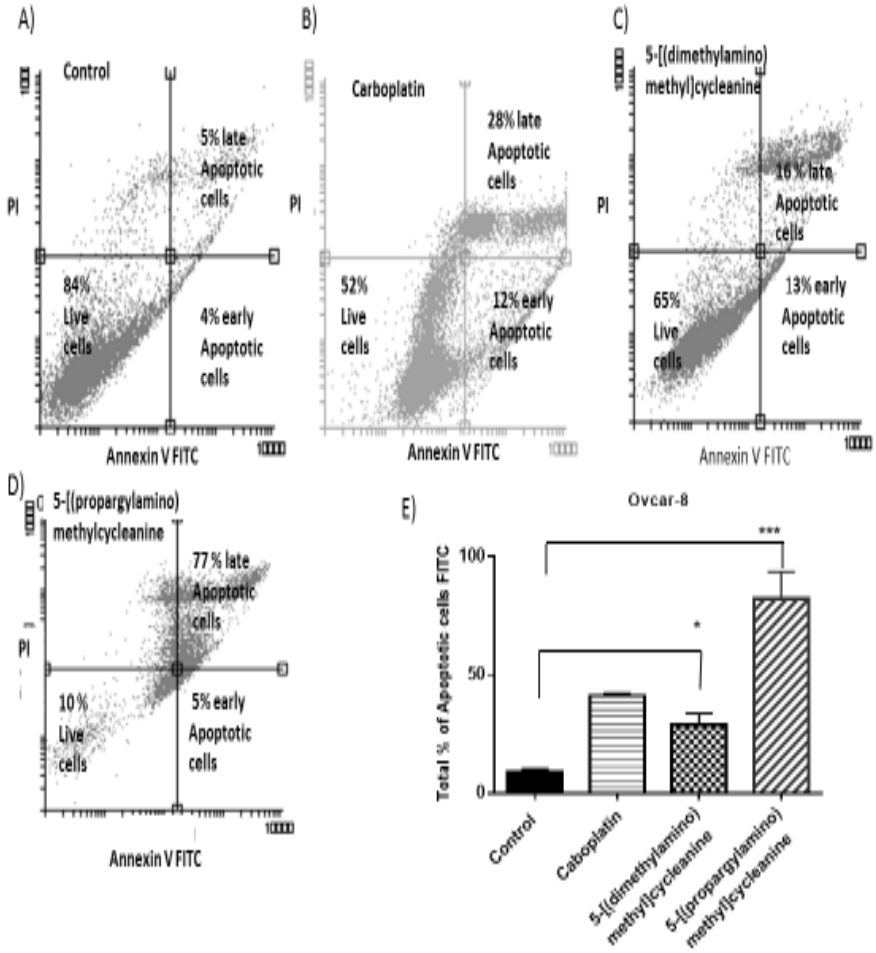

Figure 5.11 Flow cytometry analysis of apoptotic effects of 5-[(dimethylamino)methyl]cycleanine (**4**) and 5-[(propargylamino)methyl]cycleanine (**5**) on Ovcar-8 cells. The scattering dot plots indicating the percentage of live, early and

late apoptotic cells under treatment of medium (control) (**A**), carboplatin (**B**), **4** (**C**), and **5** (**D**) (20 μM) for 48 hours by using Annexin V & PI assay. The percentages of the total apoptotic cells caused by **4** (**C**), **5** (**D**) and positive control (carboplatin) (**B**) were significant compared to negative control (**A**) (one way ANOVA for group analysis, $P<0.001$; post hoc paired *t*-test relative to control was done (* $P<0.05$, t-test) (E).

5.6 Cell cycle effects of 4 and 5 on Ovcar-8 cell line

To further confirm the quantification of apoptosis induced by 5-[(dimethylamino)methyl]cycleanine (**4**) and 5-[(propargylamino)methyl]cycleanine (**5**) on ovcar-8 cells, cell cycle analysis was done using propidium iodide and flow cytometer (Figure 5.12 and 5.13). The effect of **4** and **5** on cell cycle distribution of Ovcar-8 cells is shown in Figure 5.12 and Figure 5.13. Carboplatin was used as a positive control. Medium was used as negative control. The percentage of Ovcar-8 cells in subG_1 increased after exposure to carboplatin, **4** and **5** for 48h compared to negative control. This was consistent with apoptosis observed in Figure 5.12 and 5.13. The percentage of cells at the G_0/G_1 phase (live cells) decreased significantly compared to control (Figure 5.12 and 5.13). This was consistent with results of isolated alkaloids, parent alkaloid (cycleanine) and other alkaloids in this study (Figure 4.14).

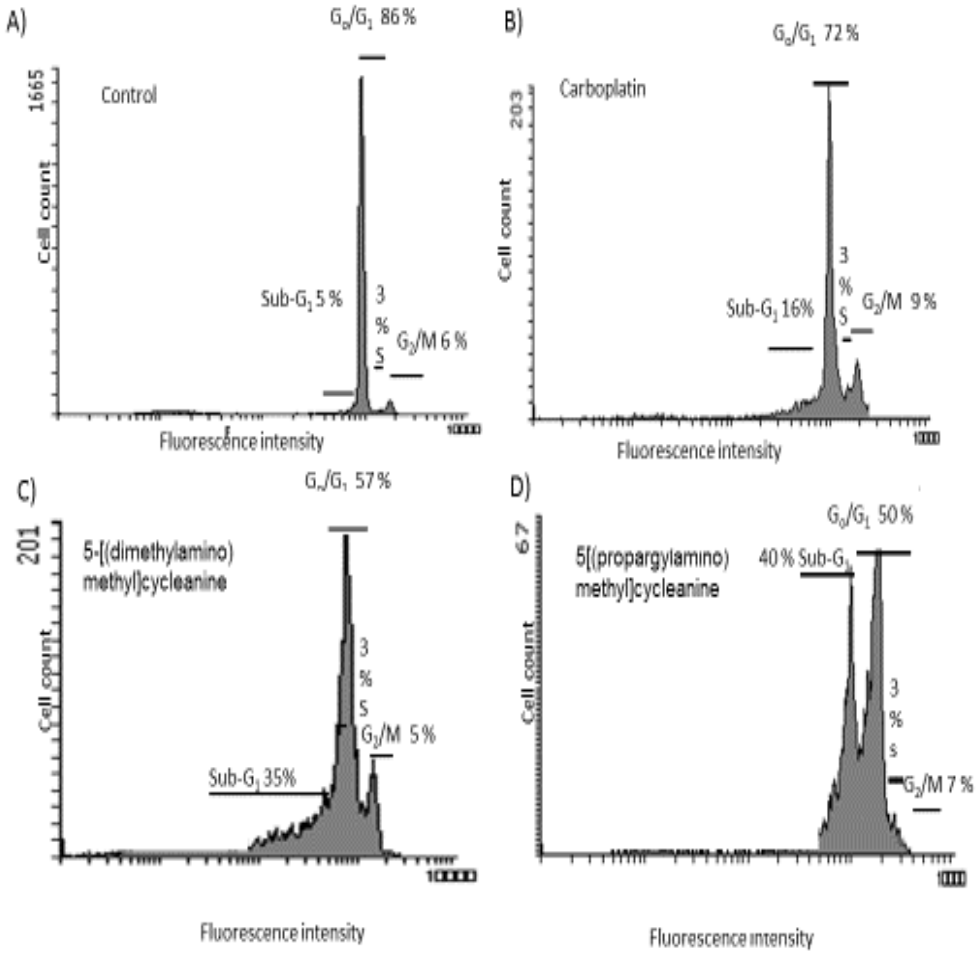

Figure 5.12 Effects of **4** and **5** on cell cycle distribution in Ovcar-8 cells. The effects of control (A), carboplatin (B), **4** (C) and **5** (D) on the cell cycle determined by use of flow cytometry analysis revealed that the percentage of subG_1 phase (apoptotic cells) of the ovcar-8 cell cycle was significantly increased compared to cells exposed to control (no drug, A).

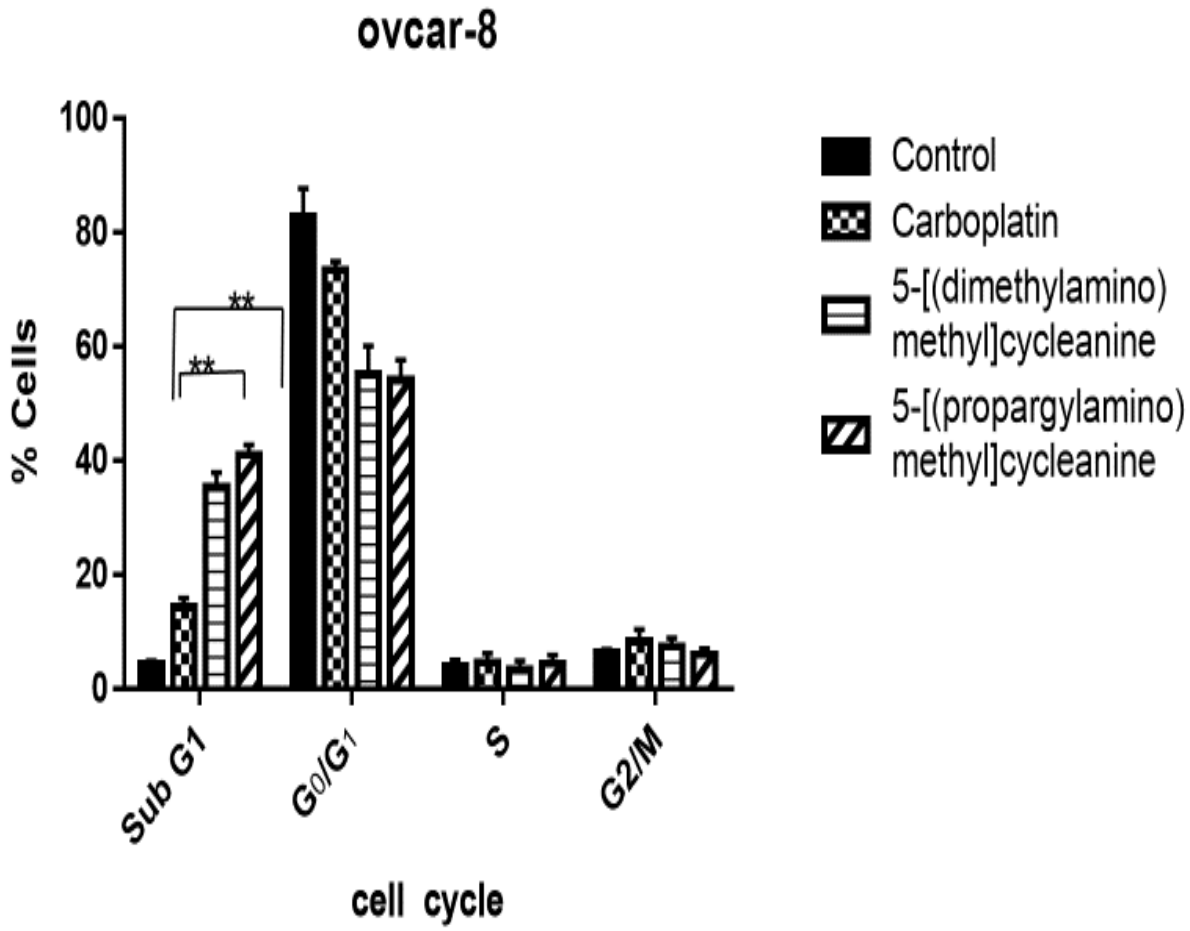

Figure 5.13 Cell cycle distribution analysis of apoptotic effects of **4** and **5** on Ovcar-8 cell lines. Data represented as mean ± SEM, n = 4 observations. The percentage of subG_1 phase (apoptotic cells) of the ovcar-8 cell cycle was significantly increased compared to cells exposed to control (no drug). While G_0/G_1 phase cells decreased significantly compared to control P< 0.0001 (one-way ANOVA) (Figure 5.12 A-D).

5.7 Alkaloid uptake in Ovcar-8 cells by use of confocal microscopy

To investigate the cellular uptake of BBIQ alkaloids and get good knowledge of the pattern alkaloids distribution in cancer cells, control, cycleanine and 5-

[(propargylamino)methyl]cycleanine (20 µM) were administered in Ovcar-8 cells. The fluorescence intensities and areas occupied by the alkaloids/control (drug distribution) were studied after 48h exposure, by use of confocal and fluorescence microscope (Figure 5.14-15). This was done by use of Alexa 488 azide (fluorescent dye) to monitor the intracellular uptake of monoalkynyl cycleanine (**5**) via specific click chemistry reaction with Alexa 488 azide per previously reported procedures (Luo et al., 2013). Cycleanine is not fluorescent compound. The fluorescence data (Figures 5.14 and 5.15) were analysed by the determination of the average fluorescence intensities of the cells in a area by use of Image J software and evaluation of the difference from the background fluorescence values. Values were evaluated from 30-90 cells determined in five independent experiments. The fluorescence intensity was used as a measure of the distribution and uptake of **5** in Ovcar-8 (Figures 5.14 – 5.16A). The fluorescence intensity is proportional to the magnitude of cellular uptake of compounds in cells (Figure 5.16 A) (Luo et al., 2013). The fluorescence intensity of compound **5** was found to be dose dependent (Figure 5.14 – 5.16 A). The mean areas occupied by the cells were proportional to the magnitude of apoptotic cell death (Figure 5.16B). Figure 5.15 A-C show 3D view of ovcar-8 cells post 48 h treatment with different doses (10 - 30 µM) of 5-[(propargylamino)methyl] cycleanine as seen under confocal microscope. A selection of limited number of cells were made from confocal microscope observation and magnified further to get a better 3D view of the representative of cells treated. (Figure 5.15 A-C).

The results revealed that treatment of Ovcar-8 with 5-[(propargylamino)methyl]cycleanine (**5**, 20 µM) caused significant dramatic increase in mean fluorescence intensities (from 300 to 1800) (Figure 5.16A), with decrease in the mean area occupied (from 1000 to 2400) (Figure 5.16B) by **5**-treated cells compared to control. There was no significant change in florescence intensity observed on cycleanine-treated cells compared to control (Figure 5.14 and 5.16A). These results confirmed the intracellular uptake of monoalkynyl cycleanine (**5**), which indicated a similar mechanism for cycleanine.

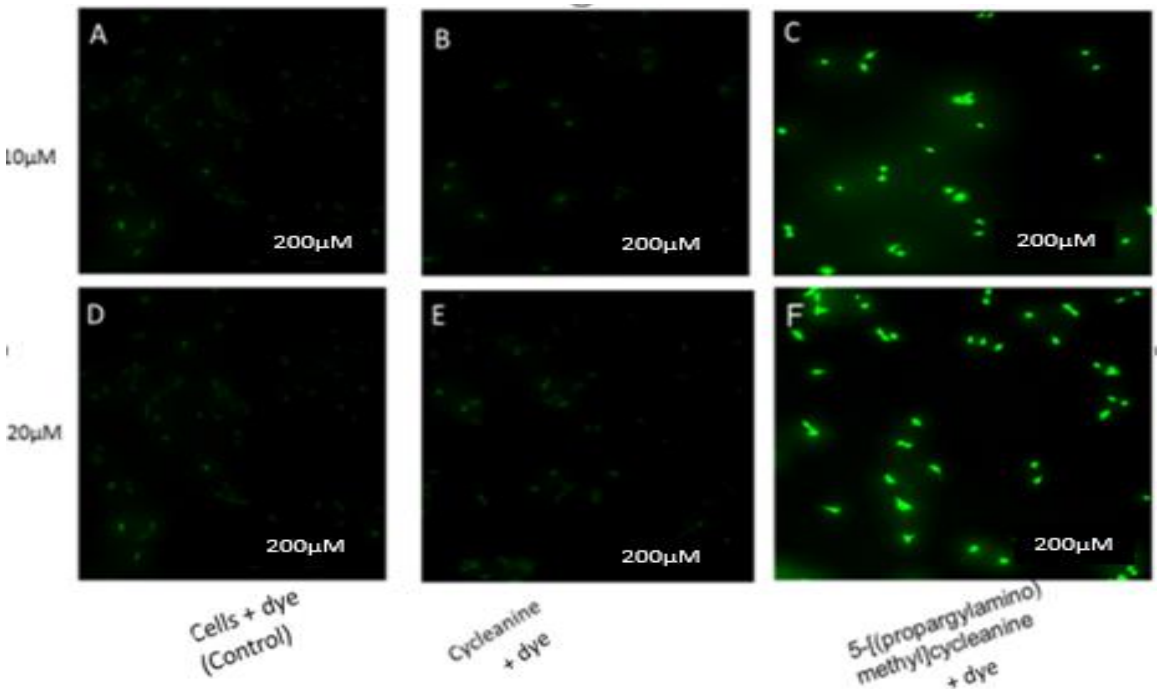

Figure 5.14 Analysis intracellular uptake of cycleanine and **5** in Ovcar-8 cells using confocal fluorescence microscopy. A and D represent cells with dye only (control); B and E, 10 and 20µM of cycleanine; C and F, 10 and 20µM of 5-[(propargylamino)methyl] cycleanine, respectively.

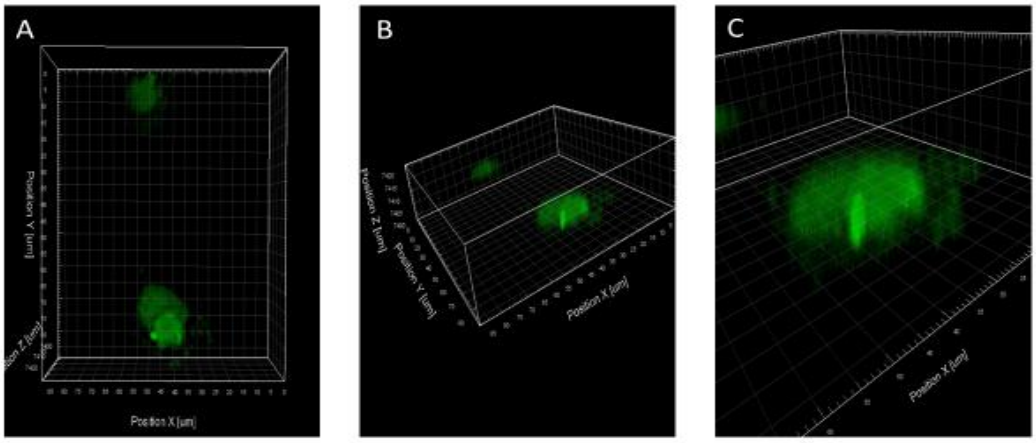

Figure 5.15 3D view of Ovcar-8 cells after treatment with 10 µM (A); 20 µM (B); 30 µM (C) of 5-[(propargylamino)methyl] cycleanine (5) over 48h as observed under

confocal microscopy. This shows the 3D view of ovcar-8 cells post 48 h treatment with different doses (10 - 30 µM) of (5) as seen under confocal microscope

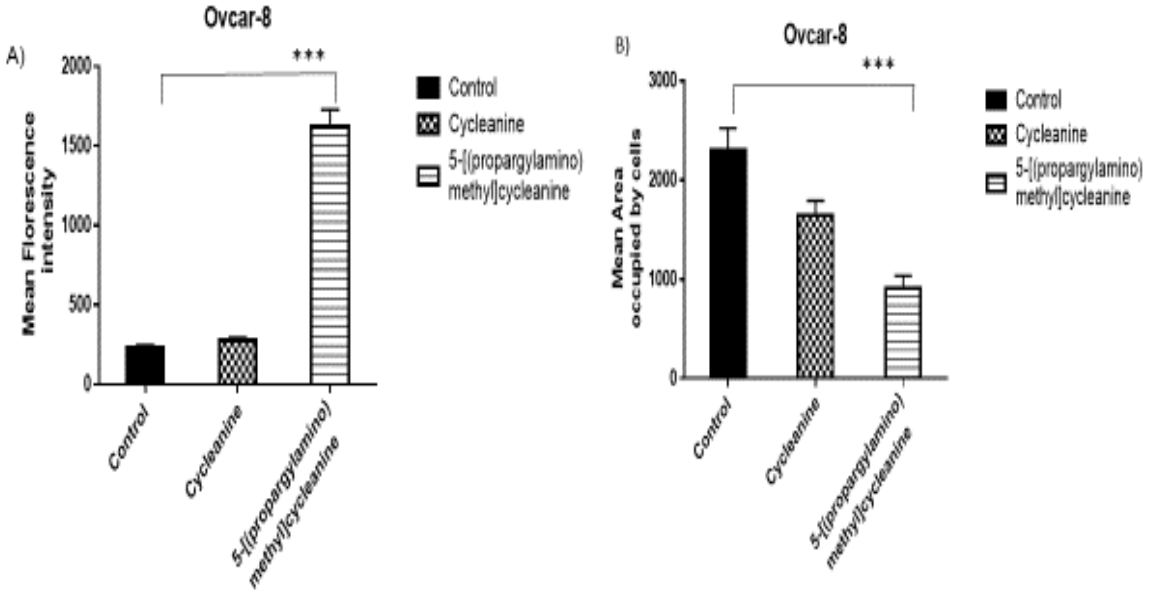

Figure 5.16 Cellular uptake of 5-[(propargylamino)methyl] cycleanine (**5**) in Ovcar-8 cells. (A): Shows the mean fluorescence intensity of ovcar-8 cells after 48h treatment with medium (control- no drug), cycleanine and 5-[(propargylamino)methyl] cycleanine. (B): the mean area occupied by ovcar-8 cells 48h post- treatment with medium (control- no drug), cycleanine and 5-[(propargylamino)methyl] cycleanine. Data represented as mean ±SEM, n = 5 independent experiments. Results were significant compared to control ***. P<0.0001 (one -way ANOVA).

5.8 Discussion

Reports showed that bisbenzylisoquinoline (BBIQ) alkaloids exerted anti-ovarian cancer activity (Liu et al., 2013). BBIQ exhibits wide range of biological activities including anti-cancer activity (Lee et al., 2002), bladder cancer (Li et al., 2011), colorectal cancer (He et al., 2011b), gallbladder carcinoma and prostate cancer cells (Liu et al., 2015). BBIQ alkaloids of *T. subcordata* exerted cytotoxicity by apoptosis induction of ovarian cancer cells. Cycleanine was also shown to possess a moderate selectivity towards ovarian cancer cells over normal cells via apoptosis, which may be used as a hit to modify its structure by semi-synthesis to improve its anti-cancer activity

Therefore, in search of BBIQ alkaloids with improved potency and optimum selective index, we have been able to synthesize two new BBIQ alkaloids using cycleanine as a hit compound (Figure 5.1 and 5.2). The new BBIQ alkaloids are 5-[(dimethylamino) methyl] cycleanine **(4)** and 5-[(propargylamino) methyl] cycleanine **(5)**. The anticancer activities of these compounds have been evaluated by SRB assay on ovarian cancer cell lines (Figure 5.5 and 5.6). The mechanism of cancer cell death induced by the new BBIQ alkaloids has been determined in this study. 5-[(dimethylamino)methyl] cycleanine **(4)** and 5-[(propargylamino)methyl] cycleanine **(5)** induced apoptosis by caspase 3/7 activation, PARP-cleavage, increase in percentage of both early and late apoptotic cells; and increase in $SubG_1$ with decrease in G_0/G_1 cell cycle phase of the Ovcar-8 cells. These were consistent with unmodified cycleanine.

The cells after exposure to **4** and **5** also showed morphological effects suggesting apoptosis in Ovcar-8 cells. The observed anti-proliferative activities of the synthesized new BBIQ alkaloids were found to be higher (about 2-3-fold increase) than the

observed effect with cycleanine (hit compound). This suggests that substitution at 5-position of cycleanine structure with dimethylamino or aminoalkynyl group could lead to improved cytotoxicity and biological activity of the cycleanine.

It was also observed that attachment of aminoalkynyl moiety to cycleanine could be used to study pattern of uptake of BBIQ alkaloids in cancer cells using click chemistry and confocal or fluorescence microscope. This agreed with past studies using a similar click chemistry approach for other natural products (Luo et al. 2013; Zhen et al. 2014).

This study is therefore, providing novel reports on cytotoxicity and apoptosis induction mechanism of 5-[(dimethylamino)methyl] cycleanine (**4**) and 5-[(propargylamino)methyl] cycleanine (**5**). The effects of **5** on uptake of BBIQ alkaloids and its evaluation in cancer cells are also novel study. Their selective index (SI) were determined to have good knowledge of the level of toxicity of these compounds on normal cells or the therapeutic index (Table 5.3). However, studies are ongoing to modify the structure of cycleanine through other chemical pathways to produce more BBIQ analogues with improved potency. The water solubility of the cycleanine analogues will also be determined for better understanding of the drug-like properties of these compounds. Future work would also be to isolate 2′-norcocsuline and isochondodendrine to get sufficient quantities as to carry out semi-synthesis of analogues of isochondodendrine and 2′-norcocsuline in search of more potent anti-cancer drugs.

CHAPTER SIX

ANTIMALARIAL ACTIVITIES OF FRACTIONS, BBIQ ALKALOIDS OF T. SUBCORDATA AND SEMI-SYNTHETIC ANALOGUES OF CYLEANINE

6.1 Anti-malarial activities of the crude extracts and fractions of *T. subcordata*

The *in vitro* antimalarial screening of extracts and fractions of total alkaloids from *T. subcordata* were done on *Plasmodium falciparum* chloroquine resistant strain using a Syber green fluorescent dye as described by Smilkstein et al., (2004) and modified by Hasenkamp et al., (2012). Results showed that among the fractions (TSS1-3) (Figure 2.2) screened, TSS1, showed the most significant antimalarial activity with about 98% parasite growth inhibition activity. TSS1 is the total alkaloids. The TSS1 was further subjected to silica gel column chromatography as previously described to produce BBIQ alkaloids of *T. subcordata*, which have potent anti-plasmodial activity (Section 6.2).

TSS3 also showed good percentage growth inhibition next to TSS1 and was fractionated by silica gel column chromatography, and its resulting fractions (TSS3.1-TSS3.8) were also evaluated for antimalarial activity (Figure 6.1). The most active fraction was TSS3.8. To identify possible bioactive compounds, gas chromatography mass spectrometer (GC-MS) was used to characterize the chemical composition of TSS3.8. After derivatization of TSS3.8 with N, O-Bis(trimethylsilyl)trifluoroacetamide (BSTFA) and pyridine. The trimethylsilyl derivatives of TSS3.8 were subjected to analysis by GC-MS. The GC-MS analysis revealed this fraction to be rich in fatty acids such cis-9-hexadecenoic acid; palmitelaidic acid; nonadecanoic acid; hexadecenoic acid and 11-cis-octadecenoic acid and glycosides (Table 6.1; Figures 6.2-6.3).

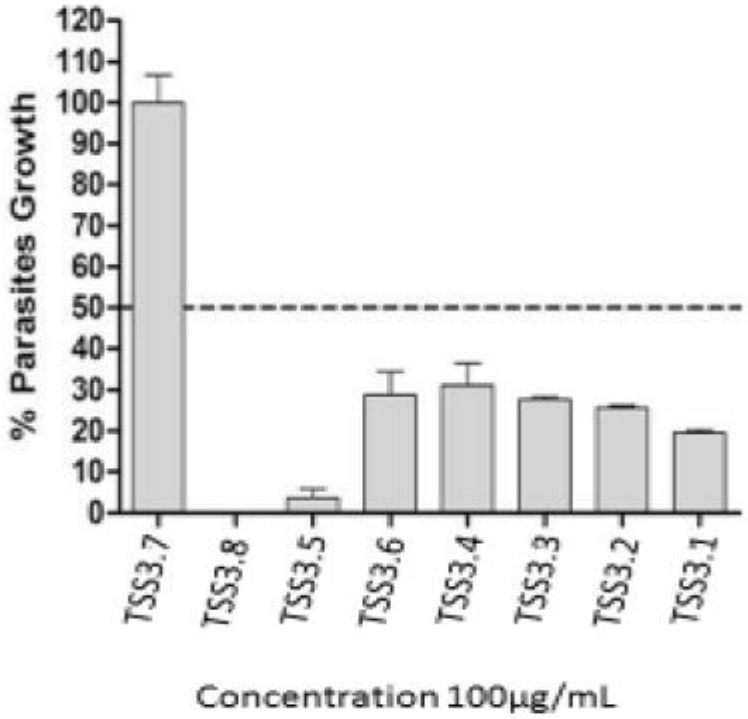

Figure 6.1 In vitro antimalarial screening results of fractions TSS3 from *T. subcordata* ethanol extract (TSS). TSS3.1-TSS3.8 are the column chromatography fractions from TSS3.

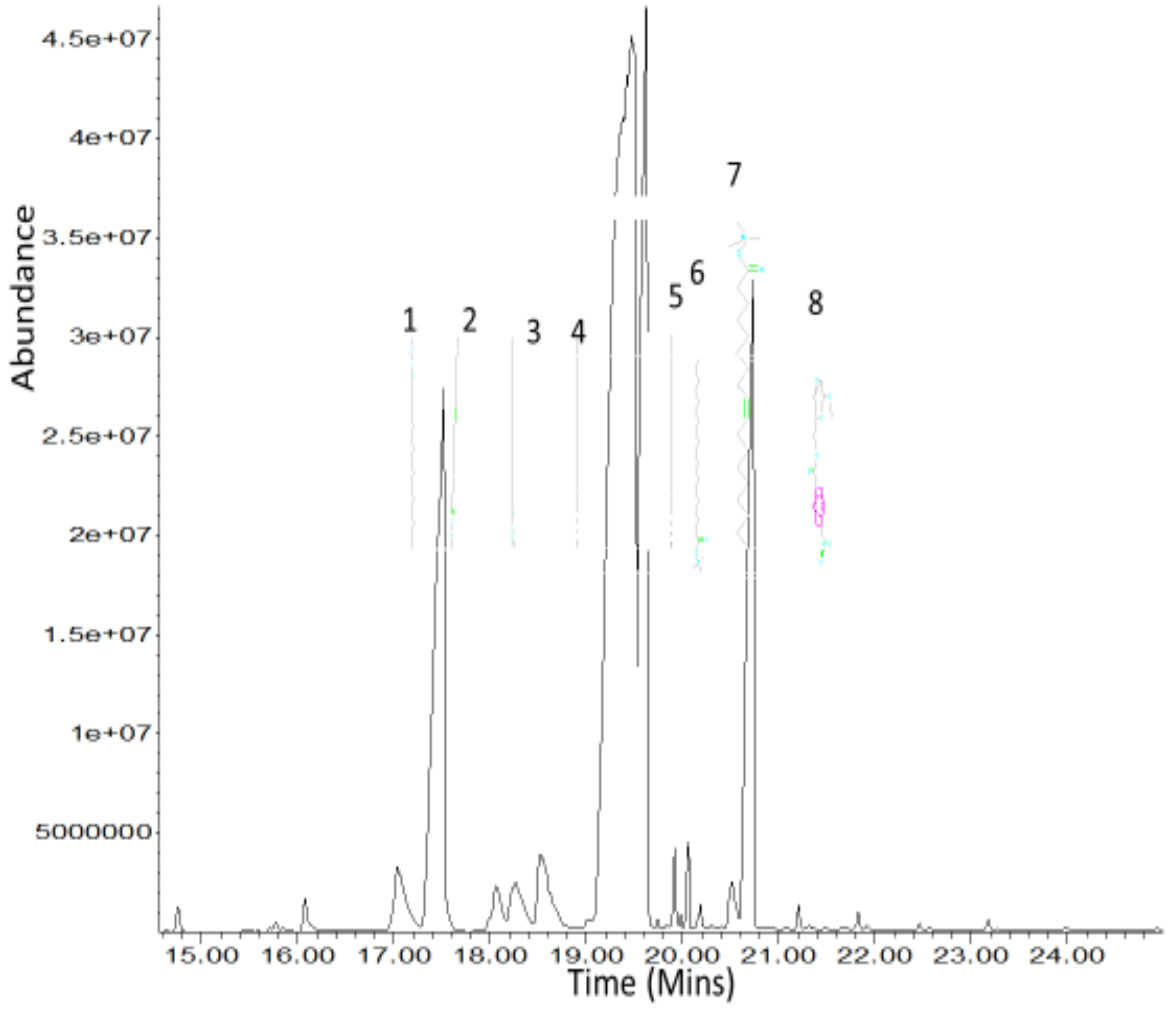

Figure 6.2 GC-MS chromatogram of TSS1.8 TMSi derivative. The numbers 1-8 are fatty acid derivatives from TSS1.8 series detected by GC-MS as named in table 6.1.

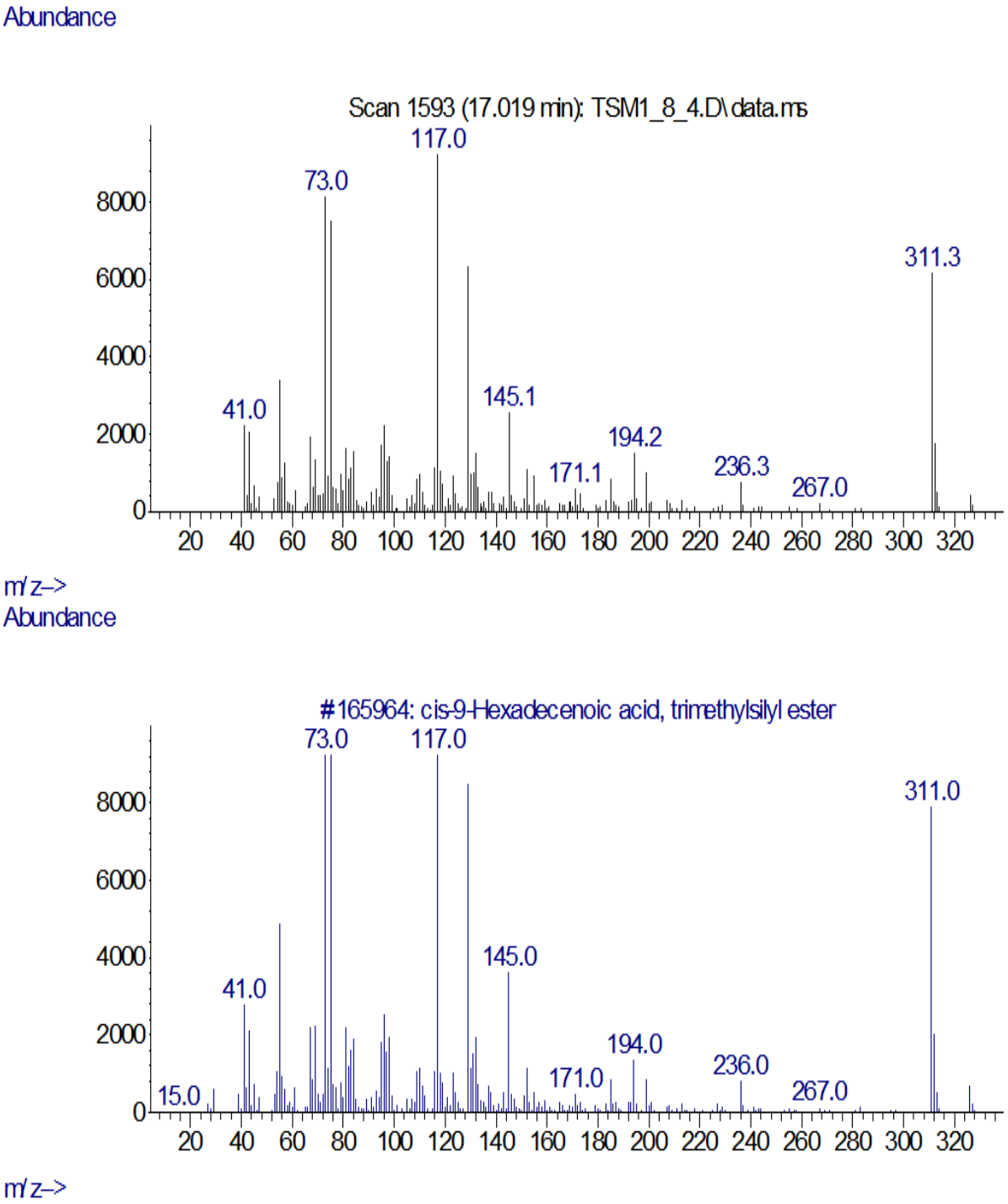

Figure 6.3 Mass spectrum of cis-9-hexadecenoic acid trimethylsilyl ester in TSS3.8.

Table 6.1 Fatty acid derivatives from TSS3.8 series detected by GC-MS.

S/No	Fatty acid/compounds	Molecular mass	RT (min)
1	N-Pentadecanoic acid	314	16.0
2	Pamitaidic acid trimethysilylester	326	17.0
3	Cis-9- hexadecanoic acid trimethysilylester	328	17.5
4	6- Heptadecanoic acid trimethysilylester	342	18.5
5	Oleic acid trimethysilyester	354	19.2
6	Octadecanoic acid trimethysilyester	356	19.5
7	11-cis-Octadecenoic acid, trimethylsilyl ester	339	19.4
8	Nanodecanoic acid trimethylsilyester	370	20.2
9	Cis-13-Eicosenoic acid, trimethylsily ester	367	20.5
10	Methy-2-3-anhydro-5-p-nitrobenzoyl-alpha-d-lyxofuranoside	295	20.7
11	Docosanoic acid, trimethylsily ester	397	21.8

6.2 Anti-malarial activities (IC_{50}) of the BBIQ alkaloids from *T. subcordata* and synthetic analogues of cycleanine

The *in vitro* antimalarial evaluation was also carried out on BBIQ alkaloids purified from chloroform fraction of *T. subcordata* and synthetic analogues of cycleanine to determine their IC_{50} on *Plasmodium falciparum* - chloroquine resistance strain(Hasenkamp et al., 2013, Smilkstein et al., 2004, Wong et al., 2011).

The results showed that the IC_{50} of isochondodendrine was least (6.1 ± 1.3 µM) among the three BBIQ alkaloids of *T. subcordata* evaluated (Table 6.2, Figure 6.4). This was seconded by 2′-norcocsuline (7.0 ± 1.6 µM) and highest with cycleanine (17.7 ± 2.0 µM). This probably implies that isochondodendrine exhibited relatively highest in vitro antimalarial activity while cycleanine showed least activity among the natural BBIQ alkaloids of *T. subcordata* assayed.

To check if there would be improved potency on antimalarial activity of cycleanine, the IC_{50} of 5-[(dimethylamino)methyl]cycleanine (**4**) and 5-[(propargylamino)methyl]cycleanine (**5**) were found to be was 0.7µM and 1.8µM, respectively (Figure 5.2, Table 6.2).

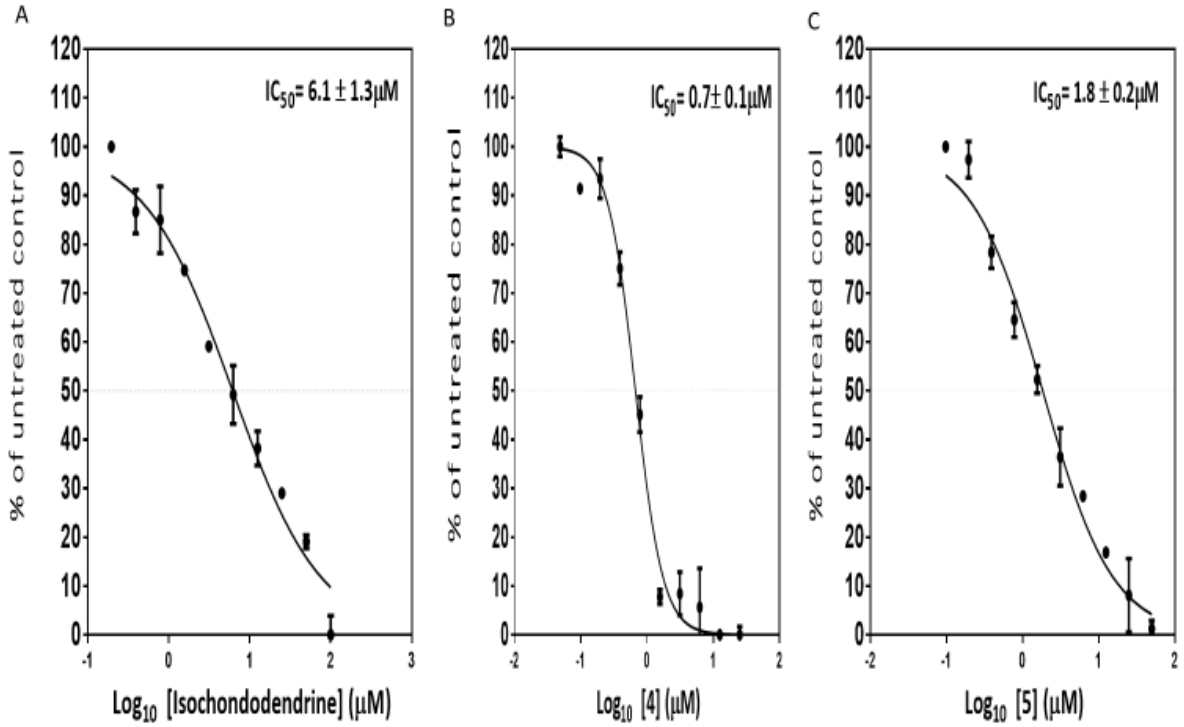

Figure 6.4 Antimalarial effects (IC_{50}) of alkaloid and derivatives of cycleanine. (A) isochondodendrine (**2**); (B) 5-[(dimethylamino)methyl]cycleanine (**4**); (C) 5-[(propargylamino)methyl]cycleanine (**5**).

Table 6.2 *In-vitro* antimalarial activities of BBIQ alkaloids and synthetic analogues of cycleanine.

BBIQ alkaloids of *T. subcordata* and cycleanine derivatives	IC_{50} on *P. falciparum*
Cycleanine (**1**)	17.7 ± 2.0 µM
Isochondodendrine (**2**)	6.1 ± 1.3 µM
2'-norcocsuline (**3**)	7.0 ± 1.6 µM
5-[(dimethylamino)methyl]cycleanine (**4**)	0.7 ± 0.1 µM
5-[(propargylamino)methyl]cycleanine (**5**)	1.8 ± 0.2 µM

6.3 Discussion

The BBIQ alkaloids possess a range of biological activities including, antiplasmodial activities (Schiff 1997; Angerhofer et al. 1999; Lin et al 1993; Mashall et al.1994; Ye and Van Dyke 2015).The total alkaloid TSS1 was purified using combined methods of column chromatography (previously described in this study), recrystallization methods and HPLC procedure. The pure BBIQ alkaloids (**1, 2** and **3**) and analogues (**4** and **5**) got in this study also showed significant antimalarial activity. This is consistent with previous reports (Ye and Dyke 2015; Angerhofer et al. 1999; Mashall et al. 1994; Mambu et al. 2000; Kaur et al. 2009; Lin et al. 1993). Here compound (**4**) showed the most potent antimalarial activity followed by (**5**). This might suggest that substitution in position 5 by amino group could result to improved antimalarial activity

of BBIQ alkaloids. The other BBIQ alkaloids showed good antimalarial activity with cycleanine having the least but good activity. For pure compounds: IC_{50} < 1µM could signify excellent or potent antimalarial activity; IC_{50} =1 – 20µM good activity; IC_{50} =21 – 100 µM moderate activity; IC_{50} =100 - 200µM low activity; IC_{50} > 200 µM inactive antimalarial (Batista et al., 2009b, Basco et al., 1994, Muriithi et al., 2002).

Cycleanine has been isolated from many other plant species of the Menispermaceae family (Schiff, 1997). It has been shown to have anti-plasmodial effects (Table 6.1) (Schiff, 1997, Angerhofer et al., 1999). Isochondodendrine also previously showed potent antiplasmodial activity (IC_{50} = 0.10 µg/ml = 0.17 µM) on the strain of 3D7 (Otshudi et al., 2005, Mambu et al., 2000). 2′-norcocsuline showed potent anti-plasmodial activity (Angerhofer et al., 1999). These were consistent with our finding here (Table 6.2, Figure 6.4).

In conclusion, the extracts and three BBIQ alkaloids - cycleanine, isochondodendrine and 2′-norcocsuline of *T. subcordata* were demonstrated to exert significant *in vitro* anti-plasmodial activities. Also, the fatty acids of *T. subcordata* such as cis-9-hexadecenoic acid; palmitelaidic acid; nonadecanoic acid; hexadecenoic acid and 11-cis-octadecenoic acid (Table 6.1; Figure 6.2 -6.3) could probably contribute to the antimalarial activities of this plant. These are also novel reports of *in vitro* antimalarial effects of *T. subcordata* and the new cycleanine analogues - 5-[(propargylamino)methyl]cycleanine and 5-[(dimethylamino)methyl]cycleanine. Compounds produced in this study were shown to exhibit up to 10 – 25-fold increase in antimalarial potency relative to the hit compound. However, further work may be necessary to determine the *in vivo* antimalarial effects of the BBIQ alkaloids of *T. subcordata* and the new analogues.

CHAPTER SEVEN

PHYTOCHEMICAL, ANTIMALARIAL AND ANTICANCER EFFECTS OF *CYLICODISCUS GABUNENSIS*

7.1 Phytochemical screening

The phytochemical screening was carried out on *C. gabunensis* crude extract, according to standard procedures (Okokon et al., 2006, Uche & Ezugwu, 2009, Trease & Evans, 1998, Sofowora, 1982, Harborne, 1998, Edeoga et al., 2005). The results revealed the presence of phytochemical constituents such as terpenes, flavonoids, saponins and glycosides (Table 7.1).

Table 7.1 Phytochemical screening results of ethanol extract of *C. gabunensis.*

Phytochemical constituents	Results of colour reaction tests
Flavonoids	++
Terpenes	++
Glycosides	+
Saponins	+
Alkaloids	-

++ represent largely present, + slightly present, - absence.

7.2 Anticancer activity of the crude extract of *C. gabunensis*

The hexane extract (CGH), ethanol crude extract (CGE) and fractions of *Cylicodiscus gabunensis* were screened for anti-proliferative activities on ovarian cancer cells using SRB. Results of anticancer assay of extracts/fractions of *Cylicodiscus gabunensis* showed that ethanol extract and different fractions of the crude ethanol extract (CGE) exhibited cytotoxicity on A2780, Igrov-1 and ovcar-8 (Table 7.1). The ethanol fractions used include ethyl acetate fraction (CGEA), butanol fraction (CGEBU), aqueous fraction (CGEAQ) and hexane extract (CGH). The CGEEA showed highest anti-proliferative activity in ovarian cancer cells with IC_{50} range of 4.5 – 17 µg/mL on A2780, Igrov-1 and Ovcar-8 cell lines. CGEAQ and CGEBU exhibited nearly similar activity with IC_{50} of 7.7 and 9.2 µg/mL respectively for CGEAQ and CGEBU on A2780 cells (Table 7.2, Figure 7.1). But CGEAQ exerted significant higher activity than CGEBU in ovcar-8 and Igrov-1 cells (Table 7.2, Figure 7.2). The hexane fraction showed the least activity with IC_{50} greater than100 µg/mL.

Table 7.2 *In vitro* anticancer activities of crude extracts and fractions of *C. gabunensis.*

Crude extract or fractions of *C. gabunensis*	50% Inhibitory concentration (IC_{50}) of cancer cell line (µg/mL)		
	A2780	Igrov-1	Ovcar-8
CGH	>100	ND	> 102
CGE	19.9 ± 1.7	13.2 ± 2.2	75 ± 2.1
CGEEA	4.5 ± 0.2	9.2 ± 1.1	17.0 ± 1.3
CGEBU	9.2 ± 0.2	16.0 ± 2.5	27 ± 1.2
CGEAQ	7.7 ± 0.5	13.9 ±1.8	7.7 ± 0.5

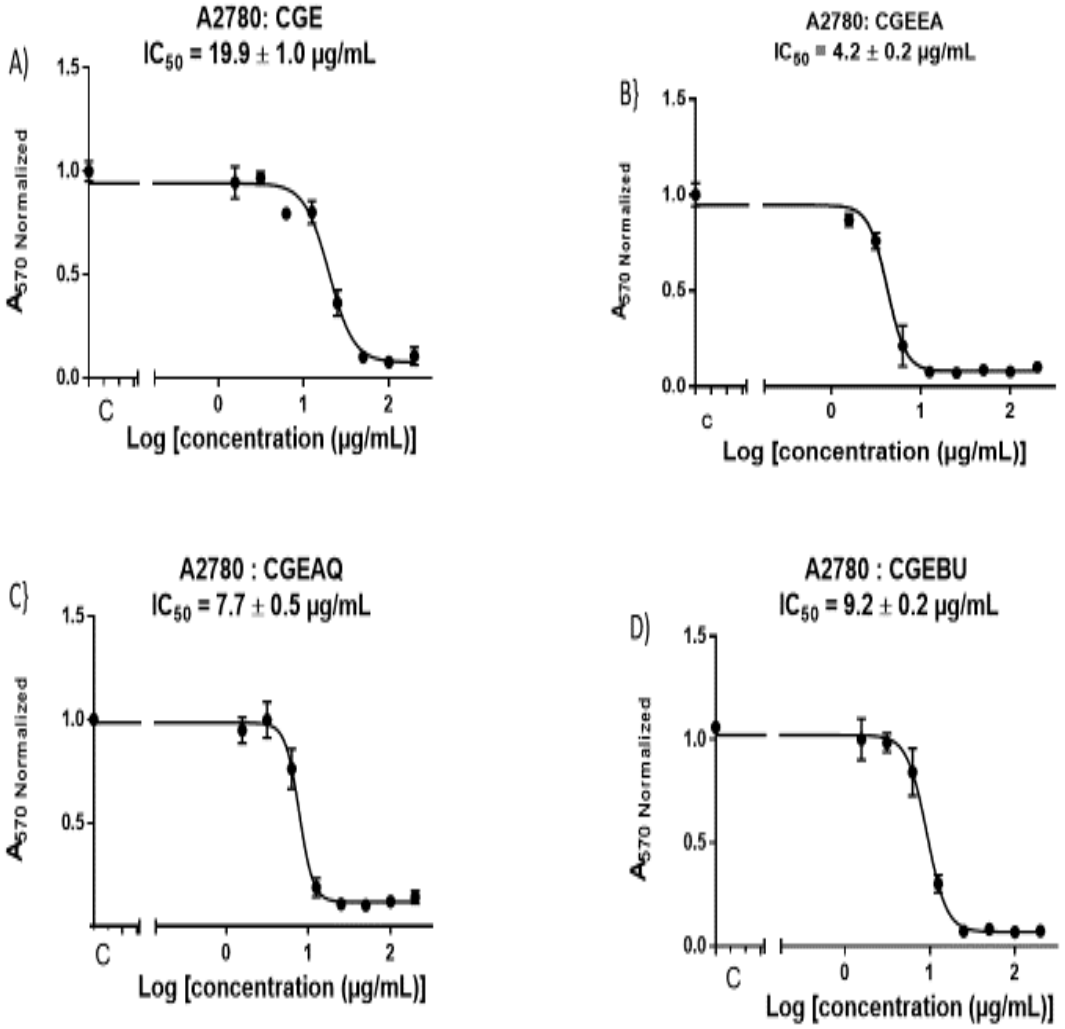

Figure 7.1 Anti-proliferative effects of *C. gabunensis* extract and fractions on A2760 cells with normalized absorbance at 570nm. **A**) The ethanol crude extracts (CGE); **B**) the ethyl acetate fraction (CGEEA); **C**) the aqueous fraction (CGEAQ); and **D**) the butanol fraction (CGEBU). C on x-axis is control. A_{570} is normalized (to control) absorbance (optical density) at 570nm

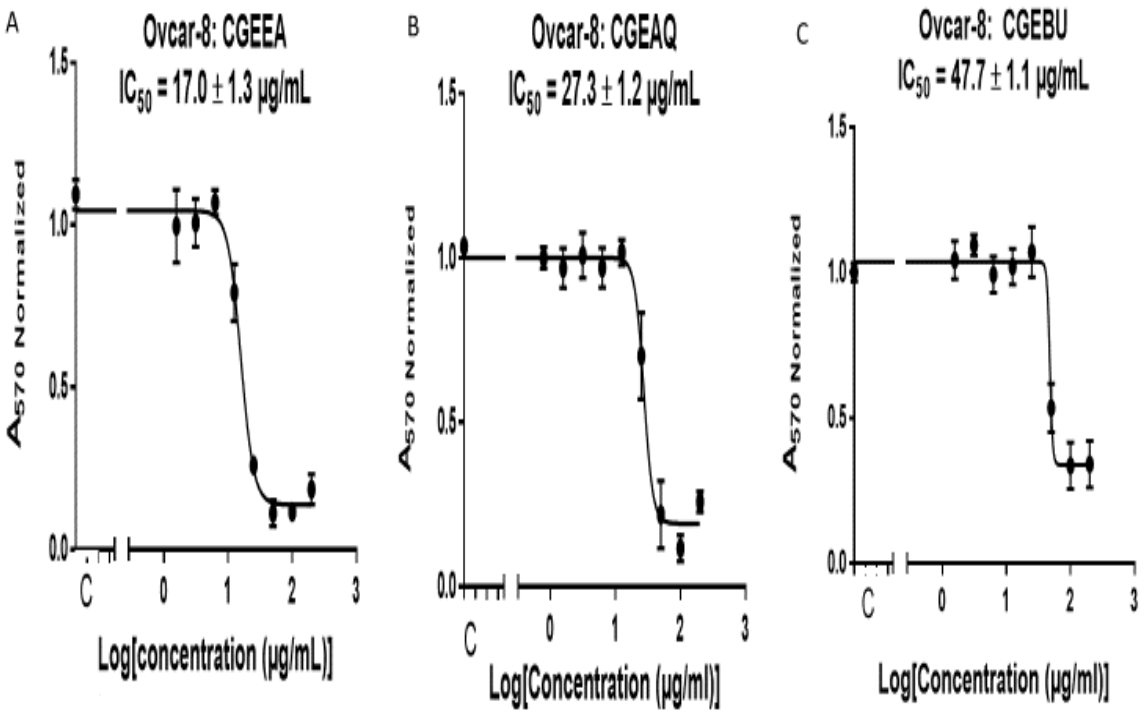

Figure 7.2 Anti-proliferative effects of *C. gabunensis* ethanol extract fractions on Ovcar-8 cells with normalized absorbance at 570nm. (A) The ethyl acetate fraction (CGEEA); (B) the aqueous fraction (CGEAQ); and (C) the butanol fraction (CGEBU). C on x-axis is control. A_{570} is normalized (to control) absorbance (optical density) at 570nm.

7.3 Antimalarial activities of *Cylicodiscus gabunensis*

Antimalarial screening of the extracts and fractions of *C. gabunensis* was carried out. The antimalarial activities of the plant extract and fractions against *P. falciparum* Dd2 were performed using Syber Green I Fluorescence assay (Henriques et al., 2012, Hasenkamp et al., 2013). The ethanol extract and fractions showed stronger

antimalarial activity than the hexane extract (Figure 7.1). The IC_{50}s of the fractions CGEEA, CGEBU, and CGEAQ were determined to be 16.06, 10.35, and 25.78 µg/ml, respectively (Figure 7.3; Table 7.3). Among them, CGEBU fraction showed the most antimalarial activity.

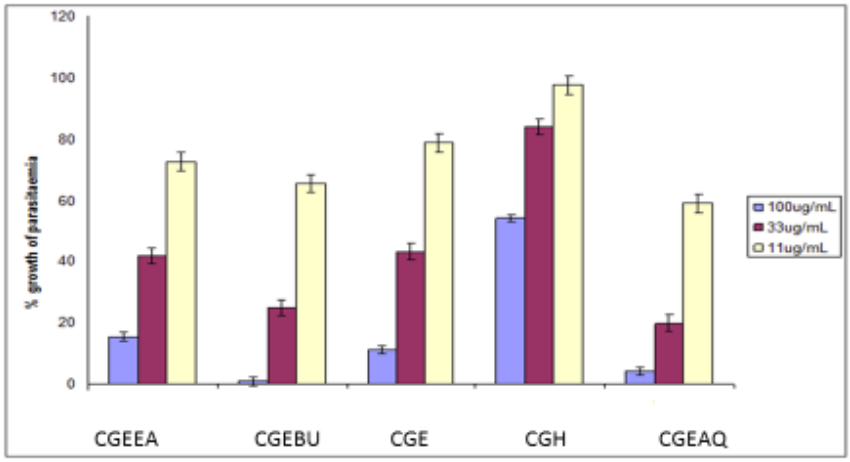

Figure 7.3 The *in vitro* antimalarial activities of different extracts and fractions of *C. gabonensis*. CGEEA represents ethyl acetate fraction from ethanol extract, CGEBU butanol fraction, CGE Ethanol extract, CGH hexane extract, and CGEAQ, aqueous fractions.

Table 7.3 In vitro antiplasmodial activity (IC_{50}) of fractions from *C. gabunensis*

Extracts and Fractions from *C. gabunensis*	IC_{50} (µg/mL)
CGEEA	16.1
CGEBU	10.4
CGEAQ	25.8

7.4 Discussion

The phytochemical screening of crude extracts of C. *gabunensis* was done to get overview of the phyto-constituents of ethanol extract of C. *gabunensis*. Results revealed the presence of terpenes, flavonoids, saponins and glycosides. This is consistent with previous studies (Okokon et al., 2006).

Due to on-going laboratory research in our group, in search of bioactive anti-ovarian cancer as part of natural product drug discovery (Li et al., 2015), coupled with the history of traditional use of *C. gabunensis* in treatment of malaria and cancer in West Africa (oral interview with herbalist in west Africa where the plant was sourced; Okonko et al., 2006), we carried out anti-proliferative assay on *C. gabunensis* to have scientific documents on the claims by Nigerian traditional medicine dealers. Results showed that *C. gabunensis* exerted *in vitro* anti-cancer activities in ovarian cancer cells (Table 7.2, Figures 7.1 and 7.2). The ethyl acetate fraction of the ethanol crude extract of *C. gabunensis* exhibited highest activity (Table 7.2, Figures 7.1 and 7.2). This is a novel report of anti-cancer activities of *C. gabunensis.* The results could provide a basis for traditional use of *C gabunensis* in cancer treatment. It could probably serve as a guide to explore more anti-cancer agents of natural origin. More studies are on-going to identify and elucidate the bioactive compounds responsible for anticancer effects of *C. gabunensis.*

Results also showed that *C. gabunensis* fractions exhibited ant-malarial activity. To identify the most bioactive anti-plasmodial compounds we used hexane to extract the non-polar materials and 70 % ethanol for polar and semi-polar materials. The results indicated that the ethanol extract has more potent activity over the hexane extract,

which is a primary indication of possible antimalarial activity and come in agreement with previous research which used an ethanol extract in an *in vivo* study in mice infected with *Plasmodium berghei*. This study could provide supporting basis for use of *C. gabunensis* as local medicine for treatment of malaria.

Plant extracts with possible antimalarial activities are classified to the highly active with $IC_{50} \leq 5$ µg/ml, promisingly active 5.1-10 µg/ml, good activity 10.1-20 µg/ml, moderate activity 20.1-40 µg/ml, marginal potency 40.1-70 µg/ml, poor or inactive 70.1 to > 100 µg/ml (Basco et al., 1994, Batista et al., 2009, Muriithi et al., 2002) According to this classification, it seems that butanol fraction CGEBU has good antimalarial activity and presents a worthy target for further investigation. This investigation is ongoing.

In conclusion, bioassay-guided extraction and fractionation of *C. gabunensis* yielded the most potent anti-plasmodial and anticancer fractions. Future study is on-going to characterize and elucidate the structure of bioactive compounds

CHAPTER EIGHT

CONCLUSIONS AND RECOMMENDED FUTURE WORK

8.1 Summary and Conclusions

In our introduction part, cyclotides were discussed as an essential cyclic protein with varied amino acid backbone which conferred to them wide biological activities including cytotoxicity. In this study, therefore cyclotides of Viola philippica and Viola yedoensis were studied as followed. The cyclotides of *Viola philippica* were isolated, purified, identified and characterized as Varv A, Kalata b1, Viba 15, Viba 17 and Varv E from *Viola philippica.* The cyclotides of *Viola yedoensis* were also identified as Varv A, Kalata B1, and Varv E (Cycloviolacin O12). The anti-ovarian cancer activities of these cyclotides were demonstrated in this study with report of Varv E as novel. Varv E was purified as a pure peptide from *Viola yedoensis*. Our results were consistent with available data in the literature which could imply that our strategy was reliable. We also got reproducible results in all our experiments. To the best of our knowledge, this is first report of anti-ovarian cancer activity of *Viola yedoensis*.

Also in our introduction, it was mentioned that bisbenzylisoquinoline (BBIQ) are commonly found in plant families including Menispermaceae. *Triclisia subcordata* belongs to Menispermaceae family. In this study, therefore, the isolation, identification and characterization of three bisbenzylisoquinoline (BBIQ) alkaloids namely, cycleanine, isochondodendrine and 2′-norcocsuline from *Triclisia subcordata* Oliv were established as a novel report. These BBIQ alkaloids and

extracts or fractions of *T. subcordata* were shown to exhibit both *in vitro* anti-cancer and antimalarial activities in this study. This is also the first-time report of cytotoxicity of Cycleanine and Isochondodendrine on ovarian cancer cells and novel report of cycleanine, isochondodendrine and 2′-norcocsuline in Triclisia subcordata, to the best of our knowledge.

Furthermore, the searches for anti-cancer and anti-malarial products with good selectivity, improved potency and bioactivities led to structural modification of cycleanine as hit, by semi-synthesis. Semi-synthesis of cycleanine yielded two new bioactive compounds which were identified and characterized in this study as 5-[(dimethylamino)methyl] cycleanine and 5-[(propargylamino)methyl] cycleanine. These new compounds showed more than 25-fold improved potency for antimalarial and about 2-fold improved potency for anticancer activities with appreciable selectivity as shown in this study. These two compounds are novel compounds with cytotoxicity effects on ovarian cancer cells and antimalarial activity on chloroquine-resistant *Plasmodium falciparum.* Their pharmacological reports are new as well.

Anti-cancer agents usually kill cancer cells in low dose by programmed cell death known as apoptosis. The mechanism of cell death induced by both BBIQ alkaloids of *T. subcordata* and synthetic analogues of cycleanine were established in this study as being likely by apoptosis induction of ovarian cancer cells. These were demonstrated by caspase Glo 3/7 activation, cleavage of PARP to PARP-1 in western blot, increased SubG1 and apoptotic cells in cell cycle and annexin V experiments in this study.

It was possible to establish the drug uptake in cells by click chemistry using the new compound produced in this study - 5-[(propargylamino)methyl] cycleanine, with the aid of confocal fluorescence microscopy. This has been shown in chapter five of this study. The BBIQ alkaloids of *T. subcordata* reported in this study and the new compounds synthesized could probably serve as hit for future semi-synthesis or structural modification to produce more potent anti-cancer and antimalarial drugs.

The *in vitro* antimalarial and anticancer activities of crude extract (50% ethanol extract) and fractions of *C. gabunensis* have been successfully investigated in this study. The ethyl acetate fraction showed the highest anti-cancer activity while the butanol fraction exerted highest antimalarial activity. This study reports anti-cancer effects of C. gabunensis as a novel report while the antimalarial activity was consistent with past studies.

Overall, our approach in this study is good because our findings and results are reproducible and consistent with available literature documentation. This study therefore, could provide scientific basis for support of use of *T. subcordata, Cylicodiscus gabunensis; V. yedoensis* and *V. philippica* in treatment of cancer or malaria. It has provided scientific evidence on the invitro cytotoxicity and ant-malarial activity of these plants.

8.2 Recommendation/future work

Work is on-going to identify and characterized the other unknown peptides present in *V. yedoensis and V. philippica.* The mechanism of cancer cell death induced by cyclotides of *V. philippica* and *yedoensis* is on-going.

Study is on the way to determine the protein targets by the anti-cancer BBIQ alkaloids of *T. subcordata* and synthesized cycleanine- analogues using a chemo-proteomics approach. It is a future work to study the BBIQ alkaloids distribution in cells using different staining for nucleus and mitochondria which is ongoing.

The bio-availability and other pharmacokinetic studies on BBIQ alkaloids and new analogues in animals are among the future studies. The *in vivo* metabolism of cycleanine in the animals - rats is currently on-going. Future work would be done on chemical modification of BBIQ alkaloids using other methods or pathways to produce more potent anti-cancer and antimalarial agents.

Finally, to be approved as anticancer drugs, *in vivo* activities or preclinical studies of these BBIQ alkaloids and analogues must be evaluated. Therefore, it is a future work to carry out the *in vivo* anti-cancer and antimalarial studies on BBIQ alkaloids and the new cycleanine analogues.

REFERENCES

Abo, K., Lawal, I. & Ogunkanmi, A. (2011). Evaluation of extracts of *Triclisia suboardata* Oliv and *Heinsia crinita* (Afz) G. Taylor for antimicrobial activity against some clinical bacterial isolates and fungi. *African Journal of Pharmacy and Pharmacology.* 5 (2): 125-131.

Adebayo, J. & Krettli, A. (2011). Potential antimalarials from Nigerian plants: a review. *Journal of Ethnopharmacology.* 133 (2): 289-302.

Angerhofer, C.K., Guinaudeau, H., Wongpanich, V., Pezzuto, J.M. & Cordell, G.A. (1999). Antiplasmodial and cytotoxic activity of natural bisbenzylisoquinoline alkaloids. *Journal of Natural Products.* 62 (1): 59-66.

Asuzu, I. &Anaga, A. (1996). The antiulcer effect of the methanolic extract of *Triclisia subcordata* leaves in rats. *Journal of Herbs, Spices & Medicinal Plants.* 3 (3): 45-53.

Ayarkwa, J. & Owusu, F.W. (2008). Cylicodiscus gabunensis Harms [Internet] Record from PROTA4U. Louppe, D., Oteng-Amoako, A.A. & Brink, M. (Editors). *PROTA (Plant Resources of Tropical Africa/Resources végétales de l'Afrique tropicale), Wageningen, Netherlands.*

Basco, L.K., Mitaku, S., Skaltsounis, A.L., Ravelomanantsoa, N., Tillequin, F., Koch, M. & Le Bras, J. (1994). *In vitro* activities of furoquinoline and acridone alkaloids against Plasmodium falciparum. *Antimicrobial Agents and Chemotherapy.* 38 (5): 1169-1171.

Batista, R., De Jesus Silva Júnior, Ademir & De Oliveira, A.B. (2009). Plant-derived antimalarial agents: new leads and efficient phytomedicines. Part II. Non-alkaloidal natural products. *Molecules.* 14 (8): 3037-3072.

Bhat, S.V., Nagasampagi ,B,A,. & Sivakumar, M. (2005). Chemistry of Natural Products. . *Berlin; New York: Springer. ISBN 81-7319481-5.*

Böhlke, M., Guinaudeau, H., Angerhofer, C.K., Wongpanich, V., Soejarto, D.D., Farnsworth, N.R., Mora, G.A. & Poveda, L.J. (1996). Costaricine, a new antiplasmodial bisbenzylisoquinoline alkaloid from *Nectandra salicifolia* trunk bark. *Journal of Natural Nroducts.* 59 (6): 576-580.

Bokesch, H.R., Pannell, L.K., Cochran, P.K., Sowder, R.C., McKee, T.C. & Boyd, M.R. (2001). A novel anti-HIV macrocyclic peptide from *Palicourea condensata*. *Journal of Natural Products.* 64 (2): 249-250.

Brouwer, N., Liu, Q., Harrington, D., Kohen, J., Vemulpad, S., Jamie, J., Randall, M. & Randall, D. (2005). An Ethnopharmacological study of medicinal plants in New South Wales. *Molecules.* 10 (10): 1252-1262.

Brunger, A.T. (1997). Nature Struct. *Bio.* 5 : 862.

Burman, R., Gunasekera, S., Strömstedt, A.A. & Göransson, U. (2014). Chemistry and biology of cyclotides: circular plant peptides outside the box. *Journal of NaturalProducts.* 77 (3): 724-736.

Burman, R., Yeshak, M.Y., Larsson, S., Craik, D.J., Rosengren, K.J. & Göransson, U. (2015). Distribution of circular proteins in plants: large-scale mapping of cyclotides in the Violaceae. *Frontiers in plant science.* 6 .

Camacho, M.d.R., Phillipson, J.D., Croft, S.L., Rock, P., Marshall, S.J. & Schiff, P.L. (2002). In vitro activity of *Triclisia patens* and some bisbenzylisoquinoline alkaloids against *Leishmania donovani* and *Trypanosoma bruce*i . *Phytotherapy Research.* 16 (5): 432-436.

Cemazar, M., Kwon, S., Mahatmanto, T., Ravipati, A.S. & Craik, D.J. (2012). Discovery and applications of disulfide-rich cyclic peptides. *Current topics in medicinal chemistry.* 12 (14): 1534-1545.

Chea, A., Bun, S., Azas, N., Gasquet, M., Bory, S., Ollivier, E. & Elias, R. (2010). Antiplasmodial activity of three bisbenzylisoquinoline alkaloids from the tuber of *Stephania rotunda. Natural Product research.* 24 (18): 1766-1770.

Chen, Y., Chen, J. & Tseng, S. (2009). Tetrandrine suppresses tumor growth and angiogenesis of gliomas in rats. *International Journal of Cancer.* 124 (10): 2260-2269.

Chen, B., Colgrave, M.L., Daly, N.L., Rosengren, K.J., Gustafson, K.R. & Craik, D.J. (2005). Isolation and characterization of novel cyclotides from *Viola hederaceae*: solution structure and anti-HIV activity of vhl-1, a leaf-specific expressed cyclotide. *The Journal of* B*iological Chemistry.* 280 (23): 22395-22405.

Chen, C., Li, X. & Zhang, H. (2010). [Inhibitory effect of matrine on proliferation of human ovary malignant teratoma cell line PA-1 in vitro]. *Zhongguo zhong xi yi jie he za zhi Zhongguo Zhongxiyi jiehe zazhi Chinese Journal of integrated traditional and Western medicine / Zhongguo Zhong xi yi jie he xue hui, Zhongguo Zhong yi yan jiu yuan zhu ban.* 30 (7): 723-725.

Claeson, P., Göransson, U., Johansson, S., Luijendijk, T. & Bohlin, L. (1998). Fractionation protocol for the isolation of polypeptides from plant biomass. *Journal of Natural Products.* 61 (1): 77-81.

Colgrave, M.L., Craik, D.J., (2004.). Thermal, chemical, and enzymatic stability of the cyclotide kalata B1: the importance of the cyclic cystine knot. . *Biochemistry.* 43, : 5965-5975.

Colgrave, M.L., Kotze, A.C., Ireland, D.C., Wang, C.K. & Craik, D.J. (2008). The anthelmintic activity of the cyclotides: natural variants with enhanced activity. *Chembiochem.* 9 (12): 1939-1945.

Colgrave, M.L., Jones, A. & Craik, D.J. (2005). Peptide quantification by matrix-assisted laser desorption ionisation time-of-flight mass spectrometry: Investigations of the cyclotide kalata B1 in biological fluids. *Journal of Chromatography a.* 1091 (1-2): 187-193.

Cordell, G.A. (1995). Changing strategies in natural products chemistry. *Phytochemistry.* 40 (6): 1585-1612.

Cragg, G.M., Grothaus, P.G. & Newman, D.J. (2009). Impact of Natural products on developing new anti-cancer agents. *Chemical Reviews.* 109 (7): 3012-3043.

Cragg, G.M., Newman, D.J. & Snader, K.M. (1997). Natural products in drug discovery and development. *Journal of Natural Products.* 60 (1): 52-60.

Craik, D.J., Daly, N.L., Bond, T. & Waine, C. (1999). Plant cyclotides: a unique family of cyclic and knotted proteins that defines the cyclic cystine knot structural motif. *Journal of Molecular Biology.* 294 (5): 1327-1336.

Craik, D.J. (2010). Discovery and applications of the plant cyclotides. *Toxicon.* 56 (7): 1092-1102.

Craik, D.J. (2001). Plant cyclotides: circular, knotted peptide toxins. *Toxicon.* 39 (12): 1809-1813.

Craik, D.J. & Conibear, A.C. (2011). The Chemistry of Cyclotides. *Journal of Organic Chemistry.* 76 (12): 4805-4817.

Craik, D.J., Henriques, S.T., Mylne, J.S. & Wang, C.K. (2012). Cyclotide isolation and characterization. *Methods in Enzymology.* 516 : 37-62.

Craik, D.J. (2009). Circling the enemy: cyclic proteins in plant defence. *Trends in Plant Science.* 14 (6): 328 - 335.

Craik, D.J. & Daly, N.L. (2007). NMR as a tool for elucidating the structures of circular and knotted proteins. *Molecular Biosystems.* 3 (4): 257-265.

Crozier, A., Clifford, M.N. & Ashihara, H. (2008). *Plant secondary metabolites: occurrence, structure and role in the human diet.* John Wiley & Sons.

de Mesquita, M.L., de Paula, J.E., Pessoa, C., de Moraes, M.O., Costa-Lotufo, L.V., Grougnet, R., Michel, S., Tillequin, F. & Espindola, L.S. (2009). Cytotoxic activity of Brazilian Cerrado plants used in traditional medicine against cancer cell lines. *Journal of Ethnopharmacology.* 123 (3): 439-445.

Delgado, S., Núñez, F., Sánchez, B., Bermúdez, E. & Rodríguez, J.M. (2011). Toxigenic microorganisms in medicinal plants used for ritual protection of infants. *Food Research International.* 44 (1): 304-309.

Demain, A.L. & Fang, A. (2000). The natural functions of secondary metabolites. In: Anonymous *History of Modern Biotechnology I.* Springer.

Deng, W., Hu, B., Dai, C., Wang, Y., Chen, H., Zito, S.W., Fu, L. & Chen, Z. (2013). Anticancer Activity of Oldenlandia Diffusa & Viola Philippica Car. *Journal of Cancer Research Updates.* 2 (2): 87-94.

Deng, X., Liu, G., Hu, N., Yuan, C., Liu, Z., Li, F., Pan, J. & Wang, C. (2015). Fangchinoline Inhibits Breast Tumor Proliferation and Induces Apoptosis in MDA-MB-231 Cell Line in Vivo. *Journal of Cancer Science and Clinical Oncology.* 2 (2): 1.

Desgrouas, C., Taudon, N., Bun, S., Baghdikian, B., Bory, S., Parzy, D. & Ollivier, E. (2014). Ethnobotany, phytochemistry and pharmacology of *Stephania rotunda* Lour. *Journal of Ethnopharmacology.* 154 (3): 537-563.

Ding, X., Bai, D. & Qian, J. (2014). Novel cyclotides from Hedyotis biflora inhibit proliferation and migration of pancreatic cancer cell in vitro and in vivo. *Medicinal Chemistry Research.* 23 (3): 1406-1413.

Dörnenburg, H. (2010). Cyclotide synthesis and supply: from plant to bioprocess. *Biopolymers.* 94 (5): 602-610.

Dörnenburg, H. (2008). Plant cell culture technology-harnessing a biological approach for competitive cyclotides production. *Biotechnology Letters.* 30 (8): 1311-1321.

Dwuma-Badu, D., Ayim, J., Tackie, A., Knapp, J., Slatkin, D. & Schiff, P. (1975). Additional alkaloids of *Triclisia patens* and *Triclisia subcordata*. *Phytochemistry.* 14 (11): 2524-2525.

Edeoga, H., Okwu, D. & Mbaebie, B. (2005). Phytochemical constituents of some Nigerian medicinal plants. *African journal of Biotechnology.* 4 (7): 685-688.

Elmore, S. (2007). Apoptosis: a review of programmed cell death. *Toxicologic Pathology.* 35 (4): 495-516.

Esmaeili, M.A., Abagheri-Mahabadi, N., Hashempour, H., Farhadpour, M., Gruber, C.W. & Ghassempour, A. (2016). Viola plant cyclotide vigno 5 induces mitochondria-mediated apoptosis via cytochrome C release and caspases activation in cervical cancer cells. *Fitoterapia.* 109: 162-168.

Fadeyi, S.A., Fadeyi, O.O., Adejumo, A.A., Okoro, C. & Myles, E.L. (2013). In vitro anticancer screening of 24 locally used Nigerian medicinal plants. *BMC Complementary and Alternative Medicine.* 13 (1): 1.

Fensterseifer, I.C., Silva, O.N., Malik, U., Ravipati, A.S., Novaes, N.R., Miranda, P.R., Rodrigues, E.A., Moreno, S.E., Craik, D.J. & Franco, O.L. (2015). Effects of cyclotides against cutaneous infections caused by *Staphylococcus aureus. Peptides.* 63: 38-42.

Fouche, G., Cragg, G.M., Pillay, P., Kolesnikova, N., Maharaj, V.J. & Senabe, J. (2008). In vitro anticancer screening of South African plants. *Journal of Ethnopharmacology.* 119 (3): 455-461.

Foye, W.O., Lemke, T.L. & Williams, D.A. (2008). *Foye's principles of medicinal chemistry.* Lippincott Williams & Wilkins.

Göransson, U., Herrmann, A., Burman, R., Haugaard-Jönsson, L.,M. & Rosengren, K.J. (2009). The conserved glu in the cyclotide cycloviolacin O2 has a key structural role. *Chembiochem: A European Journal Of Chemical Biology.* 10 (14): 2354-2360.

Goransson, U., Svangard, E., Claeson, P. & Bohlin, L. (2004). Novel strategies for isolation and characterization of cyclotides: the discovery of bioactive macrocyclic plant polypeptides in the Violaceae. *Current Protein and Peptide Science.* 5 (5): 317-329.

Goransson, U. & Craik, D.J. (2003). Disulfide mapping of the cyclotide kalata B1 - Chemical proof of the cyclic cystine knot motif. *Journal of Biological Chemistry.* 278 (48): 48188-48196.

Gran, L. (1973). Isolation of oxytocic peptides from Oldenlandia a• nis by solvent extraction of tetraphenylbo- rate complexes and chromatography on sephadex LH-20. . *Lloydia.* 36 : 207-208.

Gran, L., Sandberg, F. & Sletten, K. (2000). Oldenlandia affinis (R&S) DC - A plant containing uteroactive peptides used in African traditional medicine. *Journal of Ethnopharmacology.* 70 (3): 197-203.

Greenwood, B.M., Bojang, K., Whitty, C.J. & Targett, G.A. (2005). Malaria. *The Lancet.* 365 (9469): 1487.

Greenwood, B. & Mutabingwa, T. (2002). Malaria in 2002. *Nature.* 415 (6872): 670-672.

Gruber, C.W., Elliott, A.G., Ireland, D.C., Delprete, P.G., Dessein, S., Goransson, U., Trabi, M., Wang, C.K., Kinghorn, A.B., Robbrecht, E. & Craik, D.J. (2008). Distribution and Evolution of Circular Miniproteins in Flowering Plants. *Plant Cell.* 20 (9): 2471-2483.

Guéritte, F. &Fahy, J. (2005). The vinca alkaloids. *Anticancer agents from Natural Products.* 10 : 123-135.

Guha, K.P., Mukherjee, B. & Mukherjee, R.J. (1979). Bisbenzylisoquinoline alkaloids - A Review. *J. Nat.Prod.* 42 (1): 1-84

Gunasekera, S., Daly, N.L., Anderson, M.A. & Craik, D.J. (2006). Chemical synthesis and biosynthesis of the cyclotide family of circular proteins. *IUBMB life.* 58 (9): 515-524.

Gustafson, K.R., McKee, T.C. & Bokesch, H.R. (2004). Anti-HIV cyclotides. *Current Protein & Peptide Science.* 5 (5): 331-340.

Gustafson, K.R., Walton, L.K., Sowder, R.C., Johnson, D.G., Pannell, L.K., Cardellina, J.H. & Boyd, M.R. (2000). New circulin macrocyclic polypeptides from Chassalia parvifolia. *Journal of Natural Products.* 63 (2): 176-178.

Hanno Steen and Matthias Mann (2004). The ABC's (and XYZ's) of peptide

sequencing. Nature Review's Molecular Cell Biology 5: 699-710.

Hanson, J.R. (2003). *Natural products: the secondary metabolites.* vol. 17. Royal Society of Chemistry.

Harborne, A. (1998). *Phytochemical methods a guide to modern techniques of plant analysis.* Springer Science & Business Media.

Hasenkamp, S., Sidaway, A., Devine, O., Roye, R. & Horrocks, P. (2013). Evaluation of bioluminescence-based assays of anti-malarial drug activity. *Malaria Journal.* 12 (1): 58.

He, W., Chan, L.Y., Zeng, G., Daly, N.L., Craik, D.J. & Tan, N. (2011a). Isolation and characterization of cytotoxic cyclotides from Viola philippica. *Peptides.* 32 (8): 1719-1723.

He, B.C., Gao, J.L., Zhang, B.Q., Luo, Q., Shi, Q., Kim, S.H., Huang, E., Gao, Y., Yang, K., Wagner, E.R., Wang, L., Tang, N., Luo, J., Liu, X., Li, M., Bi, Y., Shen, J., Luther, G., Hu, N., Zhou, Q., Luu, H.H., Haydon, R.C., Zhao, Y. & He, T.C. (2011b). Tetrandrine inhibits Wnt/beta-catenin signaling and suppresses tumor growth of human colorectal cancer. *Molecular Pharmacology.* 79 (2): 211-219.

Heinrich, M. (2000). Ethnobotany and its role in drug development. *Phytotherapy Research.* 14 (7): 479-488.

Heinrich, M., Barnes, J., Gibbons, S. & Williamson, E.M. (2012). *Fundamentals of pharmacognosy and phytotherapy.* Elsevier Health Sciences.

Heinrich, M. & Bremner, P. (2006). Ethnobotany and ethnopharmacy-their role for anti-cancer drug development. *Current Drug Targets.* 7 (3): 239-245.

Heinrich, M. & Gibbons, S. (2001). Ethnopharmacology in drug discovery: an analysis of its role and potential contribution. *JPP.* 53: 425-432.

Henriques, S.T., Huang, Y.H., Castanho, M.A., Bagatolli, L.A., Sonza, S., Tachedjian, G., Daly, N.L. & Craik, D.J. (2012). Phosphatidylethanolamine binding is a conserved feature of cyclotide-membrane interactions. *The Journal of Biological Chemistry.* 287 (40): 33629-33643.

Hernandez, J.F., Gagnon, J., Chiche, L., Nguyen, T.M., Andrieu, J.P., Heitz, A., Hong, T.T., Pham, T.T.C. & Nguyen, D.L. (2000). Squash trypsin inhibitors from Momordica cochinchinensis exhibit an atypical macrocyclic structure. *Biochemistry.* 39 (19): 5722-5730.

Herrmann, A., Burman, R., Mylne, J.S., Karlsson, G., Gullbo, J., Craik, D.J., Clark, R.J. & Göransson, U. (2008). The alpine violet, *Viola biflora*, is a rich source of cyclotides with potent cytotoxicity. *Phytochemistry.* 69 (4): 939-952.

Hesham, R., El-Seedi, R.B., Ahmed, M.Z.T., LoutfyBoulos, J.G. & Goransson, U. (2013). The traditional medical uses and cytotoxic activities of sixty-one Egyptian plants: Discovery of an active cardiac glycoside from Urginea maritima. *Journal of Ethanolophamarcology*. 145 (3): 746-757.

Hu, E., Wang, D., Chen, J. & Tao, X. (2015). Novel cyclotides from Hedyotis diffusa induce apoptosis and inhibit proliferation and migration of prostate cancer cells. *International Journal of Clinical and Experimental Medicine.* 8 (3): 4059-4065.

Ijeoma, U.F., Aderonke, S.O., Ogbonna, O., Augustina, M.A. & Ifeyinwa, C. (2011). Antinociceptive and anti-inflammatory activities of crude extracts of Ipomoea involucrata leaves in mice and rats. *Asian Pacific Journal of Tropical Medicine.* 4 (2): 121-124.

Ireland, D.C., Colgrave, M.L. & Craik, D.J. (2006). A novel suite of cyclotides from Viola odorata: sequence variation and the implications for structure, function and stability. *Biochemical Journal.* 400 : 1-12.

Ireland, D.C., Wang, C.K.L., Wilson, J.A., Gustafson, K.R. & Craik, D.J. (2008). Cyclotides as natural anti-HIV agents. *Biopolymers.* 90 (1): 51-60.

Jemal, A., Siegel, R., Ward, E., Hao, Y., Xu, J. & Thun, M.J. (2009). Cancer Statistics, 2009. *Cancer Journal for Clinicians.* 59 (4): 225-249.

Jennings, C., West, J., Waine, C., Craik, D. & Anderson, M. (2001). Biosynthesis and insecticidal properties of plant cyclotides: The cyclic knotted proteins from Oldenlandia affinis. *Proceedings of the National Academy of Sciences of the United States of America.* 98 (19): 10614-10619.

Jennings, C.V., Rosengren, K.J., Daly, N.L., Plan, M., Stevens, J., Scanlon, M.J., Waine, C., Norman, D.G., Anderson, M.A. & Craik, D.J. (2005). Isolation, solution structure, and insecticidal activity of Kalata B2, a circular protein with a twist: Do Mobius strips exist in nature? *Biochemistry.* 44 (3): 851-860.

Ji, Y., Majumder, S., Millard, M., Borra, R., Bi, T., Elnagar, A.Y., Neamati, N., Shekhtman, A. & Camarero, J.A. (2013). In vivo activation of the p53 tumor suppressor pathway by an engineered cyclotide. *Journal of the American Chemical Society.* 135 (31): 11623-11633.

Kajstura, M., Halicka, H.D., Pryjma, J. & Darzynkiewicz, Z. (2007). Discontinuous fragmentation of nuclear DNA during apoptosis revealed by discrete “sub-G1” peaks on DNA content histograms. *Cytometry Part A.* 71 (3): 125-131.

Kanyinda, B., Vanhaelen-Fastré, R., Vanhaelen, M. & Ottinger, R. (1997). Two new isochondodendrine-type alkaloids from the roots of Anisocycla jollyana. *Journal of Natural Products.* 60 (11): 1121-1124.

Karlovsky, P. (2008). Secondary metabolites in soil ecology. In: Anonymous *Secondary metabolites in soil ecology.* Springer.

Kaur, K., Jain, M., Kaur, T. & Jain, R. (2009). Antimalarials from nature. *Bioorganic & Medicinal Chemistry.* 17 (9): 3229-3256.

Kim, J. & Park, E. (2002). Cytotoxic anticancer candidates from natural resources. *Current Medicinal Chemistry-Anti-Cancer Agents.* 2 (4): 485-537.

Klayman, D.L. (1985). Qinghaosu (Artemisinin) - an Antimalarial Drug from China. *Science.* 228 (4703): 1049-1055.

Kliebenstein, D. (2004). Secondary metabolites and plant/environment interactions: a view through Arabidopsis thaliana tinged glasses. *Plant, Cell & Environment.* 27 (6): 675-684.

Koehbach, J., O'Brien, M., Muttenthaler, M., Miazzo, M., Akcan, M., Elliott, A.G., Daly, N.L., Harvey, P.J., Arrowsmith, S., Gunasekera, S., Smith, T.J., Wray, S., Goransson, U., Dawson, P.E., Craik, D.J., Freissmuth, M. & Gruber, C.W. (2013). Oxytocic plant cyclotides as templates for peptide G protein-coupled receptor ligand design. *Proceedings of the National Academy of Sciences of the United States of America.* 110 (52): 21183-21188.

Kossel, A. (1891). Ueber die chemische Zusammensetzung der Zelle" [The chemical composition of the cell]. *Archiv für Physiologie (in German).* : 181-186.

Kou, B., Liu, W., He, W., Zhang, Y., Zheng, J., Yan, Y., Zhang, Y., Xu, S. & Wang, H. (2016). Tetrandrine suppresses metastatic phenotype of prostate cancer cells by regulating Akt/mTOR/MMP-9 signaling pathway. *Oncology reports.* 35 (5): 2880-2886.

Kouitcheu, M.L.B., Penlap, B.V., Kouam, J., Ngadjui, B.T., Fomum, Z. & Etoa, F. (2006). Evaluation of antidiarrhoeal activity of the stem bark of *Cylicodiscus gabunensis* (Mimosaceae). *African Journal of Biotechnology.* 5 (11):1062-1066.

Lee, J.H., Kang, G.H., Kim, K.C., Kim, K.M., Park, D.I., Choi, B.T., Kang, H.S., Lee, Y.T. & Choi, Y.H. (2002). Tetrandrine-induced cell cycle arrest and apoptosis in A549 human lung carcinoma cells. *International Journal of Oncology.* 21 (6): 1239-1244.

Lee, K. (2010). Discovery and Development of Natural Product-Derived Chemotherapeutic Agents Based on a Medicinal Chemistry Approach. *Journal of bNatural Products.* 73 (3): 500-516.

LeGrand, A. &Wondergem, P. (1989). *Herbal medicine and health promotion: a comparative study of herbal drugs in primary health care.*

Li, D., Lu, Y., Sun, P., Feng, L., Liu, M., Hu, L., Wu, W., Jiang, B., Yang, M. & Qu, X. (2015a). Inhibition on Proteasome β1 Subunit Might Contribute to the Anti-Cancer Effects of Fangchinoline in Human Prostate Cancer Cells. *PloS one.* 10 (10): e0141681.

Li, J.W.H. &Vederas, J.C. (2009). Drug Discovery and Natural Products: End of an Era or an Endless Frontier. *Science.* 325 : 161-165.

Li, X., Su, B., Liu, R., Wu, D. & He, D. (2011). Tetrandrine induces apoptosis and triggers caspase cascade in human bladder cancer cells. *Journal of Surgical Research.* 166 (1): e45-e51.

Li, W.W., Johnson-Ajinwo, O.R. & Uche, F.I. (2015b). Potential of phytochemicals and their derivatives in the treatment of ovarian cancer. . In: Anonymous *Handbook on Ovarian Cancer: Risk Factors, Therapies and Prognosis, Collier BR (ed). : Nova Science publishers USA.*

Likhitwitayawuid, K., Angerhofer, C.K., Chai, H., Pezzuto, J.M., Cordell, G.A. & Ruangrungsi, N. (1993). Cytotoxic and antimalarial alkaloids from the tubers of Stephania pierrei. *Journal of Natural Products.* 56 (9): 1468-1478.

Lin, L., Shieh, H., Angerhofer, C.K., Pezzuto, J.M., Cordell, G.A., Xue, L., Johnson, M.E. & Ruangrungsi, N. (1993). Cytotoxic and antimalarial bisbenzylisoquinoline alkaloids from Cyclea barbata. *Journal of Natural Products.* 56 (1): 22-29.

Lindholm, P., Goransson, U., Johansson, S., Claeson, P., Gullbo, J., Larsson, R., Bohlin, L. & Backlund, A. (2002). Cyclotides: A novel type of cytotoxic agents. *Molecular Cancer Therapeutics.* 1 (6): 365-369.

Liu, L., Desai, S.D., Li, T.K., Mao, Y., Sun, M. & Sim, S.P. (2000). Mechanism of action of camptothecin . 2000 ;922:1-10. *Ann N Y Acad Sci.Review. PubMed PMID: 11193884.* 922: 1-10.

Liu, Y., Harinantenaina, L., Brodie, P.J., Slebodnick, C., Callmander, M.W., Rakotondrajaona, R., Rakotobe, E., Rasamison, V.E., TenDyke, K. & Shen, Y. (2013). Structure elucidation of antiproliferative bisbenzylisoquinoline alkaloids from Anisocycla grandidieri from the Madagascar dry forest. *Magnetic Resonance in Chemistry.* 51 (9): 574-579.

Liu, M.Z., Yang, Y., Zhang, S.X., Tang, L., Wang, H.M., Chen, C.J., Shen, Z.F., Cheng, K.D., Kong, J.Q. & Wang, W. (2014). A cyclotide against influenza A H1N1 virus from *Viola yedoensis*. *Yao xue xue bao Acta pharmaceutica Sinica.* 49 (6): 905-912.

Liu, W., Kou, B., Ma, Z.K., Tang, X.S., Lv, C., Ye, M., Chen, J.Q., Li, L., Wang, X.Y. & He, D.L. (2015). Tetrandrine suppresses proliferation, induces apoptosis, and inhibits migration and invasion in human prostate cancer cells. *Asian Journal of Andrology.* 17 (5): 850-853.

Luo, Z., Tikekar, R.V. & Nitin, N. (2013). Click chemistry approach for imaging intracellular and intratissue distribution of curcumin and its nanoscale carrier. *Bioconjugate Chemistry.* 25 (1): 32-42.

Lv, J., Xu, M., Wang, D., Zhu, H., Yang, C., Wang, Y., Li, Y. & Zhang, Y. (2013). Cytotoxic bisbenzylisoquinoline alkaloids from Stephania epigaea. *Journal of Natural Products.* 76 (5): 926-932.

Malagón, D., Botterill, B., Gray, D.J., Lovas, E., Duke, M., Gray, C., Kopp, S.R., Knott, L.M., McManus, D.P. & Daly, N.L. (2013). Anthelminthic activity of the cyclotides (kalata B1 and B2) against schistosome parasites. *Peptide Science.* 100 (5): 461-470.

Mambu, L., Martin, M., Razafimahefa, D., Ramanitrahasimbola, D., Rasoanaivo, P. & Frappier, F. (2000). Spectral characterisation and antiplasmodial activity of bisbenzylisoquinolines from *Isolona ghesquiereina*. *Planta Medica.* 66 (06): 537-540.

Mann, J. (2002). Natural products in cancer chemotherapy: past, present and future. *Nature Reviews Cancer.* 2 (2): 143-148.

Marshall, S.J., Russell, P.F., Wright, C.W., Anderson, M.M., Phillipson, J.D., Kirby, G.C., Warhurst, D.C. & Schiff, P.L.,Jr (1994). In vitro antiplasmodial, antiamoebic, and cytotoxic activities of a series of bisbenzylisoquinoline alkaloids. *Antimicrobial Agents and Chemotherapy.* 38 (1): 96-103.

Mei, L., Chen, Y., Wang, Z., Wang, J., Wan, J., Yu, C., Liu, X. & Li, W. (2015). Synergistic anti-tumour effects of tetrandrine and chloroquine combination therapy in human cancer: a potential antagonistic role for p21. *British journal of pharmacology.* 172 (9): 2232-2245.

Mulvenna, J.P., Wang, C., Craik, D.J (2006). CyBase: a database of cyclic protein sequence and structure. *Nucleic Acids Res.* 34: D192-D194.

Mulvenna, J.P., Sando, L. & Craik, D.J. (2005). Processing of a 22 kDa precursor protein to produce the circular protein tricyclon A. *Structure.* 13 (5): 691-701.

Murebwayire, S., Frédérich, M., Hannaert, V., Jonville, M. & Duez, P. (2008). Antiplasmodial and antitrypanosomal activity of *Triclisia sacleuxii* (Pierre) Diels. *Phytomedicine.* 15 (9): 728-733.

Muriithi, M.W., Abraham, W., Addae-Kyereme, J., Scowen, I., Croft, S.L., Gitu, P.M., Kendrick, H., Njagi, E. & Wright, C.W. (2002). Isolation and in Vitro Antiplasmodial Activities of Alkaloids from Teclea t richocarpa: In vivo Antimalarial Activity and X-ray Crystal Structure of Normelicopicine. *Journal of Natural Products.* 65 (7): 956-959.

Nakamura, K., Tsuchiya, S., Sugimoto, Y., Sugimura, Y. & Yamada, Y. (1992). Histamine release inhibition activity of bisbenzylisoquinoline alkaloids. *Planta Medica.* 58 (6): 505-508.

Nchancho, K., Kouam, J., Tane, P., Kuete, V., Watchueng, J. & Fomum, Z.T. (2009). Coumestan glycosides from the stem bark of *Cylicodiscus gabunensis*. *Natural product communications.* 4 (7): 931-934.

Newman, D.J. & Cragg, G.M. (2012). Natural Products As Sources of New Drugs Over the 30 years from 1981 to 2010. *Journal of Natural products.* 75: 311-335.

Nguyen, K.N.T., Nguyen, G.K.T., Nguyen, P.Q.T., Ang, K.H., Dedon, P.C. & Tam, J.P. (2016). Immunostimulating and Gram-negative-specific antibacterial cyclotides from the butterfly pea (Clitoria ternatea). *The FEBS journal.* 283 (11): 2067-2090.

Nguyen, G.K., Lian, Y., Pang, E.W., Nguyen, P.Q., Tran, T.D. & Tam, J.P. (2013). Discovery of linear cyclotides in monocot plant Panicum laxum of Poaceae family provides new insights into evolution and distribution of cyclotides in plants. *The Journal of Biological Chemistry.* 288 (5): 3370-3380.

Nguyen, G.K., Lim, W.H., Nguyen, P.Q. & Tam, J.P. (2012). Novel cyclotides and uncyclotides with highly shortened precursors from *Chassalia chartacea* and effects of methionine oxidation on bioactivities. *The Journal of Biological Chemistry.* 287 (21): 17598-17607.

Nguyen, G.K., Zhang, S., Wang, W., Wong, C.T., Nguyen, N.T. & Tam, J.P. (2011). Discovery of a linear cyclotide from the bracelet subfamily and its disulfide mapping by top-down mass spectrometry. *The Journal of Biological Chemistry.* 286 (52): 44833-44844.

Okokon, J.E., Ita, B.N. & Udokpoh, A.E. (2006). Antiplasmodial activity of Cylicodiscus gabunensis. *Journal of Ethnopharmacology.* 107 (2): 175-178.

Otshudi, A.L., Apers, S., Pieters, L., Claeys, M., Pannecouque, C., De Clercq, E., Van Zeebroeck, A., Lauwers, S., Frédérich, M. & Foriers, A. (2005). Biologically active bisbenzylisoquinoline alkaloids from the root bark of Epinetrum villosum. *Journal of Ethnopharmacology.* 102 (1): 89-94.

Paudel, K.R. & Panth, N. (2015). Phytochemical Profile and Biological Activity of *Nelumbo nucifera*. *Evidence-Based Complementary and Alternative Medicine.* 2015: 789124.

Peng, H. (2003.). Spermatophyta, In: Wu ZY, editor. Flora Yunnanica. *1th ed. Beijing: Science Press,* 47-48.

Pinto, M.F., Fensterseifer, I.C., Migliolo, L., Sousa, D.A., de Capdville, G., Arboleda-Valencia, J.W., Colgrave, M.L., Craik, D.J., Magalhaes, B.S., Dias, S.C. & Franco, O.L. (2012). Identification and structural characterization of novel cyclotide with activity against an insect pest of sugar cane. *The Journal of Biological Chemistry.* 287 (1): 134-147.

Poornima, P., Weng, C.F. & Padma, V.V. (2014). Neferine, an alkaloid from lotus seed embryo, inhibits human lung cancer cell growth by MAPK activation and cell cycle arrest. *Biofactors.* 40 (1): 121-131.

Poth, A.G., Chan, L.Y. & Craik, D.J. (2013). Cyclotides as grafting frameworks for protein engineering and drug design applications. *Peptide Science.* 100 (5): 480-491.

Poth, A.G., Colgrave, M.L., Philip, R., Kerenga, B., Daly, N.L., Anderson, M.A. & Craik, D.J. (2011a). Discovery of cyclotides in the Fabaceae plant family provides new insights into the cyclization, evolution, and distribution of circular proteins. *ACS Chemical Biology.* 6 (4): 345-355.

Poth, A.G., Colgrave, M.L., Lyons, R.E., Daly, N.L. & Craik, D.J. (2011b). Discovery of an unusual biosynthetic origin for circular proteins in legumes. *Proceedings of the National Academy of Sciences of the United States of America.* 108 (25): 10127-10132.

Poth, A.G., Colgrave, M.L., Philip, R., Kerenga, B., Daly, N.L., Anderson, M.A. & Craik, D.J. (2011c). Discovery of Cyclotides in the Fabaceae Plant Family Provides New Insights into the Cyclization, Evolution, and Distribution of Circular Proteins. *Acs Chemical Biology.* 6 (4): 345-355.

Poth, A.G., Mylne, J.S., Grassl, J., Lyons, R.E., Millar, A.H., Colgrave, M.L. & Craik, D.J. (2012). Cyclotides associate with leaf vasculature and are the products of a novel precursor in petunia (Solanaceae). *The Journal of Biological Chemistry.* 287 (32): 27033-27046.

Pränting, M., Lööv, C., Burman, R., Göransson, U. & Andersson, D.I. (2010). The cyclotide cycloviolacin O2 from Viola odorata has potent bactericidal activity against Gram-negative bacteria. *The Journal of Antimicrobial Chemotherapy.* 65 (9): 1964-1971.

Quimbar, P., Malik, U., Sommerhoff, C.P., Kaas, Q., Chan, L.Y., Huang, Y.H., Grundhuber, M., Dunse, K., Craik, D.J., Anderson, M.A. & Daly, N.L. (2013). High-affinity cyclic peptide matriptase inhibitors. *The Journal of Biological Chemistry.* 288 (19): 13885-13896.

Rao, S., Krauss, N.E., Heerding, J.M., Swindell, C.S., Ringel, I., Orr, G.A. & Horwitz, S.B. (1994). 3'-(p-azidobenzamido)taxol photolabels the N-terminal 31 amino acids of beta-tubulin. *The Journal of Biological Chemistry.* 269 (5): 3132-3134.

Rauh-Hain, J.A., Krivak, T.C., Del Carmen, M.G. & Olawaiye, A.B. (2011). Ovarian cancer screening and early detection in the general population. *Reviews in obstetrics & gynecology.* 4 (1): 15-21.

Reinwarth, M., Nasu, D., Kolmar, H. & Avrutina, O. (2012). Chemical Synthesis, Backbone Cyclization and Oxidative Folding of Cystine-knot Peptides -- Promising Scaffolds for Applications in Drug Design. *Molecules.* 17 (11): 12533-12552.

Robinson, E., Nandi, M., Wilkinson, L.L., Arrowsmith, D.M., Curtis, A.D. & Richardson, A. (2013). Preclinical evaluation of statins as a treatment for ovarian cancer. *Gynecologic oncology.* 129 (2): 417-424.

Rosengren, K.J., Daly, N.L., Plan, M.R., Waine, C. & Craik, D.J. (2003). Twists, knots, and rings in proteins - Structural definition of the cyclotide framework. *Journal of Biological Chemistry.* 278 (10): 8606-8616.

Roumy, V., Garcia-Pizango, G., Gutierrez-Choquevilca, A.-., Ruiz, L., Jullian, V., Winterton, P., Fabre, N., Moulis, C. & Valentin, A. (2007). Amazonian plants from Peru used by Quechua and Mestizo to treat malaria with evaluation of their activity. *Journal of Ethnopharmacology.* 112 (3): 482-489.

Saether, O., Craik, D.J., Campbell, I.D., Sletten, K., Juul, J. & Norman, D.G. (1995). Elucidation of the Primary and 3-Dimensional Structure of the Uterotonic Polypeptide Kalata B1. *Biochemistry.* 34 (13): 4147-4158.

Samuelson, G. (1999). Drugs of natural origin: a textbook of pharmacognosy.

Saxena, S., Pant, N., Jain, D. & Bhakuni, R. (2003). Antimalarial agents from plant sources. *Current science.* 85 (9): 1314-1329.

Schiff, P.L. (1997). Bisbenzylisoquinoline alkaloids. *Journal of Natural Products.* 60 (9): 934-953.

Schiff, P.B., Fant, J. & Horwitz, S.B. (1979). Promotion of microtubule assembly in vitro by taxol.

Schmidt, B.M., Ribnicky, D.M., Lipsky, P.E. & Raskin, I. (2007). Revisiting the ancient concept of botanical therapeutics. *Nature Chemical Biology.* 3 (7): 360-366.

Schoepke, T., Hasan Agha, M.I., Kraft, R., Otto, A., & Hiller, K. (1993). Haemolytisch aktive komponenten aus *Viola tricolor* L. und *Viola arvensis*. *Murray. Sci. Pharm.* 61: 145-153.

Sen, Z., Zhan, X.K., Jing, J., Yi, Z. & Wanqi, Z. (2013). Chemosensitizing activities of cyclotides from *Clitoria ternatea* in paclitaxel-resistant lung cancer cells. *Oncology letters.* 5 (2): 641-644.

Shenkarev, Z.O., Nadezhdin, K.D., Sobol, V.A., Sobol, A.G., Skjeldal, L. & Arseniev, A.S. (2006). Conformation and mode of membrane interaction in cyclotides. Spatial structure of kalata B1 bound to a dodecylphosphocoline micelle. *Febs Journal.* 273 (12): 2658-2672.

Siegel, R.L., Miller, K.D. & Jemal, A. (2015). Cancer statistics, 2015. *CA: Cancer Journal for Clinicians.* 65 (1): 5-29.

Simonsen, S.M., Sando, L., Ireland, D.C., Colgrave, M.L., Bharathi, R., Goransson, U. & Craik, D.J. (2005). A continent of plant defense peptide diversity: cyclotides in Australian Hybanthus (Violaceae). *The Plant Cell.* 17 (11): 3176-3189.

Smilkstein, M., Sriwilaijaroen, N., Kelly, J.X., Wilairat, P. & Riscoe, M. (2004). Simple and inexpensive fluorescence-based technique for high-throughput antimalarial drug screening. *Antimicrobial Agents and Chemotherapy.* 48 (5): 1803-1806.

Snow, R.W., Guerra, C.A., Noor, A.M., Myint, H.Y. & Hay, S.I. (2005). The global distribution of clinical episodes of Plasmodium falciparum malaria. *Nature.* 434 (7030): 214-217.

Sofowora, A. (1982). *Medicinal plants and traditional medicine in Africa.* John Wiley and sons LTD.

Stephen W. Fesik (2005). Promoting apoptosis as a strategy for cancer drug

discovery . Nature Review Cancer 5, 876-885 dol:10.1038/nrc1736

Sun, Y.F. & Wink, M. (2014). Tetrandrine and fangchinoline, bisbenzylisoquinoline alkaloids from Stephania tetrandra can reverse multidrug resistance by inhibiting P-glycoprotein activity in multidrug resistant human cancer cells. *Phytomedicine.* 21 (8): 1110-1119.

Svangård, E., Göransson, U., Hocaoglu, Z., Gullbo, J., Larsson, R., Claeson, P. & Bohlin, L. (2004). Cytotoxic cyclotides from Viola tricolor. *Journal of Natural Products.* 67 (2): 144-147.

Tam, J.P., Lu, Y.A., Yang, J.L. & Chiu, K.W. (1999). An unusual structural motif of antimicrobial peptides containing end-to-end macrocycle and cystine-knot disulfides. *Proceedings of the National Academy of Sciences of the United States of America.* 96 (16): 8913-8918.

Tan, N. & Zhou, J. (2006). Plant cyclopeptides. *Chemical Reviews.* 106 (3): 840-895.

Tane, P., Bergquist, K., Téné, M., Ngadjui, B.T., Ayafor, J.F. & Sterner, O. (1995). Cyclodione, an unsymmetrical dimeric diterpene from *Cylicodiscus gabunensis*. *Tetrahedron.* 51 (42): 11595-11600.

Tang, J., Wang, C.K., Pan, X., Yan, H., Zeng, G., Xu, W., He, W., Daly, N.L., Craik, D.J. & Tan, N. (2010). Isolation and characterization of cytotoxic cyclotides from *Viola tricolor*. *Peptides.* 31 (8): 1434-1440.

Tchivounda, H.P., Koudogbo, B., Besace, Y. & Casadevall, E. (1991). Triterpene saponins from *Cylicodiscus gabunensis*. *Phytochemistry.* 30 (8): 2711-2716.

Tene, M., Chabert, P., Noté, O., Kenla, T.J.N., Tane, P. & Lobstein, A. (2011). Triterpenoid saponins from *Cylicodiscus gabunensis*. *Phytochemistry Letters.* 4 (2): 89-92.

Thell, K., Hellinger, R., Sahin, E., Michenthaler, P., Gold-Binder, M., Haider, T., Kuttke, M., Liutkeviciute, Z., Goransson, U., Grundemann, C., Schabbauer, G. & Gruber, C.W. (2016). Oral activity of a nature-derived cyclic peptide for the treatment of multiple sclerosis. *Proceedings of the National Academy of Sciences of the United States of America.* 113 (15): 3960-3965.

Tian, H. & Pan, O.C. (1997). Modulation of multidrug resistance by three bisbenzyl-isoquinolines in comparison with verapamil. *Zhongguo yao li xue bao Acta Pharmacologica Sinica.* 18 (5): 455-458.

Trease, G.E. &Evans, W.C. (1998). Trease and Evans Pharmacognosy. A physician guide to Herbal medicine. *Ballere tindal London.* (15th edition).

Troeira Henriques, S., Huang, Y., Chaousis, S., Wang, C.K. & Craik, D.J. (2014). Anticancer and toxic properties of cyclotides are dependent on phosphatidylethanolamine phospholipid targeting. *Chembiochem.* 15 (13): 1956-1965.

Uche, F. & Ezugwu, C. (2009). Evaluation of antioxidant activities of some Nigerian medicinal plants. *Asian Pacific Journal of Tropical Medicine.* 2 (4): 27-32.

Uche, F.I., Drijfhout, F.P., McCullagh, J., Richardson, A. & Li, W. (2016). Cytotoxicity Effects and Apoptosis Induction by Bisbenzylisoquinoline Alkaloids from Triclisia subcordata. *Phytotherapy Research.* doi: 10.1002/ptr.5660

Valentin, A., Benoit-Vical, F., Moulis, C., Stanislas, E., Mallie, M., Fouraste, I. & Bastide, J.M. (1997). In vitro antimalarial activity of penduline, a bisbenzylisoquinoline from Isopyrum thalictroides. *Antimicrobial Agents and Chemotherapy.* 41 (10): 2305-2307.

Verpoorte, R. (1986). Methods for the structure elucidation of alkaloids. *Journal of Natural Products.* 49 (1): 1-25.

Vichai, V. &Kirtikara, K. (2006). Sulforhodamine B colorimetric assay for cytotoxicity screening. *Nature Protocols.* 1 (3): 1112-1116.

Wang, C.K., Gruber, C.W., Cemazar, M., Siatskas, C., Tagore, P., Payne, N., Sun, G., Wang, S., Bernard, C.C. & Craik, D.J. (2013). Molecular grafting onto a stable framework yields novel cyclic peptides for the treatment of multiple sclerosis. *ACS Chemical Biology.* 9 (1): 156-163.

Wang, C.K., Colgrave, M.L., Gustafson, K.R., Ireland, D.C., Goransson, U. & Craik, D.J. (2007). Anti-HIV cyclotides from the Chinese medicinal herb *Viola yedoensis*. *Journal of Natural Products.* 71 (1): 47-52.

Wang, J., Chen, Q. & Wang, F. (2010). Cytotoxic bisbenzylisoquinoline alkaloids from the roots of Cyclea racemosa. *Journal of Natural Products.* 73 (7): 1288-1293.

Wang, C.K., Kaas, Q., Chiche, L. & Craik, D.J. (2008). CyBase: a database of cyclic protein sequences and structures, with applications in protein discovery and engineering. *Nucleic Acids Res. 36 (Database isuues)*: D206-10.

Wang, C.K., Wacklin, H.P. & Craik, D.J. (2012). Cyclotides insert into lipid bilayers to form membrane pores and destabilize the membrane through hydrophobic and phosphoethanolamine-specific interactions. *The Journal Of Biological Chemistry.* 287 (52): 43884-43898.

White, N.J. (2008). Qinghaosu (artemisinin): the price of success. *Science (New York, N.Y.).* 320 (5874): 330-334.

White, N.J., Looareesuwan, S., Warrell, D.A., Warrell, M.J., Chanthavanich, P., Bunnag, D. & Harinasuta, T. (1983). Quinine Loading Dose in Cerebral Malaria. *American Journal of Tropical Medicine and Hygiene.* 32 (1): 1-5.

Williams, D.A. & Lemke, T.L. (2002). "Chapter 1: Natural Products". *Foye's Principles of Medicinal Chemistry* (5th ed.). Philadelphia: . *Lippincott Williams Wilkins. ISBN 0-683-30737-1.*

Witherup, K.M., Bogusky, M.J., Anderson, P.S., Ramjit, H., Ransom, R.W., Wood, T. & Sardana, M. (1994). Cyclopsychotride-A, a Biologically-Active, 31-Residue Cyclic Peptide Isolated from Psychotria-Longipes. *Journal of Natural Products-Lloydia.* 57 (12): 1619-1625.

Wong, E.H., Hasenkamp, S. & Horrocks, P. (2011). Analysis of the molecular chemotherapeutic agents based on a medicinal chemistry approach. 18:315–331. (18): 315-331.

Wong, C.T., Rowlands, D.K., Wong, C.H., Lo, T.W., Nguyen, G.K., Li, H.Y. & Tam, J.P. (2012). Orally active peptidic bradykinin B1 receptor antagonists engineered from a cyclotide scaffold for inflammatory pain treatment. *Angewandte Chemie (International ed.in English).* 51 (23): 5620-5624.

Wu, Z., Wang, G., Xu, S., Li, Y., Tian, Y., Niu, H., Yuan, F., Zhou, F., Hao, Z. & Zheng, Y. (2014). Effects of tetrandrine on glioma cell malignant phenotype via inhibition of ADAM17. *Tumor Biology.* 35 (3): 2205-2210.

Xiao, W., Jiang, Y., Men, Q., Yuan, L., Huang, Z., Liu, T., Li, W. & Liu, X. (2015). Tetrandrine induces G1/S cell cycle arrest through the ROS/Akt pathway in EOMA cells and inhibits angiogenesis in vivo. *International Journal of Oncology.* 46 (1): 360-368.

Xu, W., Debeb, B.G., Lacerda, L., Li, J. & Woodward, W.A. (2011). Tetrandrine, a compound common in Chinese traditional medicine, preferentially kills breast cancer tumor initiating cells (TICs) *in vitro*. *Cancers.* 3 (2): 2274-2285.

Ye, Z. & Van Dyke, K. (2016). Antimalarial Activity of Various Bisbenzylisoquinoline and AporphineBenzylisoquinoline Alkaloids and their Structure-Activity Relationships against Chloroquine â Sensitive and Resistant *Plasmodium falciparum* Malaria *in vitro*. *Malaria Control & Elimination.* 2016 .

Yoon, J., Kim, H., Yadunandam, A.K., Kim, N., Jung, H., Choi, J., Kim, C. & Kim, G. (2013). Neferine isolated from Nelumbo nucifera enhances anti-cancer activities in Hep3B cells: molecular mechanisms of cell cycle arrest, ER stress induced apoptosis and anti-angiogenic response. *Phytomedicine.* 20 (11): 1013-1022.

Yu-Jen, C. (2002). Potential role of tetrandrine in cancer therapy. *Acta Pharmacol.Sin.* 23: 1102-1106.

Zhang, J., Li, J., Huang, Z., Yang, B., Zhang, X., Li, D., Craik, D.J., Baker, A.J., Shu, W. & Liao, B. (2015). Transcriptomic screening for cyclotides and other cysteine-rich

proteins in the metallophyte *Viola baoshanensis*. *Journal of Plant Physiology.* 178 : 17-26.

Zhang, Y., Wang, C., Wang, H., Wang, K., Du, Y. & Zhang, J. (2011). Combination of Tetrandrine with cisplatin enhances cytotoxicity through growth suppression and apoptosis in ovarian cancer *in vitro* and *in vivo*. *Cancer letters.* 304 (1): 21-32.

Zhao, J & Verpoorte, R (2007). Manipulating indole alkaloid production by cartharanthus roseus cell cultures in biochereactors; from biochemical proceeing to metabolic engineering. *Phytochem Rev.* 6: 435-457.

APPENDICES

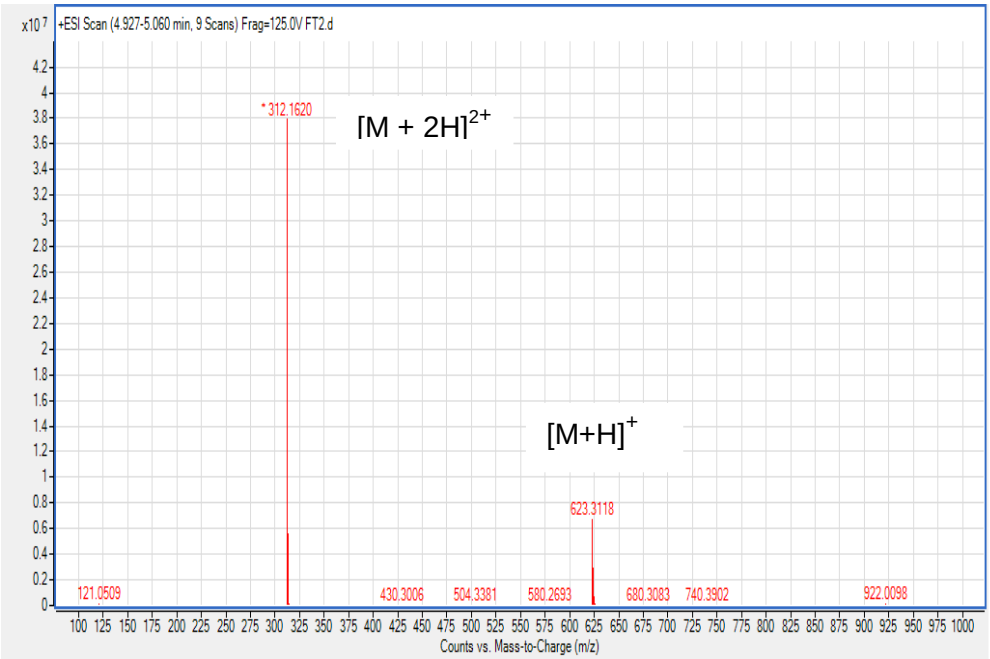

Figure A1 Positive ESI-MS of cycleanine. The mass to charge ratio (*m/z*) was found to be 623.3118.

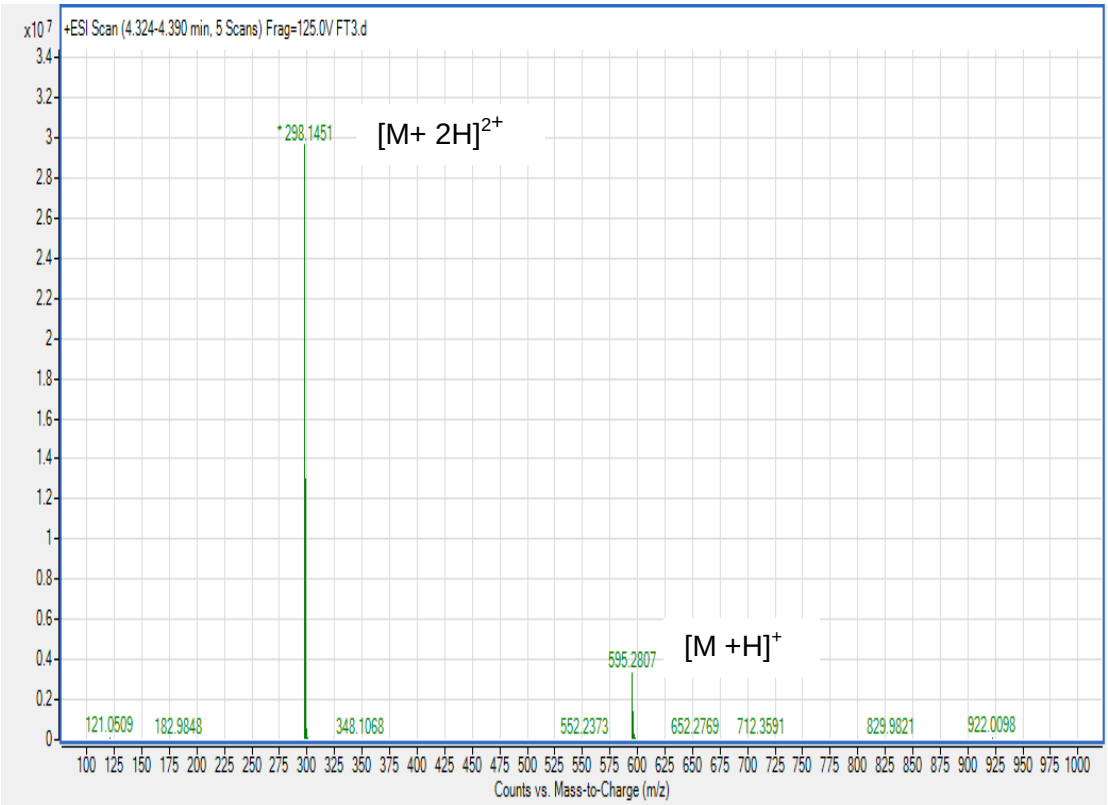

Figure A2 Positive electrospray mass spectrum of isochondodendrine.

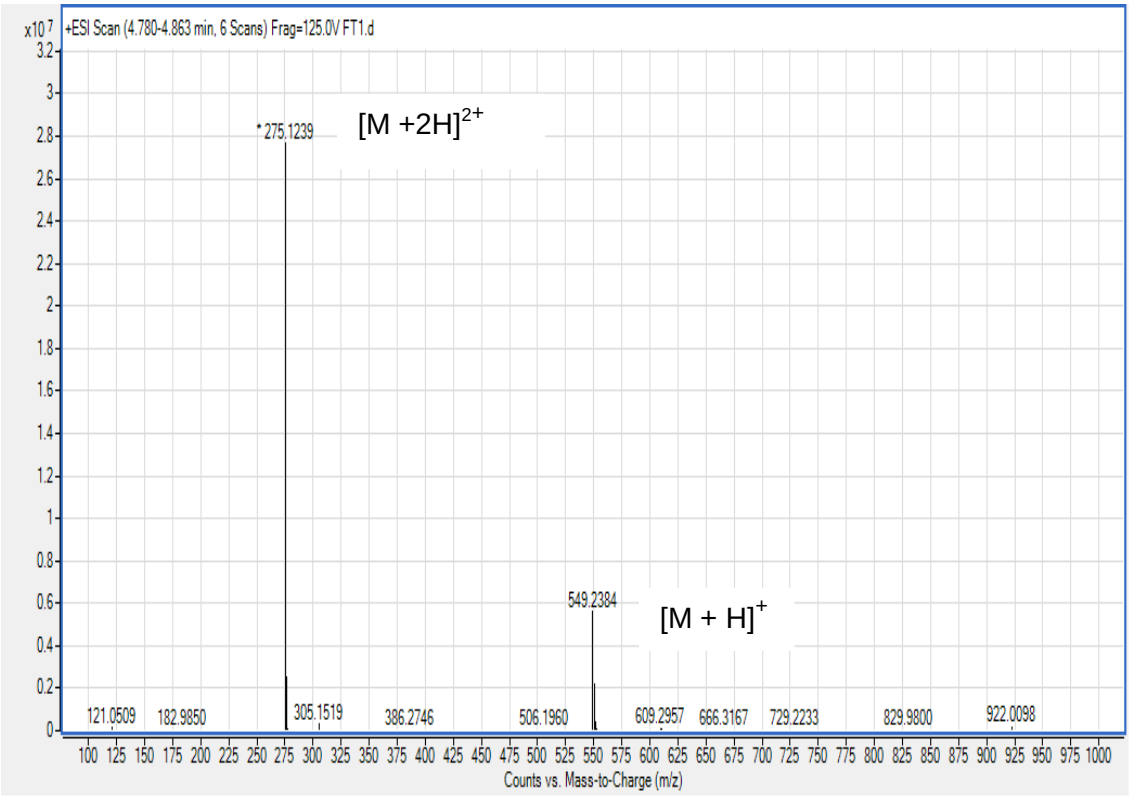

Figure A3 Positive electrospray mass spectrum of 2′-norcosculine. This shows the mass to charge (m/z) ratio of 549.2384 $[M + H]^+$ and 275.1239 $[M+2H]^{2+}$.

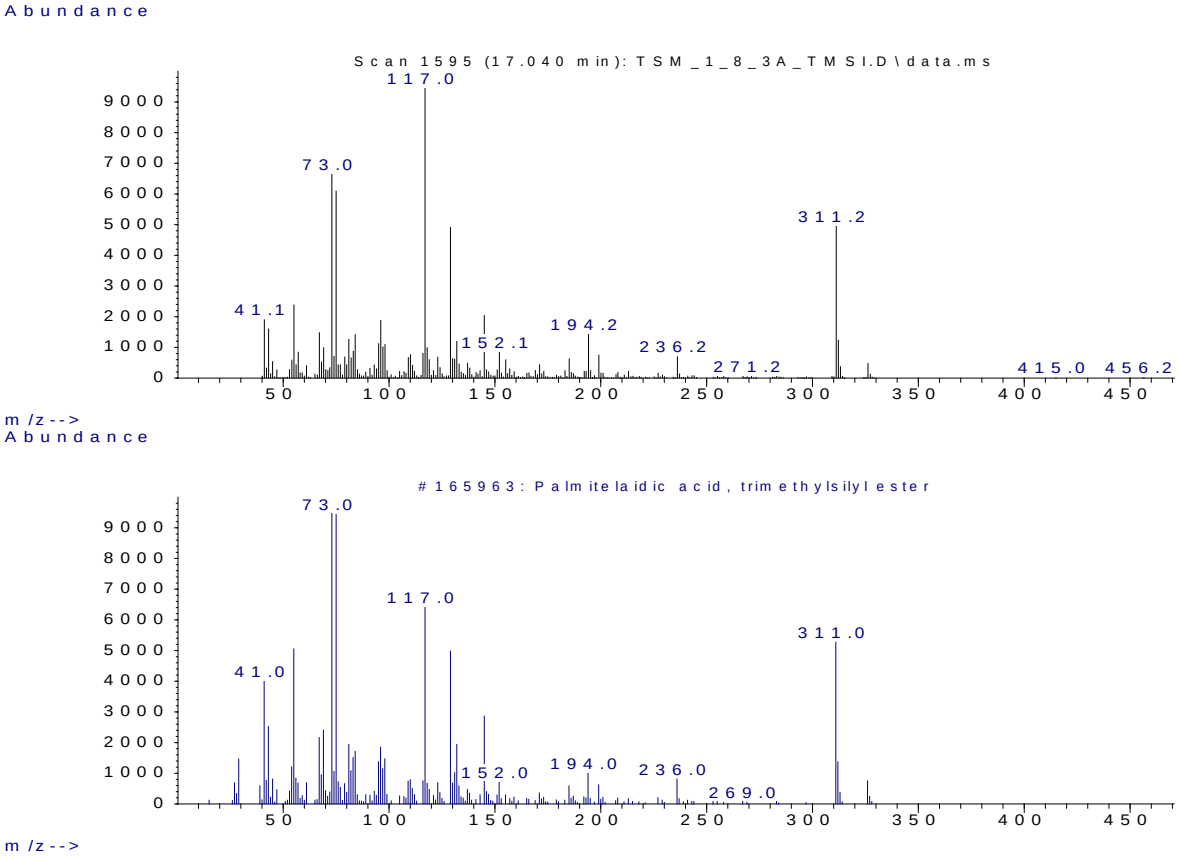

Figure *A*4 GC analysis/ spectra of palmitelaidic acid, trimethylsilyi ester from TSS3.8.

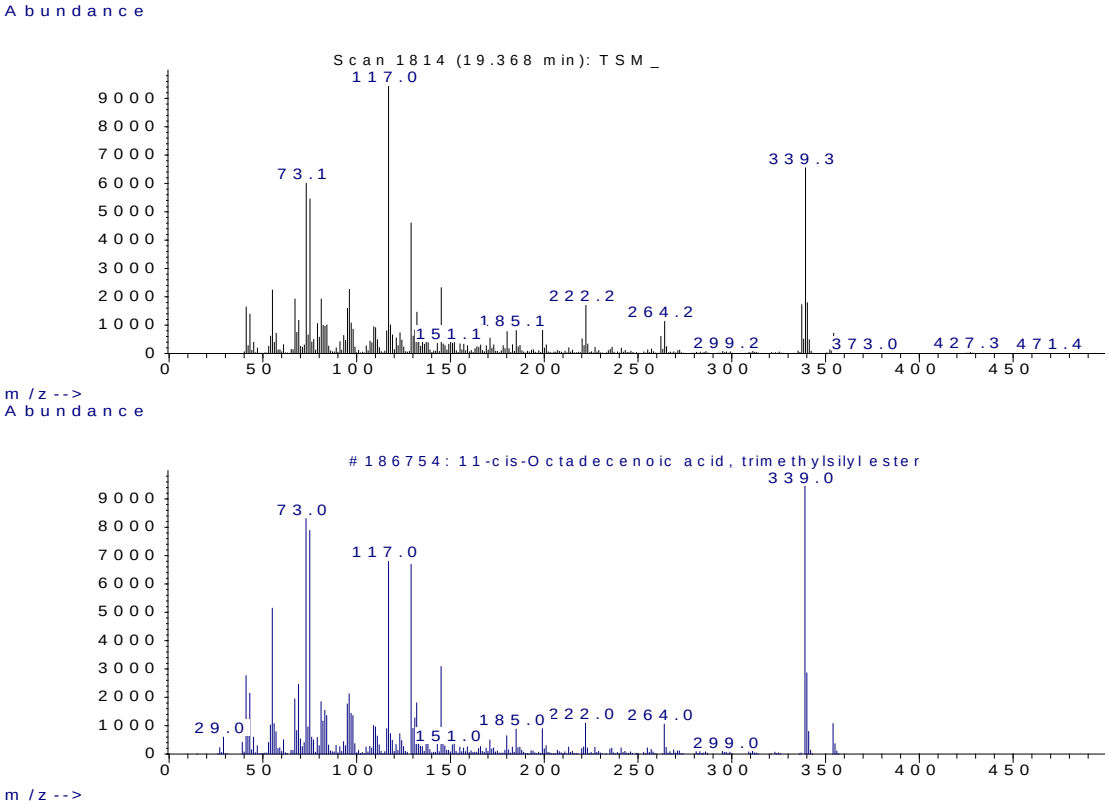

Figure A5. GC analysis/ spectra of 11-cis- Octadecenoic acid, trimethylsilyl ester of TSS3.8

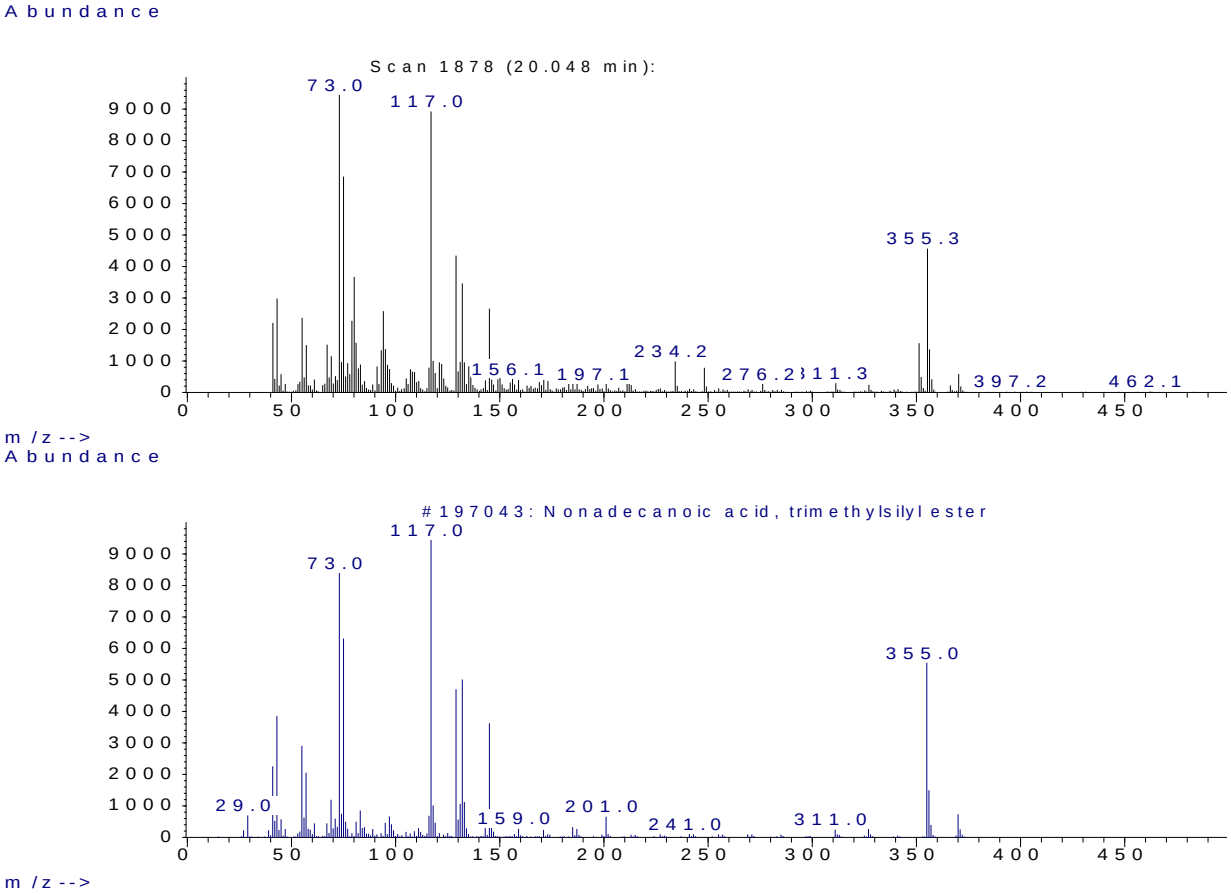

Figure A6 GC analysis/ spectra of nonadecanoic acid, trimethylsilyester in TSS3.8.

.

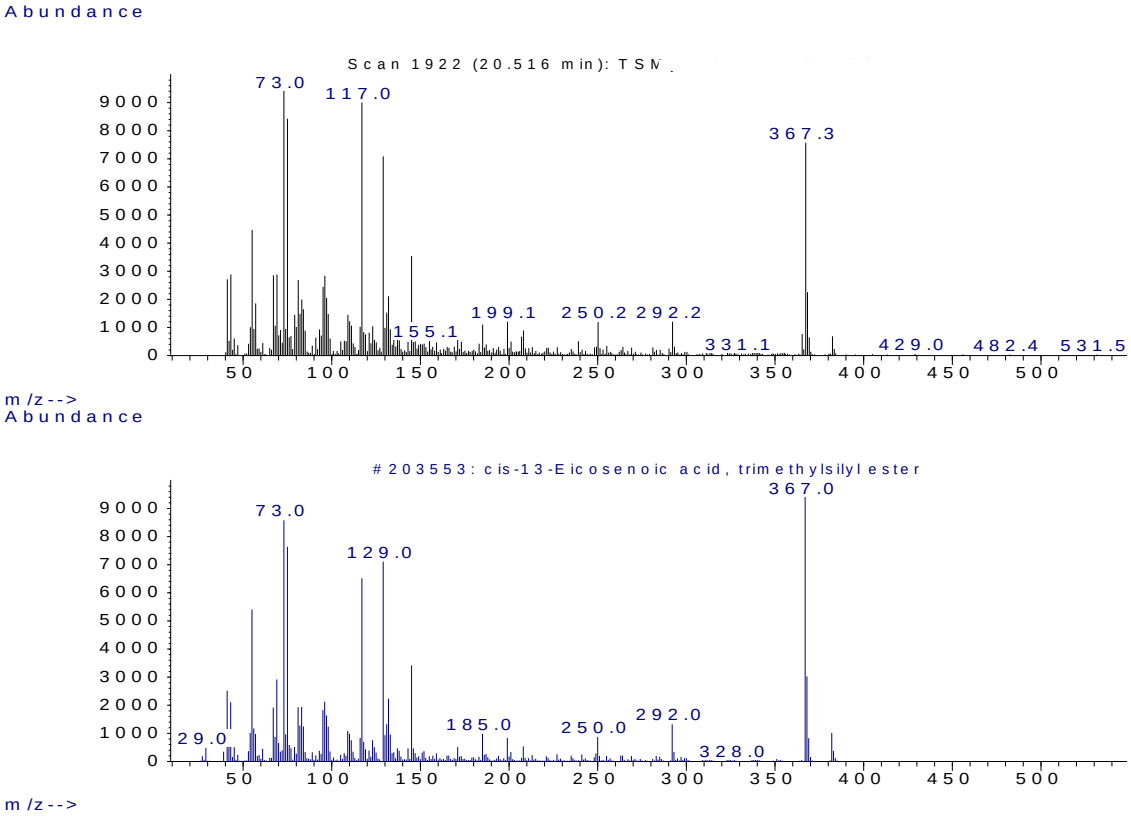

Figure A7 GC analysis/ spectra of Cis-13-Eicosenoic acid, trimethylsily ester in TSS3.8.

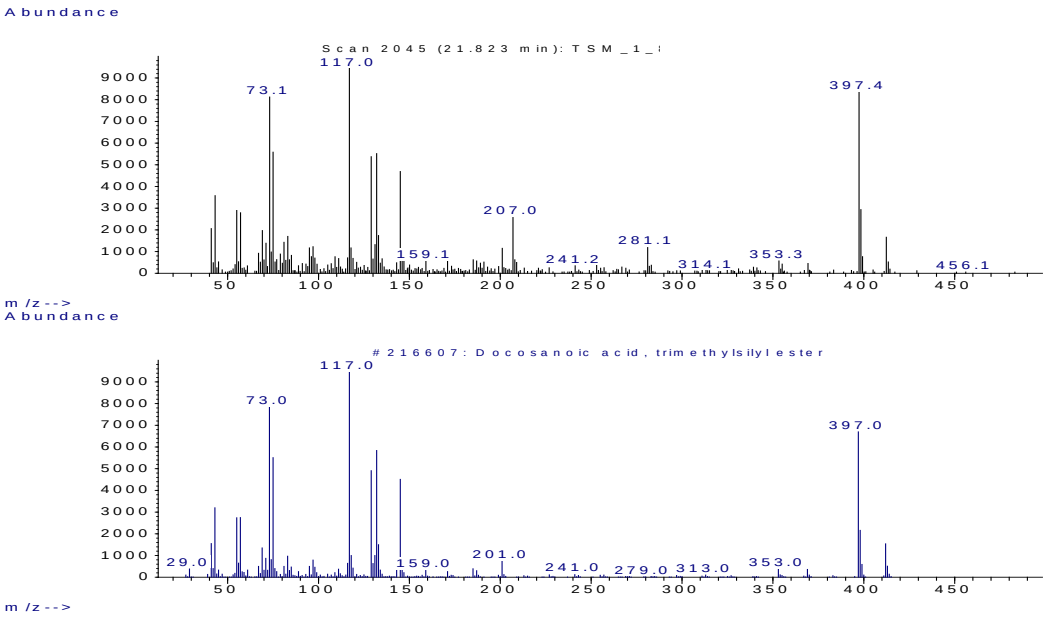

Figure A8 GC analysis/ spectra of docosanoic acid, trimethylsily ester in TSS3.8